University of Alberta

Leaf-level hyperspectral studies on leaf senescence and species recognition

by

Karen Lynne Castro

A thesis submitted to the Faculty of Graduate Studies and Research in partial fulfillment of the

requirements for the degree of *Doctor of Philosophy*

Department of *Earth and Atmospheric Sciences*

Edmonton, Alberta
Spring 2006

Library and Archives Canada

Published Heritage Branch

395 Wellington Street
Ottawa ON K1A 0N4
Canada

Bibliothèque et Archives Canada

Direction du Patrimoine de l'édition

395, rue Wellington
Ottawa ON K1A 0N4
Canada

Your file Votre référence
ISBN: 0-494-13946-3
Our file Notre référence
ISBN: 0-494-13946-3

NOTICE:
The author has granted a non-exclusive license allowing Library and Archives Canada to reproduce, publish, archive, preserve, conserve, communicate to the public by telecommunication or on the Internet, loan, distribute and sell theses worldwide, for commercial or non-commercial purposes, in microform, paper, electronic and/or any other formats.

The author retains copyright ownership and moral rights in this thesis. Neither the thesis nor substantial extracts from it may be printed or otherwise reproduced without the author's permission.

AVIS:
L'auteur a accordé une licence non exclusive permettant à la Bibliothèque et Archives Canada de reproduire, publier, archiver, sauvegarder, conserver, transmettre au public par télécommunication ou par l'Internet, prêter, distribuer et vendre des thèses partout dans le monde, à des fins commerciales ou autres, sur support microforme, papier, électronique et/ou autres formats.

L'auteur conserve la propriété du droit d'auteur et des droits moraux qui protège cette thèse. Ni la thèse ni des extraits substantiels de celle-ci ne doivent être imprimés ou autrement reproduits sans son autorisation.

In compliance with the Canadian Privacy Act some supporting forms may have been removed from this thesis.

While these forms may be included in the document page count, their removal does not represent any loss of content from the thesis.

Conformément à la loi canadienne sur la protection de la vie privée, quelques formulaires secondaires ont été enlevés de cette thèse.

Bien que ces formulaires aient inclus dans la pagination, il n'y aura aucun contenu manquant.

Canada

ABSTRACT

Understanding the variability associated with leaf spectral reflectance is critical to interpreting vegetation reflectance from remote electro-optical sensors. This variability has the potential to mask differences in spectral characteristics between species. In this thesis, a general literature review on characterizing tropical secondary forests using remote sensors is followed by four studies on leaf spectroscopy. The goal of these papers is to contribute to a better understanding of variability in leaf reflectance within species and assess the potential for tropical species discrimination at the leaf level, and to a preliminary extent, at the crown level. The first study is of a technical nature and addresses problems involved in comparing leaf spectral data gathered using multiple spectroradiometers. Recommendations include reporting on the specific wavebands used for computing indices as well as type of interpolation or smoothing performed prior to data comparison. Secondly, in a study of liana and tree leaf spectra at two sites in Panama, it was determined that the two structural groups were distinguishable at a tropical dry forest site but less so at a tropical wet forest site. In the third study, separability of tropical tree species was deemed possible within sites and seasons for a dataset of 64 tropical tree species from seven Mesoamerican sites. Across sites or seasons, separability was impeded by the large shape and amplitude differences observed within species. Lastly, in the fourth study, one of the factors causing intra-specific variability in leaf spectral reflectance, senescence, was analyzed for sunlit and shaded leaves of two temperate species, *Populus tremuloides* and *Populus balsamifera*. While changes in chlorophyll content were accurately tracked by key spectral indices, degradation of the mesophyll was not. The key future avenue of this research lies in

species separability at the crown level using high spatial resolution hyperspectral remote sensing imagery.

ACKNOWLEDGEMENT

I would like to thank my supervisor, Dr. Arturo Sánchez-Azofeifa for his limitless input, availability and flexibility during the course of my degree. As his graduate student, I have benefited from his creative and critical thinking. I particularly appreciate the opportunities I have had, through him, to carry out research from the Smithsonian canopy cranes in Panama.

There are several other people I would like to acknowledge for their support. Dr. Benoit Rivard has been very helpful with comments and ideas in general as well as through involvement in several papers of this thesis. His EAS 451 course was instrumental in my initial interest in leaf spectroscopy. As well, Dr. Joe Wright supported my work at the Smithsonian Tropical Research Institute and provided me with excellent suggestions for Chapter five, which he co-authored. I also appreciate Dr. Terry Caelli for taking the time to do an individual study course with me, in which I learned many of the spectral processing and pattern recognition techniques that were critical to my data analyses.

Fellow students with whom I have enjoyed the fieldwork experience include Margaret Kalacska and Mark Kachmar. We had some memorable times and it was a pleasure to work with such competent people. I appreciate the assistance of Mirna Samaniego, as well, who identified liana and tree species in Panama. Thank you also to my husband, Manuel Castro, for patiently enduring my years of study and for solving a number of technical problems.

Lastly, I would like to acknowledge the National Science and Engineering Research Council of Canada (NSERC PGS-B scholarship) and the Smithsonian Tropical Research Institute (Supplementary Research Award) for personal funding support. Agencies that have supported Dr. Sánchez-Azofeifa have indirectly supported my research as well, and include: the Canada Foundation for Innovation (Chapters two, three and four), the U.S. National Science Foundation (Chapter two), the Canadian National Network of Centers of Excellence - Sustainable Forest Management (Chapters three and six), the Integrated Lanscape Management (ILM) Chair at the University of Alberta (Chapter three), the Alberta Science and Research Agency (ASRA) (Chapter four), the Proyecto SEMARNAT-CONACYT (No. 2002-C01-0597 "Manejo de Bosques Tropicales: Bases Científicas para la Conservación, Aprovechamiento y Restauración de Ecosistemas", Chapters four and five), the Tinker Foundation (Chapters four and five), the Inter-American Institute for Global Change Research (IAI) (Chapter five), the Canadian International Development Agency (CIDA) (Chapter five), and NSERC under their Discovery Grant Programme (Chapter six). The Panamanian Autoridad Nacional del Ambiente (ANAM), the Ministerio del Ambiente y Energia (MINAE) of Costa Rica and the SEMANART of Mexico granted collection and/or export permits for leaf samples.

TABLE OF CONTENTS

	Page
Chapter 1—Introduction	1
Chapter synopsis	2
Summary of limitations to the research projects	3
Literature cited	5
Chapter 2—Monitoring secondary tropical forests using space-borne data: implications for Central America	7
Introduction	7
Secondary succession in the tropics	8
Estimation of biomass from remotely sensed data	10
Electo-optical image data	11
Radiation reflected from secondary forests	11
Landsat TM research on secondary forests	12
Using the biomass approach	12
Using the stand age approach	14
Accuracy assessment	14
Drawbacks of classifying by age	15
Stratification by successional pathway or other ancillary data	15
The issue of topography	16
Implications for Central America	16
National Oceanic and Atmospheric Administration (NOAA) Advanced Very High Resolution Radiometer (AVHRR) research on secondary forests	17
Research on secondary forests with SPOT	18

Limitations/future potential of electro-optical image data for secondary forest research 20

Synthetic Aperture Radar systems (SARs) 23

Microwave backscatter from secondary forests 23

SAR research on temperate forest biomass estimation 24

Tropical SAR research on forest biomass estimation 25

SAR C-band sensors 26

SAR L-band sensors 27

SAR P-band sensors 29

SAR applications for Central America 30

Limitations/future potential of SAR for secondary forest research 30

SAR/electro-optical data synergy 31

Final remarks 32

Literature cited 51

Amendment to Chapter 2 60

Literature cited 61

Chapter 3—Comparison of spectral indices obtained using multiple spectroradiometers 62

Introduction 62

Methods 63

Sample collection 63

Instruments 63

Leaf freshness test 64

Measurements of spectral reflectance 64

Analyses and statistics 66

Vegetation Indices 66

D and θ metrics 66

Statistical tests 67

Results 68

Freshness test 68

Reflectance spectra 68

Indices 68

D and θ 69

Discussion and conclusions 69

Literature cited 87

Chapter 4—Discrimination of lianas and trees with leaf-level hyperspectral data 89

Introduction 89

Methods 90

Study areas 90

Parque Natural Metropolitano 90

Fort Sherman 90

Sample collection 91

Measurements of chlorophyll content 91

Measurements of spectral reflectance 91

Spectral analysis 92

Spectral smoothing and differentiation 92

Principal components analysis 92
Pattern recognition techniques 92
Evaluation 93
Software 93
Results 94
PCA approach 94
Dataset evaluation 95
Classifier evaluation 95
Within-leaf and within-species variability 96
Discussion and conclusion 97
Literature cited 120
Chapter 5—Variability in leaf optical properties of Mesoamerican trees and the potential for species classification 122
Introduction 122
Materials and methods 124
Study sites 124
Leaf sample collection 124
Crown spectra 124
Leaf trait data 125
Leaf chlorophyll content and thickness 125
Leaf histology 125
Leaf diffuse reflectance and transmittance 125
Measurements of bi-directional spectral reflectance 126
UniSpec spectral analysis system 126

FieldSpec HandHeld 126

Spectral analysis 126

D and θ 126

Classification 128

Results 129

D and θ 129

Classification 130

Case study including leaf trait data: Parque Natural Metropolitano 131

Discussion 131

D and θ (leaf level) 132

Classification 132

Spectra and leaf traits 134

Crown spectra 134

Literature cited 154

Chapter 6—Changes in spectral properties, chlorophyll content and internal mesophyll structure of senescing *Populus balsamifera* and *Populus tremuloides* leaves 160

Introduction 161

Methods 162

Leaf spectral reflectance and chlorophyll content 162

Sample collection 162

Instruments used in this study 162

SPAD measurements and chlorophyll content (2002 samples) 163

Leaf spectral reflectance measurements (2002 samples) 163

Histology (2003 samples) 163

Sample collection 163

Leaf fixation and thin section analysis 163

Data analysis 164

SPAD calibration curves 164

Indices 164

Histological analysis 164

Correlation analysis 164

Results 165

SPAD curves 165

Indices and chlorophyll content 165

Histological analysis 166

Correlation analyses 167

Discussion 167

Comparison of species 167

Comparison of sun and shade leaves 168

Comparison of mature and senescing leaves 168

Conclusion 169

Literature cited 179

Chapter 7—Conclusions 183

Contributions and significance 183

Avenues for future research 185

Literature cited 187

LIST OF TABLES

		Page
Table 2-1.	Application of Landsat data for detecting tropical secondary forest by age or biomass	34
Table 2-2.	Examples of forest classification/stratification schemes	38
Table 2-3.	Field data gathered for remote sensing studies of regenerating forests	39
Table 2-4.	Importance of forest components to radar backscatter of different wavelengths and polarizations	42
Table 2-5.	Radar for estimation of forest biomass or stage of regeneration	44
Table 3-1.	Characteristics of spectroradiometers used in this study and an overview of illumination and viewing scenarios 1 and 2	74
Table 3-2.	Spectral indices computed in this study	75
Table 3-3.	Wavebands used for computing indices listed in Table 3-2	76
Table 3-4.	PRI computed with three spectroradiometers over 2 illumination and viewing scenarios	77
Table 3-5.	SIPI computed with three spectroradiometers over 2 illumination and viewing scenarios	78
Table 4-1.	Liana and tree species sampled for this study	100
Table 4-2.	Supervised classifiers used in this study (source: Duin, 2000)	102
Table 4-3.	Percentage of variance contained within first two eigenvectors/values in PCA1 and PCA2	103
Table 4-4.	Training and testing error (in percentage) for dataset-classifier combinations used in this study	104
Table 4-5.	Results of chlorophyll analyses for liana and tree leaves at PNM and FTS	105
Table 4-6.	Influence of number of spectral dimensions on classification accuracy (in percentage) using parametric classifiers	106
Table 4-7.	Ranking of methods used in this study for the two sites, PNM and FTS, based on overall percent classification error	107

calculated from Table 4-4 (1=lowest percentage error)

Table 5-1. Summary of study area characteristics 136

Table 5-2. Summary of data collected at each site 137

Table 5-3. Species sampled for this study 138

Table 5-4. Leaf characteristics of *Bursera simaruba* and *Byrsonima crassifolia* at multiple sites 141

Table 5-5. Best species-level classification results 142

Table 5-6. Leaf trait data for species in the Parque Natural Metropolitano October 2003 dataset 143

Table 5-7. Correlation coefficients and P-values for relationships between leaf optical properties and leaf internal mesophyll structure, PNM October 2003 dataset 144

Table 6-1. Calibration equations for SPAD and chlorophyll content of *P. tremuloides* and *P. balsamifera* sun and shade leaves 171

Table 6-2. Comparison of anatomical features and near-infrared reflectance at 800.7 nm for mature and senescing *P. tremuloides* and *P. balsamifera* leaves 172

Table 6-3. Correlation coefficients (r) for relationships between leaf optical properties and leaf chlorophyll content (2003 data) 173

LIST OF FIGURES

		Page
Figure 2-1.	Visualization of six tree temperaments. Each temperament may either remain constant from seedling to adult tree (hard strugglers, hard gamblers), or be flexible and change its shade tolerance at some stage of the life cycle (others). The vertical dimension of this diagram evaluates height above ground level, which will be different for each tree species. It also refers to processes, but the tempo and rhythm of these processes differ for each tree species, and thus this is also a relative scaling. The strugglers closely correspond to the classical "shade-bearers" or "climax species", the hard gamblers to classical "light-demanding" or "pioneer" species. The relative frequency of a temperament is indicated by the thickness of the bar. Source: Oldeman and van Dijk (1991) © Parthenon Publishing Group Ltd (Reproduced with permission).	48
Figure 2-2.	Conceptual relationship between Landsat Thematic Mapper Band 3 and Total Above Ground Biomass (TAGB) for a tropical dry forest ecosystem: t_{-0} represents pre-disturbance, t_0 represents today and t_{+1} represents the time when maximum TAGB is achieved. Breaks on both curves are related to the presence of human-induced-fires typical of this ecosystem.	49
Figure 2-3.	Spectral response of Landsat TM bands 1-5, 7 to regeneration stage. Site: Altamira (Amazon); SS=secondary succession. Source: Moran et al. (1994) © Bioscience (Reproduced with permission).	50
Figure 3-1.	Illustration of instrument set-up. Top figure shows scenario one configuration with the FR fibre-optic inserted into the port of the integrating sphere. Sphere lamp is shown on the right. Middle figure shows scenario two configuration for the FR. Bottom figure shows scenario two configuration for the UN, with the fibre-optic inserted into the leaf clip.	79
Figure 3-2.	Changes in relative reflectance (measured with UniSpec) of three wavebands (532, 571.6 and 680 nm) over time for a *Cafea arabica* (CA) leaf, *Lantana camara* (LC) leaf, and *Eriobotrya japonica* (EJ) leaf under constant illumination in the sample port of an 1800-12S integrating sphere for 30 minutes.	80
Figure 3-3.	Average visible (top three graphs) and near-infrared (bottom three graphs) reflectance spectra of 40 leaves of three species	81

as measured by three spectroradiometers under scenario one, which controlled for illumination, viewing, and FOV effects.

Figure 3-4. Average visible (top three graphs) and near-infrared (bottom three graphs) reflectance spectra of 40 leaves of three species as measured by three spectroradiometers under scenario two, a 'typical' instrument set-up. 83

Figure 3-5. Average *D* +/- one standard deviation for the instrument-pairs over the two illumination,viewing, and FOV scenarios. Instruments/scenario are indicated along the x-axis in the following manner: e.g. FRHH1=FR and HH data pair, scenario one. Additional *D* values are given for three species pairs for comparison. CALC=*Cafea arabica/Lantana camara*, CAEJ=*Cafea arabica/Eriobotrya japonica*, LCEJ=*Lantana camara/Eriobotrya japonica.* Spectra for the species-pair *D* values were measured with the ASD FR spectrometer according to scenario one configuration (using the sphere). 85

Figure 3-6. Average θ +/- one standard deviation for the instrument-pairs over the two illumination,viewing, and FOV scenarios. Instruments/scenario are indicated along the x-axis in the following manner: e.g. FRHH1=FR and HH data pair, scenario one. Additional θ values are given for three species pairs for comparison. CALC=*Cafea arabica/Lantana camara*, CAEJ=*Cafea arabica/Eriobotrya japonica*, LCEJ=*Lantana camara/Eriobotrya japonica.* Spectra for the species-pair θ values were measured with the ASD FR spectrometer according to scenario one configuration (using the sphere). 86

Figure 4-1. Classification of PNM liana and tree 1st derivative spectra using PCA method 1 and six classifiers: logistic linear (loglc, top), quadratic (qdc, 2nd from top), uncorrelated normal densities based quadratic (udc, 3rd from top), decision tree (treec, 4th from top), neural network (lmnc, 5th from top), and k-nearest neighbor (knnc, bottom). Points correspond to individual leaves (3 per species). The large filled circle represents the overall PNM liana mean; smaller filled circles are +/- one standard deviation from the mean. The large filled square indicates the overall PNM tree mean; smaller filled squares are +/- one standard deviation from the mean. 108

Figure 4-2. Classification of FTS liana and tree raw smoothed spectra by a k-nearest neighbor (knnc, k=2) classifier using PCA method 1. Points correspond to individual leaves (3 per species). The large filled circle indicates the overall FTS liana mean; smaller 111

filled circles are +/- one standard deviation from the mean. The large filled square indicates the overall FTS tree mean; smaller filled squares are +/- one standard deviation from the mean.

Figure 4-3. Principal component loadings in the spectral bands for PNM PCA1 raw smoothed data (top), PNM PCA1 1st derivative data (2nd from top), FTS PCA1 raw smoothed data (3rd from top), and FTS PCA1 1st derivative data (bottom). 112

Figure 4-4. Comparison of PNM and FTS average liana and tree spectra (top) and 1st derivative spectra (bottom) over the range 450-950 nm. 114

Figure 4-5. Comparison of PNM and FTS average liana and tree spectra (top) and 1st derivative spectra (bottom) over the visible region (450-675 nm) of the electromagnetic spectrum. 115

Figure 4-6. An illustration of within-leaf and within-species variability for two species. The three top graphs show reflectance spectra (six/leaf) measured for each of three leaves of the liana species *Tontolea ovalifolia*. The fourth through sixth graphs (from the top) show reflectance spectra (six/leaf) gathered for each of three leaves of the tree species *Simarouba amara*. In the bottom graph, average leaf spectra (three/species) are plotted for both species. 116

Figure 5-1. Partial tree crowns, as viewed from a canopy crane at Fort Sherman, Panama, at a height of 5 m. The species are A) *Jacaranda copaia*, B) *Dussia munda*, C) *Tapirira guianensis*, D) *Cordia bicolor* and E) *Vochysia ferruginea*. 145

Figure 5-2. Mean amplitude (D) (±1 SD) of leaf reflectance spectra of tropical trees at sites in Mexico, Costa Rica and Panama for various levels of comparison. Average D was calculated for all applicable UniSpec data (panel A) and ASD HandHeld data (panel B) (Table 2). Number of samples used to compute each mean is indicated, and includes all the pairwise combinations of spectra per respective level. 146

Figure 5-3. Mean shape (θ) (±1 SD) of leaf reflectance spectra of tropical trees at sites in Mexico, Costa Rica and Panama for various levels of comparison. Average θ was calculated for all applicable UniSpec (panel A) and ASD HandHeld data (panel B) (Table 2). Number of samples used to compute each mean is indicated, and includes the pairwise combinations of spectra per respective level. 147

Figure 5-4. Average crown reflectance spectra (FOV=approximately 3.6 m) for 5 species at Fort Sherman, Panama. Spectra correspond to species pictured in Figure 1 as follows: *Jacaranda copaia* (JACO), *Dussia munda* (DUMU), *Tapirira guianensis* (TAGU), *Cordia bicolor* (COBI) and *Vochysia ferruginea* (VOFE). 148

Figure 5-5. Average relative reflectance spectra of (A) *Bursera simaruba* (BUSI) and (B) *Byrsonima crassifolia* (BYCR), each at three sites in Costa Rica (SR, Santa Rosa; ER, El Rodeo; LI, Los Inocentes; LH, Los Horizontes). Accompanying leaf trait data may be found in Table 5-4. 149

Figure 5-6. Distribution of wavebands chosen in the forward feature selection process, based on the within-site species classifications (Table 5-5). The top 20 wavebands per classification were tallied for this histogram. 150

Figure 5-7. Classification analysis for 50 species from three sites, Parque Natural Metropolitano, For Sherman, and Chamela. Data gathered in the 2003 wet season using the UniSpec. Mean test data error ±1 SD was computed from 10,000 classifications each per set of 5, 10, 15, 20, 25, 30, 35, 40, and 45 species. Sets of species selected at random for each classification. 151

Figure 5-8. Average reflectance spectra for *Astronium graveolens* (ASGR) compared to average reflectance spectra ±1 SD for all species at Parque Natural Metropolitano, Panama for October 2003. 152

Figure 5-9. Leaf cross sections of three species from Parque Natural Metropolitano, Panama. (A) *Astronium graveolens*, (B) *Anacardium excelsum*, (C) *Ficus insipida*. Bracketed area indicates approximate width of the spongy mesophyll. The 100 μm scale is applicable to all cross sections. 153

Figure 6-1. SPAD calibration curves for total chlorophyll (Total Chl) of sun and shade leaves for *P. tremuloides* and *P. balsamifera*. 174

Figure 6-2. Spectral indices (mSR_{705}, mND_{705} and PSRI) plotted according to time (left) and total chlorophyll content (right) for *P. tremuloides* sun (ASU) and shade (ASH) leaves and *P. balsamifera* sun (PSU) and shade (PSH) leaves. Each symbol represents an average from three leaves. 175

Figure 6-3. Changes in total chlorophyll, chlorophyll *a* and *b* and 176

chlorophyll a/b during senescence of *P. tremuloides* and *P. balsamifera* sun and shade leaves. Each symbol represents the mean ± 1 SD from three leaves, where chlorophyll content is based on regressions in Table 6-1. Leaf drop occurred by day 288 for *P. balsamifera* and day 299 for *P. tremuloides*.

Figure 6-4. Mean palisade and spongy mesophyll thickness (± 1 SD) for mature *P. tremuloides* sun (ASU) and shade (ASH) leaves and *P. balsamifera* sun (PSU) and shade (PSH) leaves, based on measurements from August 8, 2003 thin sections (n=2-5). 177

Figure 6-5. Thin sections of mature (a) and senescing (b) *P. tremuloides* sun leaves. 178

LIST OF SYMBOLS AND ABBREVIATIONS

ASD	Analytical Spectral Device
ASH	Aspen shade leaf
ASTER	Advanced spaceborne thermal emission and reflection radiometer
ASU	Aspen sun leaf
AVIRIS	Airborne visible/infrared imaging spectrometer
D	Amplitude metric
dbh	Diameter at breast height
DEM	Digital elevation model
DMSO	Dimethyl sulphoxide
EOS	Earth observing system
ERS	European space agency
FAA	Formalin aceto-alcohol
*f*APAR	Fraction absorbed photosynthetically active radiation
FOV	Field of view
FR	Fieldspec Pro FR
FTS	Fort Sherman
HH	Fieldspec HandHeld
HVR	High resolution visible
HVRIR	High resolution visible infrared
HYDICE	Hyperspectral digital imagery collection experiment
JERS	Japan earth resources satellite

LAI	Leaf area index
LUCC	Land use/Cover change
MERIS	Medium resolution imaging spectrometer
MIR	Mid-infrared
mND_{705}	Modified normalized difference index
MODIS	Moderate resolution imaging spectroradiometer
mSR_{705}	Modified simple ratio
MSS	Multispectral scanner
NASA	National aeronautics and space administration
ND	Normalized difference index
NDVI	Normalized difference vegetation index
NIR	Near-infrared
NOAA AVHRR	National oceanic and atmospheric administration Advanced very high resolution radiometer
PCA	Principal components analysis
PNM	Parque Natural Metropolitano
PRI	Photochemical reflectance index
PSH	Poplar shade leaf
PSRI	Plant senescence reflectance index
PSU	Poplar sun leaf
SAR	Synthetic aperture radar
SD	Standard deviation
SIPI	Structure-independent reflectance index

SIR	Spaceborne imaging radar
SPOT	Satellite pour l'observation de la Terre
SR	Simple ratio
SWIR	Shortwave infrared
TAGB	Total above-ground biomass
TIR	Thermal infrared
TM	Thematic mapper
UN	UniSpec spectral analysis system
VIS	Visible
VNIR	Visible and near-infrared
θ	Shape metric

CHAPTER 1—Introduction

Green is green is green.

-Dave Simonett[1]

The above quote, from a remote sensing perspective, suggests that all vegetation types look alike. Thirty to forty years ago, this claim was more accurate than not. Early satellites supported low spatial and spectral resolution satellite sensors such as AVHRR (1 km, 2 broad spectral bands in the visible through near-infrared regions (VIS/NIR)) and Landsat MSS (80 m, 4 broad spectral bands in the VIS/NIR). Data from these instruments could be used to characterize only broad vegetation types or make course estimates of vegetation health. Remarkable advances in remote sensing technology have taken place since these early satellites were launched. Current high spatial resolution multispectral sensors, each with four broad spectral bands in the VIS/NIR, include IKONOS, Orbview-3 (both with 1 and 4m spatial resolutions) and Quickbird (0.7 and 2.8 m spatial resolutions). These sensors can be used to pinpoint individual trees, and have likely surpassed earlier expectations with regard to spatial resolution. EO-1 Hyperion, launched in 1999, represents the first spaceborne hyperspectral imager. It supports 220 wavebands over the range 400-2500 nm and a spatial resolution of 30 m. While successful development and launch of a hyperspectral sensor with fine spatial resolution has yet to be realized, the technical specifications of the failed OrbView-4 sensor (8 m, 200 spectral bands, 400-2500 nm) would indicate that it is only a matter of time. Until then, combining both high spectral and spatial resolution data is only possible with airborne hyperspectral sensors such as AVIRIS and HYDICE (224 and 200 bands, respectively, 400-2500 nm, variable spatial resolution), which are useful for research and testing, but are expensive and do not provide continuous image data.

At even finer scales, leaf spectroscopy is useful for estimation of leaf traits including chlorophyll content (Richardson et al., 2002), water content (Sims & Gamon, 2003), structural characteristics (Slaton et al., 2001), and in a broader sense, measuring leaf stress (Richardson & Berlyn, 2002), tracking leaf senescence (Gitelson & Merzlyak, 1994), or determining species type (Fung et al., 1999). The value of leaf spectroscopy also lies in gaining a better understanding of vegetation reflectance from airborne or satellite-borne electro-optical remote sensors (Schmidt & Skidmore, 2001). Classical work on leaf optical properties in the late 1960's through 1980's by authors such as Gates (1965), Allen & Richardson (1968), Allen et al. (1970), Knipling (1970), Woolley (1971), Gausman & Allen (1973), and Gausman (1974, 1985) defined the nature of the leaf reflectance spectrum in the VIS/NIR and identified the major absorption features due to pigments and water. Moreover, these authors explored the causes of perturbations to a normal healthy vegetation spectrum, such as due to leaf maturation and senescence, location (sun vs. shade), and water and nutrient stresses. Intuitively, these perturbations, which cause intra-specific variability in reflectance spectra, could cause significant confusion for species recognition using hyperspectral data, but have been ignored in many studies (Cochrane, 2000). However, these factors are important to recognize since the underlying premise for identifying species is that species are indeed separable in the

[1] Quoted in Jensen, J. R. (2000). *Remote Sensing of the Environment: An Earth Resource Perspective 2000* Upper Saddle River, New Jersey: Prentice-Hall Inc., p. 352.

spectral domain; in other words, the variance of the reflectance is greater between species than within species (Schmidt & Skidmore 2001; Skidmore et al., 1988).

To address this gap in leaf spectroscopy research, my research focuses on within and between-species variability in leaf reflectance. I begin with a literature review and then present four studies of leaf spectroscopy. Five objectives are addressed: 1) To define the current state of remote sensing of tropical secondary forests, 2) To compare leaf spectral reflectance across different spectrometers and illumination and viewing scenarios, 3) To test the separability of lianas (woody vines) and trees in two tropical forests in Panama, based on leaf reflectance spectra, 4) To quantify intra-specific and inter-specific variability in leaf optical properties for over 60 tropical tree species in Mesoamerica, and 5) To describe autumn leaf senescence of sun and shade-adapted leaves of *Populus balsamifera* and *Populus tremuloides* with respect to chlorophyll content, leaf internal anatomy and spectral reflectance characteristics. Where relevant, I link my research on leaf spectroscopy to potential remote sensing applications at the canopy level.

CHAPTER SYNOPSIS

Each of the following chapters focuses on one of the five objectives stated above. All chapters have been published or submitted to peer-reviewed journals. Chapter two, *Monitoring secondary tropical forests using space-borne data: implications for Central America* (Castro et al., 2003, published in *International Journal of Remote Sensing, 24*, 1853-1894), describes current capabilities in remote sensing research aimed at determining stage of growth in secondary tropical forests, comparing contributions from both electro-optical sensors and synthetic aperture radar (SAR). This comprehensive literature review sets the stage for subsequent chapters by revealing the necessity of interpreting spectral differences in vegetation at finer spatial and spectral scales.

Chapter three, *Comparison of spectral indices obtained using multiple spectroradiometers* (Castro-Esau et al., in press, *Remote Sensing of Environment*), addresses some of the challenges of comparing leaf spectra across different instruments and measuring methodologies. Under controlled conditions of field of view and illumination and viewing geometries, spectra of the same leaves were found to differ significantly when measured using three spectrometers. This study brings issues of standardization across studies to light and further sets the stage for Chapter five, which integrates data from multiple sites and using multiple spectrometers.

In Chapter four, leaf-level hyperspectral data are applied to a problem with ecological implications: Can two structural groups of plants be distinguished based on leaf spectra? The two structural groups are lianas (woody vines) and trees. The study, *Discrimination of lianas and trees with leaf-level hyperspectral data* (Castro-Esau et al., 2004), was published in *Remote Sensing of Environment, 90*, 353-372. Current research on lianas is gaining attention due to the finding that lianas have been increasing in dominance in tropical forests over the past two decades (Phillips et al., 2002). This increase may have serious consequences for species composition and carbon sequestration in tropical forests worldwide. Defining the spectral characteristics of lianas and identifying differences between lianas and trees is the first step in mapping their extent and distribution using remote sensors.

Whereas Chapter four focuses on separating structural groups of plants, the focus of Chapter five is even more specific: How separable are tropical tree species? Using an unprecedented database of 64 tropical species spanning seven Mesoamerican sites, this question is answered, first examining intra-specific variability in leaf spectra and comparing it with inter-specific variability. Results are extrapolated for species-rich tropical forests. The manuscript based on this research, *Variability in leaf optical properties of Mesoamerican trees and the potential for species classification*, has been accepted for publication to *American Journal of Botany*. This study explores the potential for species classification in tropical forests using leaf-level data and presents a preliminary assessment of species classification at the crown level.

Lastly, in Chapter six I analyze one of the factors causing within-species variability in leaf reflectance spectra: senescence. *Changes in spectral properties, chlorophyll content and internal mesophyll structure of senescing Populus balsamifera and Populus tremuloides leaves* has been submitted for publication to *International Journal of Remote Sensing*. During senescence, rate of chlorophyll loss and degradation of the mesophyll can vary from species to species. Understanding the time sequence and characteristics of these changes between species is an important step in interpreting remotely sensed data at certain times of the year. In this study, changes in leaf spectra and leaf traits are described, including chlorophyll content and mesophyll characteristics for two temperate species, *Populus tremuloides* and *Populus balsamifera*, over two light acclimation classes: sunlit and shaded.

SUMMARY OF LIMITATIONS TO THE RESEARCH PROJECTS

Challenges to the research projects described in this thesis were logistical or scientific in nature. Logistically, exposure of sensitive instruments to high humidity, heat and dust in the tropics sometimes led to temporary equipment failure. Weather was critical when working from the canopy cranes in Panama. Variable cloud conditions, for instance, are not suitable for crown spectral measurements, and operation of the cranes is not permitted when raining for safety reasons.

Two main scientific limitations I perceive in this thesis, secondly, relate to sample size and the use of leaf-level hyperspectral data. Sample sizes were constrained by a number of factors. Working from the canopy cranes in Panama, we were limited by institutional regulations as to number of allowable samples per tree (10 leaves/tree). High species diversity but low species frequency per unit area also made it difficult at many sites to sample multiple trees per species. Based on time constraints, we tried to make a reasonable compromise between number of species sampled and number of samples per species. This was the case both in the field and in the laboratory, performing time-consuming tasks such as leaf thin section preparation. There were also a small minority of species that were discarded prior to analysis because their leaf quality degraded quickly after harvest, leading to symptoms of necrosis and wilting.

Beyond the constraints of working with limited sample sizes is the looming fact that the research for this thesis involves primarily leaf-level, rather than crown-level, hyperspectral data. The reasons behind this limitation are outlined in the introduction to Chapter five. For the study of leaf senescence and intra-specific variability in leaf optical properties, leaf-level hyperspectral data are ideal. However, for species classifications, they are not, since it is not possible to predict similar classifications from remote sensors.

To overcome this limitation, we have included crown-level data for five species at Fort Sherman, Panama in Chapter five, and include discussions of potential for crown-level species identification in Chapters four and five. Furthermore, current research at the Earth Observation Systems Laboratory (EOSL) includes 1) a preliminary study of crown spectra of one tree species at Parque Natural Metropolitano, Panama (*Anacardium excelsum*) with varying proportions of liana coverage (Sánchez-Azofeifa & Castro-Esau, in press, *International Journal of Remote Sensing*), 2) an evaluation of data reduction approaches for distinguishing lianas and trees at both leaf and canopy levels, using an airborne HYDICE hyperspectral dataset from Parque Natural Metropolitano, Panama (Kalacska et al., submitted, *Remote Sensing of Environment*), and 3) an analysis of tropical tree species identification for five species from an airborne HYDICE image over La Selva, Costa Rica (Zhang et al., submitted, *Remote Sensing of Environment*). Airborne hyperspectral datasets of tropical forests remain, at this time, difficult to acquire. However, we anticipate this difficulty will be overcome with time, and will facilitate the transition to crown-level tropical tree species classification.

LITERATURE CITED

Castro, K. L., Sanchez-Azofeifa, G. A. & Rivard, B. (2003). Monitoring secondary tropical forests using space-borne data: implications for Central America. *International Journal of Remote Sensing*, *24*, 1853-1894.

Castro-Esau, K. L., Sanchez-Azofeifa, G. A. & Caelli, T. (2004). Discrimination of lianas and trees with leaf-level hyperspectral data. *Remote Sensing of Environment*, *90*, 353-372.

Castro-Esau, K. L., Sanchez-Azofeifa, G. A. & Rivard, B. (in press). Comparison of spectral indices obtained using multiple spectroradiometers. *Remote Sensing of Environment*.

Castro-Esau, K. L. & Sanchez-Azofeifa, G. A. (submitted). Changes in spectral properties, chlorophyll content and internal mesophyll structure of senescing *Populus balsamifera* and *Populus tremuloides* leaves. *International Journal of Remote Sensing*.

Castro-Esau, K. L., Sanchez-Azofeifa, G. A., Rivard, B., Wright, S. J. & Quesada, M. (in press). Variability in leaf optical properties of Mesoamerican trees and the potential for species classification. *American Journal of Botany*.

Cochrane, M. A. (2000). Using vegetation reflectance variability for species level classification of hyperspectral data. *International Journal of Remote Sensing*, *21*, 2075-2087.

Fung, T., Ma, F. Y. & Siu, W. L. (1999). Band Selection using hyperspectral data of subtropical tree species. http://www.gisdevelopment.net/aars/acrs/1999/ps3/ps3055pf.htm.

Gates, D. M., Keegan, H. J., Schleter, J. C. & Weidner, V. R. (1965). Spectral Properties of Plants. *Applied Optics*, *4*, 11-20.

Gitelson, A. & Merzlyak, M. N. (1994). Spectral Reflectance Changes Associated with Autumn Senescence of Aesculus-Hippocastanum L and Acer-Platanoides L Leaves - Spectral Features and Relation to Chlorophyll Estimation. *Journal of Plant Physiology*, *143*, 286-292.

Kalacska, M., Bohlman, S., Sanchez-Azofeifa, A., Castro-Esau, K. L. & Caelli, T. (submitted). Hyperspectral discrimination of tropical dry forest lianas and trees: Comparative data reduction approaches at the leaf and canopy levels. *Remote Sensing of Environment*.

Phillips, O. L., Martinez, R. V., Arroyo, L., Baker, T. R., Killeen, T., Lewis, S. L., Malhi, Y., Mendoza, A. M., Neill, D., Vargas, P. N., Alexiades, M., Ceron, C., Di Fiore, A., Erwin, T., Jardim, A., Palacios, W., Saldias, M. & Vinceti, B. (2002). Increasing dominance of large lianas in Amazonian forests. *Nature*, *418*, 770-774.

Richardson, A. D. & Berlyn, G. P. (2002). Spectral reflectance and photosynthetic properties of Betula papyrifera (Betulaceae) leaves along an elevational gradient on Mt. Mansfield, Vermont, USA. *American Journal of Botany*, *89*, 88-94.

Richardson, A. D., Duigan, S. P. & Berlyn, G. P. (2002). An evaluation of noninvasive methods to estimate foliar chlorophyll content. *New Phytologist*, *153*, 185-194.

Sanchez-Azofeifa, G. A. & Castro-Esau, K. (in press). Canopy observations on the hyperspectral properties of a community of tropical dry forest lianas and their host trees. *International Journal of Remote Sensing*.

Schmidt, K. S. & Skidmore, A. K. (2001). Exploring spectral discrimination of grass species in African rangelands. *International Journal of Remote Sensing*, *22*, 3421-3434.

Sims, D. A. & Gamon, J. A. (2003). Estimation of vegetation water content and photosynthetic tissue area from spectral reflectance: a comparison of indices based on liquid water and chlorophyll absorption features. *Remote Sensing of Environment*, *84*, 526-537.

Skidmore, A. K., Forbes, G. W. & Carpenter, D. J. (1988). Non-parametric test of overlap in multipspectral classification. *International Journal of Remote Sensing*, *9*, 777-785.

Slaton, M. R., Hunt, E. R. & Smith, W. K. (2001). Estimating near-infrared leaf reflectance from leaf structural characteristics. *American Journal of Botany*, *88*, 278-284.

Zhang, J. L., Rivard, B., Sánchez-Azofeifa, G. A. & Castro-Esau, K. L. (submitted). Intra and inter-class spectral variability of tropical tree species at La Selva, Costa Rica: Implications for species identification using HYDICE imagery. *Remote Sensing of Environment*.

CHAPTER 2—Monitoring secondary tropical forests using space-borne data: implications for Central America[1]

INTRODUCTION

Two reasons for which successional tropical forests are considered at least of equal importance to mature tropical forests are their potential for providing food and fiber for humans, based on their positive net primary productivity, and their large expanse, due to shifting agriculture, logging, and abandonment of cattle pastures (Ewel, 1977). More recently, heightened attention on tropical secondary forests can be attributed to their capacity to act as carbon sinks and their potential role to serve as regulators of climate change. Brown and Lugo's (1990) often-quoted biomass accumulation estimate of 100 Mg/ha over the first 15 years indicates that tropical secondary forests have the facility to decrease atmospheric carbon concentrations, to some degree, in relatively short periods of time.

The most practical tools available for making these estimates are space-borne remote sensors. Since the 1970s, a series of multi-spectral scanners (Landsat MSS, TM and SPOT), and more currently, hyper-spectral scanners (Hyperion) as well as satellite-borne radars (RADARSAT 1 and 2) have been monitoring the earth. Through analysis of their data, valuable information may be extracted on the presence and regeneration progress of secondary forests. A good deal of headway has already been made, particularly using Landsat TM data over the Amazon (Steininger, 1996; Foody & Curran, 1994; Moran et al., 1994). However, limitations in the methods to date make it difficult to make estimations of secondary forest biomass precise enough for calculation of carbon content, which has been estimated as 45% of total dry matter (Guimarães, 1993, cited in Fearnside, 1996, based on secondary vegetation in the Brazilian Amazon).

This review article will focus on the relevance of space-borne data to characterize secondary forests, and how they can be applied to Central America, where such techniques have been generally underutilized. There are a number of factors that distinguish this region from the Amazon, where the majority of research in the neotropics has taken place to date. One of these is its varied topography, a special challenge for remote sensing research. Volcanic mountain ranges are a characteristic feature of the Central American landscape, and give rise to a variety of climates. Based on the Holdridge (1947) life zone system, which is the predominant vegetation classification system used in Central and South America and is based on seasonal precipitation and annual biotemperature (defined as 'the mean of unit-period temperatures with the substitution of zero for all unit-period values below 0°C and above 30°C'), there are 12 life zones represented in Costa Rica alone, from tropical wet forest in the lowlands through to tropical subalpine rain páramo (Holdridge et al., 1971). The main focus of both ecological (Ewel, 1980) and remote sensing study (Helmer et al., 2000) of tropical succession, however, has been the lowland humid tropics under conditions of gentle topography. Issues of land tenure also lead to differences in the typical size of clearings. In Central America these tend to be relatively small, producing more heterogeneous land cover than might be typically found in the Amazon. Furthermore, soils in Central

[1] A version of this chapter has been published. Castro, K. L., Sanchez-Azofeifa, G. A. & Rivard, B. (2003). *International Journal of Remote Sensing, 24*, 1853-1894. (http://www.tandf.co.uk)

America are young and mineral rich (eutrophic), in contrast to those of eastern and central Amazonia, which are old and mineral poor (oligotrophic) (Kricher, 1989; Jordan & Herrera, 1981). These contrasts are important because they influence the speed and nature of recovery of secondary forests, which in turn has implications for their interpretation from space-borne data.

In addition to the former biophysical variables, Central America is probably one of the richest biodiversity sites in the world. Costa Rica, because of its unique combination of microclimates, soils, topography, variety of biological processes and the bridge effect between North and South America, hosts an estimated 4% of all plant and 5% of all bird species in the world. The country contains around 12,000 plant species (including 1,500 orchid species alone), 850 bird species, 218 reptile species, 205 mammal species and 130 fresh water fish species. The latest Costa Rican national biodiversity study (INBio, 1999) concluded that there are more than 500,000 species of organisms in the country, of which 84% are unknown to science. In some specific cases, such as insects, fungi, bacteria and viruses, the percentage unknown to science is greater than 90%.

The environmental degradation of tropical environments is a major concern for developing countries in the Central American region. Deforestation and its impact on biodiversity loss, soil erosion, water pollution, and the degradation of scenic values influences the economic productivity and quality of life there, and is considered to represent one of the most pressing environmental issues in the region. Despite growing public concern and increasing political rhetoric, actions have been relatively ineffective in managing this problem. Tropical forests in the Central American region are being destroyed and degraded in critical ecosystems, and forest resources suitable for timber production are being lost at rates exceeding reforestation efforts.

The objective of this paper is to review the progress and future potential of neotropical research for estimating secondary forest biomass (total above-ground biomass, TAGB) from space-borne data for the purpose of monitoring carbon sequestration for the Central American Region. The paper begins with a discussion of tropical succession and factors that influence it, followed by a review of different approaches to estimate biomass from space-borne data. This is followed by how the progress of succession is interpretable through trends in reflectance characteristics and a comparison of the utility of various sensors, current and prospective, including multi-spectral scanners and synthetic aperture radars (SARs).

SECONDARY SUCCESSION IN THE TROPICS

There is a general pattern to tropical forest succession, and a myriad of variations. It initiates with some type of perturbation, which may be natural (fire, hurricane, tree fall), or human-induced (logging, slash-and-burn, clearing for pastureland). Succession is the progress of returning from that disturbance to a 'biologic steady state' that is characteristic of climax, undisturbed forest (Hartshorn, 1980). This progress includes increases in biomass over time to pre-disturbance levels.

In tropical moist and wet forests, a mono-layer of vegetation quickly forms in early succession. This vegetation consists mainly of herbs and grasses, and possibly sedges, small shrubs and/or coppice shoots from pre-existing plants (3-4 months). Taller shrubs, vines and lianas then appear, creating additional layers of leaves (7-10 months) (Ewel, 1977; Opler et al., 1977). After two years, pioneer trees begin to emerge from the

4 to 5 meter high canopy of shrubs, vines and lianas. These fast-growing trees increase in dominance, under which slower-growing, shade-tolerant climax tree seedlings establish and gradually take over. While these generalizations regarding pioneer and climax tree species are often typical, growth strategies of tropical trees may take one of several paths in response to light availability during succession, as shown in Figure 2-1. Thirty to fifty years after the onset of succession, the secondary forest is similar in structure to pre-disturbance forest (Ewel, 1980). Maturity is reached when several indicators predominate, including high species richness, a multi-layered canopy, presence of large, often-buttressed trees ('dominants'), and an impressive variety of epiphytes, vines and lianas (Hartshorn, 1980). Low light levels limit the understory by this stage (Kenoyer, 1929). Brown and Lugo (1990) describe biomass accumulation of secondary forest components through succession in tropical moist and wet life zones. Leaf biomass maximizes early (within approximately 15 years), then remains fairly constant. Woody biomass also increases rapidly during this period, after which it increases at a steady but slower pace. Root biomass increases more slowly with age. Tropical dry forests undergo similar processes, but have lower biomass accumulation rates and are more affected by fire than tropical moist and wet forests (Figure 2-2).

Within a single life zone, rate of recovery may be affected by a number of factors. Type of land use is one of these. Degraded cattle pastures accumulate biomass at lower rates than most other land use types, such as shifting cultivation (Hughes et al., 1999; Fearnside & Guimarães, 1996; Uhl et al., 1988). Duration of land use likewise imposes a strong negative effect on biomass accumulation rates (Hughes et al., 1999) and may also affect species composition. Foody et al. (1996, 1997) observed that Amazonian secondary forests that had been allowed to regenerate within a year after clearing were dominated by *Cecropia* whereas those that had been used for pasture for several years were dominated by non-*Cecropia* species, a fact which influenced their classification from remotely sensed data. Soils may also be a contributing factor. Guariguata et al. (1997) postulated that faster woody regeneration in Costa Rica compared to lowland Amazonia could be attributed to its richer volcanic soils, a factor that is hardly mentioned in many remote sensing papers dealing with secondary growth. Regeneration rates also decrease with increasing clearing size and distance to seed sources. Remnant trees, however, can provide a positive stimulus, providing not only seed sources, but habitat for seed dispersal vectors such as birds and microsites with cooler soil temperatures for seed germination as well as shade for shade-tolerant species (Finegan, 1996). Sprouting from pre-existing stumps and roots can also speed up succession by providing a source of climax species on the site.

Between life zones, variations in precipitation and temperature regimes lead to even greater differences in the recovery processes of secondary forests. This is of particular relevance to Central America, which hosts a collage of ecological life zones. Such differences are not surprising since secondary forests of different climates are headed towards different endpoints of mature forest biomass, canopy height and structure, and species richness and composition. Ewel (1980) found recovery of colder, drier sites much slower than warmer, wetter sites. His comparison of 13-month old regrowth biomass from five life zones gave the following results: tropical wet forest (1,159 gm^{-2}), tropical dry forest (951 gm^{-2}), subtropical wet forest (634 gm^{-2}), subtropical dry forest (459 gm^{-2}) and tropical montane rain forest (135 gm^{-2}). In another study,

Houghton et al. (1991) estimated carbon accumulation rates in tropical moist, seasonal and open forests as 500, 400, and 300 $gm^{-2}yr^{-1}$ respectively (carbon content of secondary forests, mentioned above, has been estimated as 45% of total dry matter in Guimarães, 1993). Structural differences were also apparent in a comparison of successional wet and dry tropical ecosystems by Ewel (1977), who found spotty cover development and discontinuous height growth in dry sites in contrast to rapid, uniform structural development on wet sites. Other structural variables that may vary between life zones include number of canopy layers, height and continuity of the upper canopy, and the presence and number of emergent trees. It is also well known that warmer, wetter sites are often more species rich than cooler and/or drier sites (Ewel, 1977, 1980).

Just how all the attributes of a secondary forest individually and collectively interact with incoming radiation and consequently reflect some portion back to space, a sample of which is caught by a passing sensor, is a highly complex issue. That is why it is important to note the changes that a secondary forest undergoes as it matures, and the possible variations in development patterns from one secondary forest to the next depending on their biophysical conditions. It is only by realizing these differences at the ground level that one can hope to interpret variations in satellite imagery for the identification of secondary forest characteristics.

ESTIMATION OF BIOMASS FROM REMOTELY SENSED DATA

The most direct means of estimating forest biomass is through evaluation of TAGB/spectral reflectance correlation, or in the case of radar, TAGB/backscattered microwave radiation. Biomass levels are validated at the plot level through destructive harvesting or, more commonly, through allometric equations in the literature provided through previous destructive harvesting activities (e.g. Nelson et al., 1999). Such equations cover a range of specificity: from individual tree species or genera through to broader height/wood density classes and even broader forest types (e.g. see equations applied in Foody et al., 2001; Steininger, 2000). This approach is the most common in SAR studies, since microwave radiation is considered sensitive to forest biomass. A variation of this approach would be the correlation of space-borne data with portions of TAGB: leafy biomass, branch biomass and stem/trunk biomass. This method, which has not been tested in tropical secondary forest research, has been suggested by Kasischke et al. (1997) as having good potential for overcoming current SAR saturation levels, and could be implemented by using several frequency/polarization combinations, taking advantage of varying penetration depths to describe the different segments of the forest structure and provide a more accurate picture of the whole.

A second method of measuring forest biomass is through its correlation with forest age. This has been the most common approach for analysis of satellite multi-spectral imagery such as Landsat Thematic Mapper (TM) data. Using this approach, an image is classified into a number of age groups, after which biomass may be calculated as a function of age, again based on known and independently-derived relationships between age and biomass. For example, Uhl et al. (1988) studied growth of secondary forests in Paragominas, Pará (in Brazilian Amazonia) and determined simple biomass-age relationships for secondary growth on abandoned pasturelands of various previous land use intensities (10 $tha^{-1}yr^{-1}$ for low intensity, 5 $tha^{-1}yr^{-1}$ for moderate intensity). Although these techniques seem to be adequate for the region from where they were developed,

caution must be exercised when using these types of relationships as they are inapplicable outside the environmental conditions (e.g. land use intensity, climate, soil type, etc.) under which they were developed. A second consideration is the degree of error introduced into the biomass estimation, first through age classification using imagery, and second through calculation of biomass as a function of age using previously derived relationships. In the example by Uhl et al. (1988), there were high coefficients of determination for linear regression of TAGB as a function of age for lightly R^2=0.97) and moderately (R^2=0.90) used sites, but not for heavily-used sites (R^2=0.50).

Although single-date images may be classified according to age, higher accuracy can be achieved from multitemporal imagery. Using several images, change detection permits the tracking of regeneration over time as well as land cover changes due to re-clearing, for instance. Furthermore, if the year of forest clearing can be documented, then one can be certain of regrowth age in subsequent images as long as the land has not been re-cleared. Unfortunately, in many cases the age of clearing is not documented and assumptions are necessary to estimate specific age conditions. As such, this approach, which is often the only one available, promotes the introduction of errors and uncertainties in the development of relationships between TAGB and spectral reflectance.

Using these approaches with careful field validation, it will be possible to determine the TAGB, and consequently, carbon content of a secondary forest at various points in time. Rates of biomass or carbon accumulation are also necessary for anticipating future carbon sequestration and/or to fill in gaps in the imagery when cloud-free data are unavailable. These may also be determined by field measurements of biomass at various stages (e.g. Uhl et al., 1988) or from the imagery in conjunction with ground data.

These two methods of biomass estimation: direct biomass-reflectance correlation and classification according to age will be considered in this review. Forest biomass can also be estimated with a number of stand variables (or combinations of them) other than age, such as diameter at breast height (dbh), tree height or forest volume. However, identification of these variables from tropical secondary forests using remotely sensed data is still largely unexplored and will not be the focus of this review.

ELECTRO-OPTICAL IMAGE DATA

Radiation reflected from secondary forests

A satellite-borne electro-optical sensor detects radiation reflected and emitted from the vegetative cover and any exposed soil, and is influenced by illumination and imaging geometry (e.g. topography). The reflectance patterns shown in Figure 2-3 for the Landsat TM bands 1-5 and 7, based on results from regenerating forest in the Amazon, are typical. Band 1 (blue: 0.45-0.52 μm), which is preferentially absorbed by chlorophyll a and b, but is hindered by the influence of atmospheric attenuation, and band 2 (green: 0.52-0.60 μm), which is reflected by healthy vegetation to result in green leaf color, are fairly flat, changing little after the quick formation of monolayered successional vegetation. Band 3 (red: 0.63-.69 μm) is also absorbed by chlorophyll a and b for photosynthesis; observed red reflection decreases slightly with the advancement of succession as increasing leaf area absorbs increasing amounts of radiation in this range, however, this effect maximizes early and overall, red reflectance is low throughout succession as well (Jensen, 2000; Steininger, 2000; Moran et al., 1994). The near-infrared

band, band 4 (0.76-0.90 μm), is more variable. Near-infrared reflectance (NIR) increases initially via leaf additive reflectance from the spongy mesophyll as additional leaf layers are added to a canopy (increased leaf biomass) (Jensen, 2000). However, these increases are not sustained; as the canopy matures, creating more layers and increasing in complexity, shadowing acts as a spectral trap for incoming energy and reduces the amount of radiation returning to the sensor (Steininger, 1996; Moran et al., 1994). Shadowing also depresses short wave infrared reflectance (SWIR) (bands 5: 1.55-1.75 μm and 7: 2.08-2.35 μm) as forests mature. SWIR is also influenced by water absorption; therefore, a combination of shadowing and increasing canopy moisture content lead to decreases in SWIR through secondary forest succession (Jensen, 2000; Steininger, 2000; Moran et al., 1994). The SWIR bands have carried the most information relevant to regeneration stage in a number of studies (Steininger, 2000; Boyd et al., 1996). The thermal infrared band, band 6 (10.40-12.5 μm), with lower spatial resolution (120 m vs. 30 m) and potential calibration problems, has been ignored in most studies, but was shown to have good discriminating power in a study by Boyd et al. (1996), more so than TM bands 3 and 4. Thermal infrared emittance (TIR) has been related to both forest age and green leaf biomass (Sader, 1986, 1987, cited in Boyd et al., 1996).

Despite strong correlations observed between measures of leaf biomass and the normalized difference vegetation index (NDVI) in temperate forests (Danson & Curran, 1993, cited in Foody & Curran, 1994; Curran et al., 1992; Peterson et al., 1987), this has not been the case in tropical forests (Sader et al., 1989), due to the lack of trends in red and near-infrared reflection mentioned above. Vegetation indices in general have not been studied exhaustively for tropical regeneration, however, relationships between tropical stand age and brightness, greenness, wetness and/or (TM2*TM6)/TM7 have been observed by a number of authors (Helmer et al., 2000; Boyd et al., 1996, Steininger, 1996). On the other hand, Foody et al. (2001) found only poor correlations (insignificant at 95 percent confidence level) between 230 permutations of six conventional vegetation indices (NDVI : (TM4-TM3)/(TM4+TM3), Simple ratio: (TM4/TM3), Ratio-based: TM4/(TM1 + TM2), Stress-related: (TM1*TM2)/TM3, Complex division: TM4/(TM1*TM2*TM3*TM5*TM7), and Normalized-based: (TM4-(TM1+TM2))/(TM4+ (TM1+TM2))) and forest biomass.

Landsat TM research on secondary forests

The majority of research to date on tropical regrowth detection from remote sensors has made use of Landsat TM data. This is due to long-term availability of Landsat imagery from the 1970s onward, and its suite of spectral bands selected for study of vegetative characteristics such as leaf reflectance, leaf pigmentation, leaf and canopy structure and moisture content (Jensen, 2000). The 30 m spatial resolution is suitable for many forest classification studies.

Using the biomass approach

Sader et al. (1989) concluded that, despite observed relationships in temperate forests, NDVI was not a good predictor of biomass in tropical successional forests. Reasons for this, cited in Boyd et al. (1996), stem from the rapid accumulation of high amounts of plant tissue, which quickly maximize absorption of red radiation and reflectance of infrared radiation and thereby overcome the range of NDVI sensitivity to biophysical properties (Tucker, 1977), and the attenuation of radiation by atmospheric

water and aerosols above the canopy (Ouaidrari et al., 1994). The study by Sader et al. (1989) was one of very few in which direct biomass/spectral reflectance (in the form of NDVI) correlation has been studied for tropical secondary forests. In hindsight, of the age classes involved (Table 2-1), only the first (3-16 years) has been distinguishable in later studies. Had the youngest age class been subdivided, at least a weak NDVI-biomass relationship could possibly have been detected.

A more recent study by Steininger (2000), however, showed a significant relationship between TM mid-infrared band 5 and secondary forest biomass ($r=0.71$, $p<0.05$, $n=18$) for a site in the Brazilian Amazon and using multidate imagery. However, this correlation was not consistent at a second site in Bolivia where no significant relationship was observed. Three hypotheses for this inconsistency were given: 1.) low sun angle in one of the images, 2.) lack of relationship between canopy reflectance and the variables of concern for the tropical deciduous forest in Bolivia, or 3.) differences in development and canopy structure of regrowth between the two areas. Regarding the third possibility, canopy structure and species composition indeed seem to have an important influence on canopy reflectance as may be seen in this study as well as a number of others discussed in this review article. Whereas regrowth in Brazil was dominated by non-*Cecropia* species, regrowth in Bolivia was dominated by *Cecropia* species (Foody et al., 1996 stratified by the dominance, or not, of *Cecropia* to improve classification accuracy). Also, the successional stage dominated by pioneer species (mainly *Cecropia*) in Bolivia lasts longer (~20 years) than the equivalent stage in Brazil. In Bolivia, only two out of 14 field sites were ≥ 20 years, so successional changes that may have taken place post-20 years are not well represented, although they may potentially have resulted in changes in reflectance patterns which could have affected their conclusions. In Brazil, in contrast, early regrowth stands were dominated by different genera than at later (10+ years) stages, which was likely observed as changes in the reflectance data which could then be correlated with biomass.

Foody et al. (2001) confirm results from both Sader et al. (1989) and Steininger (2000) in a forest biomass study from Borneo at a site that had been logged at variable intensities and at different times. Vegetation indices (230 tested, including NDVI) again displayed weak and insignificant correlation with forest biomass. A different approach, using neural networks as an alternative to regression for single-date Landsat TM data, provided much better results when tested with field data ($R^2=0.65$ for network with best performance, significant at 99% confidence level). Field plot biomass levels ranged between 65 and 647 tha^{-1}, above the sensitivity level of synthetic aperture radar in most studies (see below). Neural networks have the advantage over traditional vegetation indices or regression techniques in that they do not make assumptions about the dataset, they learn by example and they can weigh the importance of each input channel and accommodate their interdependency. These nonlinear networks are capable of identifying the most essential information for classification purposes while avoiding irrelevant input. Research using neural networks is becoming more common and is consistently improving image classification results (Kimes et al., 1999; Atkinson et al., 1997). Atkinson et al. (1997) note the requirement of continuous training data as one drawback to the implementation of the artificial neural network. Results from these studies agree with Steininger (2000) in that TM band 5 provided the most information, followed by bands 2 and 4; band 3 provided the least information.

Using the stand age approach

Although limited, considerable progress has also been made in classifying neotropical secondary forests according to age using Landsat TM data. Currently, most Landsat TM studies of secondary forest have separated few broad regrowth classes (often two or three, less than five) of fairly young age (usually up to 20 years old or less) and with varying degrees of accuracy (Table 2-1). To maintain a reasonable level of accuracy (usually >80%), efforts to differentiate a greater number of classes are typically reduced to the levels mentioned above, an issue that may also be affected by the lack of information regarding when the plot was abandoned. The majority of this work has involved multitemporal images of sites in the Brazilian Amazon; some, but not all specify the objective of determining age as a means for deriving biomass or carbon levels.

Accuracy assessment

Classification accuracy of secondary forest age groups has been increased using various strategies, which typically involve increasing complexity in either the classification itself or in the field data. The greater the number of images, and/or the greater the amount of ancillary data, the greater the classification accuracy is for regenerating tropical forest stages. The first of these may be almost impossible to obtain in the Central American region due to the high frequency of cloud cover. While multitemporal imagery obviously provides much more information about land use and secondary forest history, thereby improving classification accuracy, it is very difficult to obtain multiple cloud-free images. Kimes et al. (1998) evaluated errors introduced into secondary forest age measurements due to gaps in multi-year imagery. In their study from Rondonia, in the Brazilian Amazon, it was determined that gap errors could cause TAGB overestimations of 8-23%. Errors were 'a function of the number of gaps, the placement of the gaps within the time-series of images, the length of each gap, the relative proportion of pixels in each possible trajectory of land use, and the estimated transitional probabilities between land use classes in a particular study site.'

Using single-date imagery, however, Brondizio *et al.* (1996) were successful in identifying three stages of secondary succession in the Brazilian Amazon with accuracies of 90-99 percent. However, in this case authors stressed the importance of detailed field measurements (species composition, density, frequency, dominance and basal area, % soil cover, height to first branch, total height) and historical data (interviews on land management) to achieve this level of accuracy. A texture-based classifier was also important in this study. Unfortunately, gathering ancillary data to this extent is not practical at many tropical sites due to poor accessibility, poor historical records of land use, and/or time and funding constraints. Sohn et al. (1999) achieved similar high accuracy levels for three successional stages in two Landsat TM images that were analyzed independently. In this case, the cosine of the angle concept was adopted in favor of more traditional minimum distance or maximum likelihood classifiers, and resulted in higher accuracies when compared with the latter. Using this method, spectral angles were calculated between defined spectral clusters and known reference signatures. Each spectral cluster was then assigned to one of the reference classes based on the minimum spectral angle rule.

Other improvements to classification accuracy have involved stratification of secondary forests by species composition and/or land use history (discussed below, Table 2-2), but again require additional field knowledge. MIR (TM bands 5 and 7), rather than

red or NIR, has consistently provided a sound basis for separation of tropical secondary forest age classes (e.g. Boyd et al., 1996), as was the case for estimating biomass.

Drawbacks of classifying by age

There are some inherent problems with biomass calculations from forest age, however. For one, further fieldwork is required to establish the relationship between biomass and age. In some areas, this information is available from the literature, in others, not. For another, even when that relationship has been established, it is often specific to certain conditions (*e.g.* related to land use history), making it difficult for regional extrapolation. For example, the biomass-age equations established by Uhl et al. (1988), mentioned above, were specific to abandoned pastures of various previous use intensities in a region of the Amazon. There are numerous additional site quality characteristics that will influence the rate of succession if not held constant. This results in very limited applicability of results from these types of studies.

The lack of adequate information on the real age of succession is probably one of the main reasons why specific relationships between biomass/age and spectral reflectance are weak. This is a problem difficult to resolve not only in the Central American region but also in the neotropics in general, where little or no information exists regarding land cover change practices and their effect on canopy succession. Although surveys with local farmers can help to shed some light on the age issue (Brondizio et al., 1996), this may be difficult to accomplish for large areas in the Central American region where migration in-country and between countries can affect the pool of local knowledge. The reality is that assumptions based on density of pioneer species, their presence or absence and their relationship to age as done by Lucas et al. (2000a) may be difficult to achieve in most of the neotropics. For example, Kellman (1970) showed that variability in the number of species and biomass ($kgha^{-1} \times 10^{-3}$) between selected plots of the same age in a study in Mindanao, Phillipines, suggested that age was not a good indicator of stand characteristics. Moreover, even within regions, canopy structure, light transmittance and development of secondary forest stands can vary with respect to age (Montgomery & Chazdon, 2001). These variations will depend on site characteristics (i.e. soils and topography), and more importantly, land use history and seed availability to promote succession (Denslow 1996; Corlett, 1994).

Stratification by successional pathway or other ancillary data

Studies by Boyd *et al.* (1996) and Foody et al. (1996) took these variations into consideration and broke down successional classes by age as well as by successional pathway. Higher classification accuracy was achieved by dividing regenerating forest classes into two successional pathways (accuracy increased from 79% to 87% in the study by Foody et al. 1996). The first pathway, on sites abandoned within a year of clearing, was dominated by *Cecropiaceae* species and the second, on fire-cleared land used several years for pasture, was dominated by *Clusiaceae, Flacourtiaceae*, and *Melastomataceae* species. This distinction was important not only for classification accuracy but in terms of their carbon sink strength, which could differ by a factor of two (Uhl et al., 1988, cited in Foody et al., 1996). Foody et al. (1996) noted higher variability between young classes, with increasing similarity in older classes as each pathway developed towards maturity, which was confirmed before by Kellman (1970). This was likely due to initial differences in seed bank status and soil health, which would have

been affected by differences in land use intensity; tree density varied widely in these plots.

Use of successional pathway is not the only method that has been used to subdivide secondary forest classes in studies using Landsat spectral data (Table 2-2). Tucker et al. (1998) proposed a standardized structural classification of regrowth stages that would be independent of age. The key takes soil fertility and local land use differences into account. Structural features used to identify successional stages included height, basal area and dbh indices. Sohn et al. (1999) defined three regrowth stages based on a combination age of fallow and canopy height with good results using the cosine of the angle concept, as mentioned above. Nelson et al. (2000) attempted to classify 16 successional stages based on 1-yr age classes (up to 7 yr) and 'degree', the number of times the land had been cleared. Although these examples exhibit the inadequacy of defining successional stage solely by age since abandonment, attempts to include succession-influencing variables have thus far been limited and inconsistent.

The issue of topography

Besides the complication of successional variability, uneven topography further complicates regrowth classification from data from Landsat sensors or any other remote sensing system. Topography can cause misclassification of pixels due to brightness variation between horizontal and sloped surfaces of the same land cover class (Fahsi et al. 2000). Helmer et al. (2000), lacking a digital elevation model (DEM) of suitable scale, stratified land cover classes from Landsat TM imagery by topographic illumination, into either shadowed or sunlit categories, based on visual interpretation. Her research for Costa Rica, as well as research from Thenkabail (1999) for southern Cameroon, is dissimilar to that for the Amazon in that it incorporates topographical effects into a land cover classification system that also includes several regrowth stages, an issue that must be considered necessary for any work in the Central American region. Stratification by illumination proved effective for the classification by Helmer et al. (2000); however, the final classes derived are not very useful for biomass estimations (for instance, tree/shrub crops could not be reliably distinguished from secondary forest < 6 years, also, there is only one secondary forest age category in the shadowed slope category) (Table 2-1). The same was true for results by Thenkabail (1999) in which lowland and upland areas were segregated and analyzed separately.

Implications for Central America

The study by Helmer et al. (2000) exposes some of the challenges for remote sensing of tropical secondary forests in Central America. Although their method of topographic illumination alleviated some confusion, results were limited. There is currently no study known to the authors that incorporates a DEM of suitable spatial scale into a tropical secondary forest age classification or biomass estimation from Landsat imagery. Fine-detailed investigation of secondary forests in Central America will require this at least; further refinement of topographic normalization techniques will be essential to map them with any reasonable degree of accuracy.

There was also difficulty encountered in distinguishing tree/shrub crops from young secondary shrub/forest in the study by Helmer et al. (2000). The issue of spectral similarity between tree/shrub crops or plantations and secondary forest has not been dealt with (or is perhaps irrelevant) in the prevalent studies coming from the Amazon. In Central America, however, this distinction will be crucial as small-scale agroforestry

systems such as coffee interspersed with shade trees dot the landscape. Although much research is required, it is possible that accurate classification of secondary forests in such areas will necessitate the use of imagery at either finer spatial scale (e.g. IKONOS data), from which tree or crop species can be identified visually, or higher spectral resolution (e.g. AVIRIS (airborne) data), from which unique spectral signatures for certain common crops might be determined for their distinction from secondary forests. The integration of Landsat TM data with selected Hyperion Satellite scenes, the latter providing ancillary information on the nature of the mixing present in the Landsat TM pixel, can also be useful for the separation of secondary forests from land cover types that have thus far appeared spectrally similar.

Helmer et al. (2000) noted an interesting distinction between research from the Amazon and research from montane regions in Costa Rica. Secondary forest ≥ 17 years remained distinct (brighter, greener, less wet) from old growth forest. By this time in the Brazilian Amazon, secondary forest and old growth would have been indistinguishable. Thus, despite the added challenges that altitudinal gradients and tree/shrub crops impose, there is potential for mapping later successional stages in montane life zones, where forests are cooler and growth is slower than at lower elevations. The distinction could also be related to the dominance of *Quercus* in old growth, which was still lacking in secondary forests of this age.

National Oceanic and Atmospheric Administration (NOAA) Advanced Very High Resolution Radiometer (AVHRR) research on secondary forests

Electro-optical imaging systems other than those aboard Landsat satellites have had only very limited application for the characterization of tropical secondary forests. Despite the usefulness of AVHRR data for large scale land cover monitoring, particularly using the NDVI, studies focusing on forest regeneration are few due to the limitations imposed by coarse spatial resolution (1.1 km) and limited spectral bands. NOAA AVHRR may be useful for identifying a single secondary forest class over large, homogeneous study areas such as can be found in the Amazon, however, further dissection of this class is unlikely without aggressive pixel unmixing techniques (see research by Atkinson et al., 1997 involving neural networks), and even then it would be difficult to attain reasonable accuracy levels.

Lucas et al. (2000a) made the first attempt at mapping tropical forest regeneration stages using AVHRR data in the Brazilian Amazon. Four stages of succession were considered: Stage I: <5 years, Stage II: 5-9 years, Stage III: 9-20 years, and Stage IV: 20+ years. Age was used to establish the classes in this case because data collection of properties to generate relationships within regenerating forests was considered impractical. The outcome of the analysis was a user accuracy of only 24 to 49% for mapping a single regenerating forest class at different sites and an overall accuracy of 39.6% for classification of the different stages of regrowth, meaning that any estimation of secondary growth will have, on average, 70% error. The breakdown is as follows (User's/Producer's accuracy): Stage 1: 48.6%/79.0%, Stage II: 22.4%/6.5%, Stage III/IV: 33.0/38.1%. By combining Stages II, III and IV, accuracy was increased to 87.7%/63.9%. Thus, in a best-case scenario, general division of secondary forests into those less than and greater than five years is possible to a limited degree. From these results, however, it is clear that this level of categorization and accuracy could not be considered acceptable

for further estimation of biomass and carbon accumulation rates. This process of age clustering in order to increase accuracy combined with current uncertainties related to estimations of carbon pools in the neotropics may pose important questions regarding regional estimates of carbon sequestration in the Amazon. This research group conducted a similar study using AVHRR data in Cameroon (Lucas et al., 2000b). Ground data were used for validation rather than Landsat imagery as in the previous study. The potential of AVHRR imagery to delineate forest regeneration stages was again considered limited. Use of finer spatial resolution satellite imagery was recommended in both cases.

The difficulties in mapping regenerating forest with NOAA AVHRR data would only be compounded in Central America. In Central America, pixels with mixed classes would be the norm instead of the exception, and an entire area of interest with secondary forests of varying ages might occupy only a few pixels. This was made obvious in a recent land cover characterization of Central America by Muchoney et al. (2000), in which tropical broadleaf evergreen forest in Costa Rica is grossly overestimated using monthly composited AVHRR NDVI data (secondary forest was not even mapped) when compared with a product from higher resolution Landsat TM data (Castro-Salazar & Arias-Murillo, 1998).

Research on secondary forests with SPOT

SPOT HRV imagery has a higher spatial resolution (20 m multispectral, 10 m PAN) than Landsat TM imagery despite lower spectral content, which is approximately equivalent to Landsat TM channels two through four. The newer SPOT 4 High Resolution Visible Infrared (HRVIR) instrument has a spectral content similar to Landsat TM/ETM+ channels two through five and therefore contains data from the critical SWIR region. The daily coverage SPOT 4 VEGETATION, launched in 1998, has a spatial resolution of 1.15 km X 1.15 km (a similar spatial resolution to AVHRR imagery).

Work by Thenkabail (1999) and Kimes *et al.* (1999) represent two very different approaches to secondary forest classification using SPOT HRV data. The importance of texture indicators (which has not been largely exploited using Landsat TM data for secondary forests) and the achievement of high classification accuracy, however, are common to both. Thenkabail (1999) developed a user-specific classification with relevance to slash-and-burn agriculture in southern Cameroon. The intensive methodology involved stratifying the image into discrete subsets, separate unsupervised classifications on each subset, identification of subset classes using detailed field knowledge and ground-truthing, and final mosaicking of subsets. As part of the stratification, upland and lowland areas were isolated and analyzed separately to avoid problems of spectral mixing between upland and lowland classes (compare with Helmer et al. 2000, who stratified by illumination in mountainous areas). Of a total of 19 classes, three secondary forest classes were identified: 1. Young and mature secondary forest (dense, lesser NDVI, fewer, but more vigorous shrubs and fewer trees than class 2), 2. Young and mature secondary forest (dense, greater NDVI), 3. Mature secondary forest: swampy, humid (very dense, least NDVI). The objective in this case was not biomass nor age estimation, and as such, these classes do not appear very descriptive in that respect; however, the methodology merits review as the classes were mapped with reasonable accuracy: 1: 82% (User's accuracy)/75% (Producer's accuracy), 2: 77%/71%, 3: 84%/76% (overall accuracy 82.4%). As part of the methodology, for classes that

exhibited significant mixing between each other but not with other classes (such as was the case for secondary forest classes 2 and 3), the areas were masked and reclassified to improve accuracy.

Whereas the study by Thenkabail (1999) relied on heavy user input to improve accuracy, Kimes et al. (1999) relied on the adaptability of neural networks to establish a solid classification of secondary forest age classes in the Brazilian Amazon. Using single-date SPOT HRV imagery, accurate prediction of secondary forest age as a continuous variable was not possible; however, using multitemporal imagery and texture data, results were significantly improved (R2=0.75; RSME (years)=1.3). Individual class accuracies were as follows: 1-2 years: 98.3%, 3 years: 93.1%, 4-5 years: 96.9%, 6 years: 96.0%, 7-8 years: 95.1%, and >9years: 86.5%. This new approach was found superior to linear analysis techniques for determining secondary forest age as a continuous variable. The results of this work look very promising for prediction of secondary forest age using neural networks in conjunction with spectral data, with the requirement of multidate imagery still a limitation.

Similar to conclusions from several studies using Landsat TM data, a suitable classification system was important in both studies to accurately characterize the landscape. In the study by Kimes et al. (1999), secondary forests that were cleared once, used for agricultural purposes, then abandoned, were segregated from secondary forests with more complex clearing histories, identifying the fact that rate of regeneration is influenced by land use intensity and frequency of clearing activities, which affect soil fertility and carbon fixation. Thenkabail (1999) used a classification with relevance to slash-and-burn agriculture. Although not specifically referring to secondary forests, this author felt that user-specific land cover classifications should be developed since biodiversity, water and nutrient cycles, and management techniques vary greatly among vegetation types. With respect to tropical secondary forests, however, the authors of this review article feel that a hierarchical tropical secondary forest key could be developed that would be useful for biomass estimation over a wide variety of ecosystems. Such a key could first identify the potential vegetation type on a site (by life zone, for instance), and then follow through on a number of site quality characteristics (such as land use intensity and duration, soil type, distance to seed source, size of clearing) that affect the rate of succession. Stratification of sites based on such a key would undoubtedly improve classifications/biomass correlations by comparing only secondary forests of different successional stages within a certain life zone and within a narrow set of site quality characteristics.

In Central America, the studies of Kimes (1999) and Thekabail (1999) suggest that imagery from the SPOT sensors could be very useful in mapping regenerating forest stages. Although the newer SPOT 4 HRVIR lacks the equivalent of TM bands 6 and 7, it does provide an equivalent to TM band 5 (SWIR), which is also highly useful in regeneration studies and was lacking in the earlier SPOT sensors. Three drawbacks to SPOT 4 HRVIR imagery are higher cost, lower coverage, and lack of historical data (from the mid-infrared region) when compared to Landsat TM data; however, it might be very useful in conjunction with Landsat TM data, for instance, by providing extra opportunity for cloud-free data. The SPOT 4 VEGETATION instrument, which was designed specifically for vegetation study, will certainly surpass NOAA AVHRR (which was not designed specifically for vegetation study) capabilities of tracking global

vegetation changes; however, at a similar resolution (1 km), it is unlikely to have much application to secondary forest characterization in Central America.

Limitations/Future potential of electro-optical image data for secondary forest research

The main criticisms of research in this field to date are 1.) broadness of age classes defined, 2.) inability to distinguish secondary forests > 15 years from mature forests, 3.) overall inability to tie in the research using age classes with accurate secondary forest biomass estimates, 4.) difficulty distinguishing secondary forests from plantations (which is largely undealt with), 5.) lack of relevant research on topographic correction techniques, 6.) lack of broad-scale applicability of studies, 7.) lack of consideration of the ecology of the site (in many, not all studies), 8.) poor field validation accompanied by lack of standardization of field validation techniques, and 9.) difficulty in obtaining cloud-free images in the neotropics with enough frequency to define accurate trends.

The capability of delineating forest age or biomass from Landsat or SPOT multi-spectral imagery has so far been limited. Although methods are dominated by variations of traditional unsupervised and supervised classification techniques, application of new and innovative methodologies continues to provide new insight on existing data. Sohn et al. (1999), for example, achieved greater accuracy with their classification using the cosine of the angle concept as compared with a maximum likelihood classification. Using the maximum likelihood classification, abandoned/stubble and initial secondary succession were confused, and initial and intermediate secondary successions were confused (results not quantified), although they were distinct using the previous method. The authors state that according to their analysis, 'TM data carry more information than most of the studies suggest'. Although this method has potential merits of accounting for topographic effects in classification strategies, in this case, the study took place over flat limestone lowland where topography was not an issue. Neural networks have also improved classifications of secondary tropical forests, as have the addition of texture indicators in studies of SPOT HRV data, which have not been exploited using Landsat TM data. TM band 6, in the thermal infrared region, should be reexamined for its usefulness in these studies, as it may provide unique information to the analyses, although its coarser resolution (120 m) remains a drawback.

Comparisons of the accuracy and usefulness of secondary forest classifications in the literature are confounded by inequalities in methodologies employed, the number of classes identified and the extent of ground-truthing performed (Thenkabail, 1999). Classification accuracies decrease as the number and specificity of classes increase. At the ground level, field ground-truthing methodology has not been standardized; indeed, details on how field validation methods are developed are normally very sketchy at best and number of plots are few considering the number of classes identified (Table 2-3). Considering the variability of secondary forests within an age group (due to site characteristics), too few plots will not give an accurate representation of that class. There is a need for a simple, repeatable, statistically sound method of collecting tropical field data from regenerating secondary forests. A well-developed sampling scheme could allow scientists to systematize the number of plots required for biomass estimation (or other biophysical variables of importance for secondary forest characterization) or for

each class considered in a study. Plot size is crucial in experimental design as well; this should increase with regeneration stage as mean dbh increases to prevent the occurrence of plots occupied by only one to few large trees, in contrast to early stages in which plots contain many trees of very small dbh (such as in Luckman et al., 1997a).

Consensus is also needed on what field variables can be considered essential for field validation and how they should be gathered. Although species composition has been avoided in many studies, it has proven key to improving successional classifications by Foody et al. (1996). For another example, dbh data from studies listed in Table 2-3 have been collected on trees with dbh >3, >5, or >10 cm. Which dbh criterion is used will have a significant impact if used for biomass estimation as well as for comparing between studies, especially for young successional areas where trees are small. The estimation of biomass from previously-derived allometric equations also introduces uncertainties. Foody et al. (2001) estimated biomass from a single standard allometric equation for moist zone forests, using dbh whereas Steininger (2000) used multiple allometric equations which incorporated dbh, height, and tree density for the following tree classes: light short/tall, dense short/tall and palm trees. Greater attention to the ecology of the site in general is necessary, and should be reflected in the field data collected. The phenomena that occur in secondary forests (including changes in species composition and structure) that lead to changes in the reflectance of solar radiation are not understood in detail.

Other issues that have negatively influenced the success of secondary forest classification from multi-spectral imagery relate to the data themselves and include radiometric normalization and inadequate resolution at the spectral, spatial or temporal scale. Errors in atmospheric correction of up to 2% reflectance in a multitemporal study by Steininger (1996) were critical since the range of reflectances in the infrared bands (4, 5 and 7) varied only 3-11%. These types of errors should be improved with sensors on the Earth Observing System (EOS-1), which will allow the precise modeling of effects of atmospheric properties and improve aerosol optical models, providing corrections for MODIS, ASTER and Landsat-7 imagery (Steininger, 2000). With respect to spectral resolution, broad spectral bandwidths from traditional scanners may hide unique spectral patterns that occur within them and prevent the use of sensitive spectral tools such as derivative analysis. Regarding spatial scale, classes within the secondary forest class can only be defined at a resolution of Landsat TM (30 m) or higher. Temporal frequency is also critical; the higher it is, the better the chance of cloud-free data and the greater the sensitivity to phenological variations. Choice of dataset will mean some degree of compromise between spectral, spatial and/or temporal resolution that must be evaluated based on the goals of the project and the required accuracy level.

With current abilities to map successional age classes, only general biomass accumulation rates may be applied. Based on several sources from the literature, Nelson et al. (2000) suggested 10 $tha^{-1}yr^{-1}$ for secondary forest 1-10 years old and 4 $tha^{-1}yr^{-1}$ for secondary forest 11-15 years old. These age ranges (potentially with one further subdivision of 1-10 years) are roughly where capabilities lie for what may be distinguished from Landsat TM data consistently, based on Table 2-1. Regardless, these biomass accumulation rates should represent a starting point from which to improve over time; they are very broad and are derived from research from the Amazon basin.

The study by Foody et al. (2001) is an important exception to these limitations. Biomass estimates from plots ranging 65-647 tha^{-1} were significantly correlated with single-date Landsat TM data using a neural network. This biomass range surpasses what would be considered the saturation level based on age from related studies, although it is not clear how well the 52 plots represented this range of biomass. This study also differs from others in that forests had been logged at varying intensities, and do not represent typical successional forests that follow clearing and crop or pasture use as in the typical research from Amazonian sites. Selectively logged sites, in which mature trees are left standing, would differ in their reflectance properties from sites that were fully cleared and used for other purposes. Steininger (2000), however, also found good correlation between biomass and TM multidate reflectance for secondary forests in the Amazon, where plots ranged from 20-200 tha^{-1}. That the same was not the case for a site in Bolivia requires explanation. However, considering both studies, it would be worthwhile to study neural network analysis of single-date imagery over typical successional sites of a wide biomass range and incorporate field data on site quality characteristics that would allow stratification by those characteristics if necessary.

Overall, although improvements in delineating regeneration stage are likely using Landsat and/or SPOT sensors, greater improvements in terms of narrowing the age classes, widening the total age range identified, or in terms of biomass estimation, surpassing current saturation levels, will be more likely from newer data sources, although cloud cover will still be a hindrance. For example, ASTER (Advanced Spaceborne Thermal Emission and Reflection Radiometer), launched in 1999 onboard the Terra satellite, samples data from 14 spectral bands (twice as many as Landsat TM), including 3 visible and near-infrared (VNIR) bands sampled at 15 m spatial resolution, 6 SWIR bands at 30 m, and 5 thermal bands at 90 m. Hyper-spectral sensors sample much narrower band widths than multi-spectral sensors and should help discern unique spectral patterns of different vegetation types (such as growth stages of secondary forests) and be useful in extracting biophysical information such as biomass (Jensen, 2000). AVIRIS (Airborne visible/infrared imaging spectrometer) 20 m X 20 m data is collected over 224 spectral channels from 400 to 2500 nm, each 10 nm wide (Jensen, 2000, AVIRIS home page). This type of datum will be extremely useful for vegetation studies and should be an indication of what lies ahead for satellite-borne hyper-spectral sensors. As such, in December 1999, the National Aeronautics and Space Administration (NASA) launched its first hyperspectral imager, the EO-1 Hyperion, with 220 spectral bands, also ranging from 400 to 2500 nm, and with 30 m resolution. For a satellite-borne instrument, this sensor has unprecedented spectral resolution and its data will provide unique opportunities for detailed vegetation study. The satellite-borne MODIS instrument samples 36 spectral channels; however, spatial resolution of bands useful for vegetation study is rather coarse at 250-500 m. The same is true for the upcoming Medium resolution imaging spectrometer (MERIS), which is scheduled for 2002 launch aboard Envisat-1, which is programmable for up to 15 bands (0.39-1.04 μm) and will have spatial resolution of 300-1200 m (NASA website). While coarse resolution sensors will be valuable for global and regional evaluations of land cover change, it is unlikely that any spatial resolution less than that represented by Landsat TM (28.5 m) will be useful for tracking secondary forests for the purposes of biomass and carbon estimation, as this task is already difficult from Landsat TM data. This is especially true for Central

America, where there are many areas dotted with a variety of small-sized (<1 km^2) land usages. In terms of higher spatial resolution, the recent IKONOS sensor provides resolutions of 4m for VNIR bands, as well as an unprecedented 1 m panchromatic band. One drawback of data from these newer sources (besides its high cost per km^2) is its copiousness; however, detailed examination of data over a small study area will be ideal for modeling and extrapolation or for labeling classes and minimizing field data requirements. The utility of these new sources of data has not been explored to date nor has their combined use with traditional data, but it is clear that they will help overcome earlier limitations in characterizing tropical secondary forests.

SYNTHETIC APERTURE RADAR SYSTEMS (SARs)

Microwave backscatter from secondary forests

Radar is an alternative source of data for secondary forest characterization. In the case of airborne or satellite-borne synthetic aperture radar (SAR), the sensor receives backscattered microwaves, the product of an emitted pulse interacting with a target. This is in contrast to the reflected solar radiation recorded by passive electro-optical sensors (Jensen, 2000). Dielectric constant, surface roughness, size, shape, and orientation of forest components and topography all influence radar backscatter. Reflection of microwaves back to a radar sensor requires a discontinuity in the dielectric constants between the air (often low) and the target(s) (variable). Governed highly by moisture content, leaves tend to have high dielectric constants whereas bark has a low dielectric constant (with the exception of the phloem and vascular cambium). Rain or dew on a surface, however, can increase its dielectric constant. Gradual changes in dielectric constant between leaves, twigs, branches and trunks in the canopy also induced scattering, known as 'volume scattering', which implies a combination of surface reflection as well as reflection from elements below the canopy surface (Leckie & Ranson, 1998; Lewis et al., 1998). Surface roughness and orientation are also important; in general, rougher surfaces reflect more energy in all directions, including back toward the radar sensor. 'Microscale' roughness, which is recorded in the tone of an image, is wavelength-dependent. The longer the wavelength, the larger the target (leaves, branches, trunks, etc.) needs to be to contribute to surface roughness (Lewis et al., 1998). 'Mesoscale' roughness is measured in the texture of an image, and has been likened by Lewis et al. (1998) as the irregular surface that would result if a large cloth were draped over a forest, reducing the microscale roughness. This type of roughness is related primarily to topography but also to canopy structure and characteristics such as height and plant spacing (Lewis et al., 1998).

Depending on the sensor configuration, a single channel (wavelength/frequency) or multiple channels may be recorded. SAR sensors will also record in either single or multiple polarizations. Both wavelength (or frequency) and polarization have important implications for the information provided by the radar data gathered. Angle of incidence is an additional variable that has an important influence on backscatter interaction with forests. Forest canopies, for instance, exhibit lower backscatter at larger incident angles, which necessitates the use of correction techniques or limiting the angle range in a study (Leckie & Ranson, 1998).

Backscatter interactions with forests may be broken down into the following categories: crown scattering, direct backscatter from the trunks, direct backscatter from

the ground, crown-ground backscatter and trunk-ground backscatter (Leckie & Ranson, 1998). The longer the wavelength, the further is its penetration into the forest and the greater the importance of scattering beyond the upper canopy (Table 2-4). A general trend of increasing backscatter with increasing biomass has been observed for all wavelengths, although to varying degrees (Leckie & Ranson, 1998). With regard to polarization, like-polarized radar (e.g. HH or VV) return is stronger when the target feature is parallel to the plane of the transmitted microwave (e.g. VV return will be stronger than HH return when target has a strong vertical component) (Lewis et al., 1998). Like-polarized imagery tends to show information on wavelength-dependent surface roughness. Depolarization of the radar return (HV, VH) results from multiple scattering from rough surfaces such as the forest canopy (Leckie & Ranson, 1998).

SAR research on temperate forest biomass estimation

Use of SAR data for biomass estimation has met greater success in temperate regions than in the tropics, yet the study of radar applications to tropical forest regeneration is very much in its infancy. Forests in temperate regions generally have fewer species and lower biomass than tropical forests. They also differ in crown geometry, crown density, canopy structure, climate, moisture, as well as forest management practices (Leckie & Ranson, 1998; Thompson & Dams, 1990). There are many ways in which these differences influence backscatter. For instance, the significant contribution from understory, vines and lianas in vigorous tropical secondary growth to the reflection and attenuation of radar waves has no parallel in temperate forests. There are also phenological differences between temperate and tropical forests; deciduousness due to temperature in temperate broad-leaf and mixed-wood forests can be an aid to forest characterization from multitemporal data; in tropical regions deciduousness exists in some forests due to seasonal rainfall patterns, other forests are both broadleaf and evergreen. Wet season radar data from the tropics will be affected by the large amounts of moisture in the canopy and on the ground (Saatchi et al., 1997), often much more so than in temperate forests. Because of these differences, results from studies in temperate forests are not entirely applicable in tropical forests; however, many principles are common to both.

Although this Review focuses on tropical forests, a brief review of advances in forest biomass estimation from temperate SAR research is warranted, as it has provided a foundation for research in the tropics. From temperate forest studies it is clear that L-band and, to a greater extent, P-band radar data are the most useful for forest biomass estimation, due to their greater penetration of the forest canopy as compared to shorter wavelengths (X- and C-band) which saturate at low biomass values (Ranson & Sun, 1994; Rauste et al., 1994; Dobson et al., 1992a; Le Toan et al., 1992). For example, comparing C-, L-, and P-band data at different polarizations, Dobson et al. (1992a) used regression techniques to relate backscatter to the logarithm of TAGB. Maritime pine plantations near Landes, France and natural loblolly pine forests near Duke, North Carolina were studied, and represented a range of biomass of 5 to 560 tha^{-1}. The R^2 values for the various band-polarization combinations were as follows: C-HH (0.55), C-VV (0.51), C-HV (0.75), L-HH (0.89), L-VV (0.92), L-HV (0.96), P-HH (0.93), P-VV (0.90), P-HV (0.98). Single species plantations such as pine have been well studied using L-band SAR data; R^2 values have typically been 0.6 to 0.8 for airborne L-band SAR

experiments and somewhat less for satellite L-band SAR experiments (Leckie & Ranson, 1998).

The backscatter ratios P-HV/C-HV and L-HV/C-HV are also correlated to forest biomass (Ranson et al., 1995; Ranson & Sun, 1994). Enhanced correlation using these ratios was based on a difference in cross-polarized backscatter between shorter and longer wavelengths depending on the vegetation density of regenerating and mature forests. At lower vegetation densities, short wavelength cross-polarized backscatter was greater than long wavelength cross-polarized backscatter, which mostly penetrates the vegetation. At higher vegetation densities, however, long wavelength cross-polarized backscatter increased and short wavelength cross-polarized backscatter tended to saturate (Ranson & Sun, 1994).

Besides the greater sensitivity of longer radar wavelengths to a wider range of forest biomass, the examples above also indicate that cross-polarized backscatter (HV, VH) often exhibits greater sensitivity to forest biomass than like-polarized backscatter (HH, VV). Vegetated surfaces tend to depolarize the radar signal via volume scattering from within the canopy, hence the increased cross-polarized backscatter. Although cross-polarized backscatter is more suitable to forest biomass estimation, the use of multi-polarization datasets with both like and cross-polarized channels can provide more information than either alone, and may improve biomass algorithms (Kasischke et al., 1997).

Overall, research in biomass estimation of temperate forests has been quite successful and current capability rests at biomass estimations of forests up to approximately 100 tha^{-1} at L-band and 200 tha^{-1} at P-band (Dobson et al., 1992b) under optimal conditions of single species plantations or forests. Increased sensitivity has been achieved using ratios (Ranson & Sun, 1994) or using correlation between multifrequency, multipolarization backscatter and principle components of TAGB, such as total branch biomass, in conjunction with correlation between the biomass components themselves (Kasischke et al., 1995).

Tropical SAR research on forest biomass estimation

As indicated, the history of radar use for forestry applications in the tropics is quite brief. A number of authors have reviewed SAR potential for use in tropical forests, including its potential for estimating regenerating forest biomass. These include Leckie & Ranson (1998), van der Sanden (1997), Kasischke et al. (1997), Thompson & Dams (1993), Sader et al. (1990), and Thompson & Dams (1990). Prior to 1990, this type of research was restricted to airborne radar flown over tropical forests. Over the last 10 years, however, several satellite-borne SARs have been launched, in some cases providing repetitive coverage over areas of interest and allowing a wider range of applications. These have typically been single-channel single-polarization systems. A summary of recent radar systems and their application to secondary forest biomass estimation is presented in Table 2-5.

SAR C-band sensors

SAR C-band research in the neotropics has come from the following sources: the airborne Canadian Centre for Remote Sensing (CCRS) Convair 580 SAR (X-, C-bands), the airborne NASA/JPL AIRSAR (C-, L-, P-bands), and spaceborne ERS-1/2 (C-VV) and RADARSAT (C-HH). Although airborne sensors are not the focus of this review

article, there have been a number of important studies involving airborne SARs for determining tropical secondary forest biomass that are relevant to this discussion and to the future of biomass estimation from satellite-borne SARs.

C-band imagery, regardless of polarization, saturates at very low biomass levels (20 tha^{-1}, Imhoff, 1995b) and has found only limited use for characterization of tropical secondary forests, which quickly exceed these biomass levels. The relatively short wavelength (~5 cm) does not penetrate beyond the leafy forest canopy (Table 2-4). Texture analysis of high resolution C-band has provided some information for discriminating between cleared land, secondary and mature forests. Luckman et al. (1997b) were able to qualitatively distinguish between three regeneration stages (Table 2-5), using CCRS Convair 580 C-band dual polarization (HH, VV) data over the Brazilian Amazon. Texture coarseness increased from very little in clear-cut areas, to intermediate in regenerating stages, to greatest coarseness in mature forests. These visual differences could not be supported quantitatively in this study, however. Texture was also considered the most important source of information in a study by van der Sanden and Hoekman (1999) using CCRS SAR data over Guyana and Colombia, in which textural attributes were considered moderate to good bases (50-85% classification accuracy) for automated land cover classification (eight land cover types, including a secondary forest class) in this case.

RADARSAT and ERS-1/2, which both provide C-band imagery, contrast in the polarization recorded: HH for RADARSAT and VV for ERS-1/2. Although general land use and land cover classes, including deforested areas, have been detected through visual interpretation of RADARSAT imagery over the Brazilian Amazon, C-HH backscatter is not considered a reliable indicator for the degree of regeneration in secondary forests (Kux et al., 1998; Shimabukuro et al., 1998). Kux et al. (1998), for example, found that even the canopy of early secondary succession was too thick to allow penetration at C-band. Similarly, uses of ERS-1/2 SAR data in the tropics have been restricted to the identification of forest/non-forest, broad forest types (based on significant differences in canopy structure) and distinct land use and land cover classes, excluding regeneration stage of secondary forest (Verhoeye & DeWulf, 1999; Conway, 1997). Luckman et al. (1997a) found ERS-1 C-VV backscatter to exhibit greater variation during the dry season than during the wet; however, they were unable to distinguish biomass levels above 20-30 tha^{-1}. Kuntz and Siegert (1999) were able to discriminate secondary forest from other land cover types with some difficulty using multitemporal datasets and visual interpretation of backscatter and texture over flat terrain in Indonesia. Texture in satellite radar imagery is not as apparent as in higher-resolution airborne radar imagery (Leckie & Ranson, 1998).

It appears that the best potential for C-band sensors over tropical secondary forests is the application of texture analysis (such as the grey level co-occurrence textural descriptor) to multitemporal, high spatial resolution data (van der Sanden, 1997), such as that anticipated from Canada's RADARSAT-2, scheduled for 2003, with 3-100 m spatial resolution. Current classification algorithms based on texture are not capable of matching even the accuracy of visual interpretation, however (Kuntz & Siegert, 1999). Even if that were the case, it is unlikely that C-band radar systems, with such limited ability to penetrate the forest canopy, will be very useful for detailed description of secondary forest beyond discrimination of a single secondary forest class (or, at best, several very

early successional stages), as would be needed to estimate their carbon sequestration capabilities.

On a related note, RADARSAT data is currently being explored for its potential for canopy height estimation in the Amazon; results were within approximately 5 m of expected heights (Toutin & Amaral, 2000). Once again, this level of accuracy would not be sufficient for describing secondary forests; however, this type of data may find its place in providing inputs to biomass algorithms in the future.

SAR L-band sensors

Of the recent satellite-borne SAR systems, only two recorded data in L-band; these are JERS-1 and SIR-C/X-SAR. In lieu of P-band SARs, these may be considered to have the best potential for studies of regenerating forest biomass. The Japanese JERS-1 provided L-band data at a single polarization (HH) from 1992 through 1998. The European SIR-C sensor recorded polarimetric C and L data on two 10-day missions in April and October 1994 (Saatchi et al., 1997).

JERS-1 L-HH data have been studied over regenerating forests of the Brazilian Amazon by Luckman et al. (1997a; 1998) and Kuplich et al. (2000). Luckman et al. (1998) developed a model for biomass retrieval of secondary forest using JERS-1 SAR data from Tapagós and Manaus in the Amazon. Only three biomass classes could be distinguished. These were: 6-13 tha^{-1} (young regrowth), 13-31 tha^{-1} (established regeneration) and >31 tha^{-1} (old regeneration to primary forest). These classes are all on the very low end when considering that undisturbed forest biomass has a value of 400 tha^{-1}. Kuplich et al. (2000), working from the same study area, determined the biomass/backscatter correlation of 18 regenerating and mature forest plots ranging from 8-387 tha^{-1} ($r=0.77$). There were notable gaps in the range of biomass of the plots sampled. TAGB of most plots ranged from 8-100 tha^{-1}, one plot approximated 180 tha^{-1} and mature plots were 387 tha^{-1}.

Data from the Space Shuttle Imaging Radar (SIR-C) may be considered superior to all other recent satellite-borne SAR sensors in that they provided every wavelength and polarization combination offered by other, more limited radar sensor systems so far. In fact, it was the first fully polarimetric radar flown in space (Foody et al., 1997). With this all-in-one dataset, immediate comparison of the effectiveness of C and L band polarimetric data for biomass determination was possible.

A number of attempts to map Amazonian secondary forests based on regrowth stage or age after abandonment have been made using SIR-C data (Table 2-5). Saatchi et al. (1997), with dual polarization (HH and HV) C- and L-band SIR-C data were able to delineate one secondary growth class (<6 years, <100 tha^{-1}) with only 62% accuracy when using all four channels. A combined secondary growth/disturbed forest class was mapped with 81% accuracy, which rose to 87% when restricted to L-HH and L-HV. Whereas C-band was useful for separating young/low vegetation types, such as pasture/crops from young regrowth (as expected), L-band was better for separating young/low vegetation types in general from forest and the L-HH and L-HV combination could separate secondary from primary forest. Similarly, Rignot et al. (1997) could only map initial regrowth (<60 tha^{-1}, approximately 4 years old or less) using SIR-C data and required Landsat TM data to map an additional intermediate regrowth class (60-120 tha^{-1}). For various SIR-C combinations, the highest Kappa Coefficient for initial regrowth (0.68) was obtained using the fully polarimetric C and L-band data, followed by L-Quad

(0.64) alone. It is interesting to note that, in keeping with results from the study by Saatchi et al. (1997), a higher K-coefficient for initial regrowth resulted from the L-HH,HV combination (0.61) than the L,C dual polarization (HH,HV) combination (0.57), although the opposite was true for the entire classification. It would seem that the additional C-HH, HV channels add noise, increasing the probability of error, although this is not consistent with a high K-coefficient for fully polarimetric C and L-band data. The K-coefficient for the L-HH polarization alone (which would be the equivalent to JERS-1 data), was very low at 0.14.

Yanasse et al. (1997), also studying in the Brazilian Amazon, examined SIR-C C- and L-band dual polarization data (similar to Saatchi et al.,1997) for the purpose of relating the radar data to regeneration stage. In this case, a greater number of stages were defined, based on age: recent activities, 0-2, 2-4, 4-6, 6-8, >9 years and primary forest. In keeping with other studies, L-HV band contained the most information for discriminating these classes; class separation was achieved for all classes except between the 4-6 and 6-8 year old successional forests. In this band, the difference in tonal means from recent activities through primary forest was approximately 5dB. The temporary 'saturation' between 4 and 8 years may have been due to the formation of a nearly closed canopy of pioneer species and vines, after which pioneer trees began emerging, creating a more broken canopy. The formation of a homogeneous canopy by successional vegetation may have been a complicating factor in other studies mentioned above, in which only an initial regrowth class could be discriminated from the data.

One additional study, again from the Brazilian Amazon and from the same year, examined the April 1994 SIR-C dataset (wet season) in contrast to the previously mentioned research which all focused on the October 1994 dataset (dry season). Foody et al. (1997) also used plots of a range typically considered beyond the L-band saturation limit for biomass. The eleven plots ranged in biomass from 64 to 141 tha^{-1}. For the following band configurations, C-HH, C-HV, C-VV, L-HH, L-HV, and L-VV, there were no significant relationships between backscatter and forest biomass observed. Use of backscatter ratios and stratification of forest type by the dominance, or not, of *Cecropia* species improved correlations however. Highest correlation observed for non-*Cecropia*-dominated secondary forests (with leaves more vertically oriented) was $r=0.81$ for the backscatter ratio L-HV/C-HV and for *Cecropia*-dominated secondary forests (with large, horizonally oriented leaves and long, bare trunks), $r=0.87$ for the ratio C-VV/L-VV.

A number of observations and questions may arise from the results of this paper. For instance, did collecting the data during the wet season affect the results? The vegetation and the ground may have been wet at the time of data acquisition, which could have affected their dielectric constants and thus the magnitude of backscatter from their surfaces. Also, despite a small number of plots ($n = 11$), dominant pioneer species (and their structure) had a profound effect on microwave reflectance. This may have been overlooked in other studies using this type of data. Third, the potential for use of radar backscatter ratios in tropical secondary forest research should be explored. They may allow extension beyond previous saturation points for mono-wavelength mono-polarization data (Foody et al., 1997). The information content of fully polarimetric data has also not been explored.

SAR P-band sensors

P-band applications for measuring forest biomass are currently restricted to data from airborne sensors. Spaceborne P-band systems have not yet been realized due to Faraday rotation of the waves as they pass through the ionosphere, which cause phase and amplitude errors and affect basic data processing (Rignot et al., 1995). One possibility for overcoming these limitations is night operation of spaceborne P-band radar at linear polarization, which has the approximate equivalent of L-band day-time Faraday rotation and to which correction techniques can be applied (Rignot et al., 1995). A second possibility is the use of P-band radiation at circular polarization, which is more insensitive to Faraday rotation. Rignot et al. (1995), however, did not find these data useful for measuring forest biomass.

P-band airborne SAR tropical forest biomass measurements have passed the saturation limits of C and L-band radar. The NASA/JPL polarimetric AIRSAR operates at C-, L-, and P-band and has been useful for comparison studies of the three bands for biomass estimation. Using data from this instrument, Imhoff (1995b) determined the following biomass saturation levels for combined data from broadleaf evergreen (based on results from Hawaii) and coniferous forests (based on results from North America and Europe): C-band (20 tha^{-1}), L-band (40 tha^{-1}) and P-band (100 tha^{-1}). For P-band multipolarization data, this value can extend to approximately 200 tha^{-1} for mono-species, even-aged forests on even terrain (Rignot et al., 1995). Although the details of biomass saturation will depend on species mix, it has been suggested that the focus of SAR forest research should be the characterization of regenerating forests up to the respective saturation levels (Imhoff, 1995b).

At P band, HV polarized signals tend to be dominated by branch scattering, and are correlated with fresh branch biomass (Table 2-4) (Rignot et al., 1995). VV polarized signals are also dominated by branch scattering, and are similarly related to fresh branch biomass (Rignot et al., 1995). HH polarized signals, however, are dominated by trunk-ground scattering rather than branch scattering when biomass reaches high levels, and are correlated more with fresh stem biomass (Rignot et al., 1995). Imhoff (1995b) observed greater P-band VV and HV return from broadleaf evergreen forests than coniferous forests, likely due to greater branch biomass and greater diversity of branching angles in the broadleaf forest as compared to the coniferous forest, with its more uniform arrangement of branches, and which exhibited greater HH return. Rignot et al. (1995) suggested that the HH polarization was the most useful at high biomass levels (regardless of forest type) due to its correlation with stem biomass, which becomes a larger component of total biomass at high biomass levels.

Imhoff (1995a) indicated that forest structure may have a significant impact on SAR backscatter. Using a microwave canopy scattering model (MIMICS), it was demonstrated that structural variation could cause C-, L- and P-band quadpolarization backscatter variation in forests of equal biomass. In light of this finding, a 'universal SAR biomass equation for Earth's forest' was not considered feasible. Rather, stratification according to structural variables was suggested to improve biomass-backscatter correlations. Dobson et al. (1995) also used the approach of classifying based on forest structural categories prior to estimation of biophysical characteristics in a study from Michigan. Interestingly, Foody et al. (1997), in the tropics, found improved biomass relationship with L-band data when stratifying secondary forests according to the

dominance, or not, of *Cecropia*, which has a distinct structure including a long, bare trunk and large, horizontally-oriented leaves in its crown (the same stratification improved classification accuracy of successional age classes using Landsat TM data in Foody et al. (1996)). Rosenqvist (1996) also found differing microwave scattering patterns between rubber trees and oil palms, which have distinctly different structures. Rubber trees, with a more typical tree structure, exhibited the usual canopy scattering at C-band, and branch, twig and trunk scattering at L-band whereas oil palms, which have huge fronds making up a very large crown area and a single, straight trunk, had dominant crown scattering at both C- and L-band.

SAR applications for Central America

SAR application to secondary forest research in Central America, which is currently scarce, will face a number of serious challenges. The biggest of these is likely to be the topographic correction that will be required over mountainous regions, as will also be required for imagery from electro-optical sensors, although it may have a critical role on flat regions (such as the Atlantic Floodplains) where significant secondary growth may be occurring as a result of land abandonment by large multi-nationals, especially those dealing with Banana Plantations (Dole and Chiquita Brand, for example). Studies over the Brazilian Amazon have taken advantage of level to gently undulating terrain; SAR tropical secondary forest research is practically nonexistent over variable terrain. Improved correction techniques for topographical effects and high resolution digital elevation models will be essential to tackle the areas of high relief which are prevalent in this region.

Another challenge is the heterogeneous nature of the Central American landscape, from which backscatter coefficients are to be extracted. Not only is there variety in forest types due to a large number of life zones, but within each, population dynamics, small farm sizes, and the presence of natural areas at different levels of protection have lead to diversity in land use and land cover types. It will be difficult to find large, homogenous tracts from which tonal means may be determined.

SAR and electro-optical sensor research in Central America should benefit from the wealth of ecological research that has taken place in Costa Rica in the past, which should provide numerous (albeit small) sites of known land use history and a variety of sites of differing regeneration age. Finding enough (accessible) plots over a wide enough biomass range is a challenge for secondary forest research (Luckman et al., 1997a).

Limitations/future potential of SAR for secondary forest research

The main limitations of SAR potential for tropical secondary forest biomass estimation to date are 1.) saturation at low biomass levels (approximately 60 tha^{-1} at L-band, potentially up to approximately 140 tha^{-1} when stratified based on dominant species, based on Foody et al., 1997), 2.) lack of research on topographic correction techniques, 3.) lack of long-term global coverage for L band spaceborne systems (JERS-1 gave repetitive coverage from 1992-1998, SIR-C/X-SAR data available from two 10-day missions in 1994), 4.) lack of broad-scale applicability of studies, 5.) lack of consideration of variable site quality characteristics and 6.) poor field validation accompanied by lack of standardization of field validation techniques. Several of these

limitations are common to those identified from research involving electro-optical sensors.

Evidently, an operational P-band SAR in orbit could overcome the present biomass saturation constraints. While this is not currently feasible, another possibility that has not been exploited is the use of SAR at different channels and polarizations to take advantage of the fact that they are reflected to different extents from the various components of the forest (Kasischke et al., 1997). By using the unique information provided by each band/polarization combination, components of forest biomass (leafy biomass, branch biomass, trunk biomass) could be characterized individually to potentially give a more accurate picture of the whole (TAGB). This type of approach may allow future studies to surpass current SAR biomass saturation levels. SIR-C/X-SAR has provided the best opportunity for this type of multi-frequency multi-polarization study so far. Backscatter ratios would also take advantage of multiple wavelength/polarization combinations, and have been used more for temperate forest research than for tropical. Stratification of forests by structurally-related variables could also improve biomass-backscatter correlations. Alternatively, stratification according to previous land use history could serve the same purpose where it is shown to influence structure (or species composition, which in turn affects structure e.g. Foody et al., 1997).

Hyyppä et al. (2000) compared accuracy of remote sensing data sources for the retrieval of a number of variables related to biomass: stem volume, basal area and mean height. Of the satellite images used, the order of accuracy was Spot XS, Spot PAN, Landsat TM, ERS SAR coherence (from repeat-pass SAR interferometry), JERS SAR intensity images, and ERS SAR intensity images. The author indicated that satellite optical images remain superior to satellite radar images for this purpose.

SAR/ELECTRO-OPTICAL DATA SYNERGY

Capitalizing on the relevant data from both multi-spectral scanners and radar systems is a very interesting approach, as not only is the information complementary, but radar data may be used to fill in data gaps where no cloud-free data are available from multi-spectral scanners. While SAR data at L-band or longer are sensitive to regrowth biomass, electro-optical data such as Landsat TM exhibit sensitivity to leaf color and structural variables (Saatchi et al., 1997). This type of synergy is more complex than analysis of either type of imagery alone and has not been a common approach for the mapping of regenerating forest stages nor biomass estimation from regenerating forests. Nezry (1993) owes the limited results using this approach to lack of microwave data. Nezry (1993) combined SIR-B and SPOT HRV data to improve classification accuracy of a site in Sumatra, which included very good delineation of forest regrowth from other land use classes. Rignot et al. (1997) also used this approach to increase classification accuracy of a site in the Brazilian Amazon. Landsat TM was used for classification of forests and open water whereas SIR-C data was used for mapping flooded dead forests, nonforest and initial regrowth. Several other classes, including intermediate regrowth, were mapped based on data from both sources. Despite the added information provided by the dual data sources, only two regrowth stages were classified: initial and intermediate. The joint use of radar and optical imagery has important potential that has not been exploited to date. Further exploration should lead to better characterization of secondary forests. While a combination of Landsat TM (unable to distinguish late

secondary forest ~15 years+ from mature forest) and L-band radar (saturation at biomass <60 tha^{-1}) is still unlikely to detect late successional forests well, some of the newer sensors may provide a much better chance to do so.

FINAL REMARKS

Overall, biomass estimation of tropical secondary forests using space-borne data requires a much higher level of sophistication in image analysis and field validation than the detection of secondary forest as a single land cover class. Reflection and absorption of radiation from regenerating forests occur in continuous trends as they mature. As a result, it is difficult to designate spectral data from secondary forests into discrete age classes, which is the most common method of extrapolating biomass from Landsat TM data. To add to the complexity of this task, variables such as previous land use, intensity and duration of land use, soil type, and seed source availability can influence the rate of recovery at different sites and lead to intermingling of the spectral signatures of different age classes.

Nevertheless, current capabilities allow the identification of approximately two to three successional stages up to a maximum of approximately 15 years of age, based on research from the Amazon using Landsat TM imagery. Biomass estimation of tropical secondary forests from SAR data is even more limiting; SAR L-band is considered sensitive to forest biomass up to approximately 60 tha^{-1}, provided the terrain is fairly flat (mature tropical forest biomass estimates range from approximately 300-500 tha^{-1} for lowland moist/wet, premontane wet/rain, lower montane moist/wet/rain and montane rain forest life zones in Costa Rica (Helmer & Brown, 2000)). Newer optical sensors, with higher spatial and spectral resolution capability, as well as the use of data sets from multiple sources will be critical for surpassing the limitations indicated above.

Two issues that have not been dealt with in the literature on tropical secondary forests but will be unavoidable in Central America are topographic correction and extreme diversity in the land cover matrix. Unfortunately, the development of digital elevation models (DEMs) of a scale that will be suitable for secondary forest research in Central America may still be a long time in coming. The Shuttle Mission Topography will be releasing only a coarse DEM (90 m resolution), which will not be fine enough for accurate topographic corrections. With respect to heterogeneity over the Central American landscape, the Holdridge life zone system should be a key to the integration of ecology and remote sensing. Neither tropical dry nor montane forest types, both present in Central America, have been adequately covered in the literature on remote sensing of secondary forests. Tropical dry forests, considered one of the most endangered ecosystems of the lowland tropics (Janzen, 1988), have probably been underestimated (Sanchez-Azofeifa et al., 2001) due to their similarity to pasture during the dry season when leaf-off conditions coincide with cloud-free image acquisition. Attention to phenology will be vital to the characterization of secondary forests from space-borne sensors in these forests. In montane regions, where recovery after disturbance is very slow, there is potential for identifying later successional stages, although once again the issue of topography is a complicating factor (Helmer et al., 2000). Dominant species in both dry and montane tropical successional lands will likely influence imagery analysis as it did in the case of *Cecropia* and non-*Cecropia* dominated secondary forests in studies from the humid lowlands by Foody et al. (1996, 1997).

Variations in ecological and site quality characteristics in Central America will likely necessitate a standardized stratification system of secondary forests according to variables such as life zone, previous land use, intensity and duration, soil quality, size of clearing and presence of seed sources prior to regional classification or biomass estimation. As well, there is clearly a need for sound, repeatable methodology in field validation. Consensus is also required on what field variables should be gathered and how they should be gathered. At present, biomass estimations do not normally include species other than trees of a minimum dbh, so a critical amount of biomass may be overlooked. Other, related variables that are measurable at the ground level, such as leaf area index (LAI) and fraction of absorbed photosynthetically active radiation (fAPAR), which were not discussed in this review, will give further insight to the development of secondary vegetation and provide additional information to carbon accounting systems.

The inherent challenges to biomass estimation of secondary forests in Central America will certainly have parallels elsewhere in the tropics (for instance, along the South American Andes mountain range). Therefore, improved methods for topographic correction and the development of a systematized methodology for dealing with ancillary variables (such as life zone, soil type and land use history) will have very valuable implications for monitoring secondary tropical forests at a global scale. The ability to determine secondary forest biomass content from remotely sensed imagery with greater precision will be fundamental to providing a better understanding of the role of secondary forests in global biogeochemical cycles as well as their potential for mitigating atmospheric carbon.

Table 2-1: Application of Landsat data for detecting tropical secondary forest by age or biomass

Author(s)	Location	Successional forest classes or biomass range		Dataset	Accuracy or conclusions
Sader et al., 1989	Puerto Rico (Luquillo Experimental Forest and Caribbean National Forest)	3-16 years 16-36 years 36-50 years > 50 years		Aerial photography, TM (3,4-NDVI), TMS: 3,4-NDVI, CAMS: 4,6-NDVI	No significant relationship between TM NDVI and regeneration age or biomass differences in this mountainous region
Lucas et al., 1993	Brazilian Amazon (N of Manaus)	<2 years 2-3 years 3-6 years 6-14 years Primary forest		M-MSS (4,5,6,7) and TM (3,4,5)	Not given
Mausel et al., 1993	Brazilian Amazon (Pará state)	SS1: tall grass interspersed with woody/forest growth (~<6 years) SS2: 8-12 m trees, immature but developing canopy (~6-10 years) SS3: trees often +20 m, maturing multicanopy (~10-15 years)		M-TM (2-5,7)	SS1: 88.3% SS2/SS3 combined: 81.8% Mature forest: 97.2%
Boyd et al., 1996	Brazilian Amazon (N of Manaus)	SP1: 0 < 2 years 2-3 years 4-6 years	SP2: 0 4-6 years 7-14 years >14 years	Same as Lucas *et al.* (1993), however examining all seven TM bands for one 1991 image	TM7 provided greatest discrimination of different regeneration stages Highest correlation (coeff.=|0.86|) achieved for indices that included

		Primary forest SP1: dominated by *Clusiaceae, Flacourtiaceae, Melastomataceae* SP2: dominated by *Cecropiaceae*			middle and thermal infrared wavebands (correlation with NDVI insignificant) (TM2*TM6)/TM7 achieved highest degree of separation between >14 years and primary forest
Foody et al., 1996	Brazilian Amazon (N of Manaus)	Forest type I (FI): A: 4-6 years B: 7-10 years C: >14 years Mature forest FI and FII distinguished by successional pathway and dominant species for each	Forest type II (FII): A: <3 years B: 4-10 years	GD, M-MSS, M-TM (3,4,5)	Overall accuracy for classification: 87%, weighted Kappa coefficient 0.9315 Producer's accuracy for individual classes: FIa: 100% FIb: 61% FIc: 100% FIIa: 25% FIIb: 100%
Brondizio et al., 1996	Brazilian Amazon (Pará state)	Initial SS Intermediate SS Advanced SS		GD, TM (1-5,7)	Initial SS: 90.5% Intermediate SS: 98.9% Advanced SS: 90%
Steininger, 1996	Brazilian Amazon (near Manaus)	1-3 years 4-8 years 9-13 years 14-19 years Mature forest		GD, M-TM (1-5,7), NDVI, brightness, greenness	Classes 1-3, 4-8, and 9-13 years inseparable from each other but separable from forest 14 years +; Classes 14-19 and mature forest inseparable from each other Regressions significant ($p<0.001$) for TM4+TM3, brightness and %shade; NDVI not useful

Rignot et al., 1997	Brazilian Amazon (Rondonia state)	Initial regrowth: 0-4 years Intermediate regrowth, 5-8 years	GD, SIR-C (C- and L-quad-pol), M-JERS-1 (L-HH), TM (1-7), M-SPOT XS (3 bands)	93% overall using combined SIR-C and Landsat TM data (Kappa coefficient range 0.67-0.79 for two regrowth classes)
Sohn et al., 1999	Yucatan, Mexico	SS1: 2-5 years, height 1-3 m SS2: 6-10 yeasr, height 5-8 m SS3: 11-30 years height 10-15 m	GD, M-TM (1-7)(two images analyzed independently)	User's accuracy reported for 1995 image: SS1: 95% SS2: 94% SS3: 100%
Helmer et al., 2000	Costa Rica (Talamanca Mountain Range)	Sunlit slopes: Pasture/agriculture Tree/shrub crops + secondary shrub forest <6 years Secondary shrub/forest >6 years Secondary forest 6-16 years Secondary forest >17 years Old growth Shadowed slopes: Pasture/agriculture Secondary shrub/forest> 6 years Old growth	GD, aerial photography, MSS (5), M-TM, TM TC indices, (TM2*TM6)/TM7, TM4/TM5, three TM difference bands	87% overall accuracy for five combined classes using all three TC indices and one or two image dates (K. coeff.=0.83-NS): Pasture/agriculture: 96% Tree/shrub crops and secondary shrub/forest <6 years: 100% Sunlit secondary shrub/forest≥6years: 63% Secondary forest≥ 6 years: 80% Old-growth forest: 87%

Nelson et al., 2000	Brazilian Amazon (Rondonia state)	First degree secondary forest: 1, 2, 3, 4, 5, 6, 7+ years Second degree secondary forest: 1, 2, 3, 4, 5 years Third degree secondary forest: 1, 2, 3 years Fourth degree secondary forest: 1 year 'Degree' based on no. of times cleared)	M-TM (1-5,7)	Not possible to accurately predict one-year secondary forest age classes using neural nets and single-date TM data Clearing history cannot be reliably deduced from single-date TM imagery
Steininger, 2000	Brazilian Amazon (near Manaus), Bolivia (Santa Cruz de la Sierra)	Brazil: 20 sites of biomass 20-200 tha^{-1}, ages 4-30 years Bolivia: 14 sites of biomass 24-134 tha^{-1}, ages 4-25 years	GD, M-TM (1-5, 7)	Brazil: significant relationships between middle-infrared reflectance and regrowth stage and biomass Bolivia: no significant relationships observed
Foody et al., 2001	Borneo	Regenerating forests of biomass 65 tha^{-1} to 647 tha^{-1}	GD, TM (1-5, 7) (single-date)	Biomass estimates from field strongly correlated (r=0.80) with neural network, bands 5, 2 ,4 most important

List of abbreviations: TM=Landsat Thematic Mapper, NDVI=Normalized difference vegetation index , CAMS=Calibrated airborne multispectral scanner , M=multitemporal, MSS=Landsat multi-spectral scanner, SS=secondary succession, SP=successional pathway, GD=ground data, SIR-C=NASA's Spaceborne Imaging Radar C, JERS-1=Japan Earth Resources Satellite, quad-pol=quad polarization, SPOT=Satellite pour l'observation de la Terre, TC=Tasselled Cap indices (brightness, greenness, wetness), NS=not significant

Table 2-2: Examples of forest classification/stratification schemes

Author	Stratification/classification	Variables(s) other than age
Foody et al., 1996	Classification system for regrowth stages	Successional pathway (based on dominant species and land use history
Tucker et al.,1998	Classification system for regrowth stages	Height, basal area and dbh indices
Sohn et al.,1999	Classification system for regrowth stages	Canopy height
Nelson et al., 2000	Classification system for regrowth stages	'Degree', meaning number of times land had been cleared
Helmer et al., 2000	Stratification prior to classification of regrowth stage/land use	Life zone and illumination

Table 2-3. Field data gathered for remote sensing studies of regenerating forests

Reference	Study site	Total no. of classes identified	No. of sample sites/plots	Size of plots	Data collected (forest parameters)	Interviews	Notes
Lucas et al., 1993	Brazilian Amazon (N of Manaus)	-	-	-	-	-	No field validation performed
Mausel et al., 1993	Brazilian Amazon (Pará state)	9	300 site observations of vegetation type, density, condition	-	-	Acquired 25 field histories (to 10+ years)	-
Foody & Curran, 1994	Ghana, West Africa	Relationships between reflectance and tree density studied	29 from 3 forest reserves	1 ha	Detailed biophysical and floristic records, density of trees with diameter >10, 30, and 50 cm	-	-
Foody et al., 1996	Brazilian Amazon (N of Manaus)	11	15	100 x 10 m	Forest tree species >3 cm, biophysical properties such as LAI	-	-
Brondizio et al., 1996	Brazilian Amazon (Pará state)	14	27 (1-4 per land cover feature)	Not given, however, four adjacent plots (25 x 25 m) and four nested sub-plots (2 x 5 m) randomly distributed in managed area	For 27 sample areas: Species composition, density, frequency, dominance and basal area, percent of soil covered, height of first branch, total height, species "importance value" Plot level: Trees	Yes – included date since forest thinning, pruning activities, planting, yields	

					(dbh>10 cm) identified, dbh, stem and total height measured, Açaí with dbh>5 cm counted, stems per clump noted Subplot level: All individuals identified and counted, saplings (dbh>2 cm) measured for dbh and total height		
Steininger, 1996	Brazilian Amazon (near Manaus)	9	33 stands: 9 pastures, 8 agricultural fields, 16 regrowth stands	2-6 ha	Land utilization and regrowth ages	Yes	-
Sohn et al., 1999	Yucatan, Mexico	9	-	-	Age of fallow, estimated height	122 households	
Helmer et al., 2000	Costa Rica (Talamanca Mountain Range)	9	356 reference polygons; 80% from direct field observations made by traveling on roads	-	Presence of remnant old-growth trees, evidence of pasture use, aspect/illumination category, visual estimation of % cover of soil, grasses, shrubs, trees for subset of 96 polygons	-	-
Nelson et al., 2000	Brazilian Amazon (Rondonia state)	-	-	-	-	-	No field validation performed

Steininger, 2000	Brazilian Amazon (near Manaus), Bolivia (Santa Cruz de la Sierra)	Biomass correlation with reflectance studied	20 stands in Brazil, 14 stands in Bolivia	0.07-0.10 ha	Structural measurements of trees with dbh>5cm, volume and canopy height estimated	-	-
Foody et al., 2001	Borneo	Biomass correlation with reflectance studied	52	0.05 ha	Dbh measured for trees with dbh>5cm, used for biomass estimation	-	-

List of abbreviations: LAI=Leaf Area Index, dbh=diameter at breast height

Table 2-4: Importance of forest components to radar backscatter of different wavelengths and polarizations

Band-Polarization	Approximate wavelength (cm)	Dominating contributor to backscatter from forests	Reference
K-band (general)	1	Interaction with leaves	Leckie & Ranson, 1998
X-band (general)	3	Interaction with leaves, twigs and small branches	Leckie & Ranson, 1998
C-band (general)	5	Interaction with leaves, small and secondary branches	Leckie & Ranson, 1998
C-HH		Surface scatter	Lewis et al., 1998
C-HV; C-VH		Volume scattering from uppermost canopy	
C-VV		Volume scattering from uppermost canopy	Rosenqvist, 1996, citing Karam et al., 1993; Dobson et al., 1992a; Hsu et al., 1992
L-band (general)	25	Interaction with primary and secondary branches and trunks Trunk-ground and crown-ground interactions may be important	Leckie & Ranson, 1998
L-HH		Scattering from twigs and branches; trunk-ground interaction	Rosenqvist ,1996, citing Karam et al., 1993; Dobson et al., 1992b; Hsu et al., 1992; Sun et al., 1991; Richards et al., 1987
L-HV; L-VH		Crown scattering	Le Toan et al., 1992
L-VV		-	(No reference found)

P-band (general)	68	Interaction with main branches, trunks and ground Trunk-ground and crown-ground interactions may be important	Leckie & Ranson, 1998
P-HH		Trunk-ground scattering dominates branch scattering at high biomass levels	Kasischke, 1995; Rignot et al., 1995
P-HV; P-VH		Scattering from large, lower branches	Rignot et al., 1995; Lang et al., 1994
P-VV		Branch scattering, volume canopy scattering Backscatter less sensitive to ground conditions than HV	Kasischke, 1995; Rignot et al., 1995

Table 2-5: Radar for estimation of forest biomass or stage of regeneration

Radar system	Band	Polarization	Spatial resolution	Lifespan	Tropical study site	Biomass estimation	Stage of growth	Reference
Airborne								
STAR-1/2	X	HH	4.2 x 6 m		Costa Rica	N/A	Several stages of forest regrowth in clearcuts identified	Dams et al., 1987, cited in Thompson & Dams, 1993
					Congo	N/A	Stage of growth of pine and eucalyptus stands evaluated	Thompson & Dams, 1993
CCRS Convair 580	X, C	HH, VV	6 x 6m		Brazilian Amazon	N/A	1-3, 4-6, >6 years (Qualitative distinction only)	Luckman et al., 1997b
NASA/JPL AirSAR	C, L, P	HH, HV, VH, VV	7 x 12 m		Combined data from Hawaii , France, North Carolina, USA	C-band saturation: ~20 tha^{-1} L-band saturation: ~40 tha^{-1} P-band saturation: ~100 tha^{-1}	N/A	Imhoff, 1995b
Satellite								
Radarsat	C	HH	10 x 10 m – 100 x 100 m	1995-		Poor except for very low biomass levels	N/A	Kasischke et al., 1997

					Brazilian Amazon	N/A	Unable to determine degree of regeneration	Kux et al., 1998; Shimabukuro et al., 1998
ERS-1/2	C	VV	25 x 25 m	ERS-1:1991-2000 ERS-2: 1995-		Poor except for low biomass levels	N/A	Kasischke et al., 1997
						Biomass density theshold value of approximately 20-30 tha^{-1}	N/A	Luckman et al., 1997
						N/A	Discrimination of secondary forest class possible with multitemporal data; degree of regeneration not determined	Kuntz & Siegert, 1999
JERS-1	L	HH	18 x 18 m	1992-1998	Brazilian Amazon	Good for lower biomass levels, but still limited	N/A	Kuplich et al., 2000; Luckman et al., 1998; Kasischke et al., 1997; Luckman et al., 1997a; Rignot et al., 1997

					Brazilian Amazon	Biomass threshold density value of approximately 60 tha^{-1}	N/A	Luckman et al., 1997a
SIR-C/X-SAR	X, C, L	C and L (HH, VV, VH, HV) X (HH, VV)	25 x 25 m	Two 10 day missions: April and October 1994 (Saatchi et al. 1997)		Provides good estimates, but lower frequency (P-band) still optimum	N/A	Kasischke et al., 1997
					Brazilian Amazon	Biomass threshold density value of approximately 60 tha^{-1}	N/A	Luckman et al., 1997a
				April 1994 imagery (wet season)	Brazilian Amazon	r=0.64 for LHV/LHH for sites of biomass 64tha^{-1}-141tha^{-1}; higher correlation when forests stratified by dominant pioneer species	N/A	Foody et al., 1997

12.5 x 12.5 m	Oct. 1994 imagery (dry season)	Brazilian Amazon	N/A	Secondary forests < 6 yrs	Saatchi et al., 1997 (L,C-HH and –HV dataset only)
	Oct. 1994 imagery (dry season)	Brazilian Amazon	N/A	Recent activities, 0-2, 2-4, 4-6, 6-8, >9 yrs, primary forest	Yanasse et al., 1997 (L,C-HH and HV dataset only)
12.5 x 12.5 m	Oct. 1994 imagery (dry season)	Brazilian Amazon	N/A	Initial regrowth (<60 tha^{-1})	Rignot et al., 1997

Additional source: van der Sanden (1997); List of abbreviations: CCRS=Canadian Centre for Remote Sensing , NASA=National Aeronautics and Space Administration, JPL=Jet Propulsion Laboratory, ERS=European Space Agency, JERS-1=Japan Earth Resources Satellite, SIR-C=Spaceborne Imaging Radar C

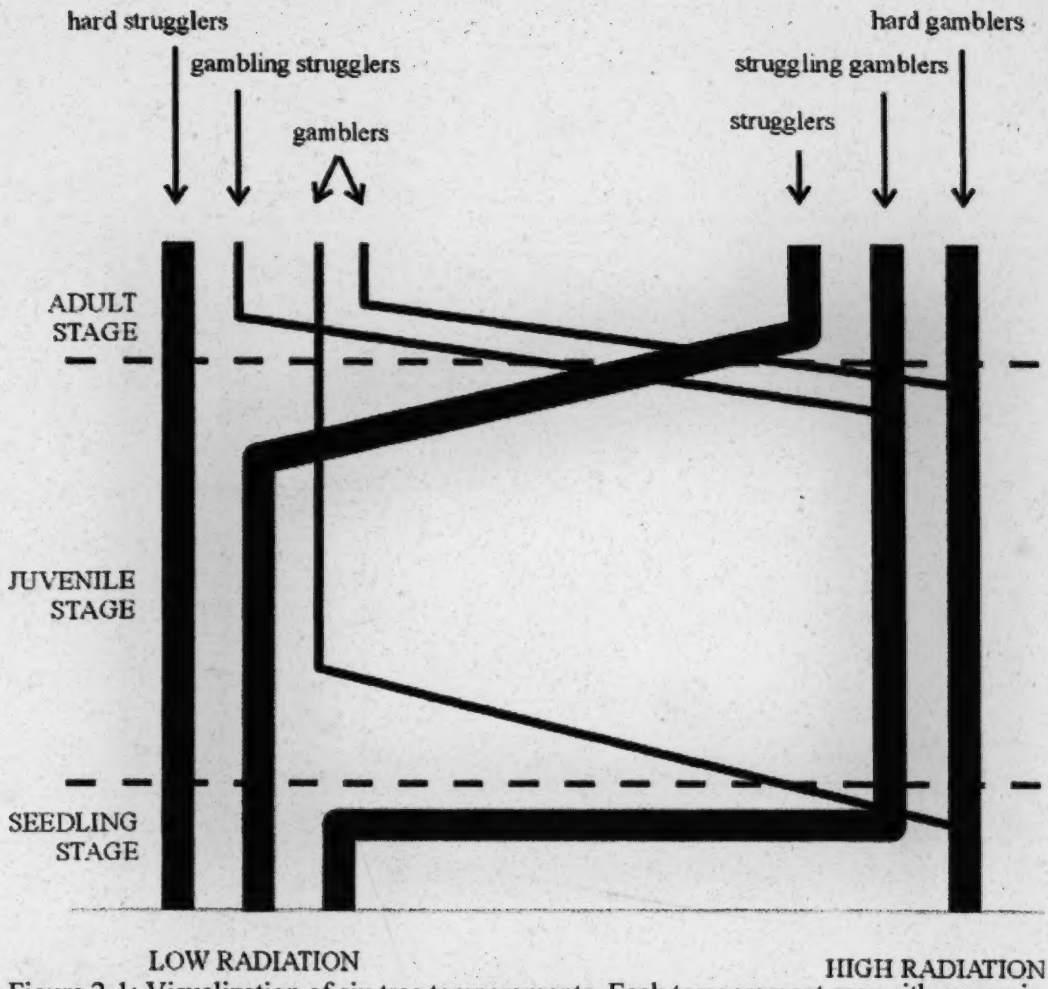

Figure 2-1: Visualization of six tree temperaments. Each temperament may either remain constant from seedling to adult tree (hard strugglers, hard gamblers), or be flexible and change its shade tolerance at some stage of the life cycle (others). The vertical dimension of this diagram evaluates height above ground level, which will be different for each tree species. It also refers to processes, but the tempo and rhythm of these processes differ for each tree species, and thus this is also a relative scaling. The strugglers closely correspond to the classical "shade-bearers" or "climax species", the hard gamblers to classical "light-demanding" or "pioneer" species. The relative frequency of a temperament is indicated by the thickness of the bar. Source: Oldeman & van Dijk (1991) © Parthenon Publishing Group Ltd (Reproduced with permission).

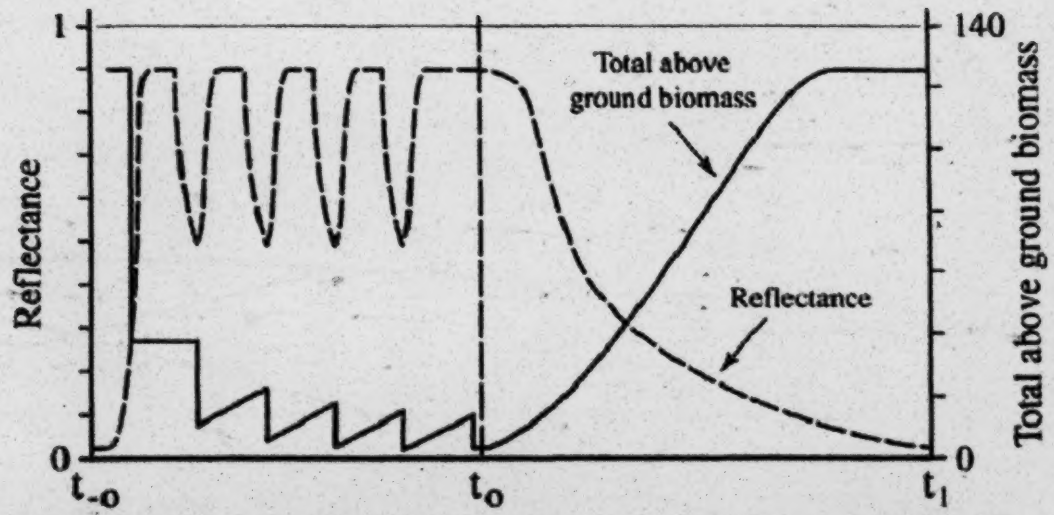

Figure 2-2: Conceptual relationship between Landsat Thematic Mapper Band 3 and Total Above Ground Biomass (TAGB) for a tropical dry forest ecosystem: t_{-o} represents pre-disturbance, t_o represents today and t_{+1} represents the time when maximum TAGB is achieved. Breaks on both curves are related to the presence of human-induced-fires typical of this ecosystem.

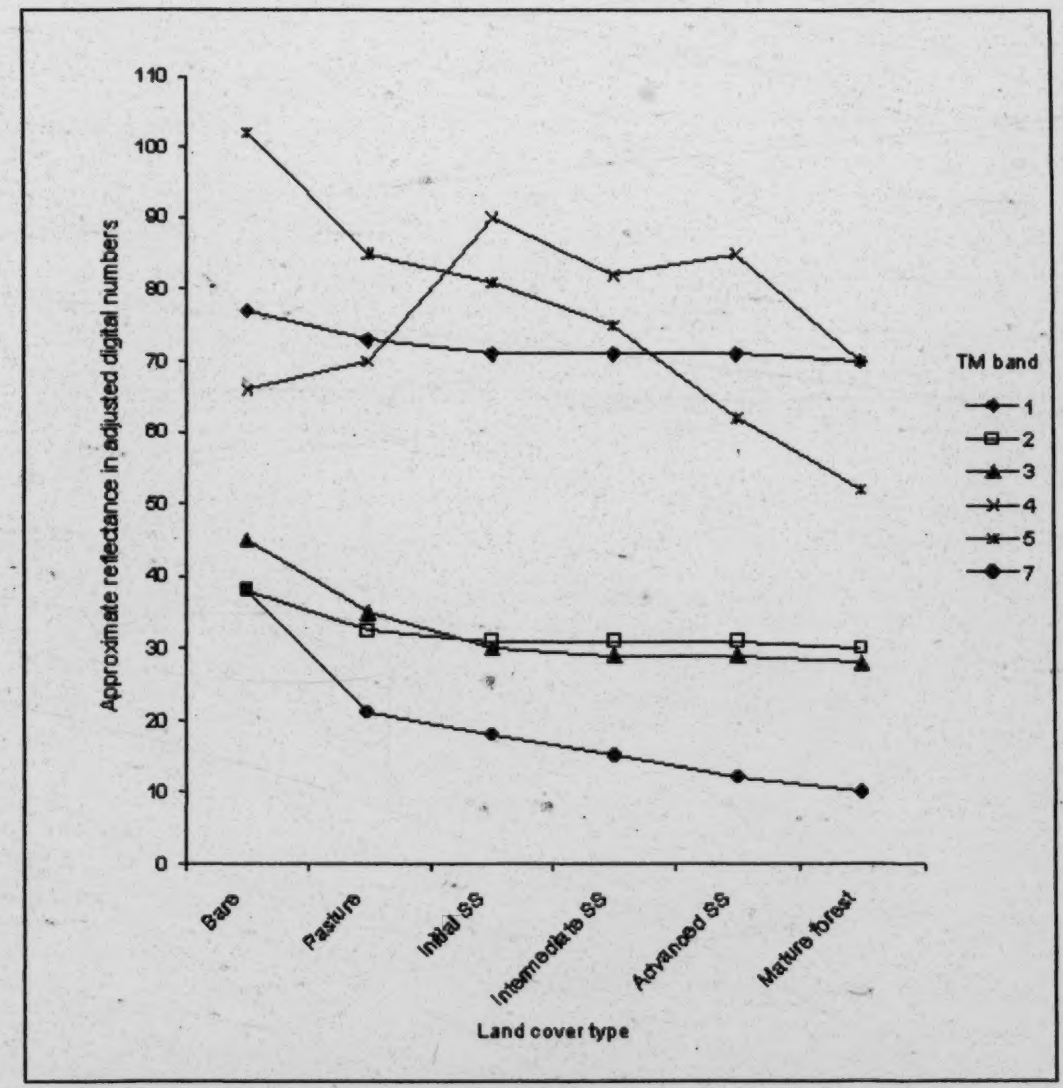

Figure 2-3: Spectral response of Landsat TM bands 1-5, 7 to regeneration stage Site: Altamira (Amazon); SS=secondary succession. Source: Moran et al. (1994) © Bioscience (Reproduced with permission).

LITERATURE CITED

Atkinson, P. M., Cutler, M. E. J., & Lewis, H. (1997). Mapping sub-pixel proportional land cover with AVHRR imagery. *International Journal of Remote Sensing, 18*, 917-935.

AVIRIS home page. http://makalu.jpl.nasa.gov/

Boyd, D. S., Foody, G. M., Curran, P. J., Lucas, R. M., & Honzak, M. (1996). An assessment of radiance in Landsat TM middle and thermal infrared wavebands for the detection of tropical forest regeneration. *International Journal of Remote Sensing, 17*, 249-261.

Brondizio, E., E. Moran, P. Mausel, & Wu, Y. (1996). Land cover in the Amazon Estuary: Linking of the Thematic Mapper with Botanical and Historical Data. *Photogrammetric Engineering and Remote Sensing, 62*, 921-929.

Brown, S., & Lugo, A. E. (1990). Tropical secondary forests. *Journal of Tropical Ecology, 6*, 1-32.

Castro-Salazar, R., & Arias-Murillo, G. (1998). Costa Rica: Toward the sustainability of its forest resources. San Jose, Costa Rica: Technical Report Fonda Nacional de Financiamiento Foresta (FONAFIFO).

Conway, J. (1997). Evaluating ERS-1 SAR data for the discrimination of tropical forest from other tropical vegetation types in Papua New Guinea. *International Journal of Remote Sensing, 18*, 2967-2984.

Corlett, R. (1994). What is secondary forest? *Journal of Tropical Ecology, 10*, 445-447.

Curran, P. J., Dungan, J. L., & Gholz, H. I. (1992). Seasonal LAI in slash pine estimated with Landsat TM. *Remote Sensing of Environment, 39*, 3-13.

Dams, R. V. et al. (1987). SAR image analysis for Costa Rican tropical forestry application. II simposio Latinamericano sobre sensores remotos. Bogota, Colombia.

Danson, F. M. & Curran, P. J. (1993). Factors affecting the remotely sensed response of coniferous forest plantations. *Remote Sensing of Environment, 43*, 55-65.

Denslow, J. (1996). Functional group diversity and responses to disturbance. In G. Orians et al. (Eds.), *Biodiversity and Ecosystems Processes in Tropical Forest* (229 p.) Springer.

Dobson, M. C., Pierce, L., Sarabandi, K., Ulaby, F. T., & Sharik, T. (1992a). Preliminary analysis of ERS-1 SAR for forest ecosystem studies. *IEEE Transactions on Geoscience and Remote Sensing, 30*, 203-211.

Dobson, M. C., Ulaby, F. T., Letoan, T., Beaudoin, A., Kasischke, E. S., & Christensen, N. (1992b). Dependence of radar backscatter on coniferous forest biomass. *IEEE Transactions on Geoscience and Remote Sensing, 30*, 412-415.

Dobson, M. C., Ulaby, F. T., Pierce, L. E., Sharik, T. L., Bergen, K. M., Kellndorfer, J. Kendra, J. R., Li, E., Lin, Y. C., Nashashibi, A., Sarabandi, K., & Siqueira, P. (1995). Estimation of forest biophysical characteristics in northern Michigan with SIR-C/X-SAR. *IEEE Transactions on Geoscience and Remote Sensing, 33*, 877-895.

Ewel, J.J. (1977), Differences between wet and dry successional tropical ecosystems. *Geo-Eco-Trop, 1*, 103-117.

Ewel, J. (1980). Tropical succession: manifold routes to maturity. *Biotropica, 12* (supplement), 1-95.

Fahsi, A., T. Tsegaye, W. Tadesse, & Coleman, T. (2000). Incorporation of digital elevation models with Landsat-TM data to improve land cover classification accuracy. *Forest Ecology and Management, 128*, 57-64.

Fearnside, P. M. (1996). Amazonian deforestation and global warming: carbon stocks in vegetation replacing Brazil's Amazon forest. Forest *Ecology and Management, 80*, 21-34.

Fearnside, P. M. & Guimarães, W. M. (1996). Carbon uptake by secondary forests in Brazilian Amazonia. *Forest Ecology and Management, 80*, 35-46.

Finegan, B. (1996). Pattern and process in neotropical secondary rain forests: the first 100 years of succession. *Trends in Ecology and Evolution, 11*, 119-124.

Foody, G. M., & Curran, P. J. (1994). Estimation of tropical forest extent and regenerative stage using remotely sensed data. *Journal of Biogeography, 21*, 223-244.

Foody, G. M., Palubinskas, G., Lucas, R. M., Curran, P. J., & Honzak, M. (1996). Identifying Terrestrial Carbon Sinks: Classification of Successional Stages in Regenerating Tropical Forest from Landsat TM Data. *Remote Sensing of Environment, 55*, 205-216.

Foody, G. M., Green, R. M., Lucas, R. M., Curran, P. J., Honzak, M., & Amaral, I. D. (1997). Observations on the relationship between SIR-C radar backscatter and the biomass of regenerating tropical forests. *International Journal of Remote Sensing, 18*, 687-694.

Foody, G. M., Cutler, M. E., Mcmorow, J., Dieter, P., Tangki, H., Boyd, D. S., & Douglas, I. (2001). Mapping the biomass of Bornean tropical rain forest from remotely sensed data. *Global Ecology and Biogeography, 10*, 379-387.

Guariguata, M. R., Chazdon, R. L., Denslow, J. S., Dupuy, J. M., & Anderson, L. (1997). Structure and floristics of secondary and old-growth forest stands in lowland Costa Rica. *Plant Ecology, 132*, 107-120.

Guimarães, W. M. (1993). Liberação de carbono e mudanças nos estoques dos nutrients contidos na biomassa aérea e no solo resultante de queimadas de florestas secundárias em areas de pastagens abandonadas, em Altamira, Pará. Masters Thesis, Manaus, AM: Instituto Nacional de Pesquisas da Amazônia/Fundação Universidade do Amazonas (INPA/FUA).

Hartshorn, G. S. (1980). Neotropical Forest Dynamics. *Biotropica, 12* (supplement), 23-30.

Helmer, E. H., & Brown, S. (2000). Gradient analysis of biomass in Costa Rica and a first estimate of countrywide emissions of greenhouse gases from biomass burning. In C. A. S. Hall (Ed.), *Quantifying Sustainable Development: The Future of Tropical Economies* (pp. 503-526). San Diego: Academic Press.

Helmer, E. H., Brown, S., & Cohen, W. B. (2000). Mapping montane tropical successional stage and land use with multi-date Landsat imagery. *International Journal of Remote Sensing, 21*, 2163-2183.

Holdridge, L. R. (1947). Determination of world plant formations from simple climatic data. *Science, 105*, 367-368.

Holdridge, L. R., Grenke, W. C., Hatheway, W. H., Liang, T. & Tosi, J.A. (1971). Forest environments in tropical life zones: A pilot study. Pergamon Press.

Houghton, R. A., Skole, D. L., & Lefkowitz, D. S. (1991). Changes in the landscape of Latin America between 1850 and 1985 II. Net release of $C0_2$ to the atmosphere. *Forest Ecology and Management, 38*, 173-199.

Hughes, R.F., Kauffman, J. B., & Jaramillo, V. J. (1999). Biomass, Carbon, and Nutrient Dynamics of Secondary Forests in a Humid Tropical Region of Mexico. *Ecology, 80*, 1892-1907.

Hsu, C. C., Shin, R. T., Kong, J. A., Le Toan, T., & Beaudoin, A. (1993). Application of theoretical model for microwave remote sensing of forest. In Proceedings of the International Geoscience and Remote Sensing Symposium (IGARSS '93), (pp. 595-597). Tokyo, Japan, 18-21 August 1993, Piscataway, NJ: IEEE.

Hyyppä, J., Hyyppä, H., Inkinen, M., Engdahl, M., Linko, S., & Zhu, Y. (2000). Accuracy comparison of various remote sensing data sources in the retrieval of forest stand attributes. *Forest Ecology and Management, 128*, 109-120.

Imhoff, M. L. (1995a). A Theoretical Analysis of the Effect of Forest Structure on Synthetic Aperture Radar Backscatter and the Remote Sensing of Biomass. *IEEE Transactions on Geoscience and Remote Sensing, 33*, 341-352.

Imhoff, M. L. (1995b). Radar Backscatter and Biomass Saturation: Ramifications for Global Biomass Inventory. IEEE *Transactions on Geoscience and Remote Sensing, 33*, 511-518.

Costa Rica National Biodiversity Institute (INBio) (1999). Annual memory. Santo Domingo de Heredia, Costa Rica, Central America.

Janzen, D. H. (1988). Tropical dry forest: The most endangered major tropical ecosystem. In E. O. Wilson (Ed.), *Biodiversity* (pp. 130-137). Washinton, DC: Natural Academy Press.

Jensen, J. R. (2000). *Remote Sensing of the Environment: An Earth Resource Perspective 2000*. Upper Saddle River, New Jersey: Prentice-Hall Inc..

Jordan, C. F., & Herrera, R. (1981). Tropical rain forests: Are nutrients really critical? *American Naturalist, 117*, 167-180.

Karam, M. A., Levine, D. M., Amar, F., Fung, A. K., Mougin, E., & Lopes, A. (1993). Understanding the relation between forest biomass and the radar backscatter signals. In Proceedings of the International Geoscience and Remote Sensing Symposium (IGARSS '93) (pp. 573-575). Tokyo, Japan, 18-21 August 1993, Piscataway, NJ: IEEE.

Kasischke, E. S., Christensen, N. L., & Bourgeau-Chavez, L. (1995). Correlating radar backscatter with components of biomass in loblolly pine forests. *IEEE Transactions on Geoscience and Remote Sensing, 33*, 643-658.

Kasischke, E. S., Melack, J.M., & Dobson, M.C. (1997). The Use of Imaging Radars for Ecological Applications-A Review. *Remote Sensing of Environment, 59*, 141-156.

Kellman, M.C. (1970). Secondary plant succession in tropical montane Mindanao.Canberra, Australia, Australian National University, Dept. Biogeogr. Geomorph., Pub BG/2, 174 p.

Kenoyer, L. A. (1929). General and Successional Ecology of the Lower Tropical Rain-Forest at Barro Colorado Island, Panama. *Ecology, 10*, 201-221.

Kimes, D. S., Nelson, R. F., Skole, D. L., & Salas, W. A. (1998). Accuracies in mapping secondary tropical forest age from sequential satellite imagery. *Remote Sensing of Environment, 65*, 112-120.

Kimes, D. S., Nelson, R. F., Salas, W. A., & Soles, D.K. (1999). Mapping secondary tropical forest age from SPOT HRV data. International *Journal of Remote Sensing, 20*, 3625-3640.

Kricher, J. C. (1989). *A Neotropical Companion.* Princeton, New Jersey: Princeton University Press.

Kuntz, S., & Siegert, F. (1999). Monitoring of deforestation and land use in Indonesia with multitemporal ERS data. *International Journal of Remote Sensing, 20*, 2835-2853.

Kuplich, T. M., Salvatori, V., & Curran, P. J. (2000). JERS-1/SAR backscatter and its relationship with biomass of regenerating forests. *International Journal of Remote Sensing, 21*, 2513-2518.

Kux, H.J.H., dos Santos, J.R., Ahern, F.J., Pietsch, R.W., & Lacruz, M. S. P. (1998). Evaluation of Radarsat for Land Use and Land Cover Dynamics in the Southwestern Brazilian Amazon State of Acre. *Canadian Journal of Remote Sensing, 24*, 350-359.

Lang, R. H., Chauhan, N. S., Ranson, K. J., & Kilic, O. (1994). Modeling P-band SAR returns from a red pine stand. *Remote Sensing of Environment, 47*, 132-141.

Leckie, D. G., & Ranson, K. J. (1998). In F. M. Henderson & A. J. Lewis (Eds.), *Principles and Applications of Imaging Radar*. Manual of Remote Sensing, Third Edition, Volume 2 (pp. 457-508), New York: John Wiley & Sons.

Le Toan, T., Beaudoin, A., Riom, J., & Guyon, D. (1992). Relating forest biomass to SAR data. *IEEE Transactions on Geoscience and Remote Sensing, 30*, 403-411.

Lewis, A. J., Henderson, F. M., & Holcomb, D. W. (1998). Radar Fundamentals: The GeoScience Perspective. In F. M. Henderson & A. J. Lewis (Eds.), *Principles and Applications of Imaging Radar*. Manual of Remote Sensing, Third Edition, Volume 2 (pp. 131-181), New York: John Wiley & Sons.

Lucas, R. M., Honzak, M., Foody, G. M., Curran, P. J., & Corves, C. (1993). Characterizing tropical secondary forests using multi-temporal Landsat sensor imagery. *International Journal of Sensing, 14*, 3061-3067.

Lucas, R. M., Honzák, M., Curran, P. J., Foody, G. M., Milne, R., Brown, T., & Amaral, S. (2000a). Mapping the regional extent of tropical forest regeneration stages in the Brazilian Legal Amazon using NOAA AVHRR data. *International Journal of Remote Sensing, 21*, 2855-2881.

Lucas, R. M., Honzák; M., Curran, P. J., Foody, G. M., & Nguele, D. T. (2000b). Characterizing tropical forest regeneration in Cameroon using NOAA AVHRR data. *International Journal of Remote Sensing, 21*, 2831-2854.

Luckman, A. J., Baker, J., Kuplich, T. M., Yanasse, C. C. F., & Frery, A. C. (1997a). A study of the relationship between radar backscatter and regenerating tropical forest biomass for spaceborne SAR instruments. *Remote Sensing of Environment, 60*, 1-13.

Luckman, A. J., Frery, A. C., Yanasse, C. C. F., & Groom, G. B. (1997b). Texture in airborne SAR imagery of tropical forest and its relationship to forest regeneration stage. *International Journal of Remote Sensing. 18*, 1333-1349.

Luckman, A., Baker, J., Honzak, M., & Lucas, R. (1998). Tropical Forest Biomass Density Estimation Using JERS-1 SAR: Seasonal Variation, Confidence Limits, and Application to Image Mosaics. *Remote Sensing of Environment, 63*, 126-139.

Mausel, P., Wu, Y., Li, Y., Moran, E. F., & Brondizio, E. S. (1993). Spectral Identification of Succesional Stages Following Deforestation in the Amazon. *Geocarto International, 4*, 61-71.

Montgomery, R. A., & Chazdon, R. L. (2001). Forest structure, canopy architecture, and light transmittance in tropical wet forests. *Ecology, 82*, 2707-2718.

Moran, E. F., Brondizio, E., Mausel, P., & Wu, Y. (1994). Integrating Amazonian Vegetation, Land-Use, and Satellite Data: Attention to differential patterns and rates of secondary succession can inform future policies. *BioScience, 44*, 329-338.

Muchoney, D., Borak, J., Chi, H., Friedl, M., Gopal, S., Hodges, J., Morrow, N., & Strahler, A. (2000). Application of the MODIS global supervised classification model to vegetation and land cover mapping of Central America. *International Journal of Remote Sensing, 21*, 1115-1138.

NASA website. http://geo.arc.nasa.gov/sge/health/sensor/sensor.html

Nelson, B. W., Mesquita, R., Pereira, J. L. G., Aquino de Souza, S. G., Batista, G. T., & Couto, L. B. (1999). Allometric regressions for improved estimate of secondary forest biomass in the central Amazon. *Forest Ecology and Management, 117*, 149-167.

Nelson, R. F., Kimes, D. S., Salas, W. A., & Routhier, M. (2000). Secondary Forest Age and Tropical Forest Biomass Estimation Using Thematic Mapper Imagery. *BioScience, 50*, 419-437.

Nezry, E., Mougin, E., Lopes, A., & Gastellu-Etchegorry, J. P. (1993). Tropical vegetation mapping with combined visible and SAR spaceborne data. *International Journal Remote Sensing, 14*, 2165-2184.

Oldeman, R. A. A., & Van Dijk, J. (1991). Diagnosis of the temperament of tropical rain forest trees. In A. Gómez-Pompa, T. C. Whitmore & M. Hadley (Eds.), *Rain Forest Regeneration and Management* vol. 6 (pp. 21-65), New Jersey: The Parthenon Publishing Group Ltd.

Opler, P. A., Baker, H. G., & Frankie, G. W. (1977). Recovery of Tropical Lowland Forest Ecosystems. In Cairns, Jr., K. L. Dickson & E. E. Herricks (Eds.), *Recovery and Restoration of Damaged Ecosystems*, Charlottesville, VA: University Press of Virginia.

Ouaidrari, H., Ibernon, J., & Dedieu, G. (1994). Use of a meterological model to correct atmospheric effects in NOAA-AVHRR data. *International Journal of Remote Sensing, 15*, 2257-2271.

Peterson, D. L., Spanner, M. A., Running, R. W., & Teuber, K. B. (1987). Relationship of Thematic Mapper Simulator data to leaf area index of temperate coniferous forests. *Remote Sensing of Environment, 22*, 323-341.

Ranson, K. J., & Sun, G. (1994). Mapping biomass of a northern forest using multifrequency SAR data. *IEEE Transactions on Geoscience and Remote Sensing, 32*, 388-396.

Ranson, K. J., Saatchi, S., & Sun, G. (1995). Boreal Forest Ecosystem Characterization with SIR-C/XSAR. *IEEE Transactions on Geoscience and Remote Sensing, 33*, 867-876.

Rauste, Y., Häme, T., Pulliainen, J., Heiska, K., & Hallikainen, M. (1994). Radar-based forest biomass estimation. *International Journal of Remote Sensing, 15*, 2797-2808.

Richards, J. A., Sun, G., & Simonnet, D. S. (1987). L-band radar backscatter modeling forest stands. *IEEE Transactions on Geoscience and Remote Sensing, 25*, 487-498.

Rignot, E. J., Zimmermann, R., & Van Zyl, J. (1995). Spaceborne Applications of P Band Imaging Radars for Measuring Forest Biomass. *IEEE Transactions on Geoscience and Remote Sensing, 33*, 1162-1169.

Rignot, E., Salas, W.A., & Skole, D.L. (1997). Mapping Deforestation and Secondary Growth in Rondonia, Brazil, Using Imaging Radar and Thematic Mapper Data, *Remote Sensing of Environment, 59*, 167-179.

Rosenqvist, Å. (1996). Evaluation of JERS-1, ERS-1 and Almaz SAR backscatter for rubber and oil palm stands in West Malaysia, *International Journal of Remote Sensing, 17*, 3219-3231.

Saatchi, S. S., Soares, J. V., & Alves, D. S. (1997). Mapping Deforestation and Land Use in Amazon Rainforest by Using SIR-C Imagery. *Remote Sensing of Environment, 59*, 191-202.

Sader, S. A. (1986). Analysis of effective radiant temperatures in a Pacific northwest forest using thermal infrared multi-spectral scanner data. *Remote Sensing of Environment, 19*, 105-115.

Sader, S. A. (1987). Airborne remote sensing of forest biomes. *Geocarto International, 1*, 9-17.

Sader, S. A., Waide, R. B., Lawrence, W. T., & Joyce, A. T. (1989). Tropical Forest Biomass and Successional Age Class Relationships to a Vegetation Index Derived from Landsat TM Data. *Remote Sensing of Environment, 28*, 143-156.

Sader, S. A., Stone, T. A., & Joyce, A. T. (1990). Remote Sensing of Tropical Forests: An Overview of Research and Applications Using Non-Photographic Sensors. *Photogrammetric Engineering and Remote Sensing, 56*, 1343-1351.

Sanchez-Azofeifa, G.A. & Rivard, B. (2001). Advancing frontiers in tropical biology: The future of remote sensing research in tropical environments. In Ganeshaiah, Shaanker & Bawa (Eds.), *Tropical Ecosystems: Structure, Diversity and Human Welfare*. Association for Tropical Biology.

Shimabukuro, Y. E., Amaral, S., Ahern, F. J., & Pietsch, R. W. (1998). Land Cover Classification from RADARSAT Data of the Tapajós National Forest, Brazil. *Canadian Journal of Remote Sensing, 24*, 393-401.

Sohn, Y., Moran, E., & Gurri, F. (1999). Deforestation in North-Central Yucatan (1985-1995): Mapping Secondary Succession of Forest and Agricultural Land Use in Sotuta Using the Cosine of the Angle Concept. *Photogrammetric Engineering and Remote Sensing, 65*, 947-958.

Steininger, M. K. (1996). Tropical secondary forest regrowth in the Amazon: age, area and change estimation with Thematic Mapper data. *International Journal of Remote Sensing, 17*, 9-27.

Steininger, M. K. (2000). Satellite estimation of tropical secondary forest above-ground biomass: data from Brazil and Bolivia. *International Journal of Remote Sensing, 21*, 1139-1157.

Sun, G., Simonnet, D. S., & Strahler, A. H. (1991). A radar backscatter model for discontinuous coniferous forests. *IEEE Transactions on Geoscience and Remote Sensing, 29*, 639-650.

Thenkabail, P. S. (1999). Characterization of the alternative to slash-and-burn benchmark research area representing the Congolese rainforests of Africa using near-real-time SPOT HRV data. *International Journal of Remote Sensing, 20*, 839-877.

Thompson, M. D., & Dams, R. V. (1990). Forest and land cover mapping from SAR: a summary of recent tropical studies. Proceedings of the Twenty-third International Symposium on Remote Sensing of Environment, 18-25 April 1990 (pp. 509-516), Bangkok, Thailand: ERIM.

Thompson, M. D., Macdonald, B. C., & Jeffries, W. C. (1993). Progress in forest mapping using airborne radar in tropical regions. *ITC Journal, 4*, 347-354.

Toutin, T., & Amaral, S. (2000). Stereo RADARSAT Data for Canopy Height in Brazilian Forests. *Canadian Journal of Remote Sensing, 26*, 189-199.

Tucker, C. J. (1977). Asymptotic nature of grass canopy reflectance. *Applied Optics, 16*, 1151-1157.

Tucker, J. M., Brondizio, E. S., & Morán, E. F. (1998). Rates of Forest Regrowth in Eastern Amazonia: A Comparison of Altamira and Bragantina Regions, Pará State, Brazil. *Interciencia, 23*, 64-73.

Uhl, C., Buschbacher, R., & Serrao, E. A. S. (1988). Abandoned pastures in Eastern Amazonia. I. Patterns of plant succession. *Journal of Ecology, 76*, 663-681.

van der Sanden, J. J. (1997). Radar remote sensing to support tropical forest management. Wageningen, The Netherlands (Wageningen Agricultural University), Tropenbos-Guyana Series 5, doctoral thesis, 330 p.

van der Sanden, J. J., & Hoekman, D. H. (1999). Potential of Airborne Radar to Support the Assessment of Land Cover in a Tropical Rain Forest Environment. *Remote Sensing of Environment, 68*, 26-40.

Verhoeye, J., & De Wulf., R. (1999). An Image Processing Chain for Land-Cover Classification Using Multitemporal ERS-1 Data. *Photogrammetric Engineering & Remote Sensing, 65*, 1179-1186.

Yanasse, C.C.F., Sant'Anna, S.J.S., Frery, A.C., Rennó, C.D. Soares, J.V. & Luckman, A.J. (1997). Exploratory Study of the Relationship between Tropical Forest Regeneration Stages and SIR-C L and C Data. *Remote Sensing of Environment, 59*, 180-190.

AMENDMENT TO CHAPTER 2

Since Chapter 2 was published in 2003, scientists have continued to explore methods of improving tropical secondary forest biomass estimates. Landsat TM and ETM+ persist as important data sources for this goal. Foody et al. (2003), for example, compared three predictive approaches (vegetation indices, multiple regression, neural networks) for biomass estimation at sites in Brazil, Malaysia and Thailand using Landsat TM data. The strongest relationships occurred using the neural network approach at each site ($r>0.71$), although transferring predictive relations between sites was problematic. Also successful with neural networks and Landsat ETM+ data, Ingram et al. (2005) found strong predictive relationships for basal area (a structural feature related to successional stage) in tropical forests of southeastern Madagascar. Furthermore, Arroyo-Mora et al. (2005), using Landsat ETM+ imagery and IKONOS high spatial resolution imagery, have contributed to improved mapping of successional stages in tropical dry forests of Costa Rica. Their work, in keeping with the findings of our review, stresses the importance of describing secondary forests in terms of successional stage rather than chronological age.

Beyond the use of data from Landsat sensors, advances in technology are providing the means to benefit secondary forest biomass estimates in tropical forests even further. For instance, large improvements in classifying land-use and land-cover classes have been achieved using hyperspectral Hyperion data over data from more traditional multispectral sensors (Thenkabail et al. 2004). Although a combination of hyperspectral and hyperspatial satellite imagery remains to be achieved, airborne imagery of this nature has been used successfully for identifying tree species in tropical forests (Clark et al., 2005). Similarly, lidar (light detection and ranging), an active remote sensing system that measures return time for a laser pulse, has been used effectively to estimate sub-canopy elevation and tree heights in a tropical wet forest of Costa Rica (Clark et al. 2004). Radar technology also continues to advance rapidly. The anticipated ALOS PALSAR instrument (http://www.eorc.jaxa.jp/ALOS/about/palsar.htm) (scheduled for launch in January 2006) is a fully polarimetric L-band SAR with spatial resolutions of 10 and 100 m. PALSAR data may become an excellent data source for tropical secondary forests, providing a compliment to electro-optical data without the impediment of cloud-cover. Through new capabilities such as these, it follows that improved characterization of successional status in tropical forests should be possible, and we expect to see evidence of this in the literature in the near future.

LITERATURE CITED

Arroyo-Mora, J. P., Sanchez-Azofeifa, G. A., Kalacska, M. E. R., Rivard, B., Calvo-Alvarado, J. C. & Janzen, D. H. (2005). Secondary forest detection in a Neotropical dry forest landscape using Landsat 7 ETM+ and IKONOS imagery. *Biotropica*, *37*, 497-507.

Clark, M. L., Clark, D. B. & Roberts, D. A. (2004). Small-footprint lidar estimation of sub-canopy elevation and tree height in a tropical rain forest landscape. *Remote Sensing of Environment*, *91*, 68-89.

Clark, M. L., Roberts, D. A. & Clark, D. B. (2005). Hyperspectral discrimination of tropical rain forest tree species at leaf to crown scales. *Remote Sensing of Environment*, *96*, 375-398.

Foody, G. M., Boyd, D. S. & Cutler, M. E. J. (2003). Predictive relations of tropical forest biomass from Landsat TM data and their transferability between regions. *Remote Sensing of Environment*, *85*, 463-474.

Ingram, J. C., Dawson, T. P. & Whittaker, R. J. (2005). Mapping tropical forest structure in southeastern Madagascar using remote sensing and artificial neural networks. *Remote Sensing of Environment*, *94*, 491-507.

Thenkabail, P. S., Enclona, E. A., Ashton, M. S., Legg, C. & De Dieu, M. J. (2004). Hyperion, IKONOS, ALI and ETM+ sensors in the study of African rainforests. *Remote Sensing of Environment*, *90*, 23-43.

CHAPTER 3—Comparison of spectral indices obtained using multiple spectroradiometers[1]

INTRODUCTION

Vegetation indices such as the Normalized Difference Vegetation Index (NDVI=NIR-Red/NIR+Red) and Simple Ratio (SR=NIR/Red) are computed from both broadband sensors (e.g. Landsat, where NIR (TM band 4) = 760-900 nm and Red (TM band 3) = 630-690 nm) and narrowband sensors, such as high spectral resolution spectroradiometers with a bandwidth of one to a few nanometers. These sensors may vary greatly in spatial resolution as well, from images with pixel dimensions of approximately 1 km^2 to less than 1 m^2, to laboratory spectra, with fields of view of several centimetres to a few millimetres. Within this range of spatial resolutions, the area of interest may range from homogeneous to highly heterogeneous with regard to reflectance properties and topography.

The spectral and spatial resolution of the instrument used to gather the data from which spectral indices are computed obviously impact the outcome and interpretation of such indices. Recently, the use of narrowband indices has proliferated in studies involving either leaf-level (e.g. Richardson & Berlyn, 2002; Sims & Gamon, 2002; Tambussi et al., 2002; Thenot et al., 2002) or *in situ* canopy-level reflectance spectra (e.g. Stylinski et al., 2002; Trotter et al., 2002). These types of indices, such as the photochemical reflectance index (PRI), structure-insensitive pigment index (SIPI), and variations of the simple ratio (SR) and normalized difference index (the narrow-band formulation designated here as ND to distinguish it from the broad-band based NDVI) are generally used to detect subtle differences in vegetation pigment content, previously impossible with broadband sensors.

The purpose of this paper is to present the results of a comparative study in which reflectance of the same leaves was recorded using three spectrometers, each with a unique spectral resolution and sampling interval. We discuss the variability exhibited by spectral indices (PRI, SIPI, SR_{705}, mSR_{705}, ND_{705}, mND_{705}) obtained using the different spectroradiometers under two scenarios: first, with a fixed illumination and viewing geometry and eliminating field of view effects between instruments, and second, using a 'typical' illumination and viewing configuration for each instrument. The three species used for the experiment, coffee (*Cafea arabica*), lantana (*Lantana camara*), and loquat (*Eriobotrya japonica*) represent a variety of leaf surface morphologies.

This research is intended to form part of the Spectral Network (SpecNet) data-sharing cooperative and addresses its theme of instrument comparison and standardization of sampling procedures. In particular, it has implications for reporting and interpretation of indices derived from multiple spectroradiometers.

---

[1] A version of this chapter has been accepted for publication. Castro-Esau, K. L., Sanchez-Azofeifa, G. A. & Rivard, B. (in press). *Remote Sensing of Environment*. Reprinted with permission from Elsevier.

METHODS

Sample collection

The three species sampled for this study have contrasting leaf surface characteristics: 1) coffee (*Cafea arabica*, Family: Rubiaceae), has smooth, shiny, dark green leaves, 2) lantana (*Lantana camara*, Family: Verbenaceae), has rough, lighter green leaves, and 3) loquat (*Eriobotrya japonica*, Family: Rosaceae) has thick, leathery leaves with a heavy greyish pubescence on the surface. If rubbed off, the leaf surface underneath is dark and shiny. Forty healthy, mature leaves were collected per species from an atrium at the University of Alberta. They were placed in sealable plastic bags with moistened paper towels, and brought immediately (within 15 minutes) back to the spectroscopy laboratory for spectral measurements.

Instruments

Spectral reflectance of the forty leaves was measured using three spectroradiometers under different set-up configurations described in section 2.4. The three spectroradiometers employed in the study are the Analytical Spectral Devices FieldSpec Pro FR (Analytical Spectral Devices, Boulder, CO, USA) (abbreviated here as FR), Analytical Spectral Devices FieldSpec HandHeld, (Analytical Spectral Devices, Boulder, CO, USA) (abbreviated as HH) and UniSpec Spectral Analysis System (PP Systems, Amesbury, MA, USA) (abbreviated as UN). Instrument specifications are described in Table 3-1. It should be noted that the actual FieldSpec Pro FR wavebands (at 1.4 nm (VNIR) and 2 nm (SWIR) spacings, Table 3-1) are not reported, but undergo an automatic interpolation to 1 nm spacings. The interpolation is accomplished using a linear equation in the VNIR region and a polynomial equation in the SWIR.

In this paper, spectral resolution refers to the Full Width at Half Maximum (FWHM) of the typical Gaussian-shape of the detector sensitivity (Jensen, 2000). There are typically >1 sampling intervals within the spectral resolution of the instrument, and this oversampling reduces degradation when spectra are resampled to match wavelengths of other sensor bands (van Aardt, 2000).

Additionally, an 1800-12S External Integrating Sphere (LI-COR Inc., Lincoln, NE, USA) was used to measure directional-hemispherical reflectance for this study. The integrating sphere is internally coated with barium sulfate, which is highly diffuse. There are six ports on the sphere. Four of these consistently hold the same item during diffuse reflectance measurements. These include the spectrometer fibre-optic port, the reference standard (barium sulphate) port, the leaf sample port, and the transmittance lamp port (this port is located behind the sample port and contains a hollow black plug during reflectance measurements). The remaining two ports contain either the sphere lamp, the 1800-12S illuminator, or a white plug. These two items are interchanged based on what is measured (dark reading, white reference reading, or sample reflectance). The reflectance reference is recorded while the sphere lamp is directed toward the barium sulphate reference standard. Diffuse reflectance of a sample is recorded when the light source is directed towards the sample, and a spectrometer fibre-optic, inserted in a sphere port, views the sphere wall.

Leaf freshness test

Prior to the main experiment, a freshness test was performed to determine if leaf reflectance changed while the leaf was held in the sample port of the integrating sphere under constant illumination, as was necessary for scenario one, described in section 2.4. The test was performed using the UniSpec and the 1800-12S External Integrating Sphere. At the onset of the test, the UniSpec and sphere illuminator warmed up for one hour. The UniSpec integration time was then adjusted followed by a dark scan and white reference (barium sulfate) scan. With a single leaf in the sample port, spectral reflectance was measured, first at one-minute intervals for the first ten minutes, and then at five-minute intervals for the remainder of the time (one hour for the *Cafea arabica* leaf, 30 minutes each for *Lantana camara* and *Eriobotrya japonica*). A new white reference scan was performed prior to each measurement.

Measurements of spectral reflectance

Spectral reflectance of the forty leaves per species was recorded using two illumination and viewing scenarios. Leaves one through forty were measured in the same order for each instrument and scenario. During the period when measurements were made, leaves were kept in the sealed bags with wet towels around the petioles to maintain freshness.

For both scenarios, instruments were turned on a minimum of 45 minutes prior to taking measurements.

Scenario 1.

The first scenario was designed to compare diffuse reflectance of the 40 leaf samples using the three instruments under the same illumination and viewing conditions, while at the same time eliminating any possible effects associated to differences in FOV. This type of configuration was achieved by alternately inserting the fibre-optics of each instrument into the same port of the 1800-12S External Integrating Sphere (3- 1, top diagram).

Although the bare fibre-optic field of view (FOV) differs between the ASD instruments (25°) and the UniSpec (40°) (Table 3-1), the fact that each fibre-optic views diffusely reflected light on the sphere wall rather than viewing a portion of the sample directly eliminates any potential observation differences due to differing FOV. In other words, although they view different-sized areas of the sphere wall, since the energy per unit area on the wall is uniform, the fibre-optics receive the same photon flux.

Instrument optimization and reflectance reference measurements were performed prior to sample measurements. For the UniSpec, integration time was adjusted to the sphere conditions (UniSpec halogen lamp off, sphere lamp on) and tested periodically thereafter, but found not to change. A dark scan was taken for every one to two sample measurements and a white reference scan was taken before every sample measurement. Ten scans were averaged per sample measurement. Likewise, for the ASD FieldSpec HandHeld, the configuration was adjusted to 10 scans per dark current, white reference, and sample measurement. Integration time was adjusted with the fibre-optic exposed to white reference conditions, so that the spectrum would peak but not saturate. Periodic checks also indicated that it was unnecessary to change the integration time during scenario one measurements. A white reference measurement was taken prior to each leaf measurement. The white reference activates a dark current measurement, which was

therefore taken for each leaf also. For the ASD FieldSpec Pro FR, configuration was adjusted to that described above for the FieldSpec HandHeld, and the instrument was optimized every one to two measurements. A white reference scan was taken before every leaf spectrum, which also activated a dark scan.

With the leaf inserted into the sample port, a reflectance measurement was taken using each spectrometer. During the period of these three measurements, the leaf was not moved, but remained inside the sample port for a total of three and a half to six minutes. This sequence was repeated for each of the 40 leaves. To avoid potential systematic effects related to a combination of instrument order and/or declining leaf freshness, the order of spectrometers used to take measurements was reversed after each leaf for *Cafea arabica* (UN-HH-FR, then FR-HH-UN), and for *Lantana camara* and *Eriobotrya japonica*, which were measured at a later date, rotated among all six possible combinations of the three instruments.

In all cases, reflectance spectra were obtained by determining the ratios of data acquired for a sample (an average of 10 scans) to data acquired for a white reflectance standard (barium sulphate). When using the 1800-12S External Integrating Sphere, white reference measurements were obtained with the lamp directed toward the reference standard. To obtain sample reflectance, the lamp was moved to a new position, directed toward the leaf sample in the sample port. The barium sulphate reference was mounted in the 1800-12S reference holder and was not removed during sample measurements. Procedure for obtaining reflectance from the three spectrometers was slightly different based on instrumentation requirements, but in all cases a white reference measurement was obtained before recording each leaf spectrum for each instrument.

Scenario 2.

The second scenario involved collection of reflectance spectra of the same 40 leaves under conditions that would be considered typical for each instrument. In this case, bi-directional configurations were used rather than employing an integrating sphere (Table 3-1).

For the ASD FR and HH, an external 50 W halogen lamp was set up with an illumination angle of 45 degrees. Besides the lamp, there were no other sources of illumination in the laboratory and therefore no environmental contribution. The instrument fibre-optic was fit through a mounting gun attached to a tripod, and adjusted to a nadir viewing position (Figure 3-1, middle diagram). Between the ASD FR and HH measurements, the same mounting gun was used and the lamp was not moved from its position. The distance from the fibre-optic to the sample was 2.5 cm, which translated to a FOV of approximately 11 mm (using a 25° bare fibre-optic). Prior to sample measurements, ASD HH integration time was adjusted as required, and found not to change throughout the time of the scenario 2 measurements. ASD FR optimization was performed at the same time as each white reference (every fifth leaf for both HH and FR). Instrument configuration was adjusted as in scenario 1, with ten scans averaged per white reference, dark current, and sample reflectance spectrum. Reflectance spectra were recorded as the ratio of sample data to white reference (99% reflectance Spectralon panel) data under the same illumination and viewing conditions. Sample reflectance was recorded by placing a black 2% reflectance panel beneath the leaf. Reflectance of all 40 leaves was first measured using the ASD FR, and then the instruments were switched and all 40 were measured using the ASD HH. Leaves, which had been numbered 1 through

40, were measured in the same order for each instrument. The measurements were always taken to the same side of the leaf midrib, midway between the top and bottom of the leaf, to approximate the same FOV for the two instruments. Actual position of the FOV would have differed since placement of the leaves under each instrument fibre-optic was not an exact match, neither with respect to area of the leaf within the FOV nor the orientation of the leaf toward the sensor, since the leaf was not flat.

Bi-directional reflectance measurements with the UniSpec involved a notably different set-up involving a bifurcated fibre-optic. One branch delivers light from an internal 7.0 W halogen lamp, and the other returns the reflected light to the detector. A leaf clip was attached to the fore-optic, achieving several purposes: it shields the sample from ambient light, it limits the FOV to a constant 2.3 mm, and it holds the fore-optic at a constant 60° (Figure 3-1, bottom diagram). Since the fore-optic provides the light source, the incident and emitted light are in the same plane, unlike the set-up for the ASD FR and HH. Prior to scenario two measurements, integration time was set with the white reference standard (Spectralon) in the leaf clip, and, after periodic checks, found not to require adjusting thereafter. A dark scan and white reference were performed every 15-20 spectra (every 3-4 leaves). Sample reflectance for the UniSpec was obtained by inserting a leaf into the leaf clip and comparing leaf reflectance to reflectance of the white Spectralon standard, also inserted into the leaf clip. Since FOV for the UniSpec leaf clip (2.3 mm) was less than that of the ASD FR or HH (~11 nm), five measurements were taken in a small circular area to one side of the leaf midrib, approximating the area measured by the ASD FR and HH. The five measurements were later averaged to obtain one measurement per leaf. As previously, 10 scans were averaged per recorded spectrum.

Analyses and Statistics

Vegetation Indices

Six vegetation indices were computed from the leaf spectra: PRI, SIPI, SR_{705}, mSR_{705}, ND_{705}, mND_{705} (Table 3-2). These indices have been employed in recent literature (e.g. Richardson & Berlyn, 2002; Sims & Gamon, 2002) and make use of a good representation of wavebands throughout the visible and near-infrared regions.

These indices were computed using: 1) the nearest wavebands for each instrument, 2) identical wavebands after all data (from the three instruments) were linearly interpolated to 1 nm, 3) identical wavebands after all data were cubically interpolated to 1 nm, 4) the nearest wavebands after all data were linearly interpolated to 3.3 nm, and 5) the nearest wavebands after all data were cubically interpolated to 3.3 nm. The actual wavebands used in each case are shown in Table 3-3. We have conducted these interpolations since 1 nm is the band spacing given for the ASD FR, the instrument with the smallest band spacing (in fact, the 1nm band spacing is the result of interpolation of wider band spacings, Table 3-1), and 3.3 nm is the band spacing for the instrument with the widest band spacing, the UniSpec. Note that for all instruments, the actual bandwidth or spectral resolution (full-width half maximum) is approximately two to three times the reported band spacing.

D and θ Metrics

The metrics D and θ, described by Price (1994), were computed to determine if any existing differences between spectra were related to amplitude or shape. In each case, D and θ were calculated on pairs of spectra of the same leaf, but recorded by two

different spectrometers. These spectra are referred to as instrument-pair spectra and are computed within single species. The two metrics are calculated as follows:

$$D = \left[\frac{1}{\lambda_b - \lambda_a} \int_{\lambda_a}^{\lambda_b} \left[S_1(\lambda) - S_2(\lambda) \right]^2 d\lambda \right]^{1/2} \quad (1)$$

$$\theta = \cos^{-1} \left[\frac{\int S_1(\lambda) S_2(\lambda)\, d\lambda}{\left[\left[\int S_1(\lambda)^2 d\lambda \right]^{1/2} \left[\int S_2(\lambda)^2 d\lambda \right]^{1/2} \right]} \right] \quad (2)$$

D is the "root mean square difference between two spectra, S_1 and S_2, averaged over the spectral interval of observation, λ_a to λ_b" (Price, 1994). The second metric, θ, "corresponds to the angle between two vectors, as identified with a vector dot product, where the denominator serves to remove the amplitude dependence" (Price, 1994).

D and θ were computed with paired same-leaf data from each of the three instruments, i.e. 1) FR:HH, 2) FR:UN, and 3) HH:UN instrument-pair spectra. The range 450-900 nm was used to compute these metrics. From each combination, mean and standard deviation of the resulting 40 D and θ values was calculated. Only the data that were linearly interpolated to 1 nm were used to compute D and θ (the same calculations based on data interpolated to 3.3 nm would have given very similar results). D and θ were determined for both scenarios one and two.

To provide examples of between-species D and θ, in comparison to the within-species D and θ values reported for instrument-pair spectra, D and θ were also computed, using the ASD FR scenario one spectra only, for the three species-pairs. The species pairs were: 1) *Cafea arabica* and *Lantana camara*, 2) *Cafea arabica* and *Eriobotrya japonica*, and 3) *Lantana camara* and *Eriobotry japonica*. It would be expected that within-species D and θ values (based on instrument-pair spectra) would be smaller than between-species D and θ (based on species-pair spectra), provided by these three examples. In fact, in scenario one, within-species D and θ should be very close to zero, while deviations from zero indicate instrumental differences.

Statistical Tests

Results from section 2.5.1 were tested statistically to determine if computed indices differed based on the instrument used. The assumption of normality was assessed using normal probability plots of the data, and appeared reasonable overall. Even so, we used both parametric (t-test) and nonparametric (Wilcoxon signed rank) statistical tests to lend support to the conclusions of the hypotheses.

Since the experiments presented in this paper involve paired data; that is, the same 40 leaves measured in the same order by each instrument for each illumination and viewing scenario, two-tailed t-tests for paired data were performed. The two-tailed t-tests were conducted to evaluate the mean difference between the pairs. Three sets of t-tests were required, one for each instrument-pair (FR:HH, FR:UN, and HH:UN). Secondly, the Wilcoxon signed rank test of equality of medians (also for matched samples) was executed for each instrument-pair. This test is the nonparametric alternative to the t-test for paired data and requires less stringent assumptions.

Where the two tests agreed, we could be very confident of our results (Ott, 1993). In fact, it was found that the results of the parametric test and non-parametric alternative agreed in the large majority of cases. In the few exceptions where they did not agree, the conservative result (i.e. do not reject the null hypothesis) was reported. The null

hypothesis of each case stated that there was no significant difference (α=0.01) between a spectral index measured on the same leaves but from two different spectrometers. All analyses were performed in Matlab Version 13.

RESULTS

Freshness test

Over time, reflectance (measured by the UniSpec) of leaves maintained under illumination in the integrating sphere changed perceptibly (Figure 3-2). The three species exhibited unique responses to exposure from the sphere lamp. Visible reflectance of *Cafea arabica* declined slightly during the period of exposure. During the first ten minutes, the decrease in visible reflectance generally remained at or below two percent from the original, time zero reflectance. *Lantana camara* exhibited a noticeable rise in reflectance on either side of the green peak after a short (3-4 minute) drop. Of the three species, *Lantana camara* has the thinnest leaf, likely the most susceptible to wilt under the intense illumination of the sphere lamp. The leathery *Eriobotrya japonica* leaf exhibited slight initial drops in visible reflectance at 532 nm and 571.6 nm. At 680 nm, reflectance of all three species declined steadily. In the near-infrared wavelengths (748.6 nm and 800.7 nm), both *Cafea arabica* and *Eriobotrya japonica.*declined slightly over time, while *Lantana camara* exhibited a small initial decline in the first 2-3 minutes, and then began to rise (data not shown). Initial fluctuations in the visible wavelengths may be related to changes in the relative amounts of xanthophyll cycle pigments upon sudden exposure to high light intensity; later on, the leaf may have suffered heat stress and dehydration. Since in the main experiment of interest for this study (scenario one), leaves remained in the sphere for only 3.5-6 minutes, and the order of spectrometers was changed after each leaf, we consider the effect on spectral reflectance minimal.

Reflectance spectra

The best match between spectra obtained by the three instruments for coffee was scenario one, where illumination, viewing, and FOV conditions were held constant using the integrating sphere, in contrast to scenario two, where a 'typical' instrument configuration was used (Figures 3-3 & 3-4). In scenario two, illumination and viewing geometry were actually the same for the ASD FR and HH, but FOV was only approximated, which resulted in a notable difference between the average spectra of *Cafea arabica*, the shiny leaf, but less so for *Lantana camara* and *Eriobotrya japonica.* In the case of the UniSpec, scenario two, the same instrument recorded both the lowest average visible reflectance and the highest near-infrared reflectance for all species. This finding may be partly related to the different illumination and viewing configurations between the UniSpec and the other two spectrometers.

Indices

Indices computed from the three spectrometers differed significantly in the majority of cases, and attempts to reduce those differences using interpolation were largely unsuccessful. This was the case even under matched illumination, viewing, and FOV conditions (scenario one). The use of α =0.05 instead of α=0.01 would have changed this finding only in a small minority of cases. PRI and SIPI were the most and least affected by instrument, respectively (Tables 3-4 & 3-5). When compared, on a

percentage difference from FR values basis, *Cafea arabica* PRI values from the UN and HH differed between –22% and +86%, depending on scenario and interpolation combination. For *Lantana camara*, PRI values differed between -66% and +111%, and for *Eriobotrya japonica*, they differed between –99% and +121%. SIPI, however, consistently differed less than 1% between the three instruments (true for all three species). For the remaining four indices, SR_{705}, mSR_{705}, ND_{705}, mND_{705}, UN and HH index values typically differed between +/-6% from FR values, and never more than +/-15%.

Despite what appear to be small differences between indices derived from different instruments (with the exception of PRI), they were statistically different in many cases. For scenario one, this is likely due to the consistency of albeit small differences in reflectance spectra as measured by the three instruments under controlled conditions. In scenario two, where sample results were more variable than in scenario one, larger differences in means would have been required to observe significant differences between instruments.

***D* and θ**

Amplitude (*D*) and shape (θ) differences for instrument-pair spectra were minor in the case of scenario one, for which reflectance measuring conditions were alike (Figures 3-5 & 3-6). As expected, *D* and θ were much greater for instrument combinations in scenario two, and variability was also greater. Even the FR:HH combination for scenario two exhibited fairly large *D* and θ, despite the fact that the illumination, viewing and approximate FOV were matched; however *D* and θ were lower for the scenario two FR:HH combination than for either the FR:UN or HH:UN. With respect to the three species, *Cafea arabica*, the shiniest leaf, consistently had higher *D* and θ values for instrument-pair spectra than either *Lantana camara* or *Eriobotrya japonica*, regardless of scenario or combination of instruments. The effect of scenario two on *D* and θ values was similar in magnitude to comparing entirely different plant species (species-pair spectra), rather than the same leaves of the same species (Figures 3-5 & 3-6).

DISCUSSION AND CONCLUSIONS

Same-leaf spectra recorded by multiple spectroradiometers differed. Interpolation to match the three sampling intervals was generally ineffective at bringing each index into agreement across instruments. While this was an expected result for scenario two, in which illumination and viewing geometry differed between the UN and the ASD instruments, and FOV could not be matched exactly between the ASD FR and HH, it was unexpected for scenario one, in which these effects were eliminated. For the majority of scenario one and two interpolations and indices, significant instrument effects ($P<0.01$) were observed for each species (Tables 3-4 & 3-5). These differences were particularly acute for PRI (Table 3-4).

Why do these differences occur for scenario one? There are a number of possible reasons. Instrument sensitivities are clearly different (Table 3-1). Spectral resolution, a measure of the narrowest spectral feature that may be resolved by an instrument, is significantly poorer (<10 nm) for the UN than either the FR (3 nm) or the HH (3.5 nm), and the UN sampling interval is at least double that of the HH or FR. Small spectral

features that would be well-defined by the ASD instruments would therefore not be detected by the UN. In fact, this was observed prior to the experiment when comparing spectra of calibration standards (dysprosium oxide, erbium oxide, and holmium oxide), which had sharp absorption features. Coarser resolution may partially explain the ineffectiveness of interpolating UN spectra to 1 nm, but it does not help explain the poor results of degrading FR and HH data to 3.3 nm. It should be kept in mind that while the apparent band spacing of the FR is 1 nm, the actual band spacing (1.4 nm in the VNIR, 2 nm in the SWIR regions) is lost due to an automatic interpolation performed by FR instrument software. This is an unknown that may be an additional source of error in our paper. In any case, the argument of differing spectral resolutions as the cause of differences in same-leaf spectra is lessened by the fact that there are no sharp spectral features in a leaf spectrum, but rather gradual ones. Signal-to-noise ratios (SNR) will also differ between instruments. While SNR was not quantified in this experiment, we attempted to reduce inconsistencies by averaging ten scans per spectrum for each instrument. Integration time, however, differed between the instruments, the longest of which was for the HH. Increasing number of scans averaged per spectrum would have improved SNR for all instruments and could have influenced the results of the experiment slightly. However, within the spectral range used for this experiment (see Table 3-2 for index wavelengths, 450-900 nm for D and θ computation), spectra appeared smooth for all instruments, and improvements in SNR would not have eliminated all amplitude and shape differences between the spectra. Stray light in the integrating sphere was tested prior to the experiment using the FR fibre-optic and found to be minimal. While both the FR and HH fibre-optics fit snugly into the sphere port, the UN fibre-optic would slip if not held in place. Therefore, it was held in place for each measurement, to the point at which a wider portion of the fibre-optic cable rested flush with the entrance to the sphere port. The issue of declining leaf freshness while each leaf remained in the sphere port for 3.5-6 minutes should have been averaged out by changing the order of instrument with each successive leaf; however, in the case of *Cafea arabica*, the first species recorded, simply reversing the order of instrument signified that the HH was the middle measurement in all cases. While this could have been a source of error, the fact that discrepancies between spectra from the three spectrometers were observed for all three species seems to indicate that it is not an important one. In the case of PRI, another reason for the apparent discrepancies between instruments may be the fact that this index can be very dynamic, with actual values varying with time of light exposure and physiological state (Gamon & Surfus, 1999). While we made attempts to minimize error by varying the order of sampling, this could have been the source of some of the discrepancies between instruments when reporting PRI values. Although each of the possible sources of error mentioned above appear minor, in combination they may have led to the small but significant differences observed in same-leaf spectra from the different spectrometers.

For scenario two, as indicated, differences in spectra recorded by the three instruments were expected. The second scenario was intended to illustrate the magnitude of differences in leaf spectra that could be expected since, typically, different users will employ different set-up configurations, or, alternatively, set-up geometry may be limited by the instrument itself. UN spectra were recorded at a 60° illumination angle and 60° viewing angle geometry, with the leaf FOV and light source contained within a leaf clip.

FR and HH spectra were recorded at a 45° illumination angle and nadir viewing geometry, while the leaf was positioned on a black non-reflective panel under the illumination of an external lamp. The differences in set-up geometry would be expected to have the greatest impact on the shiny (*Cafea arabica*) leaves, which would have been most influenced by specular reflection. The leaf FOV for which spectra were recorded, although approximated, differed between all three instruments. As such, non-homogeneity in the leaf surfaces, including features such as veins, would have translated into small differences in spectral reflectance as recorded by the three instruments. Of particular note, a small (2.3 mm) area of leaf was held relatively flat by the UN leaf clip. For the FR and HH, however, leaves were placed on a surface under the mounted fibre-optic. The leaves were not flat, although some attempt was made to position them as flat as possible within the fibre-optic FOV. Therefore, the differing leaf topographies with respect to orientation toward the sensors would have caused differences between the spectra recorded by the three instruments, particularly for the *Cafea arabica* leaves in which small changes in leaf positioning could cause notable changes in specular-type reflection on different parts of the leaf surface. This was also true for the *Eriobotrya japonica* leaves, which often tended to have a convex curve with respect to the upper surface. The *Lantana camara* leaves, on the other hand, were relatively flat. Lastly, although Spectralon was used as the white reference standard for all scenario two measurements, one standard was used for the UN, and a different one for the FR and HH. A spectrum of the UN Spectralon reference as compared to the laboratory Spectralon panel used for the FR and HH showed some incongruities towards shorter wavelengths that might have contributed to the spectral differences reported in scenario 2.

The observed differences in spectra between instruments have several implications for users. Since scenario two is more the reality than scenario one, differences in reflectance spectra between instruments can be expected to be large (Figure 3-4). The use of indices will reduce these effects, but not eliminate them. The most apparent implication is that care should be taken when comparing indices across instruments, such as in multiple published studies. The same is true for cases in which particular wavebands or vegetation indices are correlated with pigment content, such as chlorophyll and/or carotenoid concentration (e.g. Buschmann & Nagel, 1993; Merzlyak et al., 1993; Richardson et al., 2002; Sims & Gamon, 2002). Separate regressions may be required for different spectrometers. Sensor choice and measurement configuration may also influence which bands are selected as optimal for correlation with pigment concentrations. In the same way, spectral reflectance inputs to inverted radiative transfer models may require adjustments based on instrument. Leaf-level spectral libraries gathered using one model of spectrometer may not be highly useful for species classifications of leaf spectra gathered by another model of spectrometer. Fine spectral features, such as the first derivative double-peak observed by Zarco-Tejada et al. (2003) may be less clear in the coarser resolution spectrometers such as the UniSpec (although see Sims et al., submitted). Similarly, measurement of the 'blue shift' requires 1- to 5 nm resolution (Ustin et al., 2004), and thus may be more accurately tracked with the ASD HH or FR. To what degree instrument affects canopy-level spectra will also be important to determine.

For some applications, however, differences in spectra recorded by multiple spectrometers may not be important on a practical level. With the exception of PRI, the

differences of within-index, between-instrument values (instrument-pair spectra), albeit significant in many cases, were within a few percent of each other for scenario one and, surprisingly, even scenario two. For example, *Cafea arabica* ND_{705} values computed on raw data were 0.5202, 0.5457, and 0.5416 for the UN, HH and FR under scenario one, respectively. When linearly interpolated to 1 nm, the values became 0.5485, 0.5316, and 0.5416. Similarly, linear interpolation to 3.3 nm resulted in ND_{705} of 0.5202, 0.5016, and 0.5118, respectively. In each of the three cases, the ND_{705} from the different spectrometers was significantly different ($P<0.01$) based on both a paired t-test as well as a non-parametric alternative, the Wilcoxon signed rank test. The magnitude of differences in ND_{705} values between instruments for scenario two were similar to those from scenario one or slightly smaller or larger. However, whether or not the magnitude of these differences is important to an investigator wishing to compare results between studies is the question. If the overall range of values observed in a study is much greater than the differences in values observed between instruments, the instrument effect is likely trivial.

Of the six indices, however, PRI is an exception in the relatively drastic manner it was affected by both instrument and interpolation method. The reason for this is likely related to the fact that both PRI wavebands, 531 and 570 nm, are in regions of slope change. Additionally, the 531 nm reflectance value has been shown to be very dynamic with physiological state and illumination history (Gamon et al., 1992). These factors render PRI unstable compared to other indices that have at least one waveband rooted in a fairly flat, stable area of the spectrum (e.g. 445 and 800 nm, both used in SIPI). Average PRI of the same 40 *Cafea arabica* leaves, measured under the same illumination and viewing configuration (scenario one), was 0.0609, 0.0624 and 0.0504, respectively, for the UN, HH, and FR, when using non-interpolated data and the nearest waveband (Table 3-4). The UN and HH values differ >20% from the FR value. For the UN alone, PRI values, again of the same 40 leaves, were 0.0609, 0.0389, and 0.0400, respectively, for non-interpolated, linearly interpolated, and cubically interpolated data (to 1nm). Again, note that wavebands in areas of slope change (such as those used to compute PRI) will be affected by interpolation much more so than wavebands in flat areas (e.g. see results for the interpolation of UN SIPI values, which barely change when interpolated). By interpolating the UN 3.3 nm data to 1 nm, matching the FR 1 nm data was attempted. However, the linear and cubic interpolated 1nm UN spectra resulted in PRI values of 0.0389 and 0.0400, respectively, which are no closer to the FR PRI of 0.0504 than the original non-interpolated UN PRI of 0.0609. Conversely, the reverse was attempted. The FR 1 nm spectra were degraded to the UN sampling interval of 3.3 nm. In this case, the FR PRI (originally 0.0504) became 0.0708 and 0.0709, respectively, using either linear or cubic interpolation, also overshooting the UN PRI of 0.0609 at the same sampling interval (3.3 nm). The sensitivity of PRI to instrument could potentially affect interpretations of plant pigment content and photosynthetic radiation use efficiency if instrument differences are not carefully considered.

In conclusion, we present the outcome of this experiment as a cautionary note against direct comparison of indices derived from reflectance spectra gathered from different spectrometers. In reality, investigators use a wider variety of instrument configurations for their studies than explored here, a fact that would likely amplify the differences observed in our experiment. Since spectral differences between instruments

occurred for all three species, we do not consider the results to be an isolated phenomenon for a single leaf type. For the three instruments used in this study, there were minor to major shape and amplitude differences between spectra of the same leaves. To use indices effectively and confidently, they should be accompanied by context, for instance an array of values, collected from the same instrument, that span a range of vegetation health, leaf maturity, functional/structural groups, or that serve to compare between species. Furthermore, authors who decide to interpolate (e.g. Sims & Gamon, 2002) or not (e.g. Trotter et al., 2002) should be well aware of the effect interpolation has on values of indices, which can be considerable. Whether spectral data are interpolated or not, and if not, what specific instrument channels are used to compute indices, should be reported in studies involving hyperspectral data.

Table 3-1. Characteristics of spectroradiometers used in this study and an overview of illumination and viewing scenarios 1 and 2

					Scenario 1	Scenario 2			
Instrument	**Spectral range**	**Spectral resolution (FWHM)[a]**	**Sampling interval**	**Bare fibre-optic FOV**	**Light source**	**Light source**	**Illumination angle**	**Viewing angle**	**Diameter of field of view**
ASD FieldSpec Pro FR (FR) (model FSP 350-2500P)	350-2500 nm	3 nm at 700 nm 10 nm at 1400 & 2100 nm	1.4 nm (350-1050 nm) 2 nm (1000-2500 nm)[b]	25°	LI-COR 1800-12S illuminator	External 50 W halogen lamp	45°	Nadir	11 mm
ASD FieldSpec HandHeld (HH) (model FSHH 325-1075P)	325-1075 nm	3.5 nm at 700 nm	1.6 nm	25°	LI-COR 1800-12S illuminator	External 50 W halogen lamp	45°	Nadir	11 mm
UniSpec Spectral Analysis System (UN) (model UniSpec, Serial No. 9742)	350-1100 nm	< 10 nm	3.3 nm	40°	LI-COR 1800-12S illuminator	Internal 7.0 W halogen bulb	60°	60°	2.3 mm

[a]FWHM=full width at half maximum of an emission line. [b]Both 1.4 nm and 2 nm sampling intervals are automatically interpolated to 1 nm intervals by this instrument.

Table 3-2. Spectral indices computed in this study

Index		Computation	Significance	Source
Photochemical reflectance index	PRI	$(R_{531}-R_{570})/(R_{531}+R_{570})$	Correlated with the epoxidation state of xanthophyll cycle pigments and photosynthetic radiation use efficiency	Gamon et al., 1992
Structure-independent pigment index	SIPI	$(R_{800}-R_{445})/(R_{800}-R_{680})$	Correlated with the carotenoid:chlorophyll *a* ratio	Peñuelas et al., 1995
Simple ratio	SR_{705}	R_{750}/R_{705}	Estimation of chlorophyll content	
Modified simple ratio	mSR_{705}	$(R_{750}-R_{445})/(R_{705}-R_{445})$	Estimation of chlorophyll content	Sims & Gamon, 2002
Normalized difference index (also called 'Chlorophyll index')	ND_{705}	$(R_{750}-R_{705})/(R_{750}+R_{705})$	Estimation of chlorophyll content	Gitelson & Merzlyak, 1994
Modified normalized difference index	mND_{705}	$(R_{750}-R_{705})/(R_{750}+R_{705}-2R_{445})$	Estimation of chlorophyll content	Sims & Gamon, 2002

Table 3-3. Wavebands used for computing indices listed in Table 3-2

	UniSpec			ASD HH			ASD FR		
Waveband of interest	Nearest waveband	Interpolated to 1 nm	Interpolated to 3.3 nm[a]	Nearest waveband	Interpolated to 1 nm	Interpolated to 3.3 nm	Nearest waveband	Interpolated to 1 nm[a]	Interpolated to 3.3 nm
445	445.9	445	445.9	445.5002	445	445.9	445	445	445.9
531	532	531	532	530.7551	531	532	531	531	532
570	571.6	570	571.6	570.2251	570	571.6	570	570	571.6
680	680	680	680	680.7408	680	680	680	680	680
705	706.2	705	706.2	704.4227	705	706.2	705	705	706.2
750	748.6	750	748.6	750.2079	750	748.6	750	750	748.6
800	800.7	800	800.7	800.7294	800	800.7	800	800	800.7

[a]Data were not actually interpolated since their original sampling interval matched the interpolation sampling interval.

Table 3-4. PRI computed with three spectroradiometers over 2 illumination and viewing scenarios

	Scenario 1			Scenario 2		
Interpolation and interval	***Cafea arabica***	*Lantana camara*	*Eriobotrya japonica*	*Cafea arabica*	*Lantana camara*	*Eriobotrya japonica*
No interpolation						
UN	0.0609 +/- 0.0076[a]	0.0306 +/- 0.0083[a]	0.0094 +/- 0.0077[a]	0.1052 +/- 0.0128	0.0672 +/- 0.0103	0.0501 +/- 0.0132
HH	0.0624 +/- 0.0075[a]	0.0325 +/- 0.0078[a]	0.0134 +/- 0.0082	0.0693 +/- 0.0234	0.0458 +/- 0.0094	0.0316 +/- 0.0092
FR	0.0504 +/- 0.0060	0.0247 +/- 0.0068	0.0101 +/- 0.0083[a]	0.0565 +/- 0.0160	0.0318 +/- 0.0083	0.0227 +/- 0.0086
Linear 1nm						
UN	0.0389 +/- 0.0063	0.0084 +/- 0.0081	0.0006 +/- 0.0066	0.0695 +/- 0.0101[a]	0.0342 +/- 0.0084	0.0319 +/- 0.0094[a]
HH	0.0625 +/- 0.0073	0.0330 +/- 0.0077	0.0135 +/- 0.0081	0.0694 +/- 0.0231[a]	0.0460 +/- 0.0093	0.0316 +/- 0.0090[a]
FR	0.0504 +/- 0.0060	0.0247 +/- 0.0068	0.0101 +/- 0.0083	0.0565 +/- 0.0160	0.0318 +/- 0.0083	0.0227 +/- 0.0086
Cubic 1nm						
UN	0.0400 +/- 0.0064	0.0092 +/- 0.0082	0.0009 +/- 0.0067	0.0714 +/- 0.0103[a]	0.0357 +/- 0.0085	0.0329 +/- 0.0097[a]
HH	0.0626 +/-0.0074	0.0331+/- 0.0077	0.0135 +/- 0.0082	0.0696 +/- 0.0233[a]	0.0462 +/- 0.0094	0.0319 +/- 0.0093[a]
FR	0.0504 +/- 0.0060	0.0247 +/- 0.0068	0.0101 +/- 0.0083	0.0565 +/- 0.0160	0.0318 +/- 0.0083	0.0227 +/- 0.0086
Linear 3.3 nm						
UN	0.0609 +/- 0.0076	0.0306 +/- 0.0083	0.0094 +/- 0.0077	0.1052 +/- 0.0128	0.0672 +/- 0.0103[a]	0.0501+/- 0.0132
HH	0.0789 +/- 0.0083	0.0505 +/- 0.0077	0.0208 +/- 0.0092[a]	0.0861 +/- 0.0281[a]	0.0647 +/- 0.0103[a]	0.0402 +/- 0.0097
FR	0.0708 +/- 0.0068	0.0468 +/- 0.0071	0.0188 +/- 0.0097[a]	0.0798 +/- 0.0226[a]	0.0561 +/- 0.0094	0.0346 +/- 0.0114
Cubic 3.3 nm						
UN	0.0609 +/- 0.0076	0.0306 +/- 0.0083	0.0094 +/- 0.0077	0.1052 +/- 0.0128	0.0672 +/- 0.0103[a]	0.0501+/- 0.0132
HH	0.0791 +/- 0.0083	0.0507 +/- 0.0078	0.0209 +/- 0.0092[a]	0.0862 +/- 0.0284[a]	0.0649 +/- 0.0104[a]	0.0402 +/- 0.0097
FR	0.0709 +/- 0.0068	0.0468 +/- 0.0071	0.0188 +/- 0.0097[a]	0.0799 +/- 0.0226[a]	0.0561 +/- 0.0094	0.0346 +/- 0.0114

Similar subscripts within an interpolation and interval scheme for a single species indicate indices that DO NOT differ significantly, based on both a paired t-test (α=0.01) and a Wilcoxon signed rank test

Table 3-5. SIPI computed with three spectroradiometers over 2 illumination and viewing scenarios

	Scenario 1			Scenario 2		
Interpolation and interval	***Cafea arabica***	*Lantana camara*	*Eriobotrya japonica*	*Cafea arabica*	*Lantana camara*	*Eriobotrya japonica*
No interpolation						
UN	1.0136 +/- 0.0078[a]	1.0091 +/- 0.0066[a]	1.0139 +/- 0.0122[a]	1.0276 +/- 0.0046[a]	1.0344 +/- 0.0046	1.0199 +/- 0.0052[a]
HH	1.0107 +/- 0.0044[a]	1.0057 +/- 0.0057	1.0111 +/- 0.0111[b]	1.0217 +/- 0.0083	1.0241 +/- 0.0094	1.0212 +/- 0.0085[a]
FR	1.0101 +/- 0.0069[a]	1.0096 +/- 0.0062[a]	1.0119 +/- 0.0108[ab]	1.0295 +/- 0.0075[a]	1.0307 +/- 0.0068	1.0288 +/- 0.0075
Linear 1nm						
UN	1.0135 +/- 0.0077[a]	1.0093 +/- 0.0065[a]	1.0141 +/- 0.0123[a]	1.0278 +/- 0.0046[a]	1.0347 +/- 0.0044	1.0199 +/- 0.0053[a]
HH	1.0099 +/- 0.0041[b]	1.0052 +/- 0.0058	1.0108 +/- 0.0111[b]	1.0203 +/- 0.0080	1.0228 +/- 0.0090	1.0202 +/- 0.0084[a]
FR	1.0101 +/- 0.0069[ab]	1.0096 +/- 0.0062[a]	1.0119 +/- 0.0108[ab]	1.0295 +/- 0.0075[a]	1.0307 +/- 0.0068	1.0288 +/- 0.0075
Cubic 1nm						
UN	1.0135 +/- 0.0077[a]	1.0092 +/- 0.0065[a]	1.0141 +/- 0.0123[a]	1.0277 +/- 0.0046[a]	1.0346 +/- 0.0044	1.0199 +/- 0.0053[a]
HH	1.0099 +/- 0.0042[b]	1.0051 +/- 0.0058	1.0108 +/- 0.0111[b]	1.0203 +/- 0.0080	1.0229 +/- 0.0090	1.0202 +/- 0.0084[a]
FR	1.0101 +/- 0.0069[ab]	1.0096 +/- 0.0062[a]	1.0119 +/- 0.0108[ab]	1.0295 +/- 0.0075[a]	1.0307 +/- 0.0068	1.0288 +/- 0.0075
Linear 3.3 nm						
UN	1.0136 +/- 0.0078[a]	1.0091 +/- 0.0066[a]	1.0139 +/- 0.0122[a]	1.0276 +/- 0.0046[a]	1.0344 +/- 0.0046	1.0199 +/- 0.0052[a]
HH	1.0099 +/- 0.0041[b]	1.0050 +/- 0.0057	1.0106 +/- 0.0110[b]	1.0204 +/- 0.0080	1.0227 +/- 0.0091	1.0201 +/- 0.0084[a]
FR	1.0101 +/- 0.0069[ab]	1.0095 +/-0.0062[a]	1.0117 +/- 0.0108[ab]	1.0294 +/- 0.0075[a]	1.0308 +/- 0.0069	1.0286 +/- 0.0074
Cubic 3.3 nm						
UN	1.0136 +/- 0.0078[a]	1.0091 +/- 0.0066[a]	1.0139 +/- 0.0122[a]	1.0276 +/- 0.0046[a]	1.0344 +/- 0.0046	1.0199 +/- 0.0052[a]
HH	1.0099 +/- 0.0042[b]	1.0050 +/- 0.0057	1.0106 +/- 0.0110[b]	1.0204 +/- 0.0080	1.0227 +/- 0.0092	1.0201 +/- 0.0084[a]
FR	1.0101 +/- 0.0069[ab]	1.0095 +/- 0.0062[a]	1.0117 +/- 0.0108[ab]	1.0294 +/- 0.0075[a]	1.0308 +/- 0.0069	1.0286 +/- 0.0074

Similar subscripts within an interpolation and interval scheme for a single species indicate indices that DO NOT differ significantly, based on both a paired t-test (α=0.01) and a Wilcoxon signed rank test

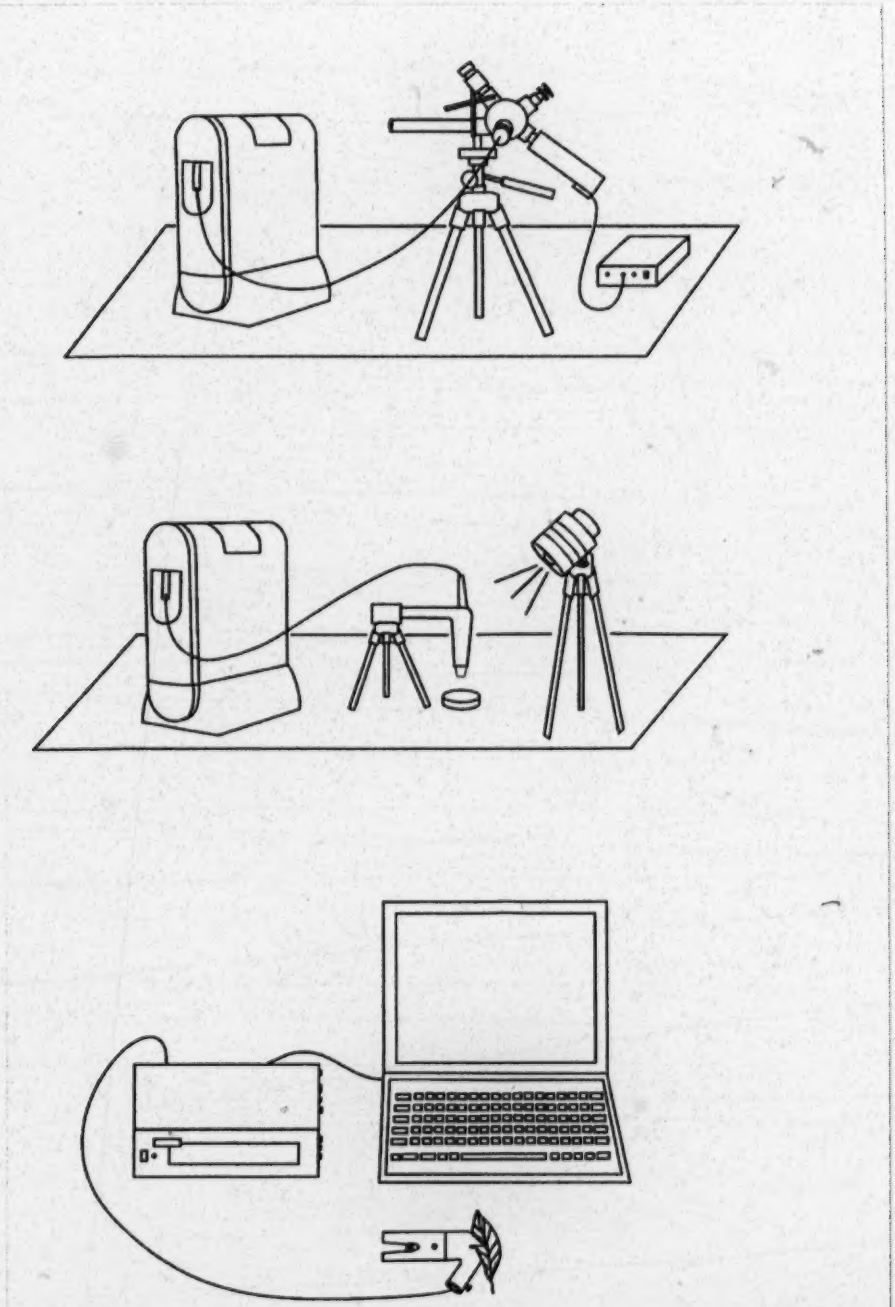

Figure 3-1. Illustration of instrument set-up. Top figure shows scenario one configuration with the FR fibre-optic inserted into the port of the integrating sphere. Sphere lamp is shown on the right. Middle figure shows scenario two configuration for the FR. Bottom figure shows scenario two configuration for the UN, with the fibre-optic inserted into the leaf clip.

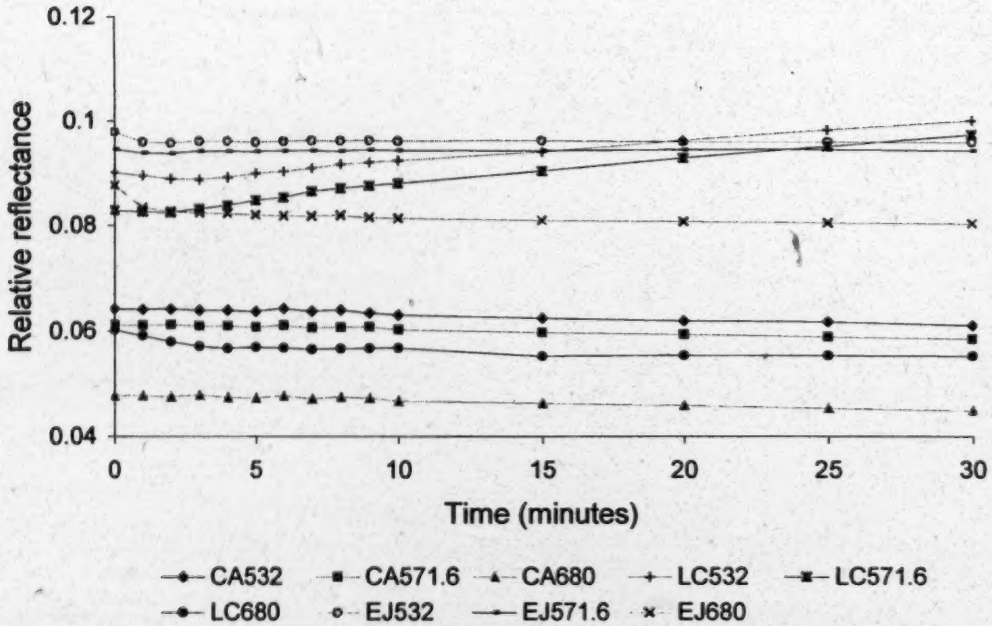

Figure 3-2. Changes in relative reflectance (measured with UniSpec) of three wavebands (532, 571.6 and 680 nm) over time for a *Cafea arabica* (CA) leaf, *Lantana camara* (LC) leaf, and *Eriobotrya japonica* (EJ) leaf under constant illumination in the sample port of an 1800-12S integrating sphere for 30 minutes.

Scenario 1

Cafea arabica

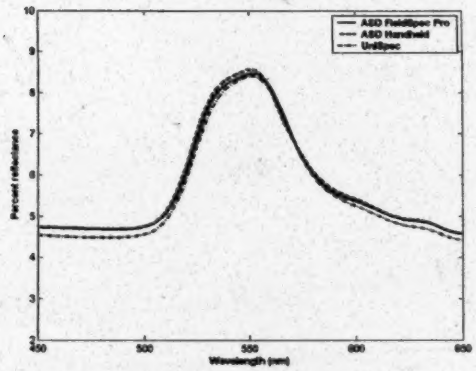

Lantana camara

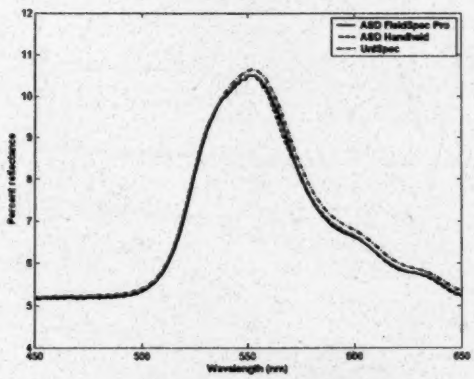

Eriobotrya japonica

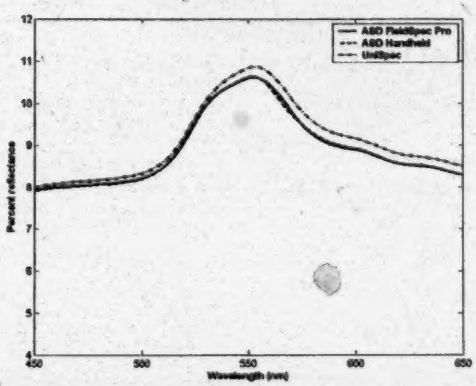

Figure 3-3. Average visible (top three graphs) and near-infrared (bottom three graphs) reflectance spectra of 40 leaves of three species as measured by three spectroradiometers under scenario one, which controlled for illumination, viewing, and FOV effects.

Scenario 1 cont'd.

Cafea arabica

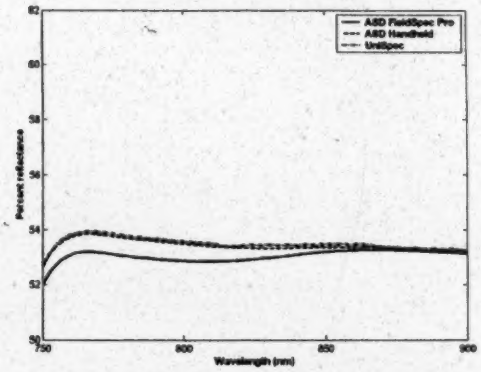

Lantana camara

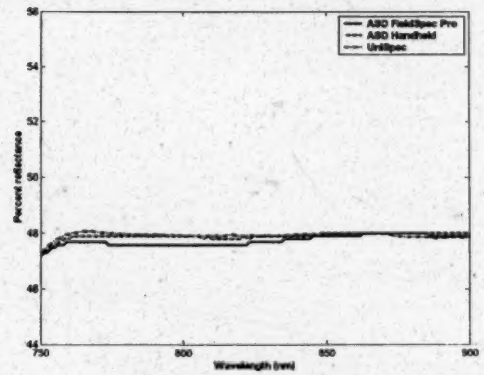

Eriobotrya japonica

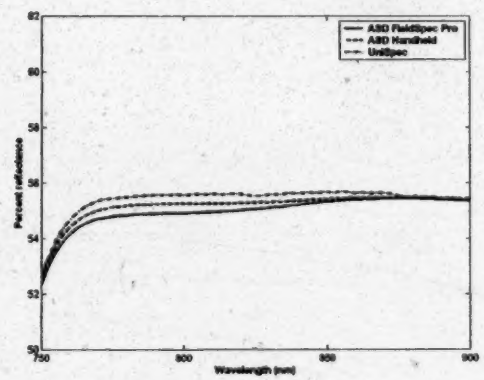

Figure 3-3 cont'd.

Scenario 2

Cafea arabica

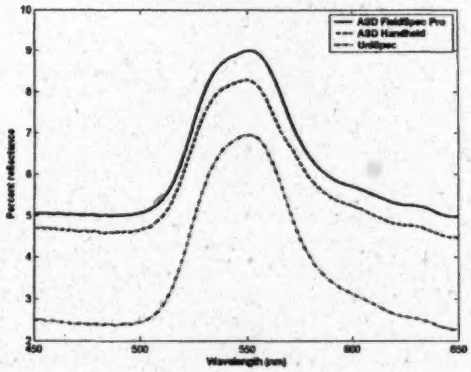

Lantana camara

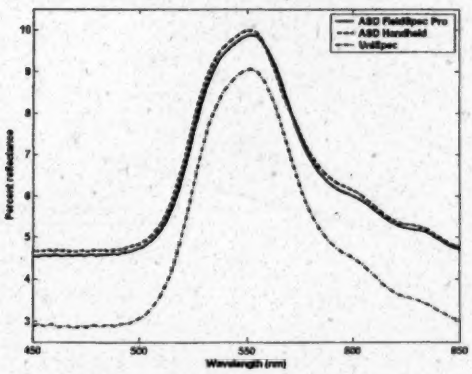

Eriobotrya japonica

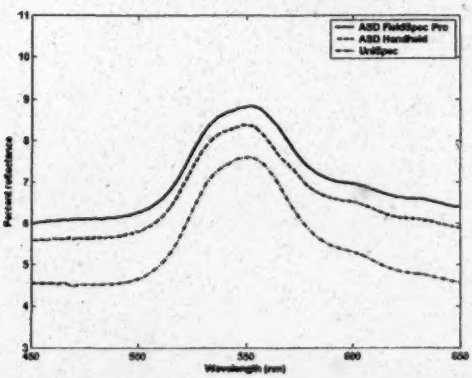

Figure 3-4. Average visible (top three graphs) and near-infrared (bottom three graphs) reflectance spectra of 40 leaves of three species as measured by three spectroradiometers under scenario two, a 'typical' instrument set-up.

Scenario 2 cont'd.

Cafea arabica

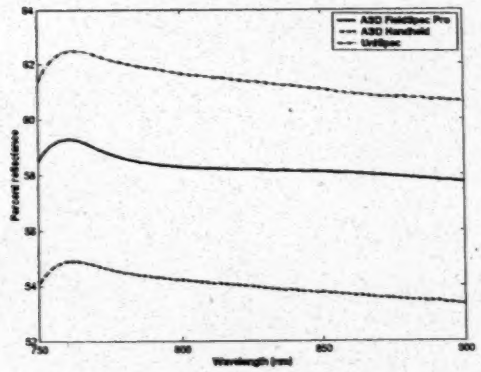

Lantana camara

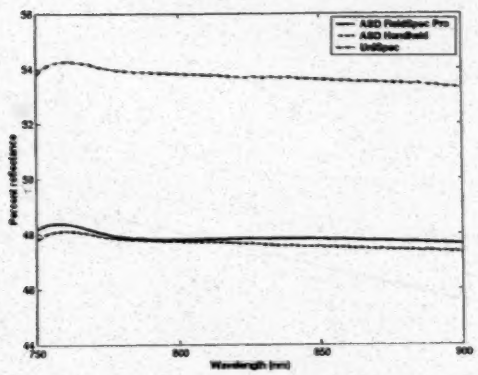

Eriobotrya japonica

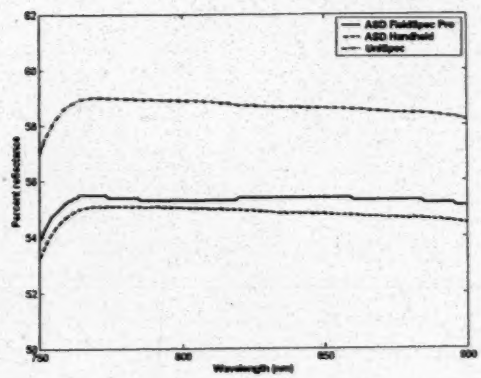

Figure 3-4 cont'd.

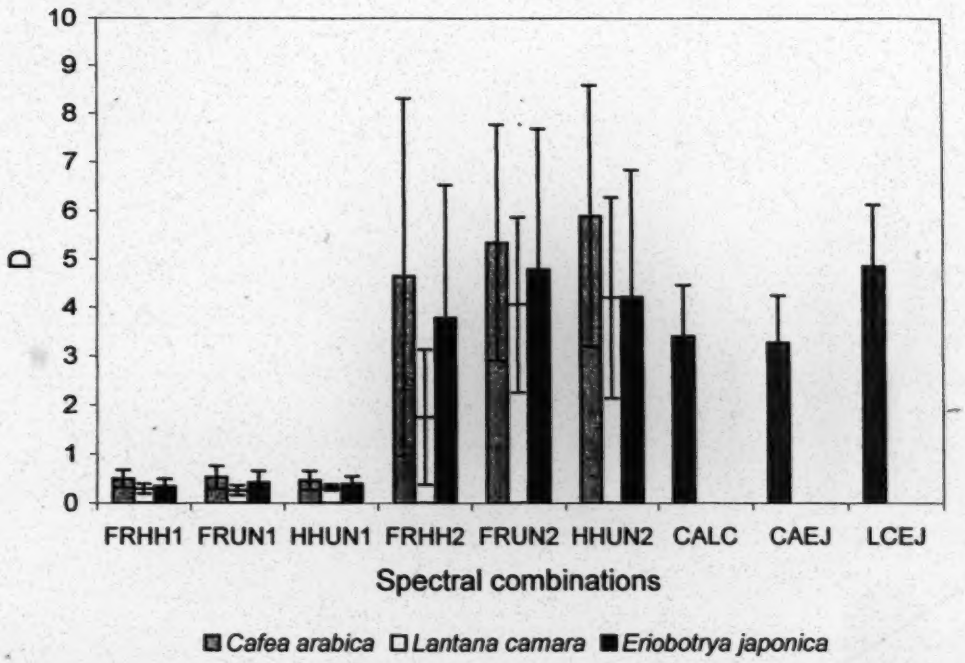

Figure 3-5. Average *D* +/- one standard deviation for the instrument-pairs over the two illumination,viewing, and FOV scenarios. Instruments/scenario are indicated along the x-axis in the following manner: e.g. FRHH1=FR and HH data pair, scenario one. Additional *D* values are given for three species pairs for comparison. CALC=*Cafea arabica/Lantana camara*, CAEJ=*Cafea arabica/Eriobotrya japonica*, LCEJ=*Lantana camara/Eriobotrya japonica.* Spectra for the species-pair *D* values were measured with the ASD FR spectrometer according to scenario one configuration (using the sphere).

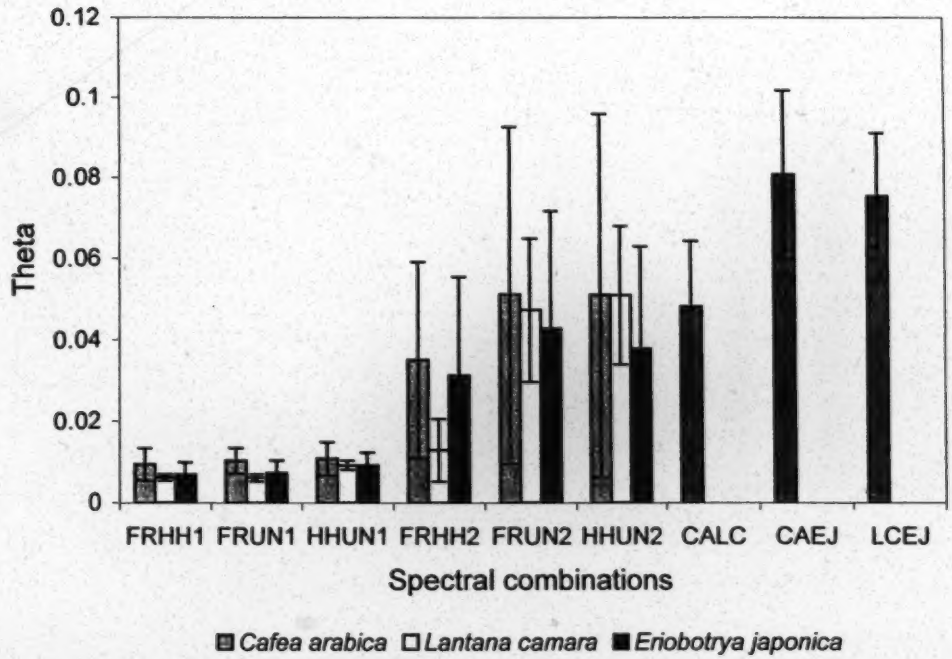

Figure 3-6. Average θ +/- one standard deviation for the instrument-pairs over the two illumination,viewing, and FOV scenarios. Instruments/scenario are indicated along the x-axis in the following manner: e.g. FRHH1=FR and HH data pair, scenario one. Additional θ values are given for three species pairs for comparison. CALC=*Cafea arabica/Lantana camara*, CAEJ=*Cafea arabica/Eriobotrya japonica*, LCEJ=*Lantana camara/Eriobotrya japonica.* Spectra for the species-pair θ values were measured with the ASD FR spectrometer according to scenario one configuration (using the sphere).

LITERATURE CITED

Buschmann, C. & Nagel, E. (1993). In vivo Spectroscopy and Internal Optics of Leaves as Basis for Remote-Sensing of Vegetation. *International Journal of Remote Sensing, 14*, 711-722.

Carter, G. A. (1993). Responses of leaf spectral reflectance to plant stress. *American Journal of Botany*, *80*, 239-243.

Gamon, J. A., Penuelas, J., & Field, C. B. (1992). A Narrow-Waveband Spectral Index That Tracks Diurnal Changes in Photosynthetic Efficiency. *Remote Sensing of Environment*, *41*, 35-44.

Gamon, J. A. & Surfus, J. S. (1999). Assessing leaf pigment content and activity with a reflectometer. *New Phytologist*, *143*, 105-117.

Gitelson, A., & Merzlyak, M. N. (1994). Spectral Reflectance Changes Associated with Autumn Senescence of *Aesculus hippocastanum* L and *Acer platanoides* L leaves - Spectral Features and Relation to Chlorophyll Estimation. *Journal of Plant Physiology*, *143*, 286-292.

Jensen, J. R. (2000). *Remote sensing of the environment: an earth resource perspective*. Upper Saddle River, New Jersey: Prentice-Hall Inc.

Merzlyak, M. N., Gitelson, A. A., Chivkunova, O. B., & Rakitin, V. Y. (1999). Non-destructive optical detection of pigment changes during leaf senescence and fruit ripening. *Physiologia Plantarum*, *106*, 135-141.

Ott, R. L. (1993). *An introduction to statistical methods and data analysis*. Belmont, California: Duxbury Press.

Peñuelas, J., Baret, F., & Filella, I. (1995). Semi-empirical indices to assess carotenoids/chlorophyll a ratio from leaf spectral reflectance. *Photosynthetica*, *31*, 221-230.

Price, J. C. (1994). How Unique are Spectral Signatures? *Remote Sensing of Environment*, *49*, 181-186.

Richardson, A. D. & Berlyn, G. P. (2002). Spectral reflectance and photosynthetic properties of *Betula papyrifera* (Betulaceae) leaves along an elevational gradient on Mt. Mansfield, Vermont, USA. *American Journal of Botany*, *89*, 88-94.

Richardson, A. D., Duigan, S. P., Berlyn, G. P. (2002). An evaluation of noninvasive methods to estimate foliar chlorophyll content. *New Phytologist*, *153*, 185-194.

Sims, D. A., & Gamon, J. A. (2002). Relationships between leaf pigment content and spectral reflectance across a wide range of species, leaf structures and developmental stages. *Remote Sensing of Environment, 81*, 337-354.

Sims, D. A., Luo, H., Hastings, S., Oechet, W. C., Rahman, A. F., & Gamon, J. A. (submitted). Parallel adjustments in vegetation greenness and ecosystem $C0_2$ exchange in response to drought in a Southern California chaparral ecosystem. *Remote Sensing of Environment*.

Stylinski, C. D., Gamon, J. A., & Oechel, W. C. (2002). Seasonal patterns of reflectance indices, carotenoid pigments and photosynthesis of evergreen chaparral species. *Oecologia, 131*, 366-374.

Tambussi, E. A., Casadesus, J., Munné-Bosch, S., & Araus, J. L. (2002). Photoprotection in water-stressed plants of durum wheat (*Triticum turgidum* var. *durum*): changes in chlorophyll fluorescence, spectral signature and photosynthetic pigments. *Functional Plant Biology, 29*, 35-44.

Thenot, F., Méthy, M., & Winkel, T. (2002). The Photochemical Reflectance Index (PRI) as a water-stress index. *International Journal of Remote Sensing, 23*, 5135-5139.

Trotter, G. M., Whitehead, D. & Pinkney, E. J. (2002). The photochemical reflectance index as a measure of photosynthetic light use efficiency for plants with varying foliar nitrogen contents. *International Journal of Remote Sensing, 23*, 1207-1212.

Ustin, S. L., Roberts, D. A., Gamon, J. A. Asner, G. A., & Green, R. O. (2004). Using imaging spectroscopy to study ecosystem processes and properties. *BioScience, 54*, 523-534.

van Aardt, J. A. N. (2000). *Spectral Separability among Six Southern Tree Species*. Master of Science. Blacksburg, Virginia: Virginia Polytechnic Institute and State University.

Zarco-Tejada, P. J., Pushnik, J. C., Dobrowski, S., & Ustin, S. L. (2003). Steady-state chlorophyll *a* fluorescence detection from canopy derivative reflectance and *double-peak* red-edge effects. *Remote Sensing of Environment, 84*, 283-294.

CHAPTER 4—Discrimination of lianas and trees with leaf-level hyperspectral data[1]

INTRODUCTION

There is mounting evidence that lianas are increasing in dominance in tropical forests (Phillips et al., 2002). With little investment in woody biomass, these aggressive climbers take advantage of existing tree trunks and other lianas to make their way to the canopy where they are capable of rapidly forming a carpet of leafy vegetation, shading the tree beneath (Avalos et al., 1999). There are numerous implications of liana infestation to the supporting tree, including increased mechanical and wind damage, increased probability of falling, and decreased growth rates (Clark & Clark, 1990; Putz, 1984). Eventually, these deleterious effects can lead to increased tree mortality. Since lianas prefer disturbed habitats, promoting disturbances likewise promotes their own proliferation (Schnitzer et al., 2000). In the long run, these trends could lead to significant alterations in forested ecosystems by affecting regeneration rates (Schnitzer et al., 2000) and tree species composition (Phillips et al., 2002).

Where lianas are abundant, their presence in the form of a monolayer on top of tree crowns has important implications for remote sensing studies. For instance, interpretation of vegetation indices relating to photosynthetic activity from hyperspectral data over such areas could be erroneous if lianas are interpreted as tree canopies. Similarly, little or no differences between spectral signatures of lianas vs. trees could also limit the potential for tree classification. From a different point of view, the ability to identify areas heavily infested with lianas would be beneficial to efforts at tracking the prevalence of lianas in tropical forests over time, a topic that demands serious attention in lieu of linkages between climate change and increased extent of liana coverage (Phillips et al., 2002).

The current status of hyperspectral research on tropical trees and/or lianas is highly preliminary. Very few datasets exist from airborne hyperspectral sensors in the Neotropics, and experimental satellite data are just now becoming available from the EO-1 Hyperion sensor, with a spatial resolution of 30 m. At the leaf level, studies by Fung (1999) and Cochrane (2000) were aimed at determining if tree species recognition is possible with subtropical and tropical tree species, respectively. Avalos et al. (1999) conducted a study to compare the optical properties of lianas and trees using absorptance, reflectance and transmittance over the photosynthetically active range rather than examining responses at individual wavebands. Their results indicated similar absorptance and reflectance between the two groups, but significantly lower transmittance of liana leaves as compared to tree leaves.

The specific objective of this paper is to determine if it is possible to distinguish between lianas and supporting trees, as groups, at the leaf level, using hyperspectral reflectance measurements taken from two communities of tropical liana/tree species in Panama, Republic of Panama: Parque Natural Metropolitano (tropical dry forest) and Fort Sherman (tropical wet forest). The approach involves principal components analysis (PCA) and pattern recognition techniques to differentiate between the two groups. The

---

[1]A version of this chapter has been published. Castro-Esau, K. L., Sanchez-Azofeifa, G. A. & Caelli, T. (2004). *Remote Sensing of Environment, 90*, 353-372. Reprinted with permission from Elsevier.

power of PCA for hyperspectral data analysis lies in the reduction of hundreds of highly correlated bands to a few highly discriminatory, uncorrelated eigenvectors, useful for isolating different groups (Chang et al., 2001; Lee et al., 1990). The study focuses on separation of the two structural groups, rather than individual species, since it would be impractical to separate individual liana species on a tree crown where multiple liana species with different abundances from season to season are present. Although the current study does not extend to the canopy level, we believe that studying leaf reflectance is a critical step for a better understanding of spectral responses at the canopy level in tropical environments.

METHODS

Study areas

Parque Natural Metropolitano

For this study, tree canopies were accessed using two canopy cranes installed by the Smithsonian Tropical Research Institute (STRI) in Panama. The first is located in a tropical dry forest at Parque Natural Metropolitano (PNM), just outside Panama City. The crane is 42 m high with a boom radius of 51 m. Annual rainfall at this site is approximately 1740 mm.

The dominant canopy species within reach of the crane is *Anacardium excelsum* (Anacardiaceae). Additional accessible tree species include *Luehea seemannii* (Tiliaceae), *Annona spraguei* (Annonaceae), *Cecropia longipes* (Cecropiaceae), *Enterolobium cyclocarpum* (Fabaceae-Mimosoideae), *Astronium graveolens* (Anacardiaceae), *Ficus insipida* (Moraceae), and *Cordia alliodora* (Boraginaceae).

Lianas contribute significantly to the biodiversity of this area. There are numerous pockets within the jib radius where lianas have proliferated and, in some cases, cover portions of or entire tree crowns. Avalos and Mulkey (1999) sampled canopy transects from this location under dry and wet season conditions (1994-1995), and found 20 liana species. During the dry season, at which time only 13 of the liana species maintained foliage, they estimated that of the canopy surface beneath the crane, 14.0 percent was occupied by lianas and 50.7 percent was occupied by the supporting trees. During the wet season, however, these figures changed to 30.9 percent and 43.8 percent, respectively.

Fort Sherman

The second STRI canopy crane is located on the Caribbean coast near Colón, Panama, in a tropical wet forest that receives an annual precipitation of approximately 3300 mm. The crane at this site has a height of 56 m and a boom length of 54 m.

Species diversity at Fort Sherman (FTS) is greater than that at PNM. There are about 180 species of trees and lianas within the crane radius. Tree species include *Tapirira guianensis* (Anacardiaceae), *Aspidosperma cruenta* (Apocynaceae), *Cordia bicolor* (Boraginaceae), several *Inga sp.* (Fabaceae-Mimosoideae), *Carapa guianensis* (Meliaceae), *Brosimum utile* (Moraceae), several *Virola sp.* (Myristicaceae), *Manilkara bidentata* (Sapotaceae), *Simarouba amara* (Simaroubaceae), and *Vochysia ferruginea* (Vochysiaceae), among others.

Lianas appear to be an important component of the biodiversity at FTS as well, although not to as great an extent as at PNM. When sampling was undertaken (March 2003), numerous medium-sized and smaller trees were supporting lianas, whereas the

tallest canopy trees were not. Lianas were particularly noticeable in the few cases where the supporting tree was in a partial to complete leaf-off condition.

Sample collection

From the gondola of each canopy crane, leaves of liana and tree species (Table 4-1) were collected March 5-14, 2003, near the end of the dry season. Ten leaves were collected per species. Leaves were immediately placed in sealable plastic bags containing moistened paper towels. These bags were placed in a cooler containing ice, brought promptly to ground level to extract samples for chlorophyll analyses, and taken to a makeshift laboratory for spectral reflectance measurements.

Measurements of chlorophyll content

For five of the ten leaves, samples were cored from one side of the leaf midrib and placed in small plastic vials that were covered in tinfoil and frozen (the remaining five leaves were retained for other analyses). The first three leaves were, in most cases, the same leaves used later for spectral reflectance measurements, which were taken on the remainder of the leaf. In the case of small leaves, different leaves were used for chlorophyll content and for spectral reflectance measurements. The corer had a diameter of 1.6 cm. Chlorophyll a and chlorophyll b content per core were determined using the dimethyl sulphoxide (DMSO) extraction technique described in Hiscox & Israelstam (1979). A standard two-sample t-test was used to determine if there were significant differences between the means of liana and tree chlorophyll contents at the two sites. Where the assumption of equal variances was not met, a Welch modified two-sample t-test was used instead (Ott, 1993).

Measurements of spectral reflectance

Spectral reflectance measurements were taken using a UniSpec Spectral Analysis System (PP Systems, Amesbury MA, USA). The UniSpec VIS/NIR incorporates a 256-element photodiode array, which covers a spectral range of 306-1138 nm at a sampling interval of 3.3 nm. It has a built-in light source (7.0 W halogen lamp) and may be fitted with a leaf clip that holds the foreoptic at 60 ° and prevents entry of ambient light. The measuring diameter of the standard foreoptic used in this study is 2.3 mm.

The following sequence was used to perform spectral reflectance measurements of liana and tree leaves with the UniSpec spectrometer: 1) integration time was adjusted automatically with a white reference standard in the leaf clip, 2) number of scans per measurement was set to 10, 3) a dark scan was performed, 4) a reference scan was acquired, again with the white reference standard in the leaf clip, and 5) a sample was scanned.

Of the 10 leaves collected per species, spectral measurements were taken for the first 3 healthy, mature leaves also used for analyses of chlorophyll content, with the exception of small-leaved species, for which different leaves were used for the two types of measurements. Single-leaf reflectance spectra were obtained for only 3 of the total 10 leaves due to time constraints; however, the main purpose for collecting all 10 leaves was for leaf stack measurements, which are not analyzed in this paper. Six reflectance spectra were recorded per leaf, avoiding the midrib, and later averaged.

Spectral analysis

Spectral smoothing and differentiation

Raw spectral reflectance data were smoothed with the Savitsky-Golay least squares filter using a quadratic polynomial and a 25-point window. This filter was chosen because it smoothed the spectral data well with minimal effect on the position, shape and depth of spectral features (Press et al., 1996). First and second derivatives of the raw smoothed data were also computed using finite central differences from adjacent wavebands. Resulting datasets, therefore, were 1) raw smoothed data, 2) 1st derivative of raw smoothed data, and 3) 2nd derivative of raw smoothed data. The wavelength range retained for analysis was 450-950 nm in the case of datasets 1) and 2) and 500-800 nm in the case of dataset 3). These regions were shortened as such due to noise on either end of the spectrum.

Principal components analysis

Principal components analysis (PCA) was used to reduce data dimensionality by isolating a small number of orthogonal (uncorrelated) spectral attributes that constitute the maximum variations in the dataset (Fernández-Cáceres et al., 2001). This approach involved computing the eigenvectors and eigenvalues of covariance matrices computed using two different sampling schemes.

In PCA method 1 (PCA1), the smoothed data array containing all liana and tree spectra for the particular site was split in half, by taking every other spectrum, into training and testing sets. The PCA was then performed on the training data, after which all sample spectra (training and testing data) were projected into the eigenspace formed by the first two to four eigenvectors.

In PCA method 2 (PCA2), the smoothed data array containing all liana and tree spectra for a particular site was split twice, first into separate liana and tree arrays, and then, within each, into training and testing sets corresponding to even and odd samples, respectively. PCA was performed twice, first for the liana training data, and then for the tree training data. The first two to four eigenvectors from each, weighted by their eigenvalues, were used to form a multi-dimensional subspace in which both the liana and tree spectra were projected for later training and classification.

The methods described above were applied to the raw smoothed, 1st derivative, and 2nd derivative datasets for the two locations.

Pattern recognition techniques

To test the hypothesis that tree and liana leaf spectra are separable, classification of spectra was attempted using a selection of supervised parametric (logistic linear classifier (loglc), normal densities based quadratic classifier (qdc), and uncorrelated normal densities based quadratic classifier (udc)) and nonparametric (neural network (lmnc), decision tree (treec), and k-nearest neighbor (knnc)) classifiers (Table 4-2). The parametric classifiers incorporate assumptions about population distributions, i.e. that classes are normally distributed, whereas the nonparametric classifiers are relatively free of assumptions about population parameters. The six classifiers included in this study are representative of currently used classifiers and were used to avoid possible biases due to the nature of the classifier, per se. The classifiers are described in PRTools (Duin, 2000) and have the following characteristics when trained using supervised learning:

1) Linear classifiers generate linear decision boundaries; they use estimates of the probability density functions to minimize the expected classification error.

2) Quadratic classifiers fit gaussian models to data clusters that maximally discriminate between training samples.
3) Uncorrelated normal densities quadratic classifiers are quadratic classifiers that make the assumption of independent features (a valid assumption when using PCA).
4) Decision trees generate classification rules based on the selection of greatest to least important attributes and their ranges.
5) Neural networks generate classification rules in terms of linear discriminate functions, over the attributes space, determined by non-linear perceptrons.
6) K-nearest neighbor classifiers classify unlabeled samples based on their similarity with k samples in the training set, where similarity is determined using a distance metric.

Classification involved training and testing stages, which were identical regardless of the classifier used. In the first stage, the scalar products of the training data generated from the PCA were labeled 1 or 2, where 1=liana and 2=tree, and used to train the various classifiers. Error estimation was generated for the training data. In the second stage, the projections of the testing data were classified based on the trained classifiers, and error estimation was performed again, this time for the testing set. In the case of PCA1, figures were plotted to show the projections of the liana and tree spectra in the eigenspace formed by the first two eigenvectors as well as the decision functions generated by each classifier. Figures were not plotted for PCA2 due to higher dimensionality. The above steps were repeated for each PCA output and each of the classifiers described in Table 4-2.

In addition to these analyses, a variation of PCA2 was included in which four additional features (chlorophyll a, chlorophyll b, total chlorophyll, chlorophyll a:b ratio) were used as ancillary data in the classification. In this case, a total of eight features were used in both training and classification, four from PCA2 (the first two eiegenvectors each from the liana and tree PCA) and the additional four based on chlorophyll analyses. Although this study is primarily aimed at remote sensing applications, the chlorophyll data were used to explore the nature of possible differences in tree and liana leaves, since chlorophyll content is the dominant factor influencing reflectance in the visible region.

Evaluation

Evaluation was made at three levels in this study. The first was to determine the effectiveness of PCA1 versus PCA2 for the separation of liana and tree spectra. The second was to assess the usefulness of the raw versus the 1st or 2nd derivative data in the classification. The last was to compare the performance of the six classifiers used to distinguish between lianas and trees.

At all three levels, performance was evaluated in terms of classification errors for both training and testing datasets.

Software

All calculations were performed using MATLAB Version No. 12 (The Mathworks, Inc.). Classification of spectra was performed using the pattern recognition toolbox, PRTOOLS Version 3.0 (Duin, 2000), developed for use within Matlab.

RESULTS

PCA approach

The use of eigenvectors beyond the first and second was ineffective or detrimental to classification accuracy in many, but not all cases (exceptions are noted below). As a result, the majority of the results shown are based on analyses involving the first two eigenvectors, which contained more than 90% of the data variance (Table 4-3).

Over both sites, neither PCA1 nor PCA2 provided consistently better separation of lianas and trees although PCA2 resulted in better classification accuracy than PCA1 with over half of the classifiers used (Table 4-4). Classification accuracy of the PNM data was improved with the addition of chlorophyll ancillary data (PCA2 + chl), for which the lowest error estimation was obtained using the first derivative and neural network classifier in combination (lmnc, 0% training error, 4% testing error). Under similar conditions, but using the raw smoothed data, the quadratic classifier (qdc) broke down likely due to overfitting (Table 4-4). Figure 4-1 presents the PNM tree and liana first derivative spectra projected into the eigenspace generated by PCA1 along with decision functions generated by the six classifiers (due to higher dimensionality it was not possible to plot the results of PCA2). Whereas most of the highest classification accuracies were obtained using PCA2 with chlorophyll ancillary data for PNM, the opposite occurred for the FTS data, for which the worst classification accuracies resulted from the PCA2 variation using chlorophyll data, although the two groups were not very distinct overall at this site. For the FTS data, the best classification resulted from the combination of the raw smoothed data and the k-nearest neighbor classifier (knnc), analyzed using PCA1 (0% training error and 16. 22% testing error) (Figure 4-2).

The addition of chlorophyll ancillary data was clearly useful for discrimination between liana and tree leaf spectra at PNM, but not so for FTS. Indeed, analysis of chlorophyll content showed highly significant differences in chlorophyll a, chlorophyll b, and total chlorophyll content between lianas and trees at the PNM site, whereas there were no significant differences at the FTS site (Table 4-5).

Although not beneficial for nonparametric classifiers, the use of principal component dimensions beyond the second led to significant improvements in classification by the parametric classifiers, particularly qdc and udc (Table 4-6). Training errors were reduced in the majority of instances. Testing error was also reduced in many cases, and most notably by over 10% for a number of the FTS data classifications.

Regardless of PCA method or site, the first principal component extracted from the raw smoothed data generally followed the shape of the leaf reflectance spectrum (Figure 4-3). In other words, since reflectance was highest in the near-infrared, the highest loadings were also in this region. The second principal component stressed the green peak region (550 nm) as well as the red edge (~710 nm). The PNM and FTS sites have similar principal component loadings; they are simply mirror images of each other. In the first principal component of the first derivative data, the areas just beyond (~730 nm) and before the red edge (the chlorophyll absorption well, ~685 nm) are stressed, followed in importance by the slopes before and after the green peak. The second principal component of the first derivative data has the greatest weightings in the red edge region (~710 nm) as well as the slope leading up to the green peak (~525 nm). These findings were fairly consistent for the PNM and FTS data as well as for the two PCA methods.

Dataset evaluation

When comparing average raw smoothed spectra of the liana group vs. the tree group at the two sites (Figures 4-4 and 4-5), the average tree leaf reflectance is lower than the average liana leaf reflectance in the visible region, and the opposite occurs in the near-infrared. The trend in the visible region is more evident for the PNM site than the FTS site. For both sites, although similar phenomena occur in the near-infrared when averaged over all spectra (higher reflectance for trees than for lianas), near-infrared reflectance was extremely variable between species of the same structural group. Despite this, it was noted above that in the PCA, the near-infrared bands were consistently highly weighted in the 1st principal component of the raw smoothed data.

Besides amplitude differences in the reflectance spectra of lianas and trees, shape differences are also confirmed by the first derivative spectra, such as in the immediate vicinity of the red edge at approximately 715 nm (Figure 4-4). As well, the slope is greater for lianas in the region approaching the green peak.

For the PNM dataset, there appears to be an advantage to using the 1st derivative of the dataset instead of the raw smoothed dataset in many cases, particularly when combined with PCA1 or the PCA2 variation involving chlorophyll data (Table 4-4). For example, there is a consistent improvement in the error of estimation for the training data when comparing, within the PNM data and PCA1, the raw and 1st derivative datasets. The opposite was true for the FTS dataset, for which classification was superior using the raw smoothed data rather than the 1st derivative. Classification results using the 2nd derivatives were inferior to those involving either the raw or 1st derivative data, and were excluded from Table 4-4. This may have been related to noisiness as well as the fact that a reduced range of spectral reflectance data was used for the analysis (500-800 nm only).

Classifier evaluation

Evidently, classifier performance is highly dependent on the PCA method (PCA1, PCA2) as well as whether the data were in the raw or 1st derivative form (Table 4-4).

The parametric classifiers (loglc, qdc, udc) provided a consistent classification in most instances; however, their performance was generally surpassed by the nonparametric classifiers (treec, lmnc, knnc), predominantly with regard to training accuracy. One noteworthy exception was the combination of PCA2 with either the raw or 1st derivative PNM data, for which training error was 7.69% and testing error was 4.00%. With respect to each other, the three parametric classifiers gave fairly similar classification results within a particular PCA method and dataset (raw or 1st derivative) combination. Uncorrelated normal densities (udc) was an appropriate assumption for PCA1 since the two eigenvectors retained from the PCA are by definition independent; however, that was not the case when the chlorophyll ancillary data was included (chlorophyll a, chlorophyll b, total chlorophyll, and chlorophyll a:b ratio).

The three nonparametric classifiers (treec, lmnc, knnc) produced higher overall classification accuracy than the parametric classifiers; however, no one was consistently superior to the other two. For instance, for the PNM data (PCA1), the neural network classifier (lmnc) had the lowest training and testing errors (Table 4-4). For the FTS data (PCA2), the lowest training and testing errors were obtained using the k-nearest neighbor classifier (knnc) (Table 4-4). It is important to remember that each classifier has its own advantages and disadvantages, however. For instance, each time the neural network was

used to classify the same dataset, the output was slightly different. This lack of reproducibility, which was a problem for this dataset, may become negligible for a larger dataset, however. Decision trees perform best when each attribute takes on a small number of disjoint possible values (Mitchell, 1997), which is not the case for this dataset. Performance on training data is excellent for decision trees while performance on testing data may be mediocre to poor. K-nearest neighbor classifiers have the disadvantage of long search times for classification of the test data. For neural networks, choice of number of neurons, and for k-nearest neighbor classifiers, choice of k, also have an important influence on classification results and must be chosen carefully after initial experimentation. For decision trees, optimal pruning also requires additional tuning.

Overall, it appears useful to test several classifiers for any classification, since their output is related to a number of factors, including the manner in which PCA is executed, the dataset used (raw, 1st or 2nd derivative), as well as the amount of training and testing data available. The use of ancillary data, such as chlorophyll content in this case, was valuable for improving the classification of the PNM leaf spectra. A summary of results is presented in Table 4-7, which ranks each combination used in the analysis.

Within-leaf and within-species variability

Thus far, results have been shown for lianas and trees as two separate structural groups. Initially, this was justified using the argument that species-level analyses would be impractical at the remote sensing level, since multiple liana species were found on single tree crowns at both sites, and their percentage abundances on the crowns are unknown and changing. This approach leaves a number of unanswered questions regarding the variability present within the species studied, as well as within and between the two groups. In addition, which liana species are most indistinguishable from the tree species, and vice versa? If the hard-to-distinguish species are the most abundant at the site, potential classification could become even more difficult.

Answering these questions requires a comprehensive discussion, which we aim to cover thoroughly in a future article, along with data to be acquired at PNM during the wet season. At this time, however, a number of preliminary observations can be made. First of all, within-leaf variability (based on six measurements per leaf) appears to be low, as does between-leaf variability (based on three leaf samples per species) for a particular species (an example is given in Figure 4-6). However, this depends highly on the condition of the leaves collected; in this case, uniform, healthy, mature leaves were collected. Leaves of the same species, but of different ages or health, will vary widely in their spectral reflectance properties. Within the PCA eigenspace, leaf samples from the same species in many cases clustered more tightly than with samples from other species within the same group, but there were exceptions. There were, therefore, species that exhibited greater within-leaf and within-species variability than others. Furthermore, three leaves per species is not a large enough sample size to make conclusive arguments on within-species variability in spectral reflectance. Within each group (lianas and trees), a large degree of variability was observed in the spectra, especially in the near-infrared region. Between the two groups, evidently some species are situated closer to decision boundaries than others, and are thus more easily confused (Figure 4-1). Within the lianas group, the main species that were confused with trees were: *Arrabidaea candicans, Doliocarpus dentatus*, and *Mikania leiostachya*. The tree species that was most often

confused with the lianas was *Anacardium excelsum*, the dominant canopy tree species within the reach of the crane. Although the difficulty rendered by this species appears to preclude classification of lianas and trees at PNM, it should be mentioned that the dominance of *Anacardium excelsum* is particularly evident within the small PNM crane radius; beyond this radius, greater heterogeneity in the tree species composition is observed.

DISCUSSION AND CONCLUSION

We have shown that lianas and trees at the tropical dry forest site of Parque Natural Metropolitano are separable based on their spectral reflectance at the leaf level and the use of pattern recognition techniques. Classification errors on the PNM test data were low (4-16% in most cases) regardless of the PCA method, use of raw or 1st derivative, or classifier, indicating that the two structural groups were clearly separable at that site (Figure 4-1). The chlorophyll ancillary data, therefore, led to improvements on what was already a reasonably accurate classification. This distinction, however, is much less clear at the tropical wet forest site of Fort Sherman, where the lowest classification error on the test data was 16% (Table 4-4), but in most cases varied between 20-40%.

PCA2 may have been advantageous over PCA1in the case of the PNM data because it projected the test data into both liana and tree eigensubspaces and then combined the two subspaces to form a 4-D feature space for classification (in contrast to a simpler 2-D feature space for PCA1). In this 4-D space, liana test spectra, if they are distinct from tree spectra, would be expected to cluster closer to the liana training spectra than the tree training spectra. As mentioned previously, this was not the case for the FTS data, for which distinctions were not clear regardless of the combination of method and classifier used.

The general effectiveness of both raw and 1st derivative datasets in these analyses indicates that both amplitude and shape differences between liana and tree spectra played a role in the classifications, although poor classifications resulted from the use of the 2nd derivative. Particularly notable, more so at the tropical dry forest site but also for the wet forest site, is a higher reflectance of liana leaves in the visible region as compared to trees, which was consistent with chlorophyll analyses that indicated lower chlorophyll a, chlorophyll b, and total chlorophyll content in lianas than in trees at PNM (not significant at FTS).

Overall, nonparametric classifiers (lmnc, knnc, treec) performed better than parametric classifiers in the analyses (Tables 4-4 and 4-7). This is most probably due to the fact that parametric classifiers, besides assumptions about population normality, need a significant amount of training data to fit the decision functions. In particular, training error estimations tended to be lower for the nonparametric classifiers than for the parametric classifiers.

Why do liana and tree leaf spectra differ at PNM? Differences in chlorophyll content between the two structural groups may provide only part of the answer. Additional differences may come to light with examination of accessory pigments (e.g. carotenoids) as well as internal leaf structural characteristics such as the degree of compactness of the mesophyll layer. Internal leaf structure is known to influence leaf reflectance in the near-infrared region such that higher reflectance occurs the greater the number of air-cell wall interfaces (Danson, 1995). Water content is another important

factor determining leaf reflectance in the near-infrared (Grant, 1987). The greater the water content, the lower the reflectance in the near-infrared, especially around water absorption bands at 1.4 μm and 1.9 μm. Another closely related question that arises is what sort of strategies have these two structural groups adopted that lead to differences in chlorophyll content and leaf reflectance? The most obvious possibility is phenological differences in the two groups. It has already been noted that, at PNM, there seems to be a greater tendency towards deciduousness in lianas than in trees (Avalos & Mulkey, 1999), and although the attempt was made to collect mature, healthy leaves, it is possible that, given the dry season conditions, some of the liana leaves were already progressing toward senescence, more so than for the tree leaves sampled, resulting in lower chlorophyll contents. A study of chlorophyll and leaf reflectance of lianas and trees at regular time intervals over the period of a year would elucidate these types of issues. Differing levels of water stress, or other stresses, such as nutrient stress (e.g. nitrogen), between the two groups, could also have induced the differences we observed in leaf reflectance between lianas and trees, and/or possibly differences in photosynthetic capacity between the two structural groups. Avalos et al. (1999) formerly detected higher transmittance in tree leaves as compared to liana leaves, which was deemed a product of the distinctive crown architecture of each group. Lianas, which typically form monolayers above tree crowns, favor high light interception and low light transmission. Trees, in contrast, which typically have many leaf layers, favor greater light transmission in order that inferior leaf layers also receive light.

Drought stress and varying phenologies under the dry season conditions at PNM may have played a role in the fact that lianas and trees could be distinguished at PNM more readily than at FTS, a tropical wet forest. The difference in chlorophyll content between lianas and trees was greater at PNM than at FTS, which was mirrored in the leaf reflectance spectra. In addition, there was a notably higher chlorophyll a content of tree leaves at PNM as compared to tree leaves at FTS. This finding may be linked to the suggestion that deciduous dry forest tree leaves have higher photosynthetic capacities and nitrogen content than evergreen tree leaves (Murphy & Lugo, 1986; Medina & Klinge, 1983). Alternatively, disparate results between PNM and FTS may be due to non-stress related factors, but rather to dissimilarities in the spectral characteristics of species adapted to two different environments. That the differences observed are related to species selection is another possibility, especially at FTS where only a few of the total number of species of lianas and trees were sampled.

The utility of finding spectral differences between liana and tree leaves will be apparent if these differences translate to the canopy level, and are detectable by airborne or satellite-borne hyperspectral sensors. If that is the case, it would be possible to map the current extent of liana communities and track their changes over time. In particular, mapping liana communities could have significance for biodiversity assessments and carbon budgets, the latter due to the fact that carbon sequestration is impeded in areas where liana proliferation hinders tree regeneration (Schnitzer & Bongers, 2002). On the other hand, where a tree species classification is the desired result, liana abundance could be a significant source of confusion.

Detecting lianas at the canopy scale will not be as straightforward as detecting differences in spectral reflectance between lianas and trees at the leaf level. Parque Natural Metropolitano, for example, is considered tropical dry forest, and both liana and

tree species have varying degrees of leaf longevity and deciduousness. Thus, for any liana-supporting tree, the proportion of liana leaves to tree leaves in the exposed upper crown area will vary throughout the year. Staggered leaf flush and leaf senescence between tree and liana species could also exaggerate or minimize spectral differences between the two groups at different times, since leaf age also is known to affect leaf spectral reflectance (Carter, 1993; Gausman, 1985). Diurnal changes in leaf angle will also affect spectral reflectance, especially if those changes are inconsistent between species, which appears to be the case. Lastly, helpful ancillary data, such as leaf chlorophyll content, may be difficult and expensive to acquire.

We therefore conclude that, at the leaf level, we have identified a highly useful combination of principal components analysis and pattern recognition techniques to distinguish between liana and tree species at a tropical dry forest site; however, we recognize that further study is required to clarify what physiological mechanisms are behind the differences between the two groups and if these differences are maintained throughout the year. As well, we recognize that additional research will be required, from both the ecological and remote sensing perspectives, to determine whether or not our results are transferable to the canopy level. At present it seems that the distinctions observed may be restricted to lianas and trees under dry season conditions.

Table 4-1: Liana and tree species sampled for this study

Parque Natural Metropolitano				Fort Sherman			
Lianas		Trees		Lianas		Trees	
Species	Family	Species	Family	Species	Family	Species	Family
Aristolochia maxima	Aristolochiaceae	*Anacardium excelsum*	Anacardiaceae	*Forsteronia myriantha*	Apocynaceae	*Aspidosperma cruenta*	Apocynaceae
Mikania leiostachya	Asteraceae	*Annona spraguei*	Annonaceae	*Odontadenia puncticulosa*	Apocynaceae	*Cordia bicolor*	Boraginaceae
Arrabidaea candidans	Bignoniaceae	*Cordia alliodora*	Boraginaceae	*Arrabidaea verrucosa*	Bignoniaceae	*Pourourma sp.*[a]	Cecropiaceae
Stizophyllum riparium	Bignoniaceae	*Ficus insipida*	Moraceae	*Phryganocydia corymbosa*	Bignoniaceae	*Marila laxiflora*	Clusiaceae
Bonamia trichantha	Convolvulaceae	*Luehea seemannii*	Tiliaceae	*Pleonotoma variabilis*	Bignoniaceae	*Terminalia amazonia*	Combretaceae
Jacquemontia sp.[a]	Convolvulaceae			*Maripa panamensis*	Convolvulaceae	*Tachigali versicolor*	Fabaceae-Caesalpiniodeae
Doliocarpus dentatus	Dilleniaceae			*Doliocarpus multiflorus*	Dilleniaceae	*Lonchocarpus longifolium*	Fabaceae-Papilionoideae
Stigmaphyllon hypargyreum	Malpighiaceae			*Dioclea wilsonii*	Fabaceae-Papilionoideae	*Carapa guianensis*	Meliaceae
Passiflora vitifolia	Passifloraceae			*Tontelea ovalifolia*	Hippocrateaceae	*Brosimum utile*	Moraceae
Gouania lupuloides	Rhamnaceae			*Unknown sp. of liana*	Hippocrateaceae	*Ficus nymphaeifolia*	Moraceae
Serjania sp.[a]	Sapindaceae					*Virola surinamensis*	Myristicaceae
Vitis tiliifolia	Vitaceae					*Tocoyena pittieri*	Rubiaceae
						Matayba apetala	Sapindaceae
						Manilkara bidentata	Sapotaceae

Parque Natural Metropolitano				Fort Sherman			
Lianas		Trees		Lianas		Trees	
Species	Family	Species	Family	Species	Family	Species	Family
						Simarouba amara	Simaroubaceae

[a]In some cases it was possible to identify lianas to genus but not to species.

Table 4-2: Supervised classifiers used in this study (source: Duin, 2000)

Code	Classifier	Description
loglc	Logistic linear classifier	Linear classifier computed by maximizing the likelihood criterion using the logistic (sigmoid) function.
qdc	Normal densities based quadratic classifier (Bayes' rule)	Quadratic classifier using the assumption of normal densities.
udc	Uncorrelated normal densities based quadratic classifier	Quadratic classifier using the assumption of normal densities with uncorrelated (independent) features.
lmnc	Train feed forward neural network by Levenberg-Marquardt rule	A neural network based on the backpropagation algorithm and Levenberg-Marquardt gradient descent.
treec	Binary decision tree classifier	Decision tree classifier using information gain as a binary splitting criterion.
knnc	k-nearest neighbor classifier	Classifier for which the class labels of the k most similar neighbors are used to predict the class of the new object. The distance metric used in this case is the Euclidean distance.

Table 4-3: Percentage of variance contained within first two eigenvectors/values in PCA1 and PCA2

	Dataset		
	Raw smoothed data	1st derivative	2nd derivative
PCA1			
PNM	97.61	94.08	95.40
FTS	98.89	97.25	96.80
PCA2			
PNM lianas	98.69	94.01	94.02
PNM trees	91.57	91.03	95.21
FTS lianas	99.79	99.33	99.16
FTS trees	97.78	94.34	93.63

Table 4-4: Training and testing error (in percentage) for dataset-classifier combinations used in this study. Analyses based on first two spectral dimensions of the PCA only.

Parque Metropolitano						
	Raw smoothed data					
Classifier	**PCA1**		**PCA2**		**PCA2 (+ chl)**	
	Training error	**Testing error**	**Training error**	**Testing error**	**Training error**	**Testing error**
loglc	19.23	20.00	3.85	20.00	0	16.00
qdc	15.38	20.00	7.69	4.00	100.00	100.00
udc	11.54	16.00	15.38	16.00	3.85	16.00
treec	0	20.00	0	24.00	0	12.00
lmnc (neurons=3)	3.85	16.00	3.85	16.00	0	8.00
knnc(k=2)	0	16.00	0	12.00	0	12.00
	1st derivative					
Classifier	**PCA1**		**PCA2**		**PCA2 (+ chl)**	
	Training error	**Testing error**	**Training error**	**Testing error**	**Training error**	**Testing error**
loglc	11.54	16.00	11.54	16.00	0	12.00
qdc	7.69	16.00	7.69	4.00	0	8.00
udc	7.69	16.00	15.38	12.00	3.85	16.00
treec	0	20.00	0	24.00	0	8.00
lmnc (neurons=3)	0	12.00	0	16.00	0	4.00
knnc(k=2)	0	20.00	0	16.00	0	12.00
Fort Sherman						
	Raw smoothed data					
Classifier	**PCA1**		**PCA2**		**PCA2 (+ chl)**	
	Training error	**Testing error**	**Training error**	**Testing error**	**Training error**	**Testing error**
loglc	26.32	35.14	23.68	32.43	33.33	36.67
qdc	23.68	40.54	13.16	29.73	50.00	50.00
udc	23.68	40.54	23.68	37.84	20.00	43.33
treec	0	21.62	0	21.62	0	43.33
lmnc (neurons=3)	15.79	27.03	0	24.32	6.67	36.67
knnc(k=2)	0	16.22	0	21.62	0	26.67
	1st derivative					
Classifier	**PCA1**		**PCA2**		**PCA2 (+ chl)**	
	Training error	**Testing error**	**Training error**	**Testing error**	**Training error**	**Testing error**
loglc	26.32	45.95	23.68	37.84	30.00	43.33
qdc	28.95	40.54	18.42	24.32	10.00	40.00
udc	23.68	37.84	26.32	45.95	20.00	40.00
treec	0	24.32	0	27.03	0	40.00
lmnc (neurons=3)	15.79	32.43	10.53	24.32	3.33	36.67
knnc(k=2)	0	24.32	0	27.03	0	46.67

Table 4-5: Results of chlorophyll analyses for liana and tree leaves at PNM and FTS. All minimum, maximum, and mean values expressed in units of mg/sample.

	PNM							FTS						
	Lianas			Trees				Lianas			Trees			
	Min	Max	**Mean**	Min	Max	**Mean**	p-value	Min	Max	**Mean**	Min	Max	**Mean**	p-value
Chl a	0.0150	0.1694	**0.0748**	0.0885	0.1451	**0.1113**	<0.001	0.0148	0.1802	**0.0846**	0.0184	0.1518	**0.0867**	0.734[a]
Chl b	0.0035	0.0523	**0.0219**	0.0178	0.0761	**0.0356**	<0.001	0.0036	0.0443	**0.0242**	0.0040	0.0719	**0.0289**	0.095
Total chl	0.0184	0.2217	**0.0967**	0.1128	0.1828	**0.1468**	<0.001	0.0184	0.2233	**0.1088**	0.0224	0.2236	**0.1158**	0.458[a]

Chl=chlorophyll. [a]tested using a standard two-sample t-test; all others tested with a Welch modified two-sample t-test due to unequal variances

Table 4-6. Influence of number of spectral dimensions on classification accuracy (in percentage) using parametric classifiers

	Classifier					
	loglc		qdc		udc	
PCA1	**Training error**	**Testing error**	**Training error**	**Testing error**	**Training error**	**Testing error**
PNM raw smoothed						
2 eig	19.23	20.00	15.38	20.00	11.54	16.00
4 eig	7.69	20.00	7.69	16.00	7.69	8.00
PNM 1st derivative						
2 eig	11.54	16.00	7.69	16.00	7.69	16.00
4 eig	11.54	16.00	11.54	8.00	7.69	12.00
FTS raw smoothed						
2 eig	26.32	35.14	23.68	40.54	23.68	40.54
4 eig	23.68	37.84	21.05	27.03	15.79	24.32
FTS 1st derivative						
2 eig	26.32	45.95	28.95	40.54	23.68	37.84
4 eig	23.68	35.14	21.05	29.73	21.05	32.43
PCA2						
PNM raw smoothed						
2 eig	3.85	20.00	7.69	4.00	15.38	16.00
4 eig	0.00	24.00	0.00	16.00	11.54	16.00
PNM 1st derivative						
2 eig	11.54	16.00	7.69	4.00	15.38	12.00
4 eig	0.00	20.00	3.85	16.00	15.38	8.00
FTS raw smoothed						
2 eig	23.68	32.43	13.16	29.73	23.68	37.84
4 eig	18.42	40.54	2.63	18.92	18.42	24.32
FTS 1st derivative						
2 eig	23.68	37.84	18.42	24.32	26.32	45.95
4 eig	15.79	40.54	2.63	21.62	18.42	29.73

eig=eigenvectors

Table 4-7: Ranking of methods used in this study for the two sites, PNM and FTS, based on overall percent classification error calculated from Table 4-4 (1=lowest percentage error).

PCA method	Dataset	Classifier	PNM	FTS
PCA2 (chl)	1st derivative	lmnc	1	7
PCA2 (chl)	raw	lmnc	2	11
PCA2 (chl)	1st derivative	qdc	2	14
PCA2 (chl)	1st derivative	treec	2	7
PCA2	Raw	qdc	3	10
PCA2	1st derivative	qdc	3	8
PCA2	Raw	knnc	4	2
PCA2 (chl)	Raw	treec	4	11
PCA2 (chl)	Raw	knnc	4	4
PCA1	1st derivative	lmnc	4	13
PCA2 (chl)	1st derivative	loglc	4	24
PCA2 (chl)	1st derivative	knnc	4	12
PCA1	Raw	knnc	5	1
PCA2 (chl)	Raw	loglc	5	22
PCA2	1st derivative	lmnc	5	6
PCA2	1st derivative	knnc	5	5
PCA1	Raw	lmnc	6	9
PCA2	Raw	lmnc	6	3
PCA2 (chl)	Raw	udc	6	19
PCA2 (chl)	1st derivative	udc	6	16
PCA1	Raw	treec	7	2
PCA1	1st derivative	treec	7	3
PCA1	1st derivative	knnc	7	3
PCA1	1st derivative	qdc	8	21
PCA1	1st derivative	udc	8	18
PCA2	Raw	loglc	9	15
PCA2	Raw	treec	10	2
PCA2	1st derivative	treec	10	5
PCA2	1st derivative	udc	11	23
PCA1	Raw	udc	12	20
PCA1	1st derivative	loglc	12	23
PCA2	1st derivative	loglc	12	18
PCA2	Raw	udc	13	18
PCA1	Raw	qdc	14	20
PCA1	Raw	loglc	15	17
PCA2 (chl)	Raw	qdc	16	25

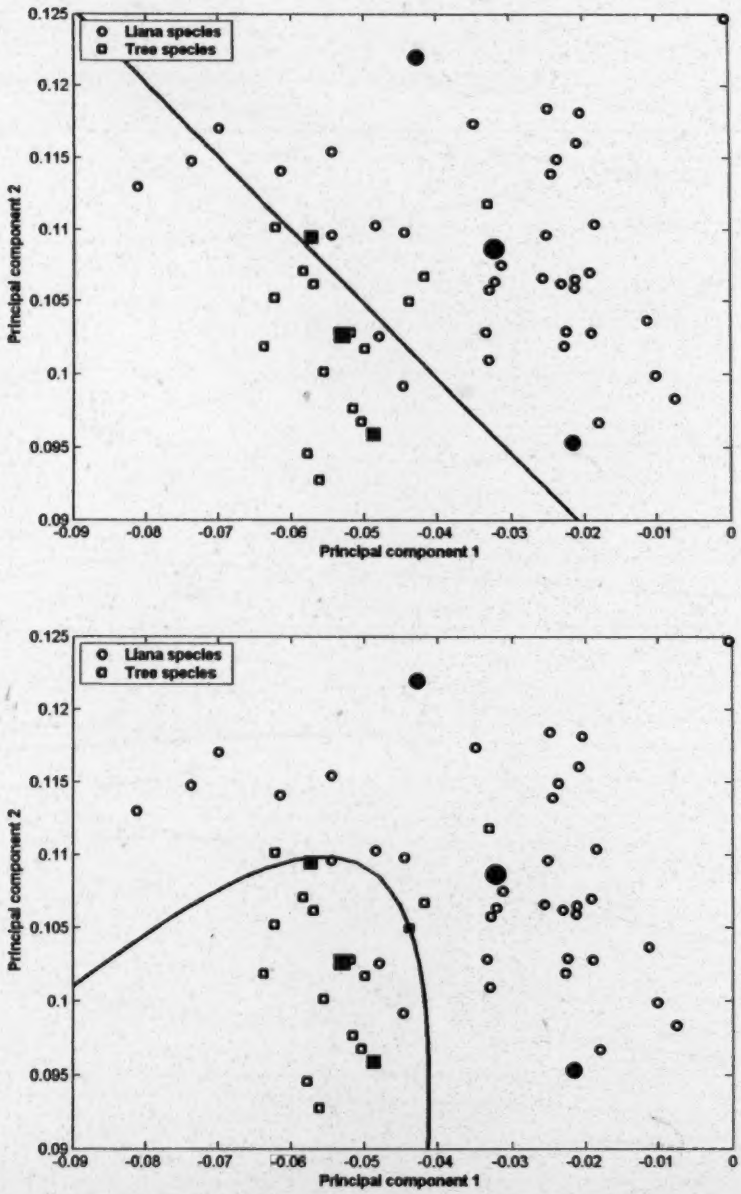

Figure 4-1. Classification of PNM liana and tree 1st derivative spectra using PCA method 1 and six classifiers: logistic linear (loglc, top), quadratic (qdc, 2nd from top), uncorrelated normal densities based quadratic (udc, 3rd from top), decision tree (treec, 4th from top), neural network (lmnc, 5th from top), and k-nearest neighbor (knnc, bottom). Points correspond to individual leaves (3 per species). The large filled circle represents the overall PNM liana mean; smaller filled circles are +/- one standard deviation from the mean. The large filled square indicates the overall PNM tree mean; smaller filled squares are +/- one standard deviation from the mean.

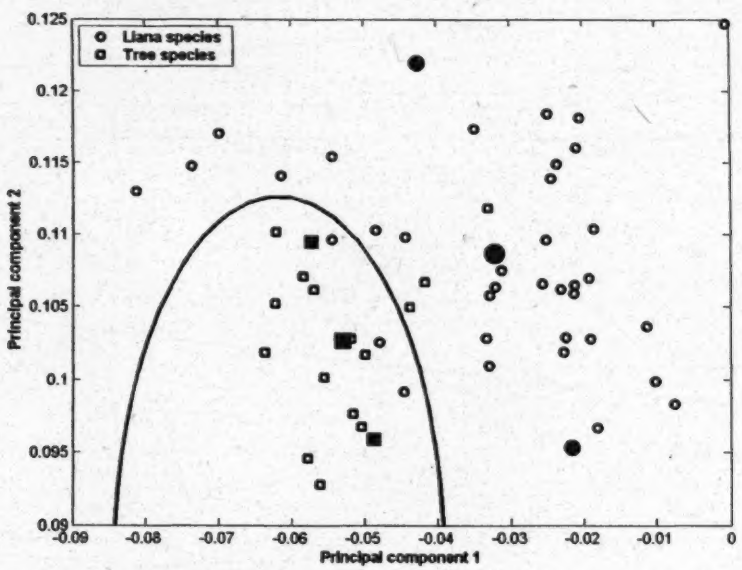

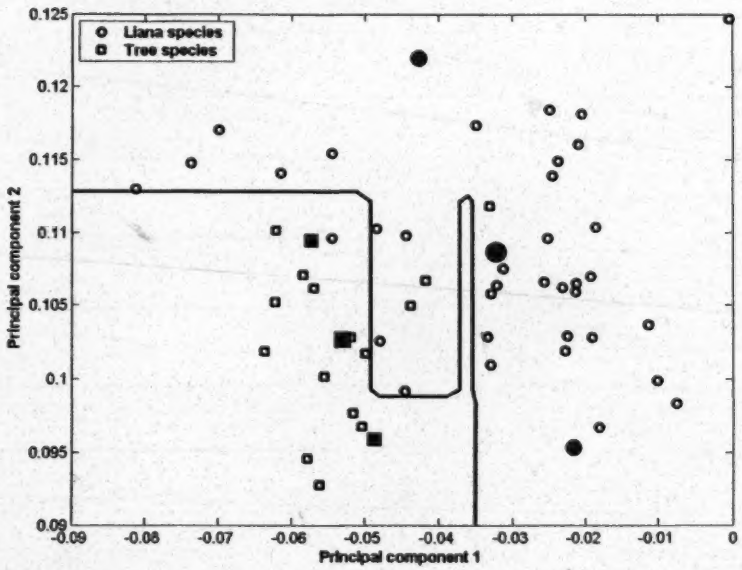

Figure 4-1 cont'd.

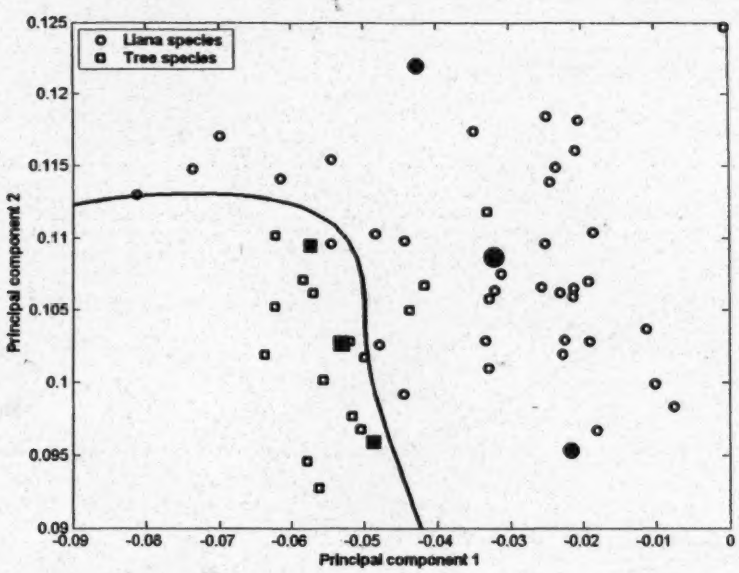

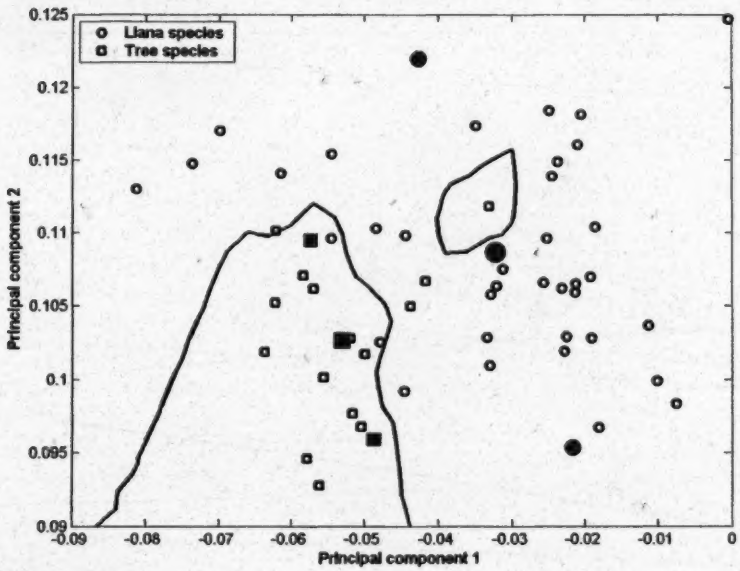

Figure 4-1 cont'd.

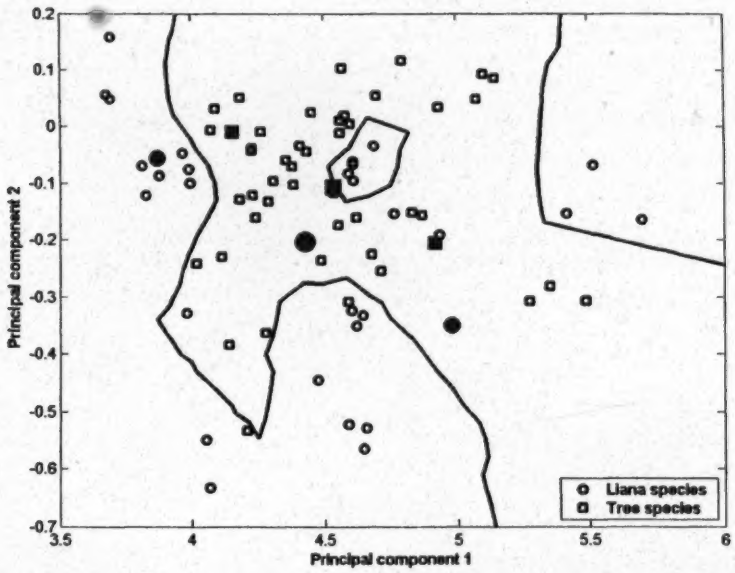

Figure 4-2. Classification of FTS liana and tree raw smoothed spectra by a k-nearest neighbor (knnc, k=2) classifier using PCA method 1. Points correspond to individual leaves (3 per species). The large filled circle indicates the overall FTS liana mean; smaller filled circles are +/- one standard deviation from the mean. The large filled square indicates the overall FTS tree mean; smaller filled squares are +/- one standard deviation from the mean.

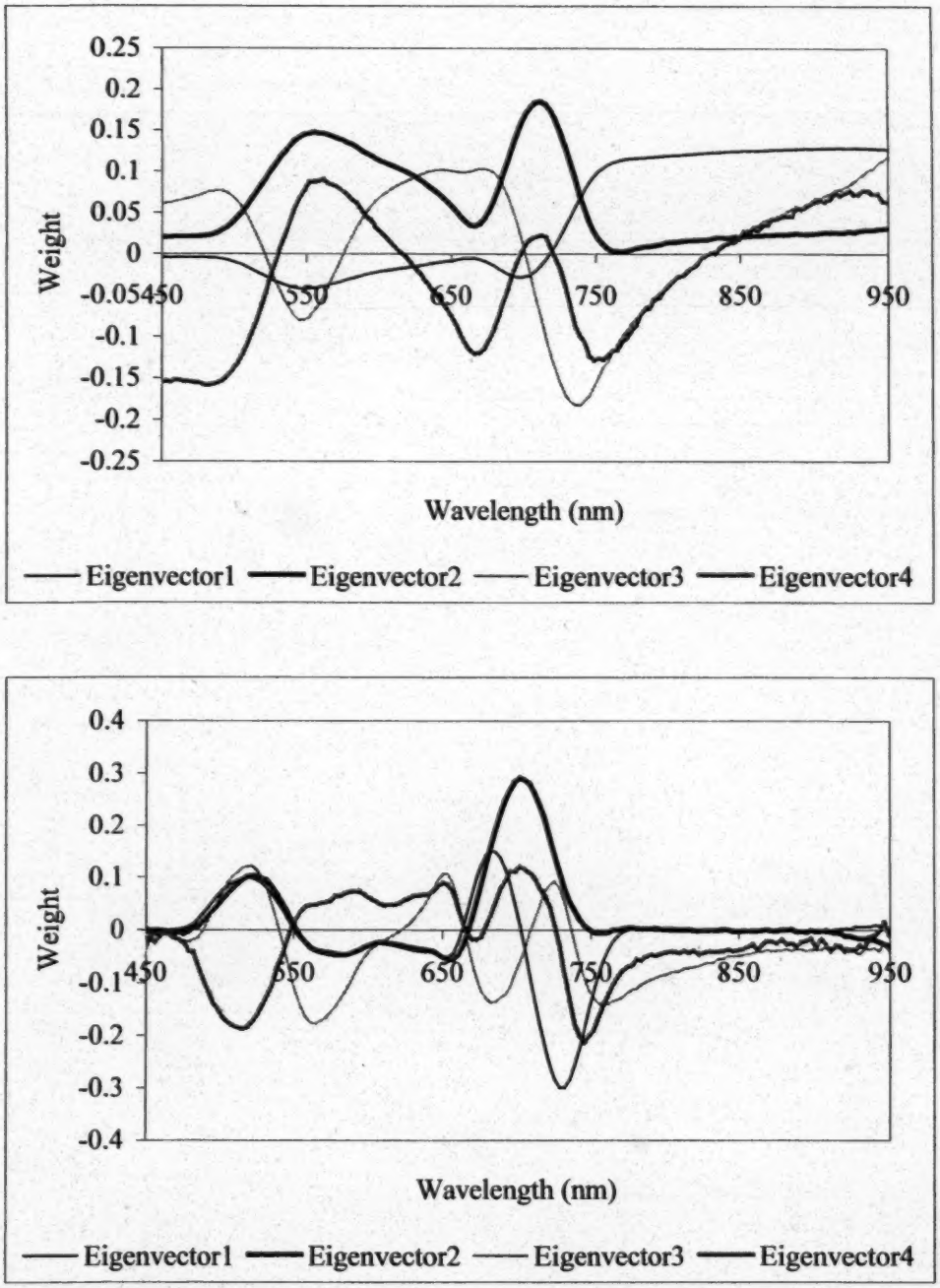

Figure 4-3. Principal component loadings in the spectral bands for PNM PCA1 raw smoothed data (top), PNM PCA1 1st derivative data (2nd from top), FTS PCA1 raw smoothed data (3rd from top), and FTS PCA1 1st derivative data (bottom).

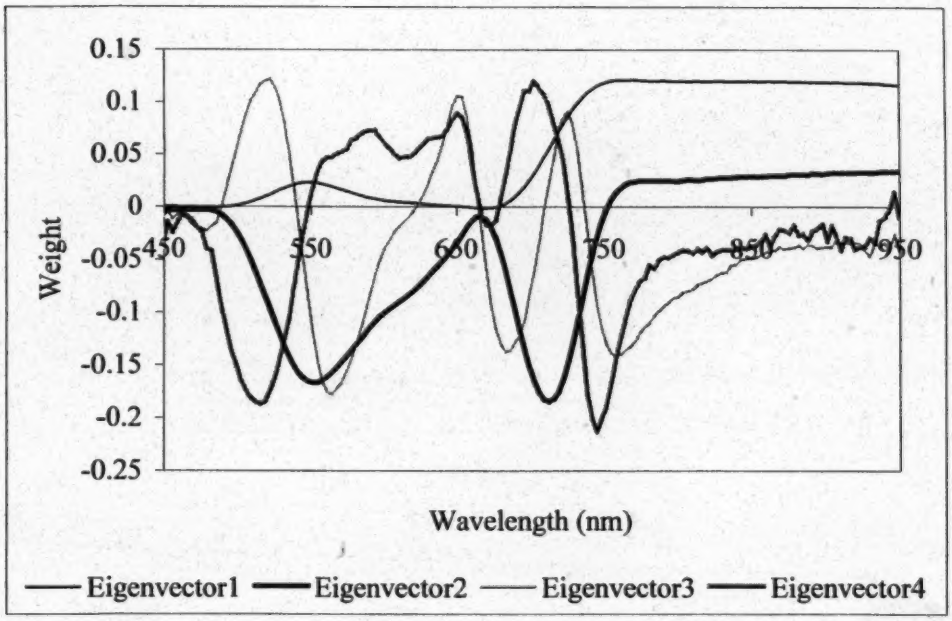

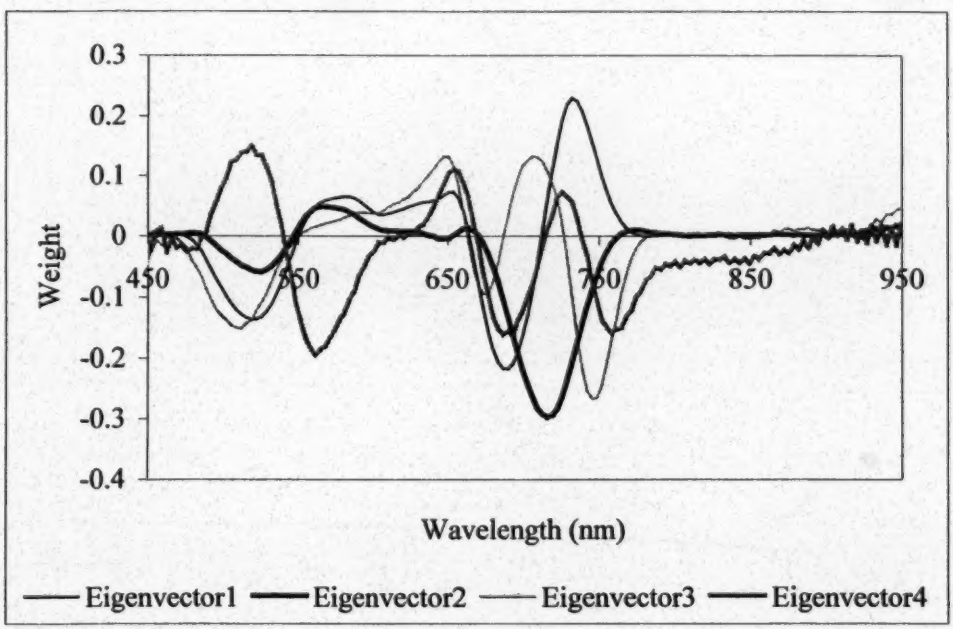

Figure 4-3 cont'd.

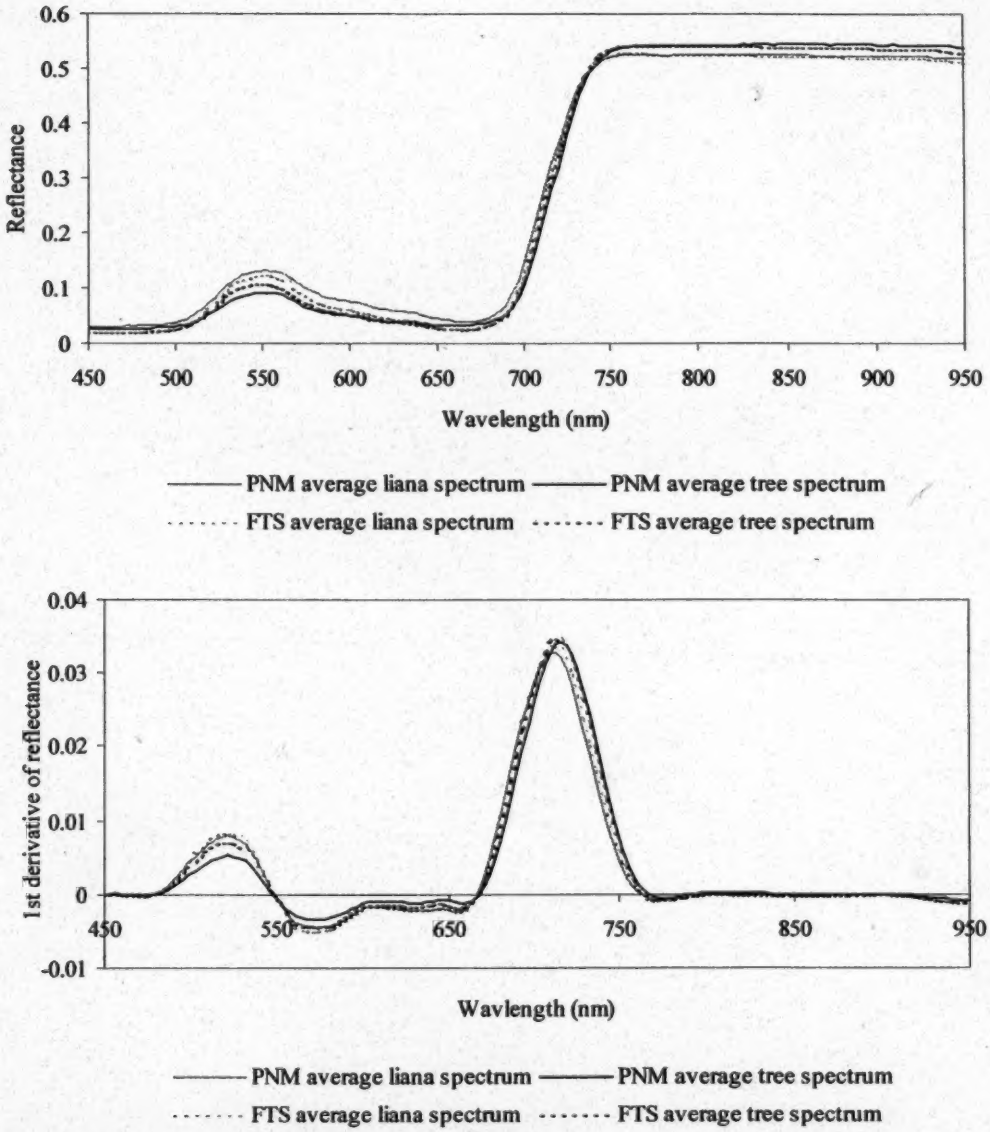

Figure 4-4. Comparison of PNM and FTS average liana and tree spectra (top) and 1st derivative spectra (bottom) over the range 450-950 nm.

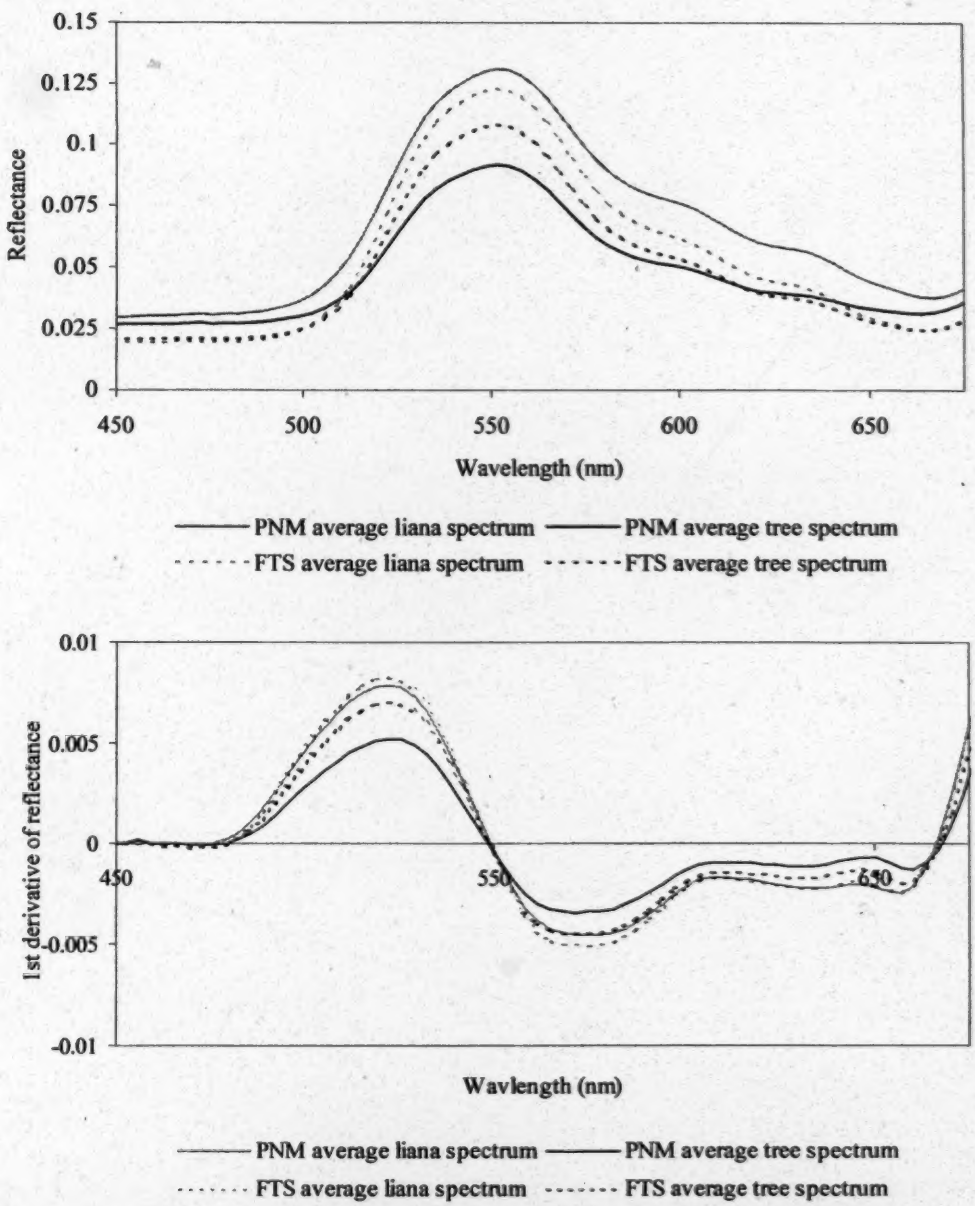

Figure 4-5. Comparison of PNM and FTS average liana and tree spectra (top) and 1st derivative spectra (bottom) over the visible region (450-675 nm) of the electromagnetic spectrum.

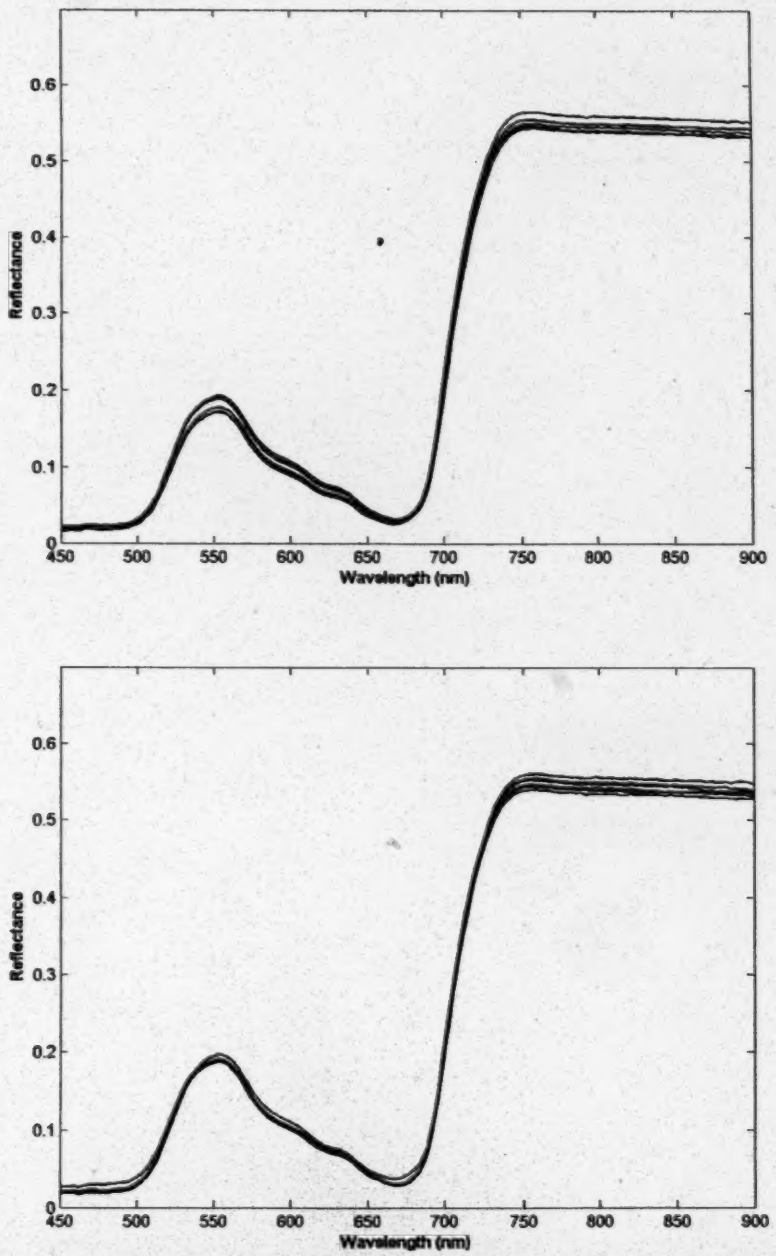

Figure 4-6. An illustration of within-leaf and within-species variability for two species. The three top graphs show reflectance spectra (six/leaf) measured for each of three leaves of the liana species *Tontolea ovalifolia*. The fourth through sixth graphs (from the top) show reflectance spectra (six/leaf) gathered for each of three leaves of the tree species *Simarouba amara*. In the bottom graph, average leaf spectra (three/species) are plotted for both species.

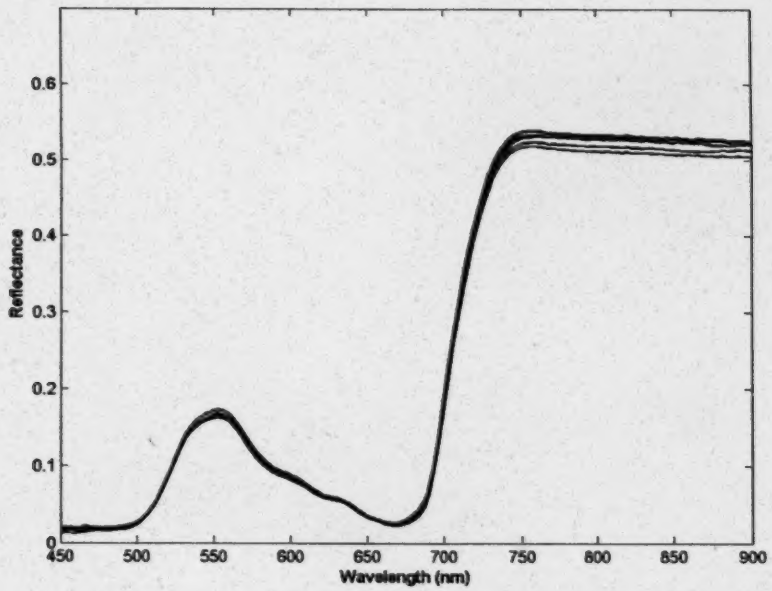

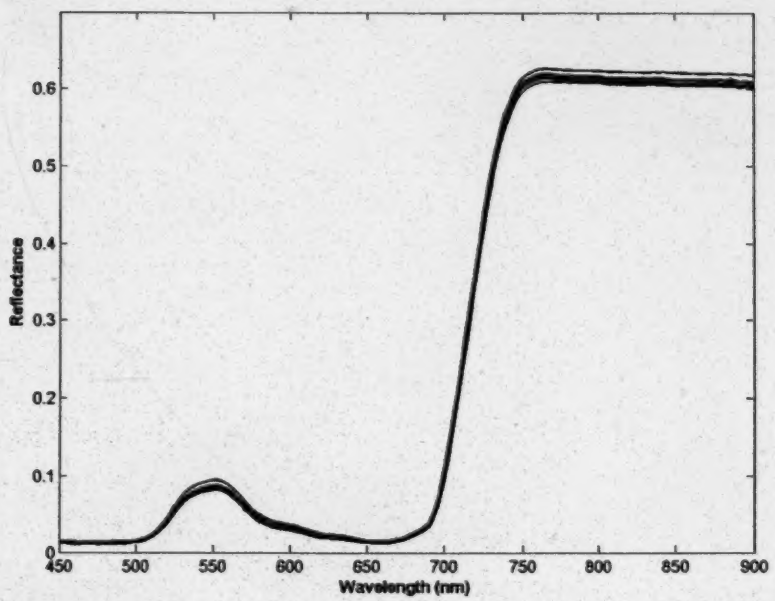

Figure 4-6 cont'd.

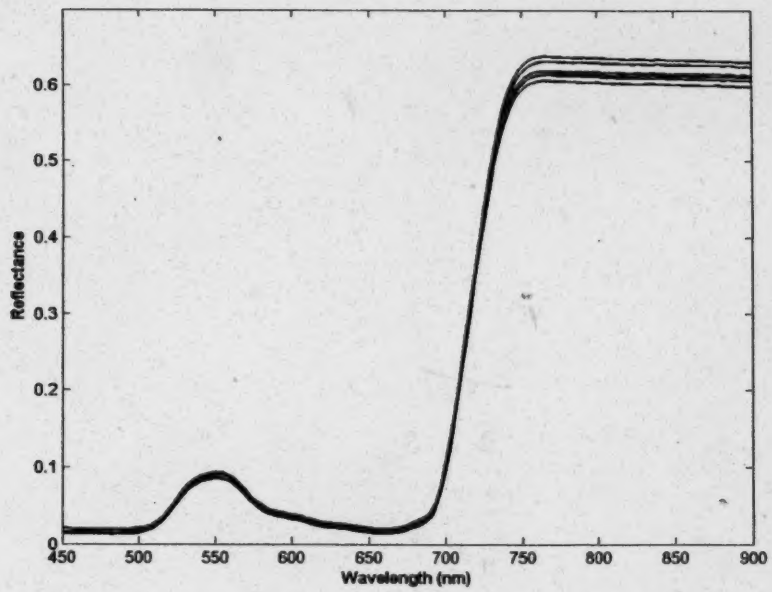

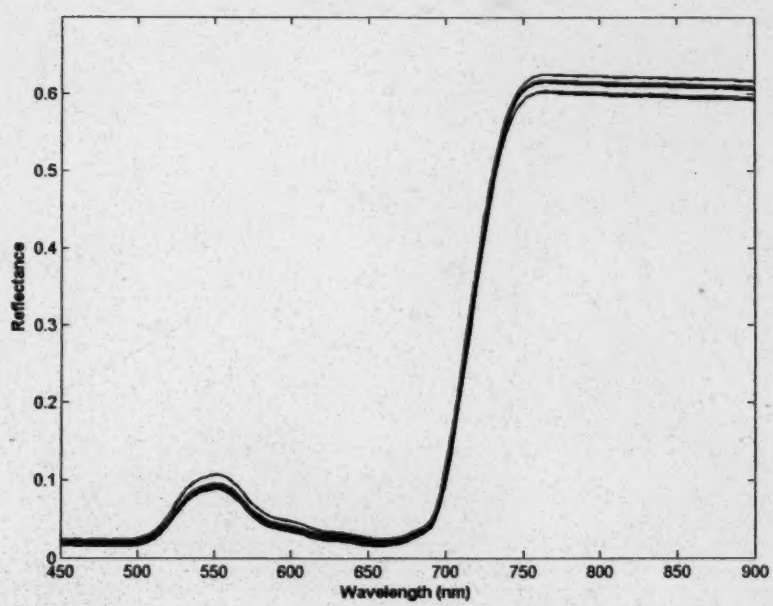

Figure 4-6 cont'd.

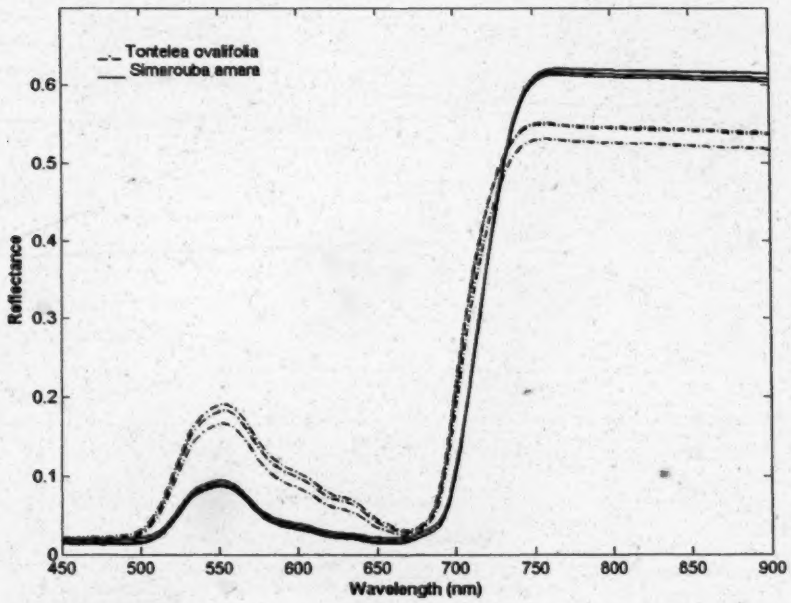

Figure 4-6 cont'd.

LITERATURE CITED

Avalos, G., & Mulkey, S. S. (1999). Seasonal changes in liana cover in the upper canopy of a neotropical dry forest. *Biotropica, 31*, 186-192.

Avalos, G., Mulkey, S. S., & Kitajima, K. (1999). Leaf optical properties of trees and lianas in the outer canopy of a tropical dry forest. *Biotropica, 31*, 517-520.

Carter, G. A. (1993). Responses of Leaf Spectral Reflectance to Plant Stress. *American Journal of Botany, 80*, 239-243.

Chang, C. W., Laird, D. A., Mausbach, M. J., & Hurburgh, C. R. (2001). Near-infrared reflectance spectroscopy-principal components regression analyses of soil properties. *Soil Science Society of America Journal, 65*, 480-490.

Clark, D. B., & Clark, D. A. (1990). Distribution and Effects on Tree Growth of Lianas and Woody Hemiepiphytes in a Costa Rican Tropical Wet Forest. *Journal of Tropical Ecology, 6*, 321-331.

Cochrane, M. A. (2000). Using vegetation reflectance variability for species level classification of hyperspectral data. *International Journal of Remote Sensing, 21*, 2075-2087.

Danson, F. M. (1995). Developments in the remote sensing of forest canopy structure. In F. M. Danson & S. E. Plummer (Eds.), *Advances in Environmental Remote Sensing* (pp. 53-69). Chichester: John Wiley & Sons.

Duin, R. P. W. (2000). *PRTools, Version 3.0: A Matlab Toolbox for Pattern Recognition.* Delft, The Netherlands: Pattern Recognition Group, Delft University of Technology.

Fernández-Cáceres, P. L., Martín, M. J., Pablos, F., & González, A. G. (2001). Differentiation of Tea (*Camellia sinensis*) varieties and their geographical origin according to their metal content. *Journal of Agricultural and Food Chemistry, 49*, 4775-4779.

Fung, T., Ma, F. Y., & Siu, W. L. (1999). Band Selection using hyperspectral data of subtropical tree species. http://www.gisdevelopment.net/aars/acrs/1999/ps3/ps3055pf.htm.

Gausman, H. W. (1985). *Plant leaf optical properties in visible and near-infrared light. Graduate Studies No. 29*. Lubbock, Texas: Texas Tech Press.

Grant, L. (1987). Diffuse and specular characteristics of leaf reflectance. *Remote Sensing of Environment, 22*, 309-322.

Hiscox, J. D., & Israelstam, G. E. (1979). A method for the extraction of chlorophyll from leaf tissue without maceration. *Canadian Journal of Botany, 57*, 1332-1334.

Lee, D. W., Bone, R. A., Tarsis, S. L., & Storch, D. (1990). Correlates of Leaf Optical-Properties in Tropical Forest Sun and Extreme-Shade Plants. *American Journal of Botany, 77*(3), 370-380.

Medina, E., & Klinge, H. (1983). Productivity of tropical forests and tropical woodlands. In O. L. Lange, P. S. Nobel, C. B. Osmond, & H. Ziegler (Eds.), *Physiological Plant Ecology IV* (pp. 281-303). New York: Springer-Verlag.

Mitchell, T. M. (1997). *Machine Learning*. New York: McGraw-Hill.

Murphy, P. G., & Lugo, A. E. (1986). Ecology of Tropical Dry Forest. *Annual Review of Ecology and Systematics, 17*, 67-88.

Ott, R. L. (1993). *An Introduction to Statistical Methods and Data Analysis*. Belmont: Duxbury Press.

Phillips, O. L., Martinez, R. V., Arroyo, L., Baker, T. R., Killeen, T., Lewis, S. L., Malhi, Y., Mendoza, A. M., Neill, D., Vargas, P. N., Alexiades, M., Ceron, C., Di Fiore, A., Erwin, T., Jardim, A., Palacios, W., Saldias, M., & Vinceti, B. (2002). Increasing dominance of large lianas in Amazonian forests. *Nature, 418(6899),* 770-774.

Press, W., Teukolsky, S., Vetterling, W., & Flannery, B. (1996). *Numerical Recipes in C*. Cambridge: Cambridge University Press.

Putz, F. E. (1984). How Trees Avoid and Shed Lianas. *Biotropica, 16*, 19-23.

Schnitzer, S. A., Dalling, J. W., & Carson, W. P. (2000). The impact of lianas on tree regeneration in tropical forest canopy gaps: evidence for an alternative pathway of gap-phase regeneration. *Journal of Ecology, 88*, 655-666.

Schnitzer, S. A., & Bongers, F. (2002). The ecology of lianas and their role in forests. *Trends in Ecology & Evolution, 17*, 223-230.

Chapter 5—Variability in leaf optical properties of Mesoamerican trees and the potential for species classification[1]

INTRODUCTION

An impressive body of literature on leaf optics to date describes the interaction of light with light-harvesting pigments and leaf structural components (e.g. Vogelmann, 1993; Gausman, 1985; Woolley, 1971; Gates et al., 1965). Three primary regions emerge from a leaf spectrum, the first (400-700 nm) dominated by light absorption from pigments (especially chlorophyll), the second (700-1200 nm), influenced by light scattering at air-cell wall interfaces and characterized by high reflectance and transmittance, and the third (1200-2500 nm) governed by water absorption (Hoffer & Johannsen, 1969). Further to this, scientists have examined perturbations to leaf absorption, reflection and transmission of light by external influences such as light availability (Gausman, 1984), disease (Knipling, 1967), freezing (Woolley, 1971), stress (Carter, 1993), and senescence (Gitelson & Merzlyak, 1994). The spectral properties of different plant types (Gates, 1965) or species (Knapp & Carter, 1998; Gausman & Allen, 1973; Allen et al., 1970) have also been compared. In more recent years, our understanding of leaf optics is being extended to larger-scale applications in the field of remote sensing, for the assessment of physiological performance of plant canopies (e.g. Gamon et al., 1990) and for distinguishing between land cover vegetation types (e.g. Salem et al., 1995). In effect, results from leaf-level studies are often used as a basis for establishing techniques for retrieving information from canopy reflectance measured by remote sensors.

Little is known about the leaf optical properties of tropical trees or about the potential for tropical tree species identification from remote sensing. Among the few exceptions are studies by Lee et al. (1990) and Lee and Graham (1986), who compared leaf optical properties of tropical sun and shade species, as well as Avalos et al. (1999), who compared leaf optical properties of tropical dry forest trees and lianas. Cochrane (2000) and Fung and Siu (1998) assessed tropical tree species separability using reflectance of leaf or branch samples. More recently, Clark et al. (2005) was successful in discriminating seven tropical rain forest tree species at leaf, pixel and crown levels in the first publication to attempt tropical tree classification using hyperspectral imagery, in which spectral reflectance is measured over numerous contiguous bands of narrow width (typically $\leq$10 nm). The study represents an important breakthrough for tropical tree species identification. Operational species classification could have numerous applications, including monitoring endangered or commercial tree species, characterizing biodiversity in ecologically important habitats, including reserves and biological corridors, monitoring changes in species composition over time as well as for tree demography studies associated with global environmental changes (Clark et al. 2005).

---

[1] A version of this chapter has been accepted for publication. Castro-Esau, K. L., Sanchez-Azofeifa, G. A., Rivard, B., Wright, S. J. & Quesada, M. (in press). *American Journal of Botany*. Reprinted with permission from the Botanical Society of America.

The precept for species discrimination is that inter-species variability in spectral reflectance exceeds intra-species variability. This presents a challenge for species identification due to inherent similarities in vegetation characteristics among species, including leaf biochemistry and anatomy, which result in similarities in leaf spectral reflectance. After posing the question 'How Unique Are Spectral Signatures?', Price (1994) determined that while some are clearly distinct, others may not be separable at all. In reality, despite the advantages of hyperspectral technologies, classification of plant species may be difficult and, at times, unfeasible. A complicating factor is the dynamic nature of plant spectral signatures. Natural cycles such as leaf flush and senescence, as well as environmental factors affecting mineral nutrition, health, light availability and water supply may contribute to changes in a species' spectral signature over time or at a given position in the canopy (Carter, 1993; Gausman, 1985; Gausman, 1984). To date, even the studies from temperate regions have not fully evaluated the seasonal dynamics of change in leaf spectral characteristics on tree classifications, nor do they explore the stability of tree spectral signatures over multiple sites with a range of climatic and edaphic conditions. Intuitively, these factors, which lead to within-species variability in reflectance spectra, could lead to significant confusion for species recognition using hyperspectral data. Although Clark et al. (2005) tested within-species variability for seven tropical tree species at one site, the degree of within-species variability over a large number of tropical tree species and a range of environmental conditions has not been adequately addressed to date.

With image-based automated tropical tree species classification in its preliminary stages of development, we believe it to be constructive at this time to provide a comprehensive assessment of intra-specific variability of leaf spectral reflectance and its potential to influence tree species classifications. The main objective of this paper, therefore, is to evaluate within-species and between-species variability in leaf spectral reflectance for a wide variety of tropical trees found at seven sites in southern Mexico and Central America. We also investigate crown-level spectra of five tree species from Fort Sherman, Panama. In effect, we ask 'How unique are spectral signatures of tropical tree species?' A large part of our study focuses on the leaf level for several reasons: 1) by necessity, since high spatial resolution (< 5 m) hyperspectral data was not available for most of our sites at the time of data collection, 2) the use of leaf spectra allows for a more controlled assessment of variability at multiple levels, and 3) spectral reflectance from leaves is usually the dominant contribution to tree crown reflectance. To evaluate variability in leaf reflectance of tropical trees, spectral metrics that describe reflectance shape and amplitude (Price, 1994) are compared at various levels within and between species. To explore the potential to identify species, we also classified the spectral data from the different sites using forward selection of features and a set of classifiers described in Castro-Esau et al. (2004). Lastly, we examined the correspondence between selected leaf traits (chlorophyll content, leaf thickness, and leaf histological features) and leaf spectral reflectance characteristics for one site to further our understanding of differences in leaf spectra between species.

MATERIALS AND METHODS

Study sites

Leaf samples were gathered from seven sites in Mexico, Costa Rica and Panama (Table 5-1). Five of the sites support tropical dry forest ecosystems, where our research group is concurrently conducting studies on leaf area index and forest complexity and their ties with remote detection of secondary growth versus mature forest. These sites are part of an international research consortium called TROPI-DRY that aims to understand the biophysical characteristics of neotropical dry forests and human interactions with these forests. Tropical dry forests undergo significant phenological changes through dry-wet season cycles, and typically contain species with varying degrees of deciduousness (Avalos & Mulkey, 1999; Bullock & Solis-Magallanes, 1990; Frankie et al., 1974). In addition, tropical dry forests can present high rates of species endemism (Kalacska et al., 2004; Lott et al., 1987).

Parque Natural Metropolitano, Panama, is the site of our case study that makes ties between leaf traits and leaf spectral reflectance. This 100-150 year-old secondary forest has a pronounced dry season from January through April, with annual precipitation averaging 1740 mm.

Crown spectra were recorded from a canopy crane at Fort Sherman, Panama, a tropical wet forest site.

Leaf sample collection

At each site, three to fifteen sun leaves were collected per tree (Table 5-2). One to five trees were sampled per species. In general, leaves were collected from the distal or middle portion of the branch. At some sites, it was not logistically feasible to sample more than one tree per species, such as Parque Natural Metropolitano and Fort Sherman, where we were restricted to trees within reach of a canopy crane and by institutional regulations regarding the size of samples that can be collected from each tree. A full list of the species sampled is provided in Table 5-3. The samples were acquired using one of the following methods: pole pruner (Mexico and Costa Rica), sling shot (Costa Rica), or canopy crane (Panama). Leaves were collected, placed in plastic bags containing moistened paper towels, labeled, and placed in a larger bag or cooler containing ice. Samples were transported to an indoor laboratory and leaf spectral reflectance was analyzed the same day. Maintaining leaf moisture prevented significant changes in leaf reflectance during this period (Foley et al., in press).

Crown spectra

Crown spectral measurements were obtained for five fairly flat, uniform crowns at Fort Sherman (Panama) by positioning the canopy crane gondola above the center of each crown and fitting the bare fibre-optic of a spectrometer through the floor grating (see *UniSpec Spectral Analysis System* below). The five species were: *Cordia bicolor* (Boraginaceae), *Dussia munda* (Fabaceae), *Jacaranda copaia* (Bignoniaceae), *Tapirira guianensis* (Anacardiaceae), and *Vochysia ferruginea* (Vochysiaceae) (Fig. 5-1, Table 5-3).

Leaf trait data

At Parque Natural Metropolitano (Panama), ancillary data on pigmentation, leaf thickness, internal leaf structure, as well as diffuse reflectance and transmittance were collected in October 2003.

Leaf chlorophyll content and thickness

Five 2.0 cm^2 leaf cores per tree species, each from a different leaf, were analyzed for chlorophyll content at Parque Natural Metropolitano. Chlorophyll *a*, chlorophyll *b* and total chlorophyll content were determined using the dimethyl sulphoxide (DMSO) extraction method (Hiscox & Israelstam 1979). A Smartspectro spectrophotometer (LaMotte, Chestertown, MD, USA) was used to determine absorbance at 645 and 663 nm. Pigment content was computed using Arnon's (1949) relationships and converted to a per area basis. In addition, nondestructive assessment of chlorophyll content was made using a SPAD 502 (Minolta Camera Co, Osaka, Japan) chlorophyll absorbance meter. The SPAD measures absorbance at 650 and 940 nm and yields a relative chlorophyll content, or 'chlorophyll index' value (Richardson et al., 2002; Markwell et al., 1995). Leaf thickness was measured for five to ten leaves per species using a Nikon digital micrometer (to nearest 0.001 mm). Five measurements were taken per leaf, avoiding large veins.

Leaf histology

Small pieces of leaf blade (approximately 1 cm long and 2-3 mm wide) were collected at Parque Natural Metropolitano in October 2003 for histological analysis. The leaf pieces were fixed under vacuum for two weeks in a formalin aceto-alcohol (FAA) solution. After fixation, the samples were run through an ethanol processing center (Fisher Histomatic 166) and embedded in paraffin molds. Thin sections (5 μm) were cut from the mounted samples using a microtome. Slides were mounted and stained (Harris' haematolxylin stain), and viewed under a Leica DM RXM light microscope (20X magnification). Digital photos were taken of the stained samples. The percentage of air space in the spongy mesophyll was determined by classifying the photos for cells versus air space. Spongy mesophyll thickness and the ratio of spongy mesophyll to total leaf thickness were calculated using a 100 μm scale given in each photo, from which a new ruler was constructed with 10 μm increments.

Leaf diffuse reflectance and transmittance

In addition to measurements of bi-directional reflectance of leaves described below, diffuse reflectance and transmittance were recorded using an 1800-12S External Integrating Sphere (LI-COR Inc., Lincoln, NE, USA) in conjunction with a UniSpec spectrometer. The spectrometer fiber-optic was fit through a port on the sphere. To record diffuse reflectance, the sphere illuminator was directed towards the leaf sample in the sample port and the spectrometer fiber-optic viewed the sphere wall. To record transmittance, the leaf was reversed so that the underside faced the sphere interior. The sphere illuminator was directed through the leaf sample, with the spectrometer fiber-optic viewing the wall. Dark scans were performed regularly and white reference scans (using barium sulfate) were repeated for every leaf sample. Both diffuse reflectance and transmittance were calculated as a ratio using the white reference data.

Measurements of bi-directional spectral reflectance

Bi-directional leaf spectral reflectance was measured at all sites, using one of two spectrometers: 1) a UniSpec Spectral Analysis System (PP Systems, Amesbury, MA, USA) or 2) a FieldSpec HandHeld spectrometer (Analytical Spectral Devices, Boulder, CO, USA). The 2002 and 2003 datasets employed the FieldSpec HandHeld (FieldSpec HH) and the UniSpec, respectively. All crown spectra (Fort Sherman, Panama) were measured using the UniSpec.

UniSpec Spectral Analysis System

The Unispec Spectral Analysis System VIS/NIR relies on a 256-element photodiode array. The spectral range is 350-1100 nm, with a sampling interval of 3.3 nm, and a spectral resolution of <10 nm. A bifurcated fibre-optic delivers light from an internal 7.0 W halogen lamp via one branch, and receives reflected light via the other. To measure spectral reflectance of leaves, we employed a leaf clip that holds the foreoptic at 60° and maintains a 2.3 mm-diameter field of view (FOV). Sample reflectance was measured by comparing leaf reflectance to reflectance of a white standard (Spectralon). Ten scans were averaged per recorded spectrum. Dark scans and white reference scans were performed frequently to prevent the effects of instrument drift on the spectra.

At Fort Sherman (Panama), crown spectra were recorded mid-morning under sunny conditions. White reference measurements were taken before measurements for each species as well as intermittently if we sensed the light conditions changed. Care was also taken to avoid taking measurements if the shadow of the gondola fell within the estimated FOV. Spectra were recorded at a height of 5 m above each crown, determined by lowering a measuring tape from the gondola. Using the bare fibre-optic of the UniSpec (40° FOV), the diameter of crown viewed was approximately 3.6 m. Six measurements were taken from the same position above each crown and averaged.

FieldSpec HandHeld

The FieldSpec HandHeld spectrometer relies on one 512-element photodiode array. Its range is 325 to 1075 nm, with a sampling interval of 1.6 nm and spectral resolution of 3.5 nm at 700 nm. The bare fibre-optic FOV is 25°.

To obtain leaf spectral reflectance measurements, an external 50 W halogen lamp was directed at the leaf at an illumination angle of 45°. Leaves were placed against a black minimal (2%) reflectance panel. The FieldSpec HandHeld fibre-optic, inserted into a mounting gun attached to a tripod, was positioned directly above the sample. In all cases, height was adjusted so that the FOV had a diameter of approximately 11 mm. Reflectance was determined by standardizing the sample data to white reference (barium sulfate) data under the same illumination and viewing conditions. White reference scans were recorded frequently. Ten scans were averaged per reflectance spectrum.

Spectral analysis

Spectra collected with the two spectrometers were analyzed separately rather than collectively due to differences between spectra measured for the same objects as described in Castro-Esau et al. (in press).

D and θ

Two spectral metrics described by Price (1994) enabled comparisons between pairs of spectra as follows:

$$D = \left[\frac{1}{\lambda_b - \lambda_a} \int_{\lambda_a}^{\lambda_b} [S_1(\lambda) - S_2(\lambda)]^2 \, d\lambda \right]^{1/2} \quad (1)$$

$$\theta = \cos^{-1} \left[\frac{\int S_1(\lambda) S_2(\lambda) d\lambda}{\left[\int S_1(\lambda)^2 d\lambda \right]^{1/2} \left[\int S_2(\lambda)^2 d\lambda \right]^{1/2}} \right] \quad (2)$$

D represents the difference in amplitude between two spectra, and is computed as the root mean square difference between a pair of spectra (S_1 and S_2) averaged over the spectral range of interest (λ_a to λ_b). The metric θ determines the angle between two spectra, and may be interpreted as the difference in shape between the pair of spectra. It is computed as a vector dot product for the pair of spectra, with amplitude dependence removed.

The spectral range retained to calculate D and θ was 445.9-949.6 nm for both the UniSpec and FieldSpec Handheld. In this region, noise from both instruments was low. In order to compute D and θ for the same spectral range and interval, FieldSpec HandHeld data were interpolated to 3.3 nm intervals to match the sampling intervals of the UniSpec. No smoothing was performed.

D and θ were compared at the following levels for leaf spectra (numbers 1-6) or crown spectra (number 7):

1) **Within-leaf**. D and θ were calculated where multiple measurements were made per individual leaf. For example, six measurements per leaf were recorded for the Parque Natural Metropolitano March 2003 dataset (Table 5-2). Therefore, D and θ were assessed for all 15 possible pairs of the six spectra (also termed 'pairwise combinations' hereafter).
2) **Within-tree.** Where multiple leaves were sampled per tree, average leaf reflectance was computed for each leaf and D and θ were then calculated on all pairwise combinations of spectra from those leaves.
3) **Between-tree and within species, site and season.** An average tree spectrum was computed from all the leaf spectra for each tree. Where multiple trees were sampled per species, D and θ were computed for all pairwise combinations of average tree spectra.
4) **Between season and within species and site.** Pairwise comparisons of D and θ were made between average tree spectra of the same species measured in the dry season and wet season. These comparisons were possible at the Parque Natural Metropolitano and Fort Sherman (Panama) sites only where sunlit leaves were collected from the same trees and measured with the same spectrometer in both seasons (Table 5-2). This comparison was not performed for Los Inocentes (Costa Rica) since the November 2002 and March 2003 datasets were obtained using different spectrometers.
5) **Between site and within species and season.** D and θ comparisons were possible for species sampled at more than one site. There were seven such species, all measured with the FieldSpec HandHeld: *Bombacopsis quinata* (Malvaceae), *Bursera simaruba* (Burseraceae), *Byrsonima crassifolia* (Malpighiaceae), *Cedrela odorata* (Meliaceae), *Gliricidia sepium*

(Fabaceae/Papilionoideae), *Guazuma ulmifolia* (Sterculiaceae), and *Hymenaea courbaril* (Fabaceae/Caesalpinoideae).

6) **Between-species and within site.** Within a site, all pairwise combinations of tree spectra of different species were made. For example, the Chamela (Mexico) August 2003 dataset provided possible combinations for 27 species.
7) **Between-species and within site (crown-level).** D and θ were computed for all pairwise combinations of the five averaged crown spectra at Fort Sherman, Panama.

A Wilcoxon Rank Sum test was used to determine if there were significant differences between levels 3 and 6. This test indicated if comparisons of individual conspecific tree crowns differed from comparisons among species. The test was performed using mean values of D and θ for comparisons of conspecific trees (level 3) and comparisons of heterospecific species pairs (level 6).

Classification

Beyond examination of shape and amplitude differences between spectra, we determined if it was possible to discriminate between species based on reflectance spectra. Steps involved in the classification included feature selection, classifier training, and classifier testing.

Forward stepwise feature selection reduced the number of variables entered into the classification. Stepwise feature selection has proven useful for studies involving species classification from hyperspectral data (Clark et al., 2005; van Aardt & Wynne, 2001), and its initial testing on our datasets led to higher classification accuracies than using a principal components-based approach described in our earlier work (Castro-Esau et al., 2004) for discriminating liana and tree species. The approach for forward feature selection involves initial selection of the single best feature, and consecutively adding features that improve performance the most. In this case, the criterion used for the procedure was first nearest neighbor leave-one-out classification performance (Duin, 2000). By taking every other spectrum, the data array was split in half into training and testing sets. Feature selection was performed using the training set only.

Spectra were classified to species using a selection of supervised parametric and nonparametric classifiers, previously described in Castro-Esau et al. (2004). The classifiers are part of a pattern recognition toolbox, PRTools, developed by Duin (2000) for use within Matlab (The MathWorks, Natick, MA, USA). Parametric classifiers included a logistic linear classifier (loglc) and a normal density based quadratic classifier (qdc). Nonparametric classifiers included a decision tree classifier (treec), a neural network classifier (based on backpropagation and Levenberg-Marquardt gradient descent) (lmnc), and a k-nearest neighbor classifier (knnc).

Classification involved several steps. Initially, training data were labeled according to species and used to train the classifiers. Secondly, the trained classifiers classified the test dataset, to validate the robustness of the model (Defernez & Kemsley, 1997). Error estimation was determined for both the training and testing data, which constituted the percentage of incorrectly classified spectra in each case. For each dataset, classifications were run several times using multiples of 10 selected features. The highest classification accuracies were reported. The classifications involved all leaf spectra for each species (a minimum of 5 spectra, but in most cases 10+). Classifications were run

on non-interpolated data in the range 445.9-949.6 nm for the UniSpec and 445.5-950.7 nm for the FieldSpec HandHeld.

A final analysis was run to determine the potential for classifying increasing numbers of tropical forest tree species. A dataset of 50 species with 10 spectra each was compiled from Parque Natural Metropolitano, Fort Sherman, and Chamela, all using UniSpec 2003 wet season data. Classifications were run on 10,000 sets each of 5, 10, 15, 20, 25, 30, 35, 40, and 45 species, where each set of species was chosen randomly from the 50 total species. A single classification was run on the full set of 50 species. For this analysis, we used the logistic linear classifier and 30 previously selected features, the top ten features from the within-site classifications for each of the three sites. Ten thousand repetitions were considered a representative sample of all possible species combinations since variation around mean classification errors stabilized by this point, as determined by testing with greater numbers of repetitions.

RESULTS

D and θ

With respect to the goal of classifying trees according to species, it is evident that the magnitude of variability in amplitude (*D*) and shape (θ) within each species presents a challenge (Figs. 5-2 and 5-3). Levels of comparison to the left of the 'between-species' category are measures of intra-specific variability. While there is a general increase in mean *D* (Fig. 5-2) and θ (Fig. 5-3) with increasing level of comparison or 'scale' from within-leaf measurements through to between-species measurements (with the exception of the 'between-sites' category for the FieldSpec HH data), there is a high degree of overlap between each of these levels. Even so, a significant difference ($P<0.05$) was found between level 3 ('between-tree') and level 6 ('between-species') with the Wilcoxon rank sum test, indicating that for one site at one date, variability between species is greater than variability between individuals of the same species. At the crown level, amplitude differences between all possible pairwise combinations of spectra of the five species were much higher than for any other category (Fig. 5-2a). This was particularly evident in the near-infrared region (Fig. 5-4).

The high variability within species but over multiple sites observed in Figs. 5-2b and 5-3b ('between-sites' FieldSpec HH data) would appear to preclude classification of leaf reflectance spectra at one site based on training data from another site or from a library of hyperspectral signatures of tropical trees. Figure 5-5 shows average reflectance spectra collected during the wet season of 2002 (October-December) for two species encountered at three sites each. Leaves of the same species collected at multiple sites may exhibit different characteristics with regard to leaf moisture content, leaf area, and chlorophyll content (represented by SPAD value) (Table 5-4).

Similarly, leaf spectra vary widely across seasons. For the majority of tree species sampled at Parque Natural Metropolitano, Panama, higher reflectance in the visible region of the spectrum during the dry season (March 2003) was a manifestation of lower chlorophyll content as compared to the wet season (October 2003) (data not shown). For example, average total chlorophyll content (n=5 samples) varied from 465.63 ± 28.10 $\mu mol/m^2$ in the dry season to $652.00 \pm 97.01 \mu mol/m^2$ in the wet season for *Astronium graveolens* (Anacardiaceae). Average reflectance at 550 nm was 7.4% and 6.5%,

respectively, for the two seasons. Differences in leaf age and stress levels from season to season may have caused additional variation in the leaf spectra.

Classification

Species from one site and season were classified with high accuracy (Table 5-5). Not unexpectedly, the highest classification error accompanies the site for which the largest number of species was sampled (Chamela, Mexico, 27 species), indicating a potential problem for complex tropical dry forest ecosystems in which species density can exceed 50-70 species per ha (Kalacska et al., 2004). Still, accuracy on the test data was 80%.

For our case study site (Parque Natural Metropolitano, Panama), classification error on the test data (47 of the total 95 leaf spectra for the site, representing 10 species) was 8.51% (Table 5-5). Misclassified test spectra included one leaf spectrum (out of 4 or 5 test spectra per species) for each of the following species: *Anacardium excelsum* (Anacardiaceae), *Luehea seemannii* (Malvaceae), *Cordia alliodora* (Boraginaceae), and *Enterolobium cyclocarpum* (Fabaceae/Mimosoideae). Since no single species was confused with greater frequency than the remainder, all species were generally well classified.

Accuracy was dependent on number of features and classifier. Highest classification accuracies were obtained with 20-40 features, beyond which classification accuracy eroded due to overfitting. The frequency at which wavebands in various regions of the spectrum were selected for the various species-level classifications, based on all classified sites and the top 20 selected features per site was higher for visible (400-700 nm) bands than for near-infrared (700-950 nm) bands (Fig. 5-6). Classifiers also affected accuracy. For example, using 40 wavebands and a logistic linear classifier produced the lowest overall classification error of 2.67% for the Fort Sherman site (Table 5-5). The second lowest error for the same site, however, was 14.67% for a k-nearest neighbor classifier (k=2) (not shown). In general, however, reasonably accurate classifications by multiple classifiers at each site lends support for the inherent separability of the species. For four of the six sites, species-level classification using the logistic linear classifier produced the lowest classification errors.

Two additional classifications were run to determine the potential for classifying species across seasons and across sites. At Parque Natural Metropolitano, there were six species for which we had bi-directional reflectance data in both dry (Mar 2003) and wet (Oct 2003) seasons. Data from the wet season (Oct 2003, 10 samples/species) were used to train classifiers to test on the dry season (Mar 2003, 3 samples/species) dataset. In this case, best-case scenario classification error on the test data was high (28%). To classify species across sites, we used data from the seven species sampled using the FieldSpec HandHeld at multiple locations. For the pooled dataset, there were 10-43 samples (spectra) per species (mean=29), and each species was sampled at 2-3 locations. Data from one site per species were used to train the classifiers, and data from the remaining site(s) were reserved for testing. Classification was poor again, with best-case scenario classification error on the test data at 51.75%.

The classification analysis using repeated classifications on random sets of 5, 10, 15, etc. species up to a total of 50 species indicated that, within this range, mean classification error on the test data rises linearly with number of species (Fig. 5-7).

Classification error on the training data was 0% in all cases. For the test data, it ranged from 13.79% for five species to 22.40% for 50 species. Variability was greater with fewer species since, from the random selection of species, entirely different sets of species were selected often. With a higher number of species, the same species would have entered into multiple classifications. It was noted that, below 5 species, the linear trend shown in Fig. 5-7 was not followed (e.g. for two classes, test data error was only 3.30%).

Case study including leaf trait data: Parque Natural Metropolitano

For each leaf trait, species at Parque Natural Metropolitano were ranked from lowest to highest value in Table 5-6. In particular, *Astronium graveolens* (Anacardiaceae) is exceptional for its low reflectance in both visible and near-infrared regions, accompanied by high transmittance in the same regions (Table 5-6, Fig. 5-8). Thin leaf section analyses displayed an unusually thin, compact spongy mesophyll for this species (Fig. 5-9). *Astronium graveolens* had both low percent intercellular space and low near-infrared reflectance, whereas *Ficus insipida* (Moraceae) had high percent intercellular space, a wide spongy mesophyll, and high near-infrared reflectance (Table 5-6, Fig. 5-9).

Correlation analyses between variables listed in Table 5-6 confirm associations between leaf pigmentation and/or structural features and leaf reflectance and/or transmittance. In addition to 548.5 nm and 800.7 nm, given in Table 5-6, the wavebands 445.9 nm, 532 nm, 571.6 nm, 680 nm, 706.2 nm, 748.6, and 959.3 nm were also tested in the correlation analyses, for both diffuse reflectance and transmittance as well as bi-directional reflectance. Transmittance in near-infrared regions was negatively correlated ($P<0.05$) with spongy mesophyll width (at 748.6 nm and 800.7 nm) and highly negatively correlated ($P<0.01$) with percentage intercellular space (at 706.2 nm, 748.6 nm, 800.7 nm and 959.3 nm) (Table 5-7). While relationships between reflectance wavebands and chlorophyll content are generally non-linear, there was a strong linear correlation ($P<0.01$) between chlorophyll content (chlorophyll *a*, chlorophyll *b*, and total chlorophyll, measured in $\mu mol/m^2$) and a common spectral index used for chlorophyll estimation, the simple ratio (R_{750}/R_{705}) (Gitelson & Merzlyak, 1994). To test these relationships, chlorophyll data from individual samples (N=5 samples per species for six species) were paired with bi-directional reflectance data for the same sample (UniSpec spectral reflectance measurements were taken of the leaf cores that were then designated for chlorophyll analysis). Leaf thickness showed significant correlations ($P<0.05$) with bi-directional reflectance at 532 nm, 548.5 nm, 571.6 nm, and 706.2 nm (not shown).

DISCUSSION

Leaf spectral reflectance is a rich data source for understanding differences in leaf traits among species and for assessing the potential for species discrimination. Differences in leaf traits are the basis for differences in leaf optical properties that permit species discrimination at the leaf-level, which within sites and within seasons, appears promising for limited species numbers. Since classification accuracy degrades with increasing numbers of species, it is more likely that, for species-rich tropical forests, a portion of species with distinctive reflectance characteristics will be separable from the larger community. At the crown scale, in the first tropical tree discrimination study using hyperspectral imagery, Clark et al. (2005) also found good potential (92% accuracy) for

a limited number of emergent tree species (7) from a single-date (1998) HYDICE image of La Selva, Costa Rica using a linear discriminant analysis and 30 wavebands. These efforts represent the initial stages of operational tropical tree species identification by hyperspectral remote sensors, which will provide an important tool to tropical biologists and ecologists for a variety of applications.

***D* and θ (leaf-level)**

Use of Price's (1994) metrics *D* and θ show that variability in a species' reflectance begins within individual leaf blades (Figs. 5-2 and 5-3). Multiple spectral measurements taken over the leaf blade show variation, particularly over leaf veins (we avoided the main vein). Similarly, multiple measurements from the SPAD chlorophyll absorbance meter, of the same leaf, also vary, indicating uneven chlorophyll distribution across the leaf blade (also documented in other species, e.g. Hew et al., 1998). This variation increases when comparing multiple leaves from the same tree, and is compounded further when examining spectra of leaves of different conspecific trees from a single site. Greater differences yet are seen for between-season and between-site spectra of the same species (Fig. 5-5).

Classification

Classification for each site was successful despite high intra-specific variability, with greater than 80% test data accuracy at all sites. These results may be attributed to the selection of a set of highly discriminating features (wavebands) from the spectral range available and the use of a variety of powerful pattern recognition tools.

The most frequently selected wavebands in our analyses were in the blue region (400-499 nm), which is strongly influenced by absorption of chlorophylls and carotenoids (Jensen, 2000). The blue-green edge leading to the green peak (500-549 nm) and chlorophyll absorption leading to the red edge (650-699 nm) were also important (Fig. 5-6). This finding is similar to Fung et al. (1999), who used stepwise linear discriminant analysis for feature selection and found selected bands to lie mainly in the green peak and red edge regions. Overall, however, the bands selected depend on the data used, and therefore differ from one suite of species to the next to optimize separability in each case. Wavebands beyond the range 400-950 nm, related to nitrogen and lignin concentration, as well as O-H stretching, may be useful in future tree discrimination studies, as was the case for Clark et al. (2005), van Aardt & Wynne (2001), and Martin et al. (1998).

The logistic linear classifier, a parametric classifier, provided the best species-level classification results at four of six sites (Table 5-5). The k-nearest neighbor classifier, a non-parametric classifier, produced the second best results overall. The quadratic classifier generally performed the worst, possibly due to correlations between features. Of the non-parametric classifiers, the decision tree classifier generally performed poorly, likely due to complex trees and the tendency toward overfitting. The decision tree classifier is not well suited to features that take on a large number of possible values (Mitchell, 1997) as was also observed when discriminating between lianas and trees (Castro-Esau et al., 2004).

The spectrometer used for data collection may possibly influence classification accuracy as well. Instruments with higher spectral resolution will better capture fine spectral details that may be used for discriminating species. In this case, the FieldSpec

HandHeld had a finer spectral resolution (3.5 nm at 700 nm) than the UniSpec (< 10 nm), but there was no obvious advantage observed in our classification results (Table 5-5).

Based on our findings, which are at this point mainly limited to the level of the leaf, the potential for using a database of species spectral signatures for classifying across sites and seasons appears low. The leaf-level spectral signature of a species from one site did not serve effectively to classify the same species at a second site (Fig. 5-5). Differences in leaf age, phenology, soil mineral nutrition, moisture availability, temperature, and other stresses (Carter, 1993) could certainly lead to the differences observed in spectral reflectance of the same species over multiple sites with varying edaphic and climatic conditions. In a similar way, progressively increasing stress with increasing elevation has been noted in the spectral reflectance properties of *Picea rubens, Abies balsamea* (Richardson et al., 2001), and *Betula papyrifera* (Richardson & Berlyn, 2002). Another possible cause of inter-site differences in conspecific leaf spectra is that genetic differences between populations can contribute to spectral differences. Winter (1998), for instance, was able to distinguish between two different varieties of avocado (*Persea americana*) in an airborne TRWIS III image. Differences in the spectral characteristics of different genotypes of crops such as barley (e.g. Fetch et al., 2004) have also been detected. However, more investigation is required in this area with respect to tropical trees.

Differences in leaf optical properties due to seasonality (wet/dry cycles) could be detrimental or beneficial to tree species identification. Temporal phenomena such as flowering, leaf flush or senescence could be confusing if not well understood, but could become useful in detecting particular species at particular times of the year if understood. In a similar way, the timing of imagery is important in crop discrimination studies (Murakami et al., 2001; Congalton et al., 1998; Collins, 1978). Thus, a creative combination of image processing and classification with in-depth knowledge of tree ecology and phenology will likely be necessary for a successful species-level classification.

Based on our leaf-level classification analysis of 50 species, there is potential for classification of up to 20 species with approximately 85% test data accuracy, and approximately 80% test data accuracy for up to 45 species (Fig. 5-7). Fung et al. (1999) achieved a similar level of overall accuracy (89%) for 25 subtropical tree species using a set of 13 bands selected using hierarchical clustering (as compared to 83.2% test data accuracy and 91.6% overall accuracy for 25 species, based on our data). For our analysis, five spectra were used for training classifiers and five for testing the classifiers. With greater amounts of training data, such as using a cross-validation approach, classification accuracies could have been higher yet.

Provided the linear relationship in Fig.5-7 continues, it may be possible to classify test data for 75 species with 73% accuracy, and 100 species with 69% accuracy. Classification accuracy erodes further beyond 100 species. At the leaf level, therefore, it would not be possible to classify all species in species-rich Neotropical forests where number of tree species can exceed 100 even in 0.1 ha plots (Gentry, 1991), although potential for discrimination would likely be improved using a spectrometer with a greater range (e.g. to 2500 nm). Also, it remains to be determined if a similar trend holds at the crown level. If it does, classification could still be successful for less species-rich tropical

forests or for detecting smaller numbers of tree species with distinct features from the remainder of the canopy.

Spectra and leaf traits

While this paper does not attempt to explore a comprehensive suite of leaf traits, the selected traits measured for species at Parque Natural Metropolitano (chlorophyll content, leaf thickness, percent intercellular space, spongy mesophyll width) provide an illustration of leaf feature variability among nine tropical dry forest tree species, which supports the differences observed in leaf reflectance for these same species (Table 5-6). Where two species differ in one or more of these traits, the resultant differences in spectral reflectance at one or multiple wavebands provide the opportunity for their discrimination.

Pigment content plays a large role in visible reflectance. The range of total chlorophyll content for the selected species at Parque Natural Metropolitano was 496-1055 $\mu mol/m^2$, and for reflectance at 550 nm, 9.10-15.36% (Table 5-6). Overall, visible wavebands (400-700 nm) were key to species identification, and were emphasized in feature selection (Fig. 5-6). Leaf thickness and internal leaf morphology appear to control near-infrared reflectance (Knapp & Carter, 1998; Knipling, 1970; Gates et al., 1965). From our samples, histological analysis of leaf thin sections (Fig. 5-9) can provide unique insight into the relative magnitude of reflectance in the near-infrared. The most striking link encountered was between the low percentage intercellular space, spongy mesophyll width, and leaf thickness of *Astronium graveolens*, and its uniquely low near-infrared reflectance. The leaf thin section of this species revealed a very thin, compact spongy mesophyll layer, allowing little opportunity for interactions of light at air-cell wall interfaces. In fact, this same species transmitted more light through the leaf than any other species sampled. Stronger correlations with near-infrared bands might have been observed using the ratio of mesophyll cell surface area exposed to intercellular spaces per unit leaf surface area (Slaton et al., 2001), which provides a better description of air-cell wall interfaces in the mesophyll than percent air space (Knipling, 1970). Water content was not studied here, but would probably correlate with leaf thickness, intercellular space, and infrared reflectance and transmittance (Sims & Gamon, 2003).

In general, accurate classification is closely associated with the presence of distinctive leaf features within the spectral range considered, as seen from the example of Parque Natural Metropolitano. Distinctive leaf spectral features that facilitate species classification will be tied to leaf traits such as 1) low or high levels of chlorophyll per unit area, 2) thick or thin leaves, and/or 3) low or high percentage of air space in the spongy mesophyll relative to other species.

Crown spectra

Although this discussion focused mainly on leaf spectra and their discrimination, the primary application for this study will be towards tree crown identification. How, then, can knowledge about intra-specific variability in leaf reflectance be applied to future crown-level tree classifications from airborne or satellite-borne imagery? First, our results will provide a partial basis for interpreting variability in tree crown reflectance spectra within and between sites and seasons, since leaf reflectance often comprises the major component of an overall crown reflectance spectrum (with exceptions, especially

in dry season conditions when many trees are deciduous). Unlike leaf spectra, tree crown spectra obtained from airborne or satellite-borne sensors are influenced by leaf area index (leaf density), leaf angle distribution, crown shape and shading, and background signals such as tree bark and soil. These additional factors may help or hinder tree crown classification. For species that have unique and predictable combinations of these factors, their overall crown spectral signatures may be even more distinguishable than their leaf spectral signatures. However, this has not been substantiated yet, and recent work by Zhang et al. (submitted) indicate that intra-crown variation within species may pose a challenge. In a tropical environment, visual inspection of the crown spectra we recorded at Fort Sherman, Panama indicate that those five species would be separable without difficulty, mainly due to large differences in spectral amplitude and, to a lesser extent, differences in shape (Figs. 5-1 and 5-4).

Classification at the canopy level is clearly the next step in determining whether tropical tree species are separable, and requires airborne or satellite-borne imagery with a combination of both high spectral and spatial resolution. Clark et al. (2005) presented pioneering work in hyperspectral tropical species discrimination at leaf to crown scales, which will likely lead to a burgeoning of research in this field. Additional efforts so far, using aerial photographs (Trichon, 2001) and high spatial resolution multispectral data (reflectance measured over a small number (4) of broad bands, each typically > 50 nm wide) such as IKONOS (1 m and 4 m resolution) and Quickbird (0.7 m and 2.8 m resolution) (Wang et al., 2004; Read et al., 2003), also support the possibility of separating a portion of the total number of tropical species. Combined with LiDAR (Light Detection And Ranging, an active remote sensor that measures return time for laser pulses), which can provide information on tree location and height as well as crown diameter and shape, the possibilities may extend even further (Gillespie et al., 2004). As these types of data become increasingly available for tropical forests, scientists may draw upon techniques developed for automated tree isolation (Leckie et al., 2003; Wulder et al., 2000) and for tree species classifications in ecosystems with more limited species diversity, such as arid environments (Lewis et al., 2001; Lewis, 2000) and temperate forests (Roberts et al., 2004; Key et al., 2001; Martin et al., 1998). The ability to accurately map tree species in tropical ecosystems will represent a significant advance that will facilitate ecosystem characterization, tree demographic studies, mapping endangered or endemic species, identifying important food sources for wildlife, and quantifying carbon pools and carbon sequestration rates.

Table 5-1. Summary of study area characteristics

Location	Latitude/Longitude	Holdridge Life Zone	Mean Annual Precipitation (mm)
1. Chamela-Cuixmala Biosphere Reserve, Mexico	19° 30' N 105° 03' W	Tropical Dry Forest	707
2. Los Inocentes, Costa Rica	11° 01' N 85° 30' W	Transition between basal Tropical Moist Forest and Premontane Tropical Moist Forest	2098
3. Santa Rosa National Park, Costa Rica	10° 48' 53" N 85° 36' 54" W	Tropical Dry Forest and Tropical Dry transition to moist	1588
4. Los Horizontes, Costa Rica	10° 45' 39" N 85° 38' 6" W	Tropical Dry Forest	2378 (1995 data only)
5. El Rodeo, Costa Rica	9° 31' 60" N 84° 4' 0" W	Tropical Dry Forest	1896
6. Parque Natural Metropolitano (PNM), Panama	8° 59' N 79° 33' W	Tropical Dry Forest	1740
7. Fort Sherman (FTS), Panama	9° 17' N 79° 58' 30" W	Tropical Wet Forest	3300

Table 5-2. Summary of data collected at each site

Location	Date	Season	Instrument	Tree species	Trees per species	Leaves per tree	Measurements per leaf
Chamela-Cuixmala Biosphere Reserve, Mexico	Aug 2003	Wet	UniSpec	27	1	15	1
Los Inocentes, Costa Rica	Nov 2002	Wet	ASD HH	10	1-3	3-5	1
	Mar 2003	Dry	UniSpec	5	1	5	3
Santa Rosa National Park, Costa Rica	Dec 2002	Wet	ASD HH	2	3	5	3
Los Horizontes, Costa Rica	Oct 2002	Wet	ASD HH	8	3-5	3	3
El Rodeo, Costa Rica	Dec 2002	Wet	ASD HH	4	3	5	3
Parque Natural Metropolitano (PNM), Panama	Mar 2003	Dry	UniSpec	6	1	3	6
	Oct 2003	Wet	UniSpec	10	1	10	4
Fort Sherman (FTS), Panama	Mar 2003	Dry	UniSpec	15	1	3	6
	Oct 2003	Wet	UniSpec	15	1	10	4

Table 5-3. Species sampled for this study

Family and Species	Field Sites	Family and Species	Field Sites
Anacardiaceae		**Fabaceae (Papilionoideae)**	
Amphipterygium adstringens (Schlecht.) Schiede.	CH	*Dalbergia retusa* Hemsl.	LH, LI_M
Anacardium excelsum (Bertero & Balb. Ex Kunth) Skeels	$LI_{N/M}$, $PM_{M/O}$	*Diphysa americana* (Mill.) M. Sousa	LH, LI_M
Astronium graveolens Jacq.	CH, LI_N, $PM_{M/O}$	*Dussia munda* C. H. Stirt.	FS_{CROWN}
Spondias purpurea L.	CH	*Gliricidia sepium* (Jacq.) Kunth ex Walp.	ER, LH, LI_M
Tapirira guianensis Aubl.	FS_{CROWN}	*Lonchocarpus heptaphyllus* (Poir.) DC.	$FS_{M/O}$
Annonaceae		**Malpighiaceae**	
Annona spraguei Saff.	$PM_{M/O}$	*Byrsonima crassifolia* (L.) Kunth	ER, LH, LI_N
Apocynaceae		**Malvaceae**	
Aspidosperma spruceanum Benth. Ex Müll. Arg	$FS_{M/O}$	*Bombacopsis quinata* (Jacq.) Dugand	LH, LI_N
Plumeria rubra L.	CH	*Ceiba aesculifolia* (Kunth) Britton & Baker	CH
Bignoniaceae		*Ceiba grandiflora* Rose.	CH
Astianthus viminalis (HBK.) Baill.	CH	*Ceiba pentandra* (L.) Gaertn.	CH
Jacaranda copaia (Aubl.) D. Don	FS_{CROWN}	*Guazuma ulmifolia* Lamarck	CH, ER, LH, $LI_{N/M}$
Tabebuia donnell-smithii Rose.	CH	*Heliocarpus pallidus* Rose.	CH
Tabebuia rosea (Bertol.) DC.	CH	*Luehea seemannii* Triana & Planch.	$PM_{M/O}$
Boraginaceae		*Pseudobombax septenatum* (Jacq.) Dugand	PM_O
Cordia alliodora (Ruiz & Pav.) Oken	$PM_{M/O}$	**Meliaceae**	

Family and Species	Field Sites	Family and Species	Field Sites
Cordia bicolor A. DC.	$FS_{M/O}$, FS_{CROWN}	*Carapa guianensis* Aubl.	$FS_{M/O}$
Cordia elaeagnoides DC.	CH	*Cedrela odorata* L.	LI_N, SR
Brassicaceae		*Swietenia humilis* Zucc.	CH
Crateva graminacea	CH	*Swietenia macrophylla* King	LI_N
Burseraceae		**Moraceae**	
Bursera simaruba (L.) Sarg.	ER, $LI_{N/M}$	*Brosimum utile* (Kunth) Oken	$FS_{M/O}$
Cochlospermaceae		*Castilla elastica* Sesse	PM_O
Cochlospermum vitifolium (Willd.) Spreng.	LH	*Ficus insipida* Willd.	$PM_{M/O}$
Combretaceae		*Ficus nymphaeifolia* Mill.	$FS_{M/O}$
Conocarpus erectus L.	CH	**Myristicaceae**	
Terminalia amazonia (J. F. Gmel.) Exell	$FS_{M/O}$	*Virola surinamensis* (Rol. ex) Rottb. Warb.	$FS_{M/O}$
Convolvulaceae		**Nyctaginaceae**	
Ipomoea wolcottiana Rose.	CH	*Guapira linearibracteata* (Heim.) Standl.	CH
Clusiaceae		**Rubiaceae**	
Marila laxiflora Rusby	$FS_{M/O}$	*Tocoyena pittieri* (Standl.) Standl.	$FS_{M/O}$
Euphorbiaceae		**Sapindaceae**	
Croton sp.	CH	*Matayba apetala* Radlk.	$FS_{M/O}$
Piranhea mexicana	CH	*Thouinidium decandrum* (Humb. & Bonpl.) Radlk.	CH
Sapium sp.	CH	**Sapotaceae**	
Fabaceae (Caesalpinoideae)		*Chrysophyllum cainito* L.	PM_O
Caesalpinia platyloba S. Watson	CH	*Manilkara bidentata* (A. DC.) Chev.	$FS_{M/O}$
Caesalpinia sclerocarpa Standl.	CH	**Simaroubaceae**	
Hymenaea courbaril L.	LH, LI_N	*Simarouba amara* Aubl.	LI_N, $FS_{M/O}$
Tachigali versicolor Standl. & L. O. Williams	$FS_{M/O}$	**Urticaceae**	
Fabaceae (Mimosoideae)		*Pourouma bicolour* Mart.	$FS_{M/O}$

Family and Species	Field Sites	Family and Species	Field Sites
Enterolobium cyclocarpum (Jacq.) Griseb.	CH, LI_M, PM_O	**Verbenaceae**	
Pithecellobium dulce (Roxb.) Benth.	CH	*Avicennia germinans* (L.) L.	CH
		Vochysiaceae	
		Vochysia ferruginea Mart.	FS_{CROWN}

Notes: CH, Chamela; ER, El Rodeo; FS, Fort Sherman; LH, Los Horizontes; LI, Los Inocentes; PM, Parque Natural Metropolitano; SR, Santa Rosa. Subscripts: $_{CROWN}$ indicates species for which crown spectra were taken at Fort Sherman (Panama); $_{M, N,}$ and $_O$ refer to the month (March, November, and October, respectively) in which the data were obtained for locations with multitemporal data. Taxonomy is based on the updated Angiosperm Phylogeny Group classification for orders and families of flowering plants (APG II, 2003).

Table 5-4. Leaf characteristics of *Bursera simaruba* and *Byrsonima crassifolia* at multiple sites

Species_site	Moisture content (%)	Leaf Area (cm^2)	Chlorophyll content
BUSI_SR	0.75 +/- 0.03	286.15 +/- 95.31	44.40 +/- 6.06
BUSI_ER	0.65 +/- 0.05	227.35 +/- 86.48	42.37 +/- 5.85
BUSI_LI	0.64 +/- 0.05	Not available	41.89 +/- 5.00
BYCR_ER	0.55 +/- 0.01	42.54 +/- 13.20	48.60 +/- 3.90
BYCR_LH	0.53 +/- 0.002	56.80 +/- 21.52	42.80 +/- 4.70
BYCR_LI	0.58 +/- 0.01	46.98 +/- 18.94	52.78 +/- 6.76

Notes: BUSI=*Bursera simaruba*, BYCR=*Byrsonima crassifolia*, SR=Santa Rosa, ER=El Rodeo, LI=Los Inocentes, LH=Los Horizontes. For moisture content and leaf area, N=15 samples (3 trees X 5 leaves). For SPAD, N=15 samples X 5 measurements/leaf = 75 measurements (exceptions: BYCR_LH and BYCR_LI, for which only 3 samples (3 trees X 1 leaf) were averaged. In those cases, 15 SPAD measurements were averaged (3 samples X 5 measurements/leaf)). Chlorophyll content was measured with SPAD, a hand-held chlorophyll absorbance meter (Richardson et al., 2002; Markwell et al., 1995).

Table 5-5: Best species-level classification results

Site	Date	Species	Samples /species	Top classifier	Number of features	Training error (%)	Testing error (%)	Overall error (%)
El Rodeo, Costa Rica	Dec02	4	15	lmnc	20	0	6.67	3.34
Los Horizontes, Costa Rica[a]	Oct02	4	10	loglc	30	0	0	0
Los Inocentes, Costa Rica[a]	Nov02	9	5-15	knnc	20	0	12.73	6.37
Parque Natural Metropolitano, Panama	Oct03	10	7-10	loglc	20	0	8.51	4.26
Fort Sherman, Panama	Oct03	15	10	loglc	40	0	5.33	2.67
Chamela-Cuixmala, Mexico	Aug03	27	15	loglc	30	0	19.37	9.69

Notes: [a]Due to insufficient data, some species were omitted from the classification. Abbreviations: lmnc, neural network classifier; loglc, logistic linear classifier; knnc, k-nearest neighbor classifier.

Table 5-6: Leaf trait data for species in the Parque Natural Metropolitano October 2003 dataset

	Chl_a ($\mu mol\ m^{-2}$)	Chl_b ($\mu mol\ m^{-2}$)	Chl_{total} ($\mu mol\ m^{-2}$)	R_{550} (%)	T_{550} (%)	R_{800} (%)	T_{800} (%)	Thick (mm)	Space (%)	SMW (μm)	SM/T
ANEX	715.2 (6)	340.1 (6)	1055.3 (6)	11.33 (6)	6.23 (5)	49.83 (3)	40.27 (5)	0.268 (4)	12.21 (4)	93.5 (6)	0.54 (6)
LUSE	570.2 (5)	144.8 (4)	715.0 (5)	11.24 (4)	1.35 (1)	60.87 (8)	26.32 (1)	0.348 (7)			
ASGR	529.9 (3)	134.3 (3)	664.2 (3)	9.10 (1)	10.96 (8)	42.22 (1)	49.45 (9)	0.164 (1)	5.40 (1)	31.0 (1)	0.22 (1)
COAL	390.7 (1)	105.5 (2)	496.2 (1)	10.90 (3)	6.22 (4)	49.90 (4)	38.52 (4)	0.290 (5)	15.47 (6)	37.0 (2)	0.35 (2)
ANSP	544.8 (4)	145.4 (5)	690.2 (4)	9.17 (2)	8.00 (6)	50.09 (5)	43.88 (8)	0.259 (3)	9.86 (2)	58.5 (3)	0.41 (3)
CAEL				11.31 (5)	8.00 (6)	51.38 (6)	41.13 (6)	0.458 (9)	10.18 (3)	65.0 (4)	0.47 (5)
PSSE				11.70 (7)	9.24 (7)	48.37 (2)	43.32 (7)	0.256 (2)	12.70 (5)	78.5 (5)	0.42 (4)
FIIN	415.0 (2)	87.9 (1)	502.9 (2)	12.34 (8)	2.70 (2)	53.57 (7)	31.97 (2)	0.378 (8)	29.30 (7)	146.5 (7)	0.42 (4)
CHCA				15.36 (9)	4.91 (3)	60.92 (9)	35.01 (3)	0.299 (6)			

Notes: ANEX, *Anacardium excelsum*, LUSE, *Luehea seemannii*, ASGR, *Astronium graveolens*, COAL, *Cordia alliodora*, ANSP, *Annona spraguei*, CAEL, *Castilla elastica*, PSSE, *Pseudobombax septenatum*, FIIN, *Ficus insipida*, CHCA, *Chrysophyllum cainito*. Chl_a, Chl_b, Chl_{total} are averages based on 5 samples/species. R_{550} refers to diffuse reflectance at 548.5 nm (average of 4 spectra/species); T_{550}, transmittance at 548.5 nm; R_{800}, diffuse reflectance at 800.7 nm; T_{800}, transmittance at 800.7 nm; Thick, average leaf thickness from 5-10 leaves (5 measurements/leaf); Space (%), percentage intercellular space, based on the classification of one internal leaf morphology image per species; SMW, spongy mesophyll width; SM/T, ratio of spongy mesophyll width to total leaf width. SMW and SM/Total both based on 5 measurements from a single leaf thin section. Species are ranked according to lowest to highest values in each column (numbers in parentheses). Spaces left blank indicate data not available. There are no leaf trait data for *Enterolobium cyclocarpum* at this site.

Table 5-7: Correlation coefficients and P-values for relationships between leaf optical properties and leaf internal mesophyll structure, PNM October 2003 dataset

	Space (%)		SMW (μm)	
Waveband[a]	**r**	**P**	**r**	**P**
$R_{706.2}$	0.760*	0.048	0.823*	0.023
$R_{748.6}$	0.626	0.133	0.632	0.128
$R_{800.7}$	0.723	0.066	0.684	0.090
$R_{959.3}$	0.786*	0.036	0.710	0.074
$T_{706.2}$	-0.879**	0.009	-0.728	0.063
$T_{748.6}$	-0.938**	0.002	-0.768*	0.044
$T_{800.7}$	-0.932**	0.002	-0.773*	0.042
$T_{959.3}$	-0.875**	0.010	-0.725	0.065

Notes: [a]$R_{subscript}$, reflectance; $T_{subscript}$, transmittance; Space (%), percentage intercellular space; SMW, spongy mesophyll width; *P≤0.05; **P≤0.01

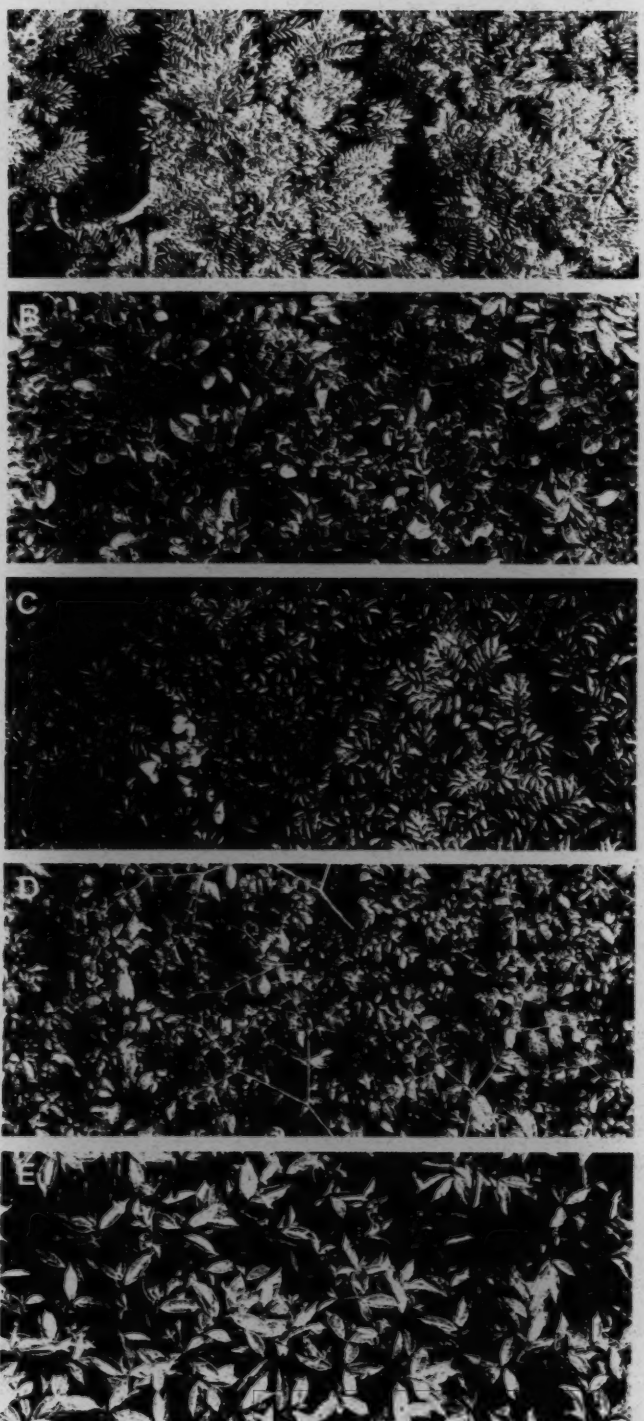

Figure 5-1. Partial tree crowns, as viewed from a canopy crane at Fort Sherman, Panama, at a height of 5 m. The species are A) *Jacaranda copaia*, B) *Dussia munda*, C) *Tapirira guianensis*, D) *Cordia bicolor* and E) *Vochysia ferruginea*.

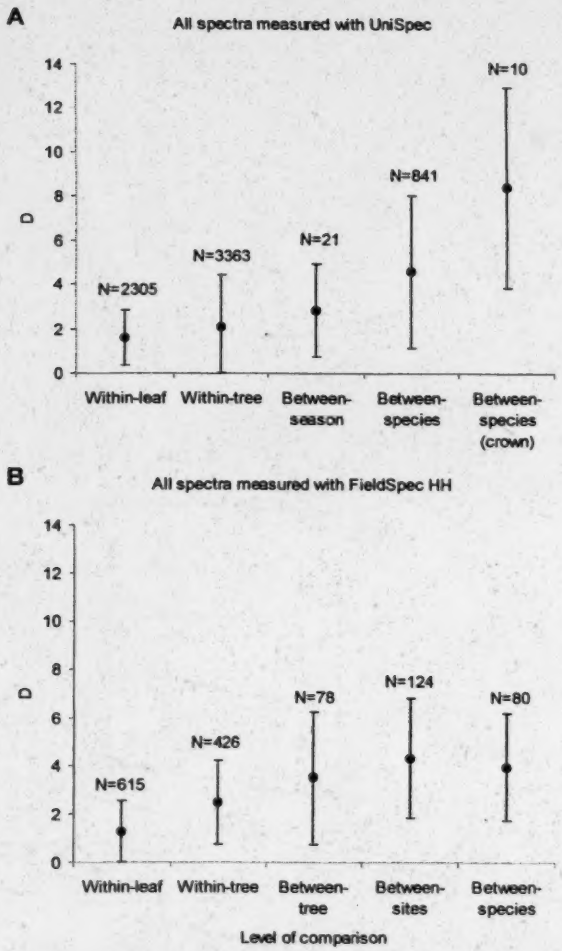

Figure 5-2. Mean amplitude (*D*) (±1 SD) of leaf reflectance spectra of tropical trees at sites in Mexico, Costa Rica and Panama for various levels of comparison. Average *D* was calculated for all applicable UniSpec data (panel A) and ASD HandHeld data (panel B) (Table 5-2). Number of samples used to compute each mean is indicated, and includes all the pairwise combinations of spectra per respective level.

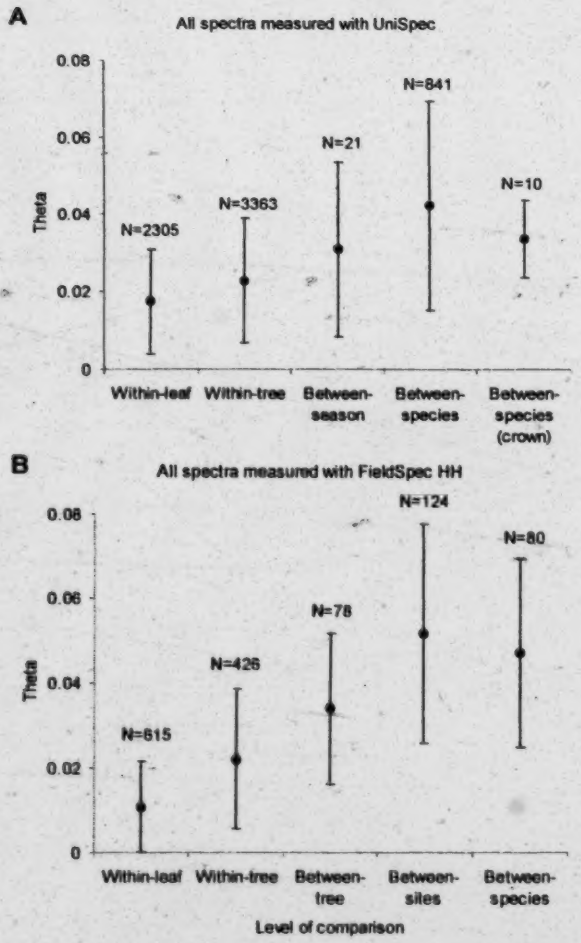

Figure 5-3. Mean shape (θ) (±1 SD) of leaf reflectance spectra of tropical trees at sites in Mexico, Costa Rica and Panama for various levels of comparison. Average θ was calculated for all applicable UniSpec (panel A) and ASD HandHeld data (panel B) (Table 5-2). Number of samples used to compute each mean is indicated, and includes the pairwise combinations of spectra per respective level.

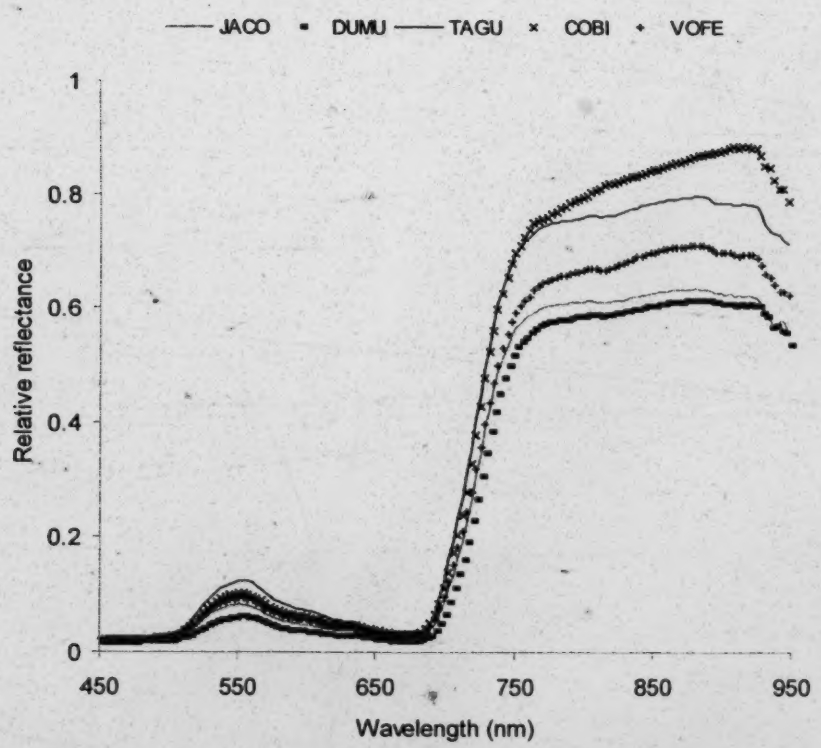

Figure 5-4. Average crown reflectance spectra (FOV=approximately 3.6 m) for 5 species at Fort Sherman, Panama. Spectra correspond to species pictured in Figure 5-1 as follows: *Jacaranda copaia* (JACO), *Dussia munda* (DUMU), *Tapirira guianensis* (TAGU), *Cordia bicolor* (COBI) and *Vochysia ferruginea* (VOFE).

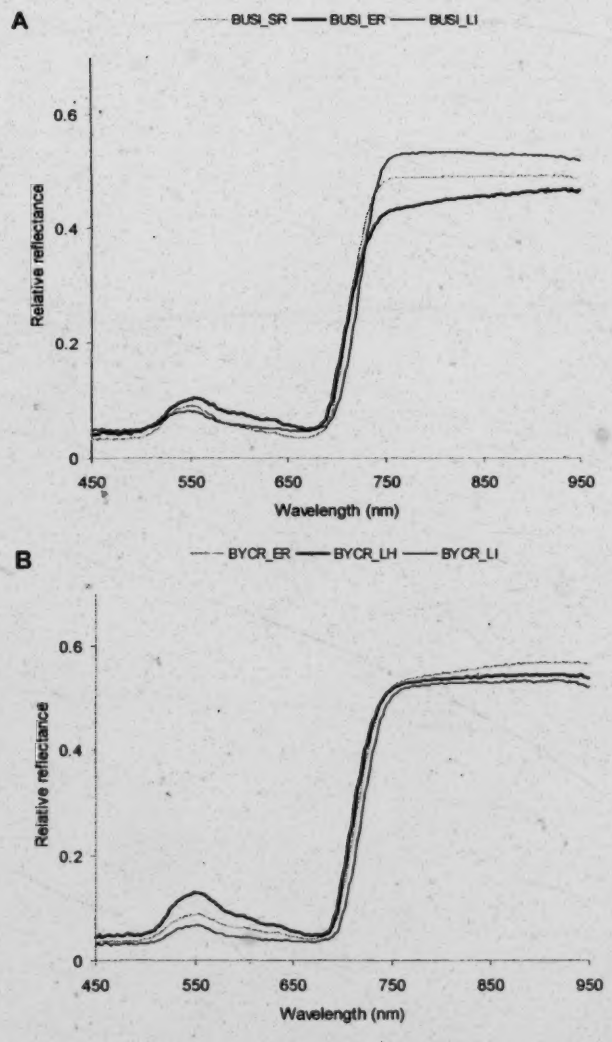

Figure 5-5. Average relative reflectance spectra of (A) *Bursera simaruba* (BUSI) and (B) *Byrsonima crassifolia* (BYCR), each at three sites in Costa Rica (SR, Santa Rosa; ER, El Rodeo; LI, Los Inocentes; LH, Los Horizontes). Accompanying leaf trait data may be found in Table 5-4.

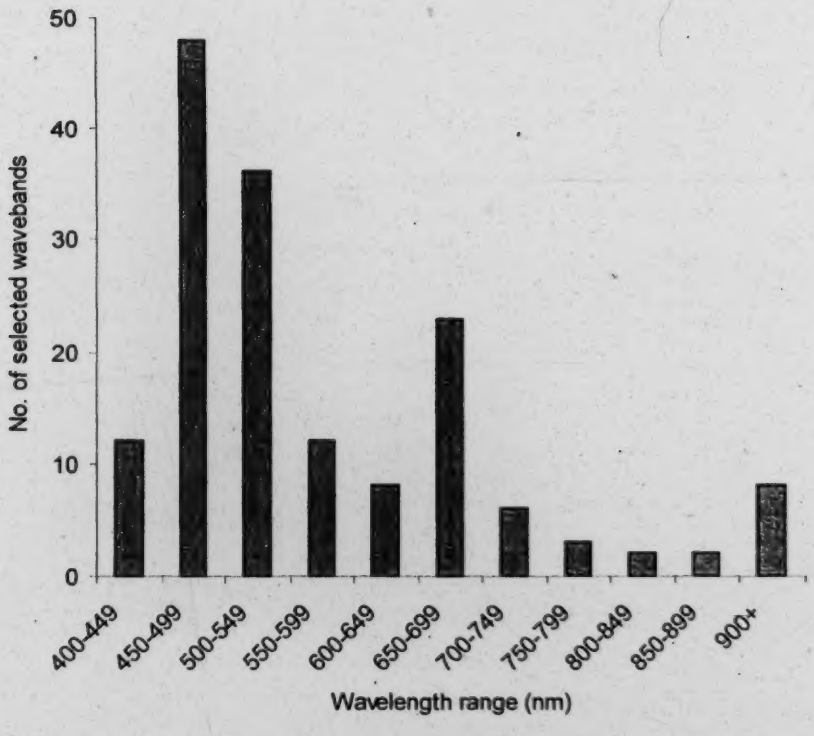

Figure 5-6. Distribution of wavebands chosen in the forward feature selection process, based on the within-site species classifications (Table 5-5). The top 20 wavebands per classification were tallied for this histogram.

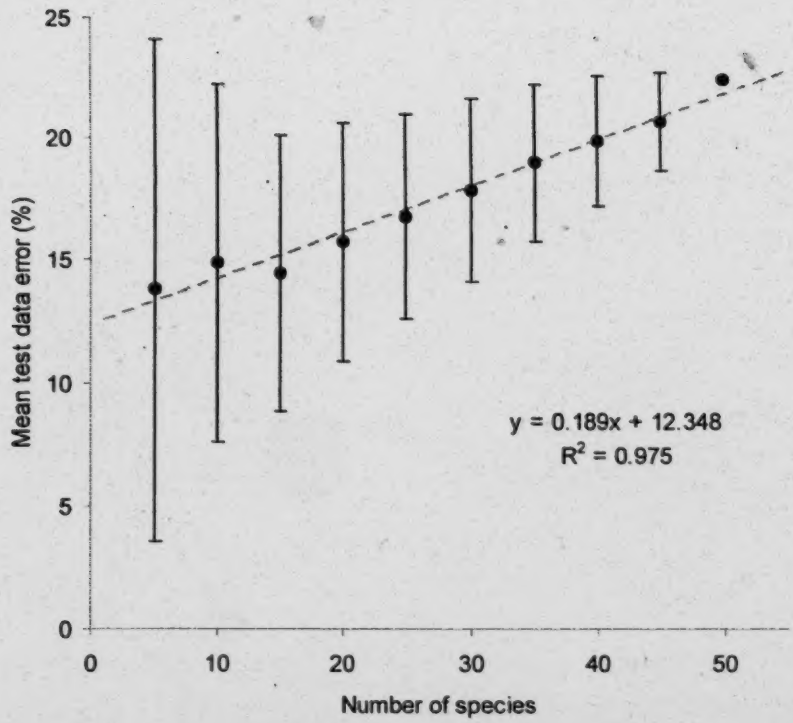

Figure 5-7. Classification analysis for 50 species from three sites, Parque Natural Metropolitano, For Sherman, and Chamela. Data gathered in the 2003 wet season using the UniSpec. Mean test data error ±1 SD was computed from 10,000 classifications each per set of 5, 10, 15, 20, 25, 30, 35, 40, and 45 species. Sets of species selected at random for each classification.

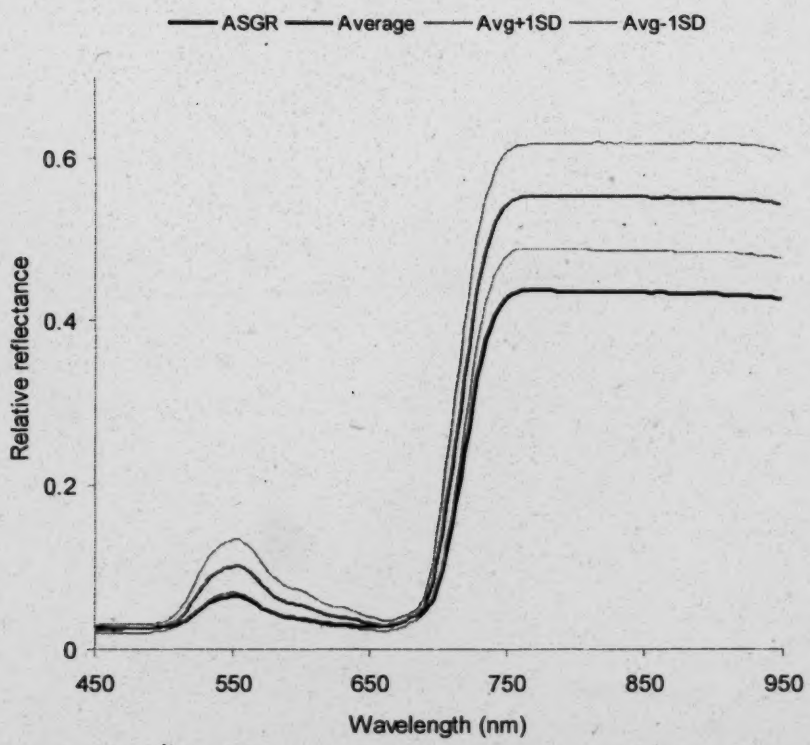

Figure 5-8. Average reflectance spectra for *Astronium graveolens* (ASGR) compared to average reflectance spectra ±1 SD for all species at Parque Natural Metropolitano, Panama for October 2003.

Figure 5-9. Leaf cross sections of three species from Parque Natural Metropolitano, Panama. (A) *Astronium graveolens*, (B) *Anacardium excelsum*, (C) *Ficus insipida*. Bracketed area indicates approximate width of the spongy mesophyll. The 100 µm scale is applicable to all cross sections.

LITERATURE CITED

Allen, W. A., Gausman, H. W., Richardson, A. J. & Wiegand, C. L. (1970). Mean effective optical constants of thirteen kinds of plant leaves. *Applied Optics, 9*, 2573-2577.

Angiosperm Phylogeny Group (APG II). (2003). An update of the Angiosperm Phylogeny Group classification for the orders and families of flowering plants: APG II. *Botanical Journal of the Linnean Society, 141*, 399–436.

Arnon, D. I. (1949). Copper enzymes in isolated chloroplasts. Polyphenoloxidase in *Beta vulgaris*. *Plant Physiology* 24: 1–15.

Avalos, G., & Mulkey, S. S. (1999). Seasonal changes in liana cover in the upper canopy of a neotropical dry forest. *Biotropica, 31,* 186–192.

Avalos, G., Mulkey, S. S. & Kitajima, K. (1999). Leaf optical properties of trees and lianas in the outer canopy of a tropical dry forest. *Biotropica, 31*, 517-520.

Bullock, S. H., & Solis-Magallanes, A. (1990). Phenology of canopy trees of a tropical deciduous forest in Mexico. *Biotropica, 22,* 23-35.

Carter, G. A. (1993). Responses of Leaf Spectral Reflectance to Plant Stress. *American Journal of Botany, 80*, 239–243.

Castro-Esau, K. L., Sánchez-Azofeifa, G. A., & Caelli, T. (2004). Discrimination of lianas and trees with leaf-level hyperspectral data. *Remote Sensing of Environment, 90,* 353–372.

Castro-Esau, K. L., Sánchez-Azofeifa, G. A., & Rivard, B. (in press). Comparison of spectral indices obtained using multiple spectroradiometers. *Remote Sensing of Environment*.

Clark, M. L., Roberts, D. A. & Clark, D. B. (2005). Hyperspectral discrimination of tropical rain forest tree species at leaf to crown scales. *Remote Sensing of Environment, 96*, 375-398.

Cochrane, M. A. (2000). Using vegetation reflectance variability for species level classification of hyperspectral data. *International Journal of Remote Sensing, 21,* 2075–2087.

Collins, W. (1978). Remote-sensing of crop type and maturity. *Photogrammetric Engineering and Remote Sensing, 44,* 43–55.

Congalton, R. G., Balogh, M., Bell, C., Green, K., Milliken, J. A., & Ottman, R. (1998). Mapping and monitoring agricultural crops and other land cover in the Lower Colorado River Basin. *Photogrammetric Engineering and Remote Sensing, 64,* 1107–1113.

Defernez, M. & Kemsley, E. K. (1997). The use and misuse of chemometrics for treating classification problems. *Trends in Analytical Chemistry, 16*, 216-221.

Duin, R. P. W. (2000). PRTools, Version 3.0: a Matlab toolbox for pattern recognition. Pattern Recognition Group, Delft, The Netherlands: Delft University of Technology.

Fetch, J., Stefenson, B. J., & Pederson, V. D. (2004). Predicting agronomic performance of barley using canopy reflectance data. *Canadian Journal of Plant Science, 84,* 1–9.

Foley, S. L., Rivard, B., Sánchez-Azofeifa, G. A. & Calvo-Alvarado, J. (in press). Foliar spectral properties following leaf clipping and implications for handling techniques. *Remote Sensing of Environment.*

Frankie, G. W., Baker, H. G., & Opler, P. A. (1974). Comparative phenological studies of trees in tropical wet and dry forests in the lowlands of Costa Rica. *Journal of Ecology, 62,* 881–899.

Fung, T. & Siu, W. L. (1998). Hyperspectral data analysis for subtropical tree species recognition. In: *Symposium Proceedings, IGARSS '98, Sensing and Managing the Environment*, pp. 1298-1300. Seattle, WA: IEEE International Geoscience and Remote Sensing.

Fung, T., Ma, F. Y., & Siu, W. L. (1999). Band Selection using hyperspectral data of subtropical tree species. *http://www.gisdevelopment.net/aars/acrs/1999/ps3/ps3055pf.htm*.

Gamon, J. A., Field, C. B., Bilger, W., Bjorkman, O., Fredeen, A. L. & Penuelas, J. (1990). Remote-Sensing of the Xanthophyll Cycle and Chlorophyll Fluorescence in Sunflower Leaves and Canopies. *Oecologia, 85*, 1-7.

Gates, D. M., Keegan, H. J., Schleter, J. C. & Weidner, V. R. (1965). Spectral Properties of Plants. *Applied Optics, 4*, 11-20.

Gausman, H. W. (1984). Evaluation of Factors Causing Reflectance Differences between Sun and Shade Leaves. *Remote Sensing of Environment, 15*, 177–181.

Gausman, H. W. (1985). Plant leaf optical properties in visible and near-infrared light. Graduate Studies No. 29. Lubbock, Texas: Texas Tech Press.

Gausman, H. W. & Allen, W. A. (1973). Optical parameters of leaves of 30 plant species. *Plant Physiology, 52*, 57-62.

Gentry, A. H. (1991). The distribution and evolution of climbing plants. In F. E. Putz & H. A. Mooney (Eds.), *The biology of vines*. Cambridge, UK: Cambridge University Press.

Gillespie, T. W., Brock, J., & Wright, C. W. (2004). Prospects for quantifying structure, floristic composition and species richness of tropical forests. *International Journal of Remote Sensing, 25*, 707–715.

Gitelson, A. & Merzlyak, M. N. (1994). Spectral Reflectance Changes Associated with Autumn Senescence of Aesculus-Hippocastanum L and Acer-Platanoides L Leaves - Spectral Features and Relation to Chlorophyll Estimation. *Journal of Plant Physiology, 143*, 286-292.

Hew, C. S., Soh, W. P., & Ng, C. K. Y. (1998). Variation in photosynthetic characteristics along the leaf blade of *Oncidium goldiana*, a C-3 tropical epiphytic orchid hybrid. *International Journal of Plant Sciences, 159,* 116–120.

Hiscox, J. D., & Israelstam, G. F. (1979). Method for the Extraction of Chlorophyll from Leaf Tissue without Maceration. *Canadian Journal of Botany-Revue Canadienne De Botanique, 57,* 1332–1334.

Hoffer, R. M. & Johannsen, C. J. (1969). Ecological potentials in spectral signature analysis. In: *Remote sensing in ecology* (Ed. P. L. Johnson), pp. 1-16. Athens: University of Georgia.

Jensen, J. R. (2000). *Remote sensing of the environment: an earth resource perspective*. Upper Saddle River, New Jersey: Prentice-Hall Inc.

Kalacska, M., Sánchez-Azofeifa, G. A., Calvo-Alvarado, J. C., Quesada, M., Rivard, B., & Janzen, D. H. (2004). Species composition, similarity and diversity in three successional stages of a seasonally dry tropical forest. *Forest Ecology and Management, 200,* 227–247.

Key, T., Warner, T. A., McGraw, J. B., & Fajvan, M. A. (2001). A comparison of multispectral and multitemporal information in high spatial resolution imagery for classification of individual tree species in a temperate hardwood forest. *Remote Sensing of Environment, 75,* 100–112.

Knapp, A. K. & Carter, G. A. (1998). Variability in leaf optical properties among 26 species from a broad range of habitats. *American Journal of Botany, 85*, 940-946.

Knipling, E. B. (1967). Physical and physiological basis for differences in reflectance of healthy and diseased plants. In: *Proc. Workshop on Infrared Color Photography and diseased plants*. Winter Haven, Florida: Florida Dept. of Agriculture.

Knipling, E. B. (1970). Physical and physiological basis for the reflectance of visible and near-infrared radiation from vegetation. *Remote Sensing of Environment, 1*, 155-159.

Leckie, D. G., Gougeon, F. A., Walsworth, N., & Paradine, D. (2003). Stand delineation and composition estimation using semi-automated individual tree crown analysis. *Remote Sensing of Environment, 85,* 355–369.

Lee, D. W. & Graham, R. (1986). Leaf Optical-Properties of Rain-Forest Sun and Extreme Shade Plants. *American Journal of Botany, 73,* 1100-1108.

Lee, D. W., Bone, R. A., Tarsis, S. L. & Storch, D. (1990). Correlates of Leaf Optical-Properties in Tropical Forest Sun and Extreme-Shade Plants. *American Journal of Botany, 77,* 370-380.

Lewis, M. (2000). Discrimination of arid vegetation composition with high resolution CASI imagery. *Rangeland Journal, 22,* 141–167.

Lewis, M., Jooste, V., & deGasparis, A. A. (2001). Discrimination of arid vegetation with airborne multispectral scanner hyperspectral imagery. *IEEE Transactions on Geoscience and Remote Sensing, 39,* 1471–1479.

Lott, E. J., Bullock, S. H., & Solís-Magallanes, J. A. (1987). Floristic diversity and structure of a tropical deciduous forest of coastal Jalisco. *Biotropica, 19,* 228–235.

Markwell, J., Osterman, J. C., & Mitchell, J. L. (1995). Calibration of the Minolta SPAD-502 leaf chlorophyll meter. *Photosynthesis Reseach, 46,* 467–472.

Martin, M. E., Newman, S. D., Aber, J. D., & Congalton, R. G. (1998). Determining forest species composition using high spectral resolution remote sensing data. *Remote Sensing of Environment, 65,* 249–254.

Mitchell, T. M. (1997). *Machine Learning.* New York, New York: McGraw-Hill.

Murakami, T., Ogawa, S., Ishitsuka, N., Kumagai, K., & Saito, G. (2001). Crop discrimination with multitemporal SPOT/HRV data in the Saga Plains, Japan. *International Journal of Remote Sensing, 22,* 1335–1348.

Price, J. C. (1994). How Unique Are Spectral Signatures. *Remote Sensing of Environment, 49,* 181–186.

Read, J. M., Clark, D. B., Venticinque, E. M., & Moreira, M. P. (2003). Application of merged 1-m and 4-m resolution satellite data to research and management in tropical forests. *Journal of Applied Ecology, 40,* 592–600.

Richardson, A. D., Berlyn, G. P., & Gregoire, T. G. (2001). Spectral reflectance of *Picea rubens* (Pinaceae) and *Abies balsamea* (Pinaceae) needles along an elevational gradient, Mt. Moosilauke, New Hampshire, USA. *American Journal of Botany, 88,* 667–676.

Richardson, A. D., & Berlyn, G. P. (2002). Spectral reflectance and photosynthetic properties of *Betula papyrifera* (Betulaceae) leaves along an elevational gradient on Mt. Mansfield, Vermont, USA. *American Journal of Botany, 89,* 88–94.

Richardson, A. D., Duigan, S. P., & Berlyn, G. P. (2002). An evaluation of noninvasive methods to estimate foliar chlorophyll content. *New Phytologist, 153,* 185–194.

Roberts, D. A., Ustin, S. L., Ogunjemiyo, S., Greenberg, J., Dobrowski, S. Z., Chen, J. Q., & Hinckley, T. M. (2004). Spectral and structural measures of northwest forest vegetation at leaf to landscape scales. *Ecosystems, 7,* 545–562.

Salem, B. B., Elcibahy, A. & Elraey, M. (1995). Detection of land-cover classes in agroecosystems of northern Egypt by remote-sensing. *International Journal of Remote Sensing, 16,* 2581-2594.

Sims, D. A., & Gamon, J. A. (2003). Estimation of vegetation water content and photosynthetic tissue area from spectral reflectance: a comparison of indices based on liquid water and chlorophyll absorption features. *Remote Sensing of Environment, 84,* 526–537.

Skidmore, A. K., Forbes, G. W., & Carpenter, D. J. (1988). Non-parametric test of overlap in multipspectral classification. *International Journal of Remote Sensing, 9,* 777–785.

Trichon, V. (2001). Crown typology and the identification of rain forest trees on large-scale aerial photographs. *Plant Ecology, 153,* 301–312.

van Aardt, J. A. N., & Wynne, R. H. (2001). Spectral separability among six southern tree species. *Photogrammetric Engineering and Remote Sensing, 67,* 1367–1375.

Vogelmann, T. C. (1993). Plant-Tissue Optics. *Annual Review of Plant Physiology and Plant Molecular Biology, 44,* 231-251.

Wang, L., Sousa, W. P., Gong, P., & Biging, G. S. (2004). Comparison of IKONOS and QuickBird images for mapping mangrove species on the Caribbean coast of Panama. *Remote Sensing of Environment, 91,* 432–440.

Winter, E. M. (1998). Classification of vegetation types using a high spectral and spatial resolution hyperspectral sensor. EUROPTO Conference on Sensors, Systems, and Next-Generation Satellites II, Barcelona, Spain: *SPIE, 3498,* 216–222.

Woolley, J. T. (1971). Reflectance and transmittance of light by leaves. *Plant Physiology, 47,* 656-662.

Wulder, M., Neimann, K. O., & Goodenough, D. G. (2000). Local maximum filtering for the extraction of tree locations and basal area from high spatial resolution imagery. *Remote Sensing of Environment, 73,* 103–114.

Zhang, J. L., Rivard, B., Sánchez-Azofeifa, G. A. & Castro-Esau, K. L. (submitted). Intra and inter-class spectral variability of tropical tree species at La Selva, Costa Rica: Implications for species identification using HYDICE imagery. *Remote Sensing of Environment.*

CHAPTER 6—Changes in spectral properties, chlorophyll content and internal mesophyll structure of senescing *Populus balsamifera* and *Populus tremuloides* leaves[1]

INTRODUCTION

Autumn foliar senescence in deciduous temperate tree species is typically induced by shortening of the photoperiod (Andersson et al., 2004). Within a leaf, a sequence of programmed changes take place during senescence, among them chlorophyll loss (Collier & Thibodeau, 1995; Merzlyak & Gitelson, 1995; Masoni et al., 1994; Matile et al., 1989), decreased chlorophyll a/b ratio (Watts & Eley 1981; Sanger, 1971; Wolf, 1956), declining photosynthetic ability (Masclaux et al., 2000; Okada et al., 1992; Peterson & Huffaker ,1975), transition from nutrient assimilation to nutrient remobilization (Hörtensteiner & Feller, 2002; Masclaux et al., 2000), and collapse of cell walls (Boyer et al., 1988). Some of these changes may be tracked with concomitant alterations in leaf optical properties. In general, visible reflectance (400-700 nm) increases in response to chlorophyll degradation (Guasman, 1985; Knipling, 1967). Near-infrared reflectance (700-1300 nm) initially rises as the number of scattering interfaces increases as cells split and cell contents shrink away from cell walls, and eventually decreases in accordance with further mesophyll breakdown (Knipling, 1970). More specifically, wavelengths near 550 nm and 700 nm have been shown to be particularly sensitive to changes in chlorophyll content during leaf senescence (Gitelson & Merzlyak,1994), while correlations of specific wavebands with the demise of mesophyll structure during senescence have not been explored. The plant senescing reflectance index (PSRI=$(R_{678}-R_{500})/R_{750}$) was developed by Merzlyak et al. (1999) for the sole purpose of describing the dynamics of senescence processes in leaves and fruits, and is sensitive to the carotenoid/chlorophyll ratio.

While the series of physiological and, to a lesser extent, anatomical events leading to leaf death have been described for numerous plant species, it remains unknown if they are equivalent for both sun and shade-acclimated leaves of the same plant. Sun-exposed and shaded leaves have been shown to exhibit considerable physiological and morphological differences. Although the degree of within-tree plasticity of leaf morphology and physiology varies among species, related to light tolerance and successional status (Feng et al., 2004; Ashton & Berlyn, 1992; St-Jacques et al., 1991), it is apparent that some species are capable of acclimating their foliage to the light environment (Gamage et al., 2003; Ashton & Berlyn, 1992; St-Jacques et al., 1991). Within a single crown, changes in leaf anatomy tend to reflect changes in light availability during development (Ashton et al., 1998). In comparison with shade-acclimated leaves, sun-adapted leaves exhibit some or all of the following features: smaller leaf surface area (Gamage et al., 2003; Roth, 1984), greater leaf width (Gamage et al., 2003; Gausman, 1984; Roth, 1984), lower chlorophyll concentration (on a per mass basis) (Gausman, 1984), higher amounts of the photoprotective xanthophyll pigment (Gamon & Surfus, 1999), thicker and/or multi-layered palisade mesophyll (Gamage et

[1] A version of this chapter has been submitted for publication. Castro-Esau, K. L. & Sanchez-Azofeifa, G. A. (submitted). *International Journal of Remote Sensing.*

al., 2003; Roth, 1984), denser mesophyll structure (Bäck et al., 1999), and higher light-saturated photosynethic rates (Gamage et al., 2003). Chlorophyll a/b ratio, besides decreasing during senescence, also tends to decrease with decreasing light availability (Lei et al., 1996; Givnish, 1988; Oberbauer & Strain, 1986). The influence of these differences on leaf optical properties is not well defined to date. Among species of sun and shade-adapted rainforest plants, similar optical properties were found in the visible region (400-700 nm) despite differing anatomical features and photosynthetic efficiencies (Lee & Graham, 1986). The same conclusion was drawn for 26 temperate species from understory, intermediate, and open light environments (Knapp & Carter. 1998).

Within a single species, however, Gausman (1984) observed greater reflectance of orange (*Citrus sinensis* (L.) Osbeck) sun leaves than shade leaves in the visible region of the electromagnetic spectrum, which was consistent with a lower chlorophyll concentration (on a per mass basis). Demarez et al. (1999) confirmed this for the case of three tree species (oak (*Quercus* spp.), beech (*Fagus sylvatica* L.), hornbeam (*Carpinus betulus* L.)), although his results were not significant. However, both visible and near-infrared transmittance of sun leaves were significantly less ($p=0.05$) than that of shade leaves. In the NIR (700-1300 nm), lower transmittance of sun leaves was attributed to their high quantity of intercepting leaf tissues, including cellular constituents and intercellular spaces. Similarly, increased NIR reflectance and decreased transmittance correlate with increases in leaf thickness (Knapp & Carter, 1998), a trend that should hold for sun versus shade leaves since sun leaves are the thicker of the two.

In the present study, the two species of interest are common to our location in central Alberta. Aspen (*Populus tremuloides* Michx.) is considered the most widely distributed tree species in North America (Rauscher et al., 1995; Dean et al., 1993). Balsam poplar (*Populus balsamifera* L.) prefers riparian sites but is also widely distributed (Amlin & Rood, 2003; Farrar, 1995). The congeneric species are shade-intolerant pioneers, often among the first recolonizers of open areas following disturbance (Farrar, 1995). Both have the capacity to reproduce vegetatively. Aspen can become extensively clonal (Mitton & Grant, 1980) and balsam poplars sprout from roots and stumps (Farrar, 1995). The clones may differ in morphological characteristics as well as in timing of leaf flush, flowering and leaf fall, which can lead to differences in autumn leaf colors in adjacent clones (Peterson & Peterson, 1992). While a few studies have focused on autumn foliar senescence of trembling aspen (Collier & Thibodeau, 1995; Dean et al., 1993; (also note that Watts & Eley, 1981 addressed senescence of *P. sargentii*, and Garcia-Plazaola et al., 2003 and Andersson et al., 2004 did the same for European aspen, *P. tremula* L.), equivalent studies on balsam poplar are nonexistent. Sanger (1971) and Dean et al. (1993) noted contrasting trends in chlorophyll a/b ratio during senescence of aspen leaves. Whereas Sanger (1971) observed fairly uniform chlorophyll a/b during the summer, and a drop during senescence, Dean et al. (1993) observed striking increases in chlorophyll a/b for five progressive stages of senescence of aspen leaves, a phenomenon not previously recorded among deciduous tree species, and possibly linked to earlier structural loss of grana lamellae compared to stroma lamellae. The reasons behind the incongruent results remain without clarification to date.

Our research aims to expand current knowledge of the dynamics of fall senescence of *P. tremuloides* and *P. balsamifera* in our region as well as potential differences in these dynamics for sun and shade-adapted leaves of each species. We do

this by exploring the spectro-temporal changes in leaf optical properties, chlorophyll content (total chlorophyll, chlorophyll *a* and *b*) and internal anatomical features (palisade and spongy mesophyll thickness, total leaf thickness, percentage intercellular space within the spongy mesophyll). The specific objectives are three-fold: 1) To compare the two species, both of which play important ecological roles in the boreal forest of Canada, 2) To compare sun and shade-adapted leaves, since light acclimation can lead to important differences in the morphology and physiology of leaves, and 3) To explore differences in mature and senescing leaves with respect to chlorophyll content and internal anatomy. We also consider our results in light of future remote sensing applications.

METHODS

Leaf spectral reflectance and chlorophyll content

Sample collection

Leaf samples of *P. tremuloides* (aspen) and *P. balsamifera* (balsam poplar) were collected over 16 sampling dates during August to October 2002, the period of autumn senescence. Leaf spectral measurements and chlorophyll analysis were performed on the 2002 samples. In 2003, additional samples were collected over seven dates during the same time period. The primary purpose of the 2003 samples was leaf thin section analysis in support of the 2002 data. Leaf spectral reflectance and SPAD readings (chlorophyll content) also accompany the 2003 samples. The two trees were situated near the top of a ravine bordering the North Saskatchewan River in south central Edmonton, Alberta, Canada. At each collection, three leaves each were harvested from the sunlit and shaded portions of both trees. Hereafter, the following acronyms will be used to refer to leaf samples: aspen sun (ASU), aspen shade (ASH), poplar sun (PSU) and poplar shade (PSH). After labelling, the petioles of the leaves were wrapped in a moist paper towel. Leaves were then packed into a black plastic bag inside a cooler containing ice and taken for analysis.

Instruments used in this study

Two spectrometers were used over the course of the study for spectral reflectance measurements. The FieldSpec Pro FR spectroradiometer (Analytical Spectral Devices, Boulder, CO, USA) (model FSP350-2500P), first of all, has three photodiode arrays and measures a spectrum from 350-2500 nm. The spectral resolution is 3 nm wide in the VNIR and 10 nm in the SWIR. The sampling interval of 1.4 nm in the visible and near-infrared (VNIR) and 2 nm in the short wave infrared (SWIR) is interpolated to a finer sampling interval of 1 nm for a total of 2151 contiguous channels. The bare fibre-optic has a FOV of 25 degrees. The FiedSpec Pro FR was used for all samples collected in 2002.

The UniSpec Spectral Analysis System VIS/NIR (PP Systems, Amesbury, MA, USA), secondly, has a 256-element photodiode array and a spectral range of 350-1100 nm. Spectral resolution is <10 nm and sampling interval is 3.3 nm. The UniSpec has a bifurcated fibre-optic: one branch delivers light from an internal 7.0 W halogen lamp while the other returns the reflected light to the detector. For measurements, a leaf clip was attached to the fore-optic, which limits the FOV to a constant 2.3 mm and prevents ambient light entry. The UniSpec was used only for samples obtained in 2003 for leaf thin section analysis (section 2.2).

Last, the SPAD 502 (Minolta Camera Co., Osaka, Japan) is a hand-held chlorophyll absorbance meter. When the meter is clamped over leafy tissue, an indexed chlorophyll content (0-99.9) reading is given, based on absorbance at 650 and 940 nm.

SPAD measurements and chlorophyll content analysis (2002 samples)

Six SPAD measurements were recorded per leaf, three per each side of the leaf blade, avoiding the main vein. A 16 mm-diameter sample was cored from each leaf, from which an additional SPAD measurement was taken. The cored samples were placed in small plastic vials, wrapped in tinfoil and frozen.

Of the over 250 leaf cores accumulated over the 16 sampling dates, 100 were selected for chlorophyll analysis. The chosen samples provided adequate representation of the four leaf types (sun and shade leaves of the two species) over a wide range of SPAD values. Total chlorophyll, chlorophyll *a*, and chlorophyll *b* content were determined using the dimethyl sulphoxide (DMSO) extraction method described by Hiscox & Israelstam (1979).

Leaf spectral reflectance measurements (2002 samples)

The FieldSpec Pro FR bare fibre-optic was fit through a mounting gun attached to a tripod, and adjusted to a nadir viewing position above a black, non-reflecting (<2%) surface on which each leaf was placed. Distance between the fibre-optic and the sample was 23 mm, which resulted in a field of view of approximately 10 mm in diameter. Illumination was provided using an external 50 W halogen, at an angle of 45 degrees. FieldSpec Pro FR optimization was performed at the same time as each white reference (initially and after groups of 9 measurements). Instrument configuration was adjusted to average 20 scans per white reference and 25 per dark current reading. Twenty scans were averaged per recorded leaf spectrum. Reflectance spectra were recorded as the ratio of sample data to white reference (99% reflectance Spectralon panel) data under the same illumination and viewing conditions. Three spectral measurements, from the side of the leaf opposite where the core was extracted, were recorded per leaf, and later averaged.

Histology (2003 samples)

Sample collection

The following autumn (August-October 2003), sun and shade leaves from the same two trees were sampled for histological analysis. For each sample, three SPAD values were recorded from one side of the leaf blade. Similarly, three UniSpec leaf spectral measurements were recorded from within the same area. For UniSpec measurements, a dark current reading and white reference (using barium sulfate), both averages of 10 scans, were performed after every other leaf. Sample reflectance was obtained by comparing leaf reflectance (also an average of 10 scans) to reflectance of the barium sulfate standard.

Leaf fixation and thin section analysis

Thin sections were made for study of changes in internal mesophyll structure over the period of fall senescence. Initially, small pieces were cut from the leaf blade (approximately 10 mm long and 2-3 mm wide, from the same side as the SPAD and reflectance measurements), avoiding the midrib. Fixation followed, in which the leaf pieces were subject to vacuum for two weeks in a formalin aceto-alcohol (FAA) solution. After fixation, samples were run through an ethanol processing center (Fisher Histomatic 166) and embedded in paraffin molds. Using a microtome, thin sections (5 μm) were then

cut from the embedded samples. Slides were mounted and stained (using two stains: Harris' haematolxylin stain and Safranin O and fast green, for comparison), and viewed and photographed under a Leica DM RXM light microscope at 20X magnification.

Data analysis

SPAD calibration curves

For each species and illumination category (sun or shade), SPAD calibration curves were developed for the estimation of chlorophyll *a*, chlorophyll *b* and total chlorophyll. In addition, we computed a collective curve for each species, which included data from both sun and shade leaves over the range of dates sampled.

Indices

Three spectral vegetation indices were computed over the time course of senescence, 1.) the modified simple ratio, mSR_{705} (Sims & Gamon, 2002), 2.) the modified normalized difference index, mND_{705} (Sims & Gamon, 2002), and 3.) the plant senescence reflectance index, PSRI (Merzlyak et al., 1999):

$$[1]\ mSR_{705} = \frac{(R_{750} - R_{445})}{(R_{705} - R_{445})}$$

$$[2]\ mND_{705} = \frac{(R_{750} - R_{705})}{(R_{750} + R_{705} - 2R_{445})}$$

$$[3]\ PSRI = \frac{(R_{678} - R_{500})}{R_{750}}$$

Indices were plotted over both time and total chlorophyll content.

Histological analysis

Total width and palisade and spongy mesophyll width were determined using the 100 μm scale provided in each photo, from which a new ruler was constructed with 10 μm increments. To determine the proportion of airspace versus cells in the spongy mesophyll, we determined the percentage of pixels in an area of interest within the range of colour that typified air space using the Matlab Image Processing Toolbox. One to three areas of interest were delineated per image, to encompass as much of the spongy mesophyll as possible while avoiding veins. There were 114 images in total for the various species/light regime combinations (ASU, 34, ASH, 23, PSU, 26, PSH, 31) covering the seven sampling dates in 2003. Per sampling date, there were 2-5 images per species/light regime combination.

Correlation analysis

Correlation analysis was performed to determine the strength of potential relationships between either chlorophyll content (total chlorophyll, chlorophyll *a* and *b*) or anatomical features (total, palisade mesophyll and spongy mespohyll width, percent intercellular space) and spectral wavebands (445.9, 499, 548.5, 676.7, 706.2, 748.6, 800.7, 849.4, 901.2, and 949.6 nm) or indices (mSR_{705}, mND_{705}, PSRI). The wavebands listed provide a representation throughout the visible and near-infrared regions and several are also used in computation of indices (Eq. 1-3). Correlation analyses involving chlorophyll content were performed using 2002 data, for which we had a greater number of sampling dates; those involving histological features were restricted to the 2003 dataset.

RESULTS

In autumn 2002, for neighbouring *P. tremuloides* and *P. balsamifera* trees along the south side of the North Saskatchewan River, visible differences in the timing of senescence events were apparent between species. *P. balsamifera* exhibited the first signs of leaf yellowing and was the first to undergo total leaf drop. By October 15 (day 288), 99% of *P. balsamifera* leaves had fallen. For *P. tremuloides*, all leaves had abscised by October 26 (day 299).

SPAD curves

Individual SPAD calibration curves developed for each species and illumination category (sun or shade) were best represented by second-order polynomials (Table 6-1, Figure 6-1). In addition, collective calibration curves, for sun and shade leaves combined, were computed for each species (Table 6-1). Coefficients of determination for curves were highest for prediction of chlorophyll *a*, followed by total chlorophyll and chlorophyll *b*.

Indices and chlorophyll content

Over the time course of autumn senescence, several key differences may be observed between species and/or illumination category (Figure 6-2). When plotted according to date, mSR_{705} and mND_{705} for ASH leaves are consistently higher than for ASU leaves. For *P. balsamifera*, sun leaves generally exhibit higher values of both indices until near the end of the study period. At day 281, this phenomenon is reversed, and at day 285, values are near equal for PSU and PSH leaves. Over both species and illumination categories, ASU leaves exhibit the highest mSR_{705} and mND_{705} values; PSH leaves generally (with exceptions) show the least. When plotted against chlorophyll content, *P. balsamifera* leaves tend to have slightly higher mSR_{705} and mND_{705} values than *P. tremuloides*, but little distinction may be made between sun and shade leaves.

For mature leaves to early senescent leaves, PSRI for *P. balsamifera* leaves are slightly positive whereas for *P. tremuloides* leaves are slightly negative. The slightly positive PSRI values for mature *P. balsamifera* leaves are of note, as other documented species with dark-green plant tissues and high chlorophyll content have all exhibited slightly negative PSRI values (Merzlyak et al. 1999). Within *P. tremuloides*, ASH PSRI values are higher than for ASU until after day 274. Thus, in later stages of senescence, higher PSRI is observed for ASU leaves. PSU and PSH PSRI values are similar in mature to early senescing leaves, but in late senescence (days 281 and 285), PSRI is higher for PSU leaves. When comparing the two species, PSRI increases sooner for *P. balsamifera* (~day 272) than for *P. tremuloides* (day 285). When plotted against chlorophyll content, PSRI curves are similar for both species and illumination category, although there are no PSRI values for *P. tremuloides* above 0.07.

Prior to chlorophyll breakdown, shade leaves of both *P. balsamifera* and *P. tremuloides* have higher total chlorophyll and chlorophyll *a* contents (Figure 6-3). Similarly, *P. balsamifera* shade leaves have higher chlorophyll *b* contents. Chlorophyll *b* for *P. tremuloides* leaves, prior to chlorophyll breakdown, is similar for sun and shade leaves, but higher in shade leaves once chlorophyll content declines. Comparing the two species, *P. tremuloides* had higher initial total chlorophyll and chlorophyll *b* contents than *P. balsamifera*. For both trees, declines in chlorophyll content in 2002 began

approximately day 255 (Sept 12). For *P. tremuloides*, the decline was faster for sun leaves than for shade leaves. *P. balsamifera* leaves reversed this role in that total chlorophyll and chlorophyll *a* contents decreased sharply for shade leaves during mid-senescence (from approximately day 255 to day 270). Overall, declines in chlorophyll *a*, *b* and total chlorophyll were sharper and more variable for *P. balsamifera* than for *P. tremuloides*.

P. balsamifera and *P. tremuloides* differ markedly in the behaviour of the chlorophyll a/b prior to and during senescence. *P. tremuloides* has lower initial chlorophyll a/b but its decline started later than in *P. balsamifera* (approximately day 262 for *P. tremuloides* versus day 254 for *P. balsamifera*). Throughout the entire period, chlorophyll a/b for *P. tremuloides* shade leaves is greater than for sun leaves whereas the reverse is observed in *P. balsamifera* (also observed for the 2003 dataset with the exception of two dates (day 268, Sept 25 and day 274, Oct 1) for *P. balsamifera*, data not shown).

In the near-infrared, reflectance at 800 nm was significantly higher for *P. balsamifera* (mean ±1 SD = 51.68 ± 5.25%) than for *P. tremuloides* (mean ± 1SD = 47.50 ± 2.86%) (based on a two-tailed t-test, $P<0.001$). Significant differences were not observed between sun and shade leaves for either species, however ($P>0.05$). Over time, reflectance at 800 nm for both species remained nearly constant data not shown).

Histological analysis

Analysis of leaf thin sections also revealed a number of important differences between *P. tremuloides* and *P. balsamifera* and their sun-lit and shaded leaves during senescence. Statistical tests were not performed due to the low number of samples in some categories, and one of the limitations of the histological analysis is a lack of *P. tremuloides* shade leaves at low chlorophyll contents (<200 mg m^{-2}) (Table 6-2). Key findings from Table 6-2 and visual observations include the following:

Comparisons between P. tremuloides and P. balsamifera

1) *P. tremuloides* leaves are thinner than *P. balsamifera* leaves
2) *P. tremuloides* leaves have lower percent intercellular space in the spongy mesophyll than *P. balsamifera* leaves

Comparisons between sun and shade leaves

1) Sun leaves are thicker than shade leaves (Figure 6-4)
2) For sun leaves, the palisade mesophyll is thicker than the spongy mesophyll (Figure 6-4)
3) For *P. tremuloides* shade leaves, the palisade mesophyll is thicker than the spongy mesophyll but for *P. balsamifera* shade leaves, the spongy mesophyll is thicker than the palisade mesophyll (Figure 6-4)
4) Both sun and shade leaves of *P. tremuloides* and *P. balsamifera* had two palisade cell layers
5) For mature leaves, percent intercellular space was greater in shade leaves than for sun leaves

Comparisons between mature and senescing leaves

1) For sun leaves, percent intercellular space is higher in senescing leaves
2) Cell disintegration in the spongy mesophyll was evident in late stages of senescence (Figure 6-5).

Correlation analyses

Highly significant ($P<0.01$) correlation coefficients were found between the chlorophyll indices (mSR_{705}, mND_{705})) and chlorophyll *a*, *b*, total chlorophyll and chlorophyll a/b (exception: ASU mSR_{705} with chlorophyll a/b, significant at $P<0.05$) (Table 6-3). Similarly, many of the wavebands involved in the computation of these indices had significant ($P<0.05$) to highly significant ($P<0.01$) correlations. A notable exception was for $R_{676.7}$ for *P. tremuloides* and *P. balsamifera* sun leaves only. Also, $R_{445.9}$ did not correlate well with chlorophyll content except for PSU. This band is used as a reference band in the indices mSR_{705} and mND_{705}, since reflectance is minimal due to combined absorptance by chlorophyll and carotenoids at all but very low chlorophyll contents (Sims and Gamon 2002). PSRI was not included in the correlation analysis with chlorophyll because the relationship is non-linear (Figure 6-2).

There were fewer significant relationships between spectral bands and leaf anatomical features (total thickness, palisade mesophyll thickness, spongy mesophyll thickness, percent intercellular space). Of particular interest, no significant correlations were found between any of these leaf traits and wavebands in the near-infrared. This is consistent with our finding that reflectance at 800.7 nm was fairly stable over a large range of chlorophyll contents within each species. However, a number of significant relationships were detected between leaf traits and wavebands in the chlorophyll absorption wells (445.9 nm, 676.7 nm) as well as with PSRI. This was the case for ASU leaves, in which all leaf traits (total thickness, palisade mesophyll thickness, spongy mesophyll thickness, percent intercellular space) were significantly ($P<0.05$) correlated with reflectance at 445.9 nm, 676.7 nm, as well as with PSRI. For *P. tremuloides* shade leaves, the only significant correlations found were between palisade mesophyll thickness and PSRI and between percent intercellular space and PSRI. For *P. balsamifera* sun leaves, palisade mesophyll thickness was correlated ($P<0.05$) with $R_{445.9}$, $R_{676.7}$ and PSRI. No significant relationships existed between *P. balsamifera* shade leaves and any of the leaf anatomical traits.

DISCUSSION

Comparison of species

Several key differences in leaf spectral reflectance and leaf traits between *P. tremuloides* and *P. balsamifera* have been identified in this study. Overall, the earlier onset of senescence in *P. balsamifera* as compared to *P. tremuloides* was reflected in an earlier rise in PSRI, an index designed for this purpose (Figure 6-2). Two additional indices, mSR_{705} and mND_{705}, which tightly correlate with chlorophyll content, were useful in monitoring trends in chlorophyll content over the progress of senescence (Table 6-3). Values of these indices were generally higher for *P. tremuloides*, with the higher total chlorophyll content. *P. balsamifera*, on the other hand, exhibited higher chlorophyll a/b. Leaf thickness and percentage intercellular space were also greater in *P. balsamifera* (Table 6-2), which corresponds well with its significantly higher mean reflectance at 800.7 nm ($P<0.001$).

Differences in reflectance indices between species at key times of the year can have important implications for detecting species from a remote sensing perspective. This will be the case only if these differences are consistent between species and are

transferred to the canopy level. Further study using hyperspectral airborne or space-borne imagery would be necessary to answer these types of questions. A significant complicating factor will be non-synchronous timing of leaf color changes and leaf fall between clones, which has been known to occur within the same stand (Peterson and Peterson 1992).

Comparison of sun and shade leaves

For both species, many of the expected differences between their sunlit and shaded leaves were observed, including greater total thickness and, in particular, greater palisade mesophyll thickness in sunlit leaves (Table 6-2). That mature shade leaves had greater percent intercellular space than mature sun leaves is consistent with Bäck et al. (1999) and Gausman (1984). Higher proportion of spongy mesophyll in shade leaves can serve to increase internal light scattering and absorptance under low light levels (DeLucia et al., 1996). The two species therefore appear capable of some degree of morphological plasticity due to light environment. Although St-Jacques et al. (1991) indicate that very shade-intolerant species tend to have little or no leaf physiological and morphological plasticity, the variability in leaf histological features of these two shade-intolerant species suggests otherwise, in accordance with Ashton and Berlyn (1992) and Feng et al. (2004). However, these differences did not result in significant differences (α =0.05) in reflectance at 800.7 nm between sun and shade leaves for either species (based on two-tailed t-tests). An earlier study by Knapp and Carter (1998) concluded similarly, for which sun-adapted plants had similar optical properties in the near-infrared to shade-adapted plants.

Although total chlorophyll was initially higher for shade leaves for both *P. tremuloides* and *P. balsamifera*, this trend continued for *P. tremuloides* but destabilized in *P. balsamifera* with the onset of senescence (Figure 6-3). The most striking difference between sun and shade leaves of the two species was observed for chlorophyll a/b. For *P. tremuloides*, shade leaves consistently had higher chlorophyll a/b whereas for *P. balsamifera*, sun leaves almost always had the higher chlorophyll a/b. Since previous studies have shown a tendency for chlorophyll a/b to decrease with decreasing light availability (Lei et al., 1996; Givnish, 1988; Oberbauer & Strain, 1986), our results for *P. tremuloides* are contrary to the norm.

Furthermore, our results indicate potential benefit for establishing independent SPAD curves for sun and shade leaves. On the one hand, for *P. tremuloides*, combining sun and shade leaves for a collective SPAD calibration curve did not negatively impact the coefficients of determination for chlorophyll *a*, chlorophyll *b*, or total chlorophyll. Rather, r^2 was improved for chlorophyll *b*. In contrast, a collective SPAD calibration curve resulted in lower coefficients of determination for *P. balsamifera* for all chlorophyll variables (chlorophyll *a*, chlorophyll *b*, and total chlorophyll). In keeping, different trajectories followed by *P. balsamifera* sun and shade leaves are evident in Figure 6-2.

Comparison of mature and senescing leaves

Higher percent intercellular space for senescing ASU and PSU than for mature ASU and PSU (Table 6-2) are an indication of changes in the mesophyll such as cell wall breakdown, also evident in thin section photographs (Figure 6-5) (for PSH, percent

intercellular space was approximately equal for mature and senescing leaves, however). Unfortunately, based on our data, it does not appear possible to track these types of changes, determined from simple leaf thin sections, using wavebands in the NIR. It is important to note here, however, that while large sample sizes were attained of reflectance spectra and for chlorophyll analyses, sample sizes for the histological analysis were small due to the greater amount of time and detail required (see Methods). Larger sample sizes could have strengthened our conclusions based on Table 6-2.

Overall, correlations between internal anatomical features and wavebands in the NIR were poor ($P>0.05$). Likewise, correlations between NIR and % intercellular space were weak in a study by Slaton et al. (2001), who used more labour-intensive oblique-paradermal sections to determine leaf section parameters. In their case, parameters highly correlated with NIR included the ratio of mesophyll cell surface area exposed to intercellular space per unit leaf area, leaf bicoloration, and the presence of a thick leaf cuticle. Their finding agrees with Knipling (1970), who indicated that the number or total area of the air-cell wall interfaces may be a more important parameter for determining reflectance than the volume of air space. He also suggested that, with regard to internal light-scattering mechanisms, the palisade mesophyll may be just as important as the spongy mesophyll. On the other hand, we found significant correlation ($P<0.05$) between transmittance at 800.7 nm and both percent intercellular space and spongy mesophyll width for nine tropical species with a much greater range for these three variables (Castro-Esau et al., in press). It appears that percent intercellular space and spongy mesophyll width may be more useful for prediction in the near-infrared in multiple species with dissimilar internal morphologies than for same-species samples covering the progress of senescence.

Chlorophyll a/b declined with time for *P. tremuloides* and *P. balsamifera* during autumn senescence (Figure 6-3). This decline is consistent with work by Sanger (1971), who also observed a decline in chlorophyll a/b in senescing *P. tremuloides* leaves. It does not correspond with findings by Dean et al. (1993), however, who observed an increase in chlorophyll a/b for this same species during senescence.

CONCLUSION

Throughout this study, we aimed to improve our understanding of the spectro-temporal dynamics of *P. tremuloides* and *P. balsamifera* leaves by characterizing changes in leaf traits in autumn and determining their correspondence with changes in leaf spectral characteristics. Since our results cover two trees over two autumn periods (2002 and 2003), we cannot make generalizations about their senescence behaviour over time or space. Changes in chlorophyll content during this period, however, were well correlated with two indices, mSR_{705} and mND_{705} (Sims & Gamon, 2002). Deterioration of the mesophyll, however, while evident in thin section photographs, was not evident in a NIR response. This result was unexpected. In fact, Knipling (1970) stated 'collapse of the mesophyll' as a common predictor for decreases of NIR. This predictor was not effective in explaining NIR levels in our data, and may not be useful over all species or leaf types. Transmittance in the NIR was not found to change with leaf senescence either in a study by Madeira et al. (2000) on beans (*Phaseolus vulgaris* L.). On the contrary, several mesophyll features (palisade and spongy mesophyll thickness and percent intercellular space) were significantly correlated with PSRI, which incorporates

wavebands from both the visible and NIR regions. This index should be explored to a greater extent for the purpose of tracking mesophyll breakdown in senescing leaves .

Sampling over multiple years, over a greater number of trees representing clones and over a broader range of sites would further extend our knowledge of the ecology of these species, particularly if coupled with study of satellite-borne hyperspectral imagery. Research of this type could indicate the potential for species discrimination and potentially clone discrimination from remotely sensed data, especially at critical times of the year such as autumn senescence. Extending the present study to cover the period of spring flush could expose additional key differences between these major hardwood components of the forest resource in western Canada.

Table 6-1: Calibration equations for SPAD and chlorophyll content of *P. tremuloides* and *P. balsamifera* sun and shade leaves

Species	Light acclimation (no. samples)	y	r^2	Calibration equation for converting from SPAD to chlorophyll content (mg m^{-2})
P. tremuloides	Sun (20)	Chl *a*	0.961	$y = 0.215x^2 + 0.352x + 15.1$
		Chl *b*	0.789	$y = 0.0781x^2 - 2.92x + 84.9$
		Total Chl	0.958	$y = 0.293x^2 - 2.57x + 99.9$
	Shade (18)	Chl *a*	0.982	$y = 0.298x^2 - 4.38x + 86.0$
		Chl *b*	0.793	$y = 0.0212x^2 + 0.486x + 4.08$
		Total Chl	0.976	$y = 0.319x^2 - 3.89x + 127$
	All (48)	Chl *a*	0.978	$y = 0.231x^2 - 0.536x + 32.4$
		Chl *b*	0.846	$y = 5.77E\text{-}03x^2 + 1.69x + 17.6$
		Total Chl	0.974	$y = 0.237x^2 + 1.15x + 50.0$
P. balsamifera	Sun (24)	Chl *a*	0.980	$y = 0.130x^2 + 2.07x - 12.1$
		Chl *b*	0.900	$y = 0.0146x^2 + 0.501x + 7.79$
		Total Chl	0.975	$y = 0.145x^2 + 2.57x - 4.30$
	Shade (25)	Chl *a*	0.980	$y = 0.218x^2 + 0.189x + 14.9$
		Chl *b*	0.934	$y = 0.0250x^2 + 0.580x + 1.07$
		Total Chl	0.979	$y = 0.243x^2 + 0.786x + 2.56$
	All (52)	Chl *a*	0.938	$y = 0.119x^2 + 2.93x - 3.26$
		Chl *b*	0.818	$y = 6.59E\text{-}03x^2 + 1.02x + 6.61$
		Total Chl	0.928	$y = 0.126x^2 + 3.95x + 3.35$

Note. r^2 is the coefficient of determination. 'All' signifies sun and shade leaves combined.

Table 6-2. Comparison of anatomical features and near-infrared reflectance at 800.7 nm for mature and senescing *P. tremuloides* and *P. balsamifera* leaves

	Mature (Total Chl>400 mg m^{-2})		**Senescing (ChlT<200 mg m^{-2})**	
	ASU (n=4)	***ASH*** (n=9)	***ASU*** (n=3)	***ASH***
Total thickness (μm)	88.43(1.42)	67.84(6.68)	84.73(16.52)	NA
Thickness palisade (μm)	49.35(2.61)	31.08(4.46)	48.13(12.24)	NA
Thickness spongy (μm)	29.90(0.58)	27.04(3.28)	26.88(4.88)	NA
Intercellular space (%)	28.35(4.00)	38.80(7.60)	41.28(10.97)	NA
$R_{800.7}$	56.07(6.87)	54.47(3.80)	52.63(3.27)	NA
	PSU (n=2)	***PSH*** (n=4)	***PSU*** (n=4)	***PSH*** (n=2)
Total thickness (μm)	115.60(21.07)	80.24(8.05)	103.55(15.70)	79.20(18.95)
Thickness palisade (μm)	56.5(9.90)	28.47(0.66)	41.25(6.60)	35.90(19.37)
Thickness spongy (μm)	49.9(10.39)	42.25(7.89)	52.65(10.22)	43.1(13.44)
Intercellular space (%)	42.84(10.67)	50.66(5.46)	54.65 (6.69)	49.74 (17.69)
$R_{800.7}$	58.78(0.14)	55.59(3.65)	56.80(2.63)	55.16(2.17)

Note. NA=not available. No ASH samples with total chlorophyll< 200 mg m^{-2} from the 2003 dataset were gathered. $R_{subscript}$ is reflectance at the indicated waveband. Sample sizes indicate number of thin sections used to compute means. For each thin section, five measurements were made and averaged.

Table 6-3: Correlation coefficients (r) for relationships between leaf optical properties and leaf chlorophyll content (2003 data)

Waveband	Chl *a*	Chl *b*	Chl a/b	Total Chl
ASU				
$R_{445.9}$	NS	NS	NS	NS
R_{499}	NS	NS	NS	NS
$R_{548.5}$	-0.938**	-0.803**	-0.949**	-0.927**
$R_{676.7}$	NS	NS	NS	NS
$R_{706.2}$	-0.946**	-0.842**	-0.918**	-0.939**
mSR_{705}	0.919**	0.961**	0.711*	0.930**
mND_{705}	0.925**	0.910**	0.790**	0.929**
ASH				
$R_{445.9}$	NS	NS	NS	NS
R_{499}	-0.741*	-0.741*	-0.738*	-0.741*
$R_{548.5}$	-0.939**	-0.943**	-0.953**	-0.939**
$R_{676.7}$	-0.762*	-0.764*	-0.765*	-0.762*
$R_{706.2}$	-0.912**	-0.917**	-0.926**	-0.913**
mSR_{705}	0.985**	0.982**	0.971**	0.985**
mND_{705}	0.980**	0.981**	0.981**	0.980**
PSU				
$R_{445.9}$	-0.744*	-0.757*	-0.893**	-0.745*
R_{499}	-0.724*	-0.738*	-0.888**	-0.726*
$R_{548.5}$	-0.960**	-0.965**	-0.972**	-0.960**
$R_{676.7}$	NS	NS	NS	NS
$R_{706.2}$	-0.955**	-0.961**	-0.984**	-0.955**
mSR_{705}	0.992**	0.990**	0.911**	0.992**
mND_{705}	0.982**	0.985**	0.962**	0.982**
PSH				
$R_{445.9}$	NS	NS	NS	NS
R_{499}	-0.779*	-0.819*	-0.944**	-0.785*
$R_{548.5}$	-0.946**	-0.963**	-0.987**	-0.949**
$R_{676.7}$	-0.745*	-0.788*	-0.927**	-0.751*
$R_{706.2}$	-0.971**	-0.974**	-0.940**	-0.972**
mSR_{705}	0.974**	0.960**	0.859**	0.972**
mND_{705}	0.982**	0.977**	0.908**	0.982**

Note. $R_{subscript}$ is reflectance at the indicated waveband. *$P \leq 0.05$; **$P \leq 0.01$

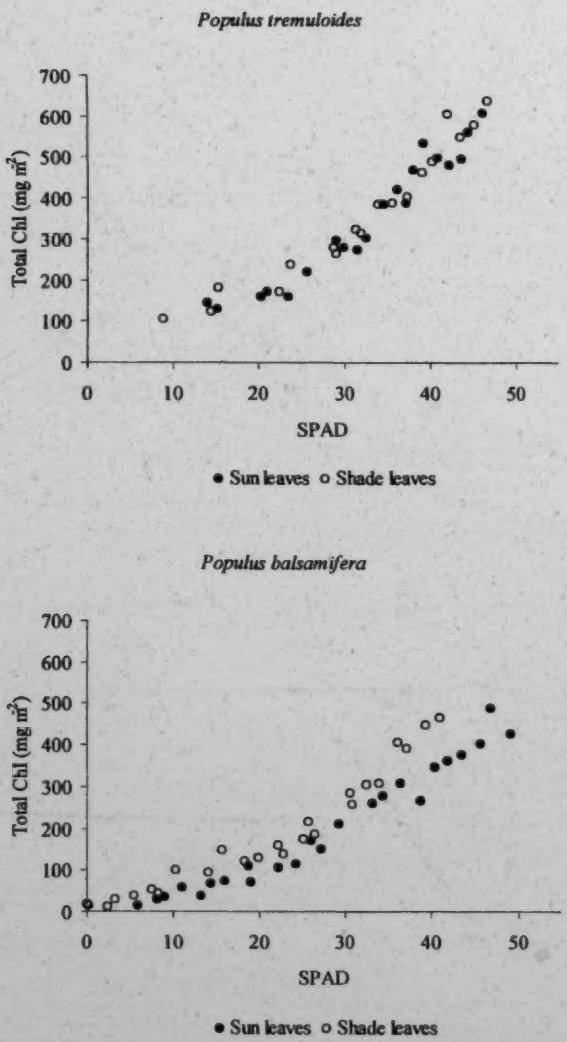

Figure 6-1. SPAD calibration curves for total chlorophyll (Total Chl) of sun and shade leaves for *P. tremuloides* and *P. balsamifera*.

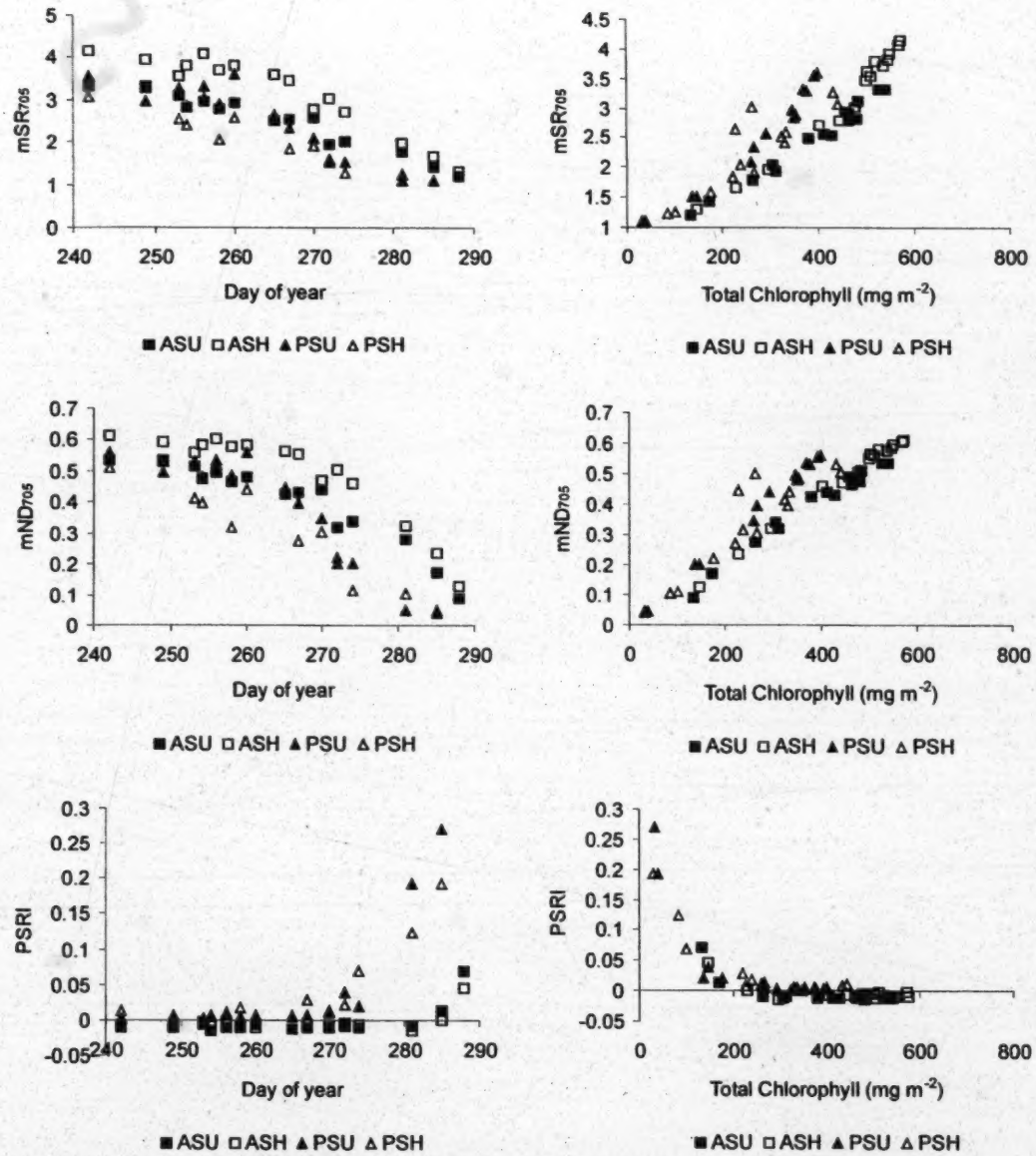

Figure 6-2. Spectral indices (mSR_{705}, mND_{705} and PSRI) plotted according to time (left) and total chlorophyll content (right) for *P. tremuloides* sun (ASU) and shade (ASH) leaves and *P. balsamifera* sun (PSU) and shade (PSH) leaves. Each symbol represents an average from three leaves.

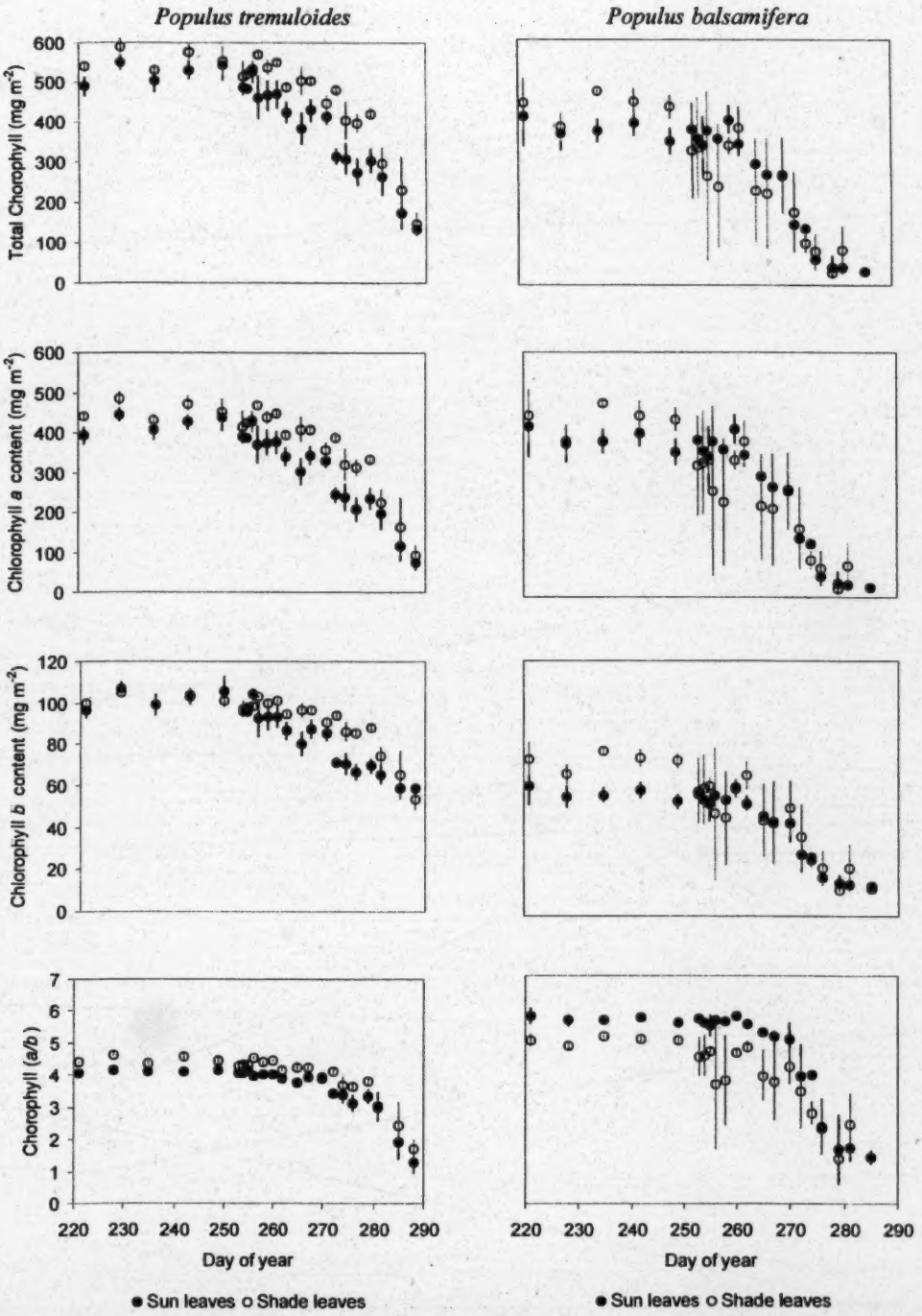

Figure 6-3. Changes in total chlorophyll, chlorophyll *a* and *b* and chlorophyll a/b during senescence of *P. tremuloides* and *P. balsamifera* sun and shade leaves. Each symbol represents the mean ± 1 SD from three leaves, where chlorophyll content is based on regressions in Table 6-1. Leaf drop occurred by day 288 for *P. balsamifera* and day 299 for *P. tremuloides.*

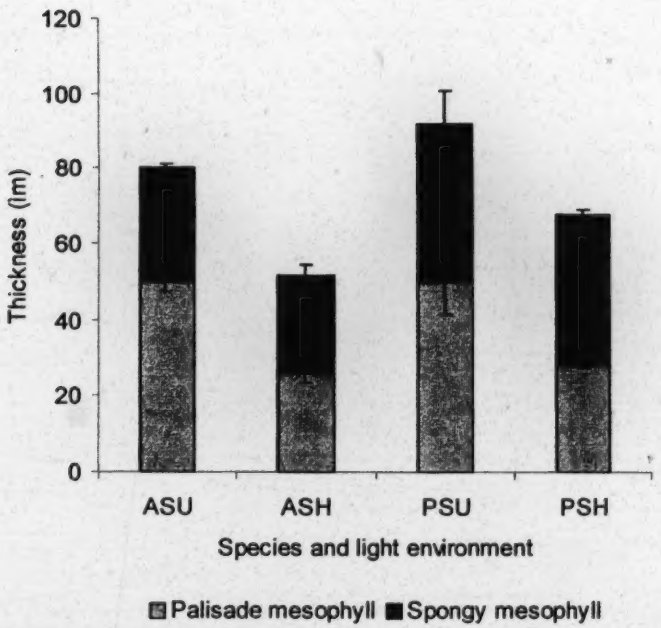

Figure 6-4. Mean palisade and spongy mesophyll thickness (± 1 SD) for mature *P. tremuloides* sun (ASU) and shade (ASH) leaves and *P. balsamifera* sun (PSU) and shade (PSH) leaves, based on measurements from August 8, 2003 thin sections (n=2-5).

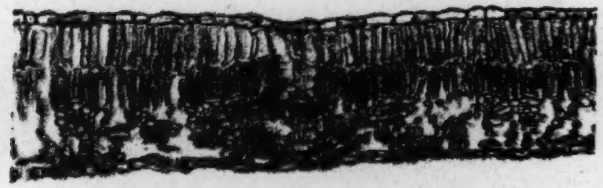

(a)

100 µm

(b)

100 µm

Figure 6-5. Thin sections of mature (a) and senescing (b) *P. tremuloides* sun leaves.

LITERATURE CITED

Amlin, N.M. & Rood, S.B. (2003). Drought stress and recovery of riparian cottonwoods due to water table alteration along Willow Creek, Alberta. *Trees-Structure and Function, 17(4),* 351-358.

Andersson, A., Keskitalo, J., Sjodin, A., Bhalerao, R., Sterky, F., Wissel, K., Tandre, K., Aspeborg, H., Moyle, R., Ohmiya, Y., Brunner, A., Gustafsson, P., Karlsson, J., Lundeberg, J., Nilsson, O., Sandberg, G., Strauss, S., Sundberg, B., Uhlen, M., Jansson, S. & Nilsson, P. (2004). A transcriptional timetable of autumn senescence. *Genome Biology, 5(4)*, R24: 1-13.

Ashton, P.M.S. & Berlyn, G.P. (1992). Leaf Adaptations of Some Shorea Species to Sun and Shade. *New Phytologist, 121(4)*, 587-596.

Ashton, P.M.S., Olander, L.P., Berlyn, G.P., Thadani, R. & Cameron, I.R. (1998). Changes in leaf structure in relation to crown position and tree size of Betula papyrifera within fire-origin stands of interior cedar-hemlock. *Canadian Journal of Botany, 76(7)*, 1180-1187.

Bäck, J., Vanderklein, D.W. & Topa, M.A. (1999). Effects of elevated ozone on CO2 uptake and leaf structure in sugar maple under two light environments. *Plant Cell and Environment, 22(2)*, 137-147.

Boyer, M., Miller, J., Belanger, M., Hare, E. & Wu, J.Y. (1988). Senescence and Spectral Reflectance in Leaves of Northern Pin Oak (Quercus-Palustris Muenchh). *Remote Sensing of Environment, 25(1),* 71-87.

Castro-Esau, K. L., Sánchez-Azofeifa, G. A., Rivard, B., Wright, S. J., & Quesada, M. (in press) Variability in leaf optical properties of Mesoamerican trees and the potential for species classification. *American Journal of Botany*.

Collier, D.E. & Thibodeau, B.A. (1995). Changes in Respiration and Chemical Content During Autumnal Senescence of Populus-Tremuloides and Quercus-Rubra Leaves. *Tree Physiology, 15(11)*, 759-764.

Dean, M.A., Letner, C.A. & Eley, J.H. (1993). Effect of Autumn Foliar Senescence on Chlorophyll a-B Ratio and Respiratory Enzymes of Populus-Tremuloides. *Bulletin of the Torrey Botanical Club, 120(3)*, 269-274.

DeLucia, E.H., Nelson, K., Vogelmann, T.C. & Smith, W.K. (1996). Contribution of intercellular reflectance to photosynthesis in shade leaves. *Plant Cell and Environment, 19(2)*, 159-170.

Demarez, V., Gastellu-Etchegorry, J.P., Mougin, E., Marty, G., Proisy, C., Dufrene, E. & Le Dantec, V. (1999). Seasonal variation of leaf chlorophyll content of a temperate

forest. Inversion of the PROSPECT model. *International Journal of Remote Sensing, 20(5),* 879-894.

Farrar, J.L. (1995). *Trees in Canada*. Ottawa, Canada: Fitzhenry & Whiteside Ltd. and the Canadian Forest Service, Natural Resources Canada..

Feng, Y.L., Cao, K.F. & Zhang, J.L. (2004). Photosynthetic characteristics, dark respiration, and leaf mass per unit area in seedlings of four tropical tree species grown under three irradiances. *Photosynthetica, 42(3)*, 431-437.

Gamage, H.K., Ashton, M.S. & Singhakumara, B.M.R. (2003). Leaf structure of Syzygium spp. (Myrtaceae) in relation to site affinity within a tropical rain forest. *Botanical Journal of the Linnean Society, 141(3)*, 365-377.

Gamon, J.A. & Surfus, J.S. (1999). Assessing leaf pigment content and activity with a reflectometer. *New Phytologist, 143(1)*, 105-117.

Garcia-Plazaola, J.I., Hernandez, A. & Becerril, J.M. (2003). Antioxidant and pigment composition during autumnal leaf senescence in woody deciduous species differing in their ecological traits. *Plant Biology, 5(5)*, 557-566.

Gausman, H.W. (1984). Evaluation of Factors Causing Reflectance Differences between Sun and Shade Leaves. *Remote Sensing of Environment, 15(2)*, 177-181.

Gausman, H.W. (1985). *Plant leaf optical properties in visible and near-infrared light.* Graduate Studies No. 29. Lubbock, Texas: Texas Tech Press.

Gitelson, A. & Merzlyak, M.N. (1994). Spectral Reflectance Changes Associated with Autumn Senescence of Aesculus-Hippocastanum L and Acer-Platanoides L Leaves - Spectral Features and Relation to Chlorophyll Estimation. *Journal of Plant Physiology 143(3)*, 286-292.

Givnish, T.J. (1988). Adaptation to Sun and Shade: A Whole-plant Perspective. In J.R. Evans, S. vonCaemmerer & W.W. Adams III (Eds.), *Ecology of Photosynthesis in Sun and Shade* (pp. 63-92). Australia: CSIRO.

Hiscox, J.D. & Israelstam, G.F. (1979). Method for the Extraction of Chlorophyll from Leaf Tissue without Maceration. *Canadian Journal of Botany, 57(12)*, 1332-1334.

Hörtensteiner, S. & Feller, U. (2002). Nitrogen metabolism and remobilization during senescence. *Journal of Experimental Botany, 53(370)*, 927-937.

Knapp, A.K. & Carter, G.A. (1998). Variability in leaf optical properties among 26 species from a broad range of habitats. *American Journal of Botany, 85(7)*, 940-946.

Knipling, E.B. (1967). Physical and physiological basis for differences in reflectance of healthy and diseased plants. In Proc. Workshop on Infrared Color Photography and diseased plants, Winter Haven, Florida: Florida Dept. of Agriculture.

Knipling, E.B. (1970). Physical and physiological basis for the reflectance of visible and near-infrared radiation from vegetation. *Remote Sensing of Environment, 1*, 155-159.

Lee, D.W. & Graham, R. (1986). Leaf Optical-Properties of Rain-Forest Sun and Extreme Shade Plants. *American Journal of Botany, 73(8)*, 1100-1108.

Lei, T.T., Tabuchi, R., Kitao, M. & Koike, T. (1996). Functional relationship between chlorophyll content and leaf reflectance, and light-capturing efficiency of Japanese forest species. *Physiologia Plantarum, 96(3)*, 411-418.

Madeira, A.C., Mendonca, A., Ferreira, M.E. & Torborda, M.D. (2000). Relationship between spectroradiometric and chlorophyll measurements in green beans. *Communications in soil science and plant analysis, 31(5-6),* 631-643.

Masclaux, C., Valadier, M.H., Brugiere, N., Morot-Gaudry, J.F. & Hirel, B. (2000). Characterization of the sink/source transition in tobacco (Nicotiana tabacum L.) shoots in relation to nitrogen management and leaf senescence. *Planta, 211(4)*, 510-518.

Masoni, A., Ercoli, L., Mariotti, M. & Barberi, P. (1994). Changes in Spectral Properties of Aging and Senescing Maize and Sunflower Leaves. *Physiologia Plantarum, 91(2)*, 334-338.

Matile, P., Duggelin, T., Schellenberg, M., Rentsch, D., Bortlik, K., Peisker, C. & Thomas, H. (1989). How and Why Is Chlorophyll Broken Down in Senescent Leaves. *Plant Physiology and Biochemistry, 27(4)*, 595-604.

Merzlyak, M.N. & Gitelson, A. (1995). Why and What for the Leaves Are Yellow in Autumn - on the Interpretation of Optical-Spectra of Senescing Leaves (Acer-Platanoides L). *Journal of Plant Physiology, 145(3)*, 315-320.

Merzlyak, M.N., Gitelson, A.A., Chivkunova, O.B. & Rakitin, V.Y. (1999). Non-destructive optical detection of pigment changes during leaf senescence and fruit ripening. *Physiologia Plantarum, 106(1),* 135-141.

Mitton, J.B. & Grant, M.C. (1980). Observations on the Ecology and Evolution of Quaking Aspen, Populus-Tremuloides, in the Colorado Front Range. *American Journal of Botany, 67(2)*, 202-209.

Oberbauer, S.F. & Strain, B.R. (1986). Effects of Canopy Position and Irradiance on the Leaf Physiology and Morphology of Pentaclethra-Macroloba (Mimosaceae). *American Journal of Botany, 73(3)*, 409-416.

Okada, K., Inoue, Y., Satoh, K. & Katoh, S. (1992). Effects of Light on Degradation of Chlorophyll and Proteins During Senescence of Detached Rice Leaves. *Plant and Cell Physiology, 33(8)*, 1183-1191.

Peterson, L.W. & Huffaker, R.C. (1975). Loss of Ribulose 1,5-Diphosphate Carboxylase and Increase in Proteolytic Activity During Senescence of Detached Primary Barley Leaves. *Plant Physiology, 55(6)*, 1009-1015.

Peterson, E.B. & Peterson, N.M. (1992). Ecology, management, and use of aspen and balsam poplar in the prairie provinces. Special Report 1, Forestry Canada Northwest Region Northern Forestry Centre.

Rauscher, H.M., Perala, D.A. & Worth, C.V. (1995). The Ecology and Management of Aspen. *AI Applications, 9(3)*, 59-59.

Roth, I. (1984). Stratification of tropical forests as seen in leaf structure. The Hague: Dr. W. Junk Publishers.

Sanger, J.E. (1971). Quantitative Investigations of Leaf Pigments from Their Inception in Buds through Autumn Coloration to Decomposition in Falling Leaves. *Ecology, 52(6)*, 1075-1089.

Sims, D.A. & Gamon, J.A. (2002). Relationships between leaf pigment content and spectral reflectance across a wide range of species, leaf structures and developmental stages. *Remote Sensing of Environment, 81*, 337-354.

Slaton, M.R., Hunt, E.R. & Smith, W.K. (2001). Estimating near-infrared leaf reflectance from leaf structural characteristics. *American Journal of Botany, 88(2)*, 278-284.

St-Jacques, C., Labrecque, M. & Bellefleur, P. (1991). Plasticity of Leaf Absorbency in Some Broadleaf Tree Seedlings. *Botanical Gazette, 152(2)*, 195-202.

Watts, D.F. & Eley, J.H. (1981). Changes in the Chlorophyll a-B Ratio During Autumn Coloration of Populus-Sargentii. *Bulletin of the Torrey Botanical Club, 108(3)*, 379-382.

Wolf, F.T. (1956). Changes in Chlorophyll-a and Chlorophyll-B in Autumn Leaves. *American Journal of Botany, 43(9)*, 714-718.

CHAPTER 7—Conclusions

Recent developments in technology and modelling techniques mean that remote sensing is in a stronger position than ever to benefit ecology.
-Paul Aplin[1]

The specific nature of inferences made from both leaf spectroscopy and remote sensing studies today are evidence that 'green' is not simply 'green'. Rather, as the quote by Aplin (2005) indicates, remote sensing is a powerful tool for ecological research at a variety of scales. At the global scale, for example, extent and rates of deforestation have been estimated using coarse spatial resolution satellite data (Lepers et al., 2005). At local scales, nonnative plants have been mapped using airborne hyperspectral imagery (e.g. Underwood et al., 2003) and height of trees has been estimated using LIDAR (e.g. Drake et al., 2003). These are but a few examples of the myriad of ecological applications for remote sensing, which include, according to Kerr & Ostrovsky (2003), 'identifying and detailing the biophysical characteristics of species' habitats, predicting the distribution of species and spatial variability in species richness, and detecting natural and human-caused change at scales ranging from individual landscapes to the entire world'.

Much of the research described in this dissertation is either directly or indirectly geared toward species recognition. Study of leaf-level species separability, as well as understanding and quantifying intra-specific variability, are precursors for interpreting high spatial resolution hyperspectral imagery. Factors other than leaf senescence that cause within-species variations in leaf spectra include leaf age, nutrient and water status, leaf position (sunlit or shaded), and other stress-related factors. Due to these factors, results from Chapter five suggest that the likelihood of classifying species across sites or seasons may be poor. However, within a site these factors may help or hinder species recognition when they cause greater between-species variations than within-species variations. For example, the presence of epiphylls on canopy dominants was useful for distinguishing among forest types in Amazon caatinga in a study by Roberts et al. (1998). Furthermore, differences in phenology among species could potentially aid classification of a single-date image. Overall, successful species recognition from hyperspectral data could have many potential ecological applications. Some of these include quantifying carbon sinks, identifying important food sources for wildlife (Clark et al., 2005), locating endangered or threatened tree species, characterizing secondary and climax forest species composition, and aiding in tree demographic studies.

CONTRIBUTIONS AND SIGNIFICANCE

The literature review in Chapter two not only critically summarizes current research on biomass estimation for tropical secondary forests (mainly from the Amazon), it synthesizes the literature into research needs specific to Central America, where research of this nature is scarce. The specific needs identified include topographic correction and stratification according to ecological and site quality variables. While at present it is possible to segregate roughly three successional stages up to 15 years of age using Landsat TM data, or up to 60 tha^{-1} of plant biomass using synthetic aperture radar, use of higher spectral and spatial resolution imagery could lead to significant improvements in biomass estimation in tropical forests. Improvements in biomass

[1] Aplin, P. (2005). Remote sensing: ecology. *Progress in Physical Geography*, 29, 104-113.

estimation of tropical secondary forests, in turn, will provide for more accurate estimates of carbon sequestration by these important carbon sinks.

Chapter three exposes the risks of inter-instrument comparison of leaf spectra and vegetation indices. The authors stress reporting specific wavebands for computing indices as well as any procedure used for interpolation or smoothing prior to index computation, to prevent faulty conclusions when comparisons are made between studies. This research was critical to Chapter five, in which leaf spectra for the tropical tree database were gathered with multiple spectrometers. As a result of conclusions from the inter-instrument comparison study, data from the multiple spectrometers were analyzed separately for Chapter five, rather than compiled.

Lianas (woody vines) are becoming a concern to the scientific community due to their increasing dominance in tropical forests over the past two decades (Phillips et al., 2002). Their increase could potentially alter carbon fixation rates and species composition. In Chapter four it was determined that, at a tropical dry forest in Panama, leaf optical properties and chlorophyll content of lianas differ significantly from trees in the visible region, possibly due to differences in drought stress and phenology between lianas and trees at this site. This finding is new to the scientific community and could have implications for monitoring liana coverage from space in the future. To study this further, differences in tree crown spectra with and without liana coverage are explored in a follow-up paper by Sanchez-Azofeifa & Castro-Esau (in press, *International Journal of Remote Sensing*). Differences between the two structural groups were not significant at a tropical wet forest site, however.

Using a dataset of leaf spectra for over 60 tree species from seven Mesoamerican sites, and leaf trait data for nine species at one site (Parque Natural Metropolitano, Panama), within-species variability in leaf spectra was quantified in Chapter four. This is likely the most extensive compilation of leaf reflectance spectra for tropical tree species at different sites and seasons conducted to date in the remote sensing and ecological literature. Large differences between same-species leaf spectra were observed between sites and between seasons. As a result, it was possible to classify up to 27 species with high accuracy within a specific site and season, but not across sites or seasons. Extrapolation for greater species numbers indicated that classification accuracy degraded to approximately 70% for 100 species. This can be an important limitation to species discrimination in species-rich tropical forests; however, further research is required at the crown level.

Prior to this research, only two studies were known to the author that approach the topic of differentiating tropical tree species (Cochrane, 2000; Fung, 1999). Of these, Fung (1999) claims that approximately 80% accuracy could be attained for a classification of 25 subtropical tree species found in Hong Kong using a backpropagation feed forward neural network and linear discriminate analysis. The second study had much more limited results, in which one species of interest (*Swietenia macrophylla*) could be distinguished from 11 other Amazonian species using a shape-space filter (Cochrane, 2000). A classification of the remaining species was not performed. A dataset of the nature and magnitude of that created and used in this dissertation has not previously been available for tropical tree species. Analysis of this dataset has presented a more comprehensive picture of the nature and magnitude of intra-specific variability in leaf spectra and the

potential for tropical tree species classification at the leaf-level, with preliminary data at the crown level.

Chapter five characterized autumn foliar senescence of two important aspen parkland species, *Populus tremuloides* and *Populus balsamifera*, both with regard to chlorophyll content and degradation of the mesophyll. Changes in reflectance indices were studied in relation to changes in these leaf traits, and differed both between species and between sunlit and shaded leaves within species. Although changes in chlorophyll content over time corresponded well with changes in reflectance indices, specifically the modified simple ratio (mSR_{705}) and the modified normalized difference index (mND_{705}), changes in mesophyll characteristics did not correspond well with changes in near-infrared reflectance. By providing a comparison of these two shade-intolerant species, as well as of sunlit and shaded leaves within each species over the spectro-temporal domain, this research represents an important contribution to the field in which the majority of leaf spectroscopy work is steady-state. This study also contributes to the understanding of the ecology and phenology of *P. tremuloides* and *P. balsamifera* in Alberta and has potential significance for remote detection of the two species during fall senescence.

AVENUES FOR FUTURE RESEARCH

Future research on factors causing intra-specific variations in leaf reflectance as well as tree species recognition has the potential to follow the same trajectory as remote sensing technology over the past three to four decades. There are still many questions to be answered about intra-specific variability in leaf reflectance, both at the leaf-level and at the crown-level, and numerous opportunities exist for further study. For instance:

- How does leaf spectral reflectance change for a single species over the course of an entire season or, for evergreen species, over the lifespan of the leaf?
- How do between-site differences, such as soil mineral levels, water availability, and climate affect spectral reflectance?
- To what extent do species retain unique spectral features from one site or one season to the next?
- How do genotype and/or phenotype influence leaf spectra of a species?
- What changes occur in leaf spectra as a result of insect galls or colonization by epiphylls?
- How does variability in reflectance spectra link with changes in photosynthetic rates or capacities?

To date, the answers to these questions are lacking. Further opportunities exist in extending the study of correlations between leaf traits and spectral wavebands over a larger number of species and from a broader range of tropical life zones (Chapter four leaf trait data were restricted to nine tree species from one tropical dry forest site, Parque Metropolitano, Panama). In addition, additional leaf components, such as water, lignin and cellulose could be compared between tropical species using spectra that extend into the 1100-2500 nm region.

Additional opportunities abound for comparing lianas and trees at leaf and crown-scales using hyperspectral data. Although differences between the two structural groups were characterized in Chapter four, spectral properties of individual liana species were not, nor the variability in leaf traits and leaf spectra among liana species. As well, further exploration into liana mapping from remote sensors is an important research area that

could imply monitoring lianas over time and space in support of recent concerns that indicates their increase in tropical forests over time (Phillips et al., 2002).

Similarly, a great opportunity exists for tropical species recognition at the crown-level, either using *in situ* data, such as gathered from a canopy crane, or from remotely sensed airborne data, and in the future, anticipated satellite data. Canopy-level studies will present new challenges and require confronting issues of leaf density, leaf angle, and background spectra from bark and soil. Research involving aerial photographs (Trichon, 2001), high spatial resolution multi-spectral imagery such as Quickbird (0.7 m) and IKONOS (1 m) (Clark et al., 2004a; Wang et al., 2004; Read et al., 2003), and LIDAR (Clark et al., 2004b) indicate that potential exists for classification of at least a portion of the total number of species, particularly emergents, as well as for gaining knowledge on tree mortality and tree structural characteristics. Similar potential was revealed in the examination of crown spectra of five species from the canopy crane at Fort Sherman (Chapter five) as well as for five to seven species in a HYDICE image over La Selva, Costa Rica (Clark et al., 2005, Zhang et al., submitted, *Remote Sensing of Environment*). Possibilities for remote mapping of greater species numbers using hyperspectral imagery have yet to be determined and are the key avenue of future research.

LITERATURE CITED

Clark, D. B., Read, J. M., Clark, M. L., Cruz, A. M., Dotti, M. F. & Clark, D. A. (2004). Application of 1-M and 4-M resolution satellite data to ecological studies of tropical rain forests. *Ecological Applications*, *14*, 61-74.

Clark, M. L., Clark, D. B. & Roberts, D. A. (2004b). Small-footprint lidar estimation of sub-canopy elevation and tree height in a tropical rain forest landscape. *Remote Sensing of Environment*, *91*, 68-89.

Clark, M. L., Roberts, D. A. & Clark, D. B. (2005). Hyperspectral discrimination of tropical rain forest tree species at leaf to crown scales. *Remote Sensing of Environment*, *96*, 375-398.

Cochrane, M. A. (2000). Using vegetation reflectance variability for species level classification of hyperspectral data. *International Journal of Remote Sensing*, *21*, 2075-2087.

Drake, J. B., Knox, R. G., Dubayah, R. O., Clark, D. B., Condit, R., Blair, J. B. & Hofton, M. (2003). Above-ground biomass estimation in closed canopy Neotropical forests using lidar remote sensing: factors affecting the generality of relationships. *Global Ecology and Biogeography*, *12*, 147-159.

Fung, T., Ma, F. Y. & Siu, W. L. (1999). Band Selection using hyperspectral data of subtropical tree species. *http://www.gisdevelopment.net/aars/acrs/1999/ps3/ps3055pf.htm*.

Kerr, J. T. & Ostrovsky, M. (2003). From space to species: ecological applications for remote sensing. *Trends in Ecology & Evolution*, *18*, 299-305.

Lepers, E., Lambin, E. F., Janetos, A. C., DeFries, R., Achard, F., Ramankutty, N. & Scholes, R. J. (2005). A synthesis of information on rapid land-cover changes for the period 1981-2000. *Bioscience, 55*, 115-124.

Phillips, O. L., Martinez, R. V., Arroyo, L., Baker, T. R., Killeen, T., Lewis, S. L., Malhi, Y., Mendoza, A. M., Neill, D., Vargas, P. N., Alexiades, M., Ceron, C., Di Fiore, A., Erwin, T., Jardim, A., Palacios, W., Saldias, M. & Vinceti, B. (2002). Increasing dominance of large lianas in Amazonian forests. *Nature*, *418*, 770-774.

Read, J. M., Clark, D. B., Venticinque, E. M. & Moreira, M. P. (2003). Application of merged 1-m and 4-m resolution satellite data to research and management in tropical forests. *Journal of Applied Ecology*, *40*, 592-600.

Roberts, D. A., Nelson, B. W., Adams, J. B. & Palmer, F. (1998). Spectral changes with leaf aging in Amazon caatinga. *Trees-Structure and Function*, *12*, 315-325.

Sanchez-Azofeifa, G. A. & Castro-Esau, K. (in press). Canopy observations on the hyperspectral properties of a community of tropical dry forest lianas and their host trees. *International Journal of Remote Sensing*.

Trichon, V. (2001). Crown typology and the identification of rain forest trees on large-scale aerial photographs. *Plant Ecology, 153*, 301-312.

Underwood, E., Ustin, S. & DiPietro, D. (2003). Mapping nonnative plants using hyperspectral imagery. *Remote Sensing of Environment, 86*, 150-161.

Wang, L., Sousa, W. P., Gong, P. & Biging, G. S. (2004). Comparison of IKONOS and QuickBird images for mapping mangrove species on the Caribbean coast of Panama. *Remote Sensing of Environment, 91*, 432-440.

Zhang, J. L., Rivard, B., Sánchez-Azofeifa, G. A. & Castro-Esau, K. L. (submitted). Intra and inter-class spectral variability of tropical tree species at La Selva, Costa Rica: Implications for species identification using HYDICE imagery. *Remote Sensing of Environment*.